Electronic supplementary information

Chemical Communications. 2021

The cage phosphoranes formation and their rearrangements in the reaction of substituted 2-(3-oxo-3-phenyl)ethoxybenzo[*d*]-1,3,2-dioxaphospholes with perfluorodiacetyl

Vladimir F. Mironov[a,b,1], Mudaris N. Dimukhametov[a], Gulnara A. Ivkova[b,2], Hasan R. Hayarov[b], Daut R. Islamov[a,b,3], Igor A. Litvinov[a,4]
[1]ORCID 0000-0002-4198-3774; [2]ORCID 0000-0001-6972-8452; [3]ORCID 0000-0002-5988-1012; [4]ORCID 0000-0003-4991-1908
[a]A.E.Arbuzov Institute of Organic and Physical Chemistry, FRC Kazan Scientific Center, Russian Academy of Sciences, Arbuzov Str. 8, 420088 Kazan, Russia, E-mail: mironov@iopc.ru
[b]Kazan (Volga Region) Federal University, Kremlevskaya Str. 18, 420008 Kazan, Russia

Table of contents

Numbers of investigated compounds

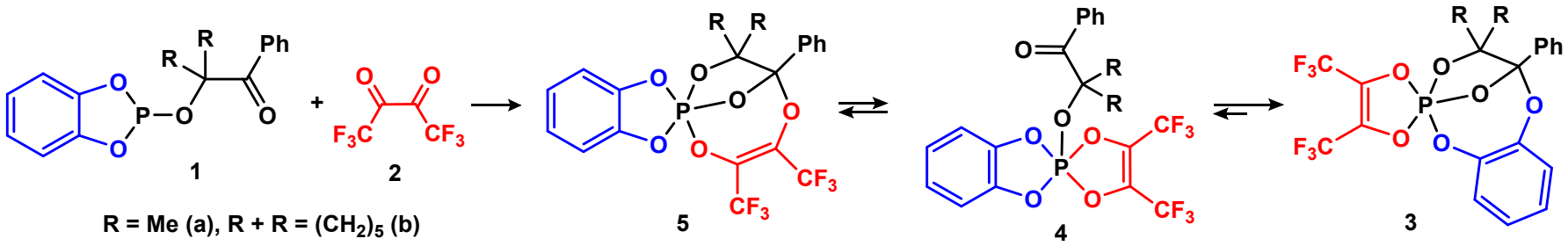

General remarks, experimental procedures and detail interpretation of NMR spectra

Commercially available solvents were purified according to the standard procedures. All reactions were run under an argon atmosphere. Mass spectra were recorded on AmaZon X (ESI) Bruker mass spectrometers. IR spectra were recorded on a Vector 22 instrument. NMR experiments were carried out on 400 MHz [400 MHz (^{1}H), 376.5 MHz (^{19}F), 161.9 MHz (^{31}P) and 100.6 MHz (^{13}C)] or 600 MHz [600 MHz (^{1}H), 242.9 MHz (^{31}P), 150.9 MHz (^{13}C)] spectrometers. ^{1}H, ^{31}P, ^{19}F, and ^{13}C NMR experiments were carried out at different temperatures (–5 °C, after 15 min; 25°C, after 6 h; after heating in dichloromethane for 1 hour). Chemical shifts (δ) are given in parts per million relative to the residual ^{1}H and ^{13}C signal of $CDCl_3$, CD_2Cl_2 or acetone-d_6 and the signals are designated as follows: s, singlet; d, doublet; t, triplet; m, multiplet. Coupling constants (*J*) are in hertz (Hz). Mass spectra (EI) were taken on a DFS Thermo Electron Corporation instrument (Germany). The energy of ionizing electrons was 70 eV, the temperature of the ion source was 280°C, a system of direct input of the sample into the ion source was used, and temperature of the evaporator was 250°C. Elemental analysis was performed on a CHNS-O analyzer; the phosphorus content was determined by the pyrolysis under oxygen flow.

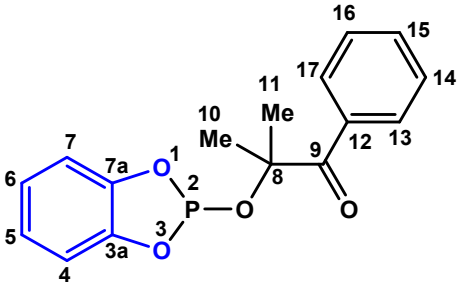

2-(Benzo[d][1,3,2]dioxaphosphol-2-yloxy)-2-methyl-1-phenylpropan-1-one (**1a**). To a mixture of 2-chlorobenzo[*d*][1,3,2]dioxaphosphole (5.28 g, 30.3 mmol) and triethylamine (4.22 ml, 30.4 mmol) in 100 ml of absolute diethyl ether, a solution of 2-methyl-1-phenylpropan-1-one (4.96 g, 30.2 mmol) in 10 ml the same solvent was added dropwise (0-5 °C). The resulting reaction mass was stirred for 3 h at 20 °C and then filtered off. The precipitate was washed with absolute diethyl ether (30 ml), the ethereal filtrate was evaporated in vacuum (subsequently from 12 to 0.01 mmHg), the resulting colorless oil was dissolved in pentane (50 ml), kept in a refrigerator for a day. A pentane solution was again filtered off and evaporated in vacuum; 8.58 g (94%) phosphole (**1a**) was obtained as a residue, which was used further without additional purification. IRS, cm^{-1} (film): 3069, 3006, 2977, 2928, 1682, 1643, 1616, 1599, 1476, 1447, 1359, 1332, 1303, 1285, 1233, 1205, 1159, 1120, 1095, 1070, 1034, 1010, 962, 889, 838, 748, 713, 693, 631, 596, 577, 562, 521, 501, 489. ^{1}H NMR spectrum (400.0 MHz, $CDCl_3$, δ ppm, *J* Hz): 7.96 d. d ($H^{13,17}$, 2H, $^{3}J_{HH}$ 8.2, $^{4}J_{HH}$ 1.2), 7.51 m (H^{15}, 1H, $^{3}J_{HH}$ 7.4, $^{4}J_{HH}$ 1.2), 7.36 m ($H^{14,16}$, 2H, $^{3}J_{HH}$ 8.2, $^{3}J_{HH}$ 7.4), 7.08 m ($H^{5,6}$, 2H, *AA'*-part of *AA'BB'*-system), 7.0 m ($H^{4,7}$, 2H, *BB'*-part of *AA'BB'*-system), 1.80 s ($H^{10,11}$, 6H). ^{31}P-{^{1}H} NMR spectrum (242.9 MHz, $CDCl_3$): δ_P 140.1 ppm.

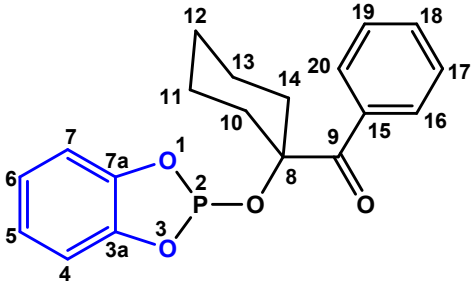

(1-(Benzo[d][1,3,2]dioxaphosphol-2-yloxy)cyclohexyl)(phenyl)methanone (**1b**) was obtained by a similar method from chlorobenzo[*d*][1,3,2]dioxaphosphole (4.39 g, 25.2 mmol), triethylamine (3.85 ml, 27.7 mmol), and (1-hydroxycyclohexyl)(phenyl)methanone (5.13 g, 25.1 mmol). The phosphole (**1b**) yield is 8.0 g (93%). ^{1}H NMR spectrum (400.0 MHz, $CDCl_3$, δ ppm, *J* Hz): 7.83 br. d ($H^{16,20}$, 2H, $^{3}J_{HH}$ 7.9), 7.36 br. m (H^{18}, 1H, $^{3}J_{HH}$ 7.5), 7.22 br. m ($H^{17,19}$, 2H, $^{3}J_{HH}$ 7.9, $^{3}J_{HH}$ 7.5), 6.87 m ($H^{5,6}$, 2H, *AA'*-part of *AA'BB'*-system), 6.81 m ($H^{4,7}$, 2H, *BB'*-part of *AA'BB'*-system), 2.0 br. m (Cy, 2H), 1.88 br. m (Cy, 2H), 1.45-1.47 and 1.61-1.62 two br. m (Cy, 5H), 1.19 br. m (Cy, 1H). ^{31}P-{^{1}H} NMR spectrum (242.9 MHz, $CDCl_3$): 141.1 ppm.

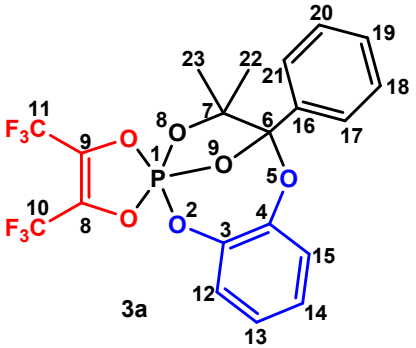

4',4'-Dimethyl-5'-phenyl-4,5-bis(trifluoromethyl)-4',5'-dihydro-2λ^5-spiro[[1,3,2]dioxaphosphole-2,2'-[2,5]epoxybenzo[d][1,3,6,2]trioxaphosphocine] (**3a**). To a solution of phosphole (**1**) (2.6 g, 8.6 mmol) cooled to –10 °C in 30 ml of dichloromethane, a solution of perfluorodiacetyl (1.68 g, 8.7 mmol) in 5 ml of dichloromethane was added dropwise. The addition of yellow perfluorodiacetyl resulted in its discoloration. The resulting reaction mass then acquired a brown color, and further brightened to a light brown color. The reaction mixture was kept at room temperature for 10 days, then it was evaporated by half and 15 ml of pentane was added. When kept in a refrigerator (5 °C), a crystalline precipitate of compound (**3a**) was gradually formed. Yield was 3.84 g (90%), m. p. 143-145 °C. Mass spectrum EI: *m/z*: 496.05 $[M]^+$. Calcd 496.05. Found, %: C, 48.33; H, 3.44; P, 6.19. $C_{20}H_{15}F_6O_6P$. Calcd, %: C, 48.40; H, 3.05; P, 6.24. IRS, cm^{-1} (nujol): 2726, 2677, 1712,1602, 1593, 1495, 1400, 1358, 1284, 1262, 1225, 1209, 1193, 1171, 1143, 1130, 1105, 1074, 1033, 1017, 998, 976, 943, 925, 915, 844, 815, 793, 779, 764, 755, 746, 737, 699, 682, 645, 616, 588, 563, 530, 484, 472, 413. IRS, cm^{-1} (pellet KBr): 3065, 3045, 2988, 2950, 1712, 1603, 1594, 1495, 1469, 1453, 1391, 1358, 1283, 1262, 1226, 1211, 1194, 1171, 1144, 1106, 1075, 1034, 1018, 999, 977, 944, 925, 915, 844, 816, 793, 779, 765, 756, 747, 737, 699, 683, 646, 616, 588, 573, 563, 530, 484, 472, 414. ^{1}H NMR spectrum (400 MHz, acetone-d_6, δ ppm, *J* Hz): 1.17 and 1.83 two s (Me, 6H), 6.95 d (H^{15}, 1H, $^3J_{HH}$ 7.9), 7.06 br d. d (H^{14}, 1H, $^3J_{HH}$ 7.9, $^3J_{HH}$ 7.3), 7.16 m (H^{13}, 1H, $^3J_{HH}$ 7.4, $^3J_{HH}$ 7.3), 7.20 m (H^{12}, 1H, $^3J_{HH}$ 7.4), 7.51-7.52 m ($H^{18\text{-}20}$, 3H), 7.69 m (H^{17}, H^{21}, 2H). ^{13}C NMR spectrum (100.6 MHz, acetone-d_6, δ_C ppm, *J* Hz) (hereinafter a view of signal in ^{13}C-{^{1}H} NMR spectrum is in parentheses): 142.68 d. d. d. d (d) (C^3, $^3J_{HC^{13}CC}$ 11.0-11.5, $^3J_{HC^{15}CC}$ 6.7-6.8, $^2J_{HC^{12}C}$ 3.8-3.9, $^2J_{POC}$ 3.5), 148.46 d. d. d. d (d) (C^4, $^3J_{HC^{14}CC}$ 10.6, $^3J_{POC^3C}$ 9.6, $^3J_{HC^{12}CC}$ 8.2, $^2J_{HC^{15}C}$ 3.5-3.6), 108.80 m (d) (C^6, $^3J_{HC^{22,23}C^7C}$ 3.6-3.8, $^2J_{POC}$ 3.2), 89.90 s (sept) (C^7, $^3J_{HCCC}$ 4.2), 125.95 q. d. q (q. d. q) (C^8, $^2J_{FC^{10}C}$ 43.0, $^2J_{POC}$ 5.3, $^3J_{FC^{11}C^9C}$ 3.0), 133.91 q. d. q (q. d. q) (C^9, $^2J_{FC^{11}C}$ 43.3, $^2J_{POC}$ 6.6, $^3J_{FC^{10}C^8C}$ 3.3), 119.51 q. d (q. d) (C^{10}, $^1J_{FC}$ 269.3, $^3J_{POCC}$ 18.5), 119.69 q. d (q. d) (C^{11}, $^1J_{FC}$ 267.6, $^3J_{POCC}$ 19.5-20.0), 120.74 d. d. d (d) (C^{12}, $^1J_{HC}$ 163.9, $^3J_{POCC}$ 10.6, $^3J_{HC^{14}CC}$ 8.8), 126.91 d. d (s) (C^{13}, $^1J_{HC}$ 164.1, $^3J_{HC^{15}CC}$ 9.0), 126.79 d. d (s) (C^{14}, $^1J_{HC}$ 164.2, $^3J_{HC^{12}CC}$ 8.0), 124.56 d. d (s) (C^{15}, $^1J_{HC}$ 163.9, $^3J_{HC^{13}CC}$ 8.0-8.1), 134.63 d. d. d (d) (C^{16}, $^3J_{POCC}$ 14.1, $^3J_{HC^{18}CC}$ 7.3, $^3J_{HC^{20}CC}$ 6.2), 127.55 br. d. d. d (s) ($C^{17,21}$, $^1J_{HC}$ 163.4, $^3J_{HC^{19}CC}$ 7.0-7.2, $^3J_{HC^{21,17}CC}$ 6.0-6.2), 129.40 br. d. m (s) ($C^{18,20}$, $^1J_{HC}$ 162.0, $^3J_{HC^{20,18}CC}$ 7.3), 130.73 d. t (s) (C^{19}, $^1J_{HC}$ 161.3, $^3J_{HC^{17,21}CC}$ 7.5), 25.90 q. q (s) (C^{22}, $^1J_{HC}$ 128.4, $^3J_{HCCC}$ 3.9), 20.76 q. d. q (d) (C^{23}, $^1J_{HC}$ 128.8, $^3J_{POCC}$ 11.7, $^3J_{HCCC}$ 3.9). ^{19}F NMR spectrum (376.5 MHz, CH_2Cl_2/$CDCl_3$ = 1 : 2, δ_F ppm, *J* Hz): –65.45 br. q (CF_3, 3F, $^5J_{FF}$ 9.3), –64.13 q (CF_3, 3F, $^5J_{FF}$ 9.3). ^{19}F NMR spectrum (376.5 MHz, acetone-d_6, δ_F ppm, *J* Hz): –66.11 q (CF_3, 3F, $^5J_{FF}$ 9.6), –64.62 q (CF_3, 3F, $^5J_{FF}$ 9.6). ^{31}P-{^{1}H} NMR spectrum (242.94 MHz, δ_P ppm): –39.7 (CH_2Cl_2/$CDCl_3$ = 1 : 2), –37.0 (acetone-d_6).

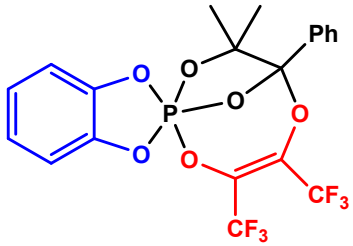

7',7'-Dimethyl-6'-phenyl-3',4'-bis(trifluoromethyl)-2',5',8',9'-tetraoxa-2λ^5-phosphaspiro[benzo[d][1,3,2]dioxaphosphole-2,1'-bicyclo[4.2.1]nonan]-3'-ene (**5a**). ^{19}F NMR spectrum (376.5 MHz, 25°C, CH_2Cl_2 / $CDCl_3$ = 1 : 2, δ_F ppm): –64.82 br. s. ^{31}P-{^{1}H} NMR spectrum (162.0 MHz, 25°C, CH_2Cl_2, δ_P ppm): –49.6 br. s.

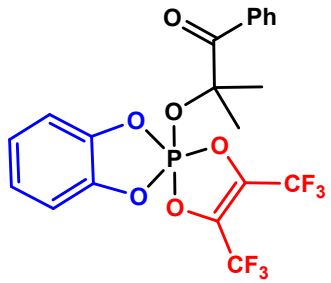

2-((4',5'-Bis(trifluoromethyl)-2λ^5-spiro[benzo[d][1,3,2]dioxaphosphole-2,2'-[1,3,2]dioxaphosphol]-2-yl)oxy)-2-methyl-1-phenylpropan-1-one (**4a**). ^{19}F NMR spectrum (376.5 MHz, 25°C, CH_2Cl_2 / $CDCl_3$ = 1 : 2, δ_F ppm): –64.24 br. q ($^4J_{FF}$ 11.0), –64.72 br. q ($^4J_{FF}$ 11.0). ^{19}F NMR spectrum (376.5 MHz, 25°C, acetone-d_6, δ_F ppm): –64.67 br. q ($^4J_{FF}$ 10.6), –65.10 br. q ($^4J_{FF}$ 10.6). ^{31}P-{^{1}H} NMR spectrum (242.9 MHz, 25°C, CH_2Cl_2, δ_P ppm): –40.3 s. ^{31}P-{^{1}H} NMR spectrum (162.0 MHz, 25°C, acetone-d_6, δ_P ppm): –37.2 s.

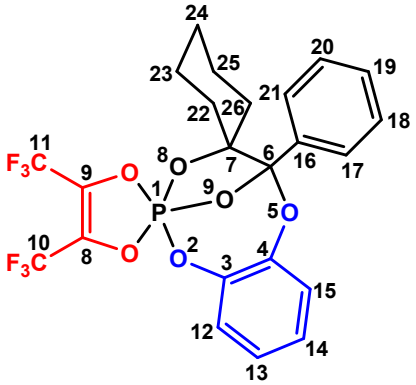

5'-Phenyl-4'',5''-bis(trifluoromethyl)-5'H-2'λ^5-dispiro[cyclohexane-1,4'-[2,5]epoxybenzo[d][1,3,6,2]trioxa phosphocine-2',2''-[1,3,2]dioxaphosphole] (**3b**). To a solution of phosphole (**1**) (3.57 g, 11.8 mmol) cooled to –10 °C in 30 ml of dichloromethane, a solution of perfluorodiacetyl (2.3 g, 11.9 mmol) in 5 ml of dichloromethane was added dropwise. After reaching room temperature in 2 h, the resulting reaction mixture was heated at reflux of dichloromethane for 1 h, then the solvent was removed in vacuum, the remaining thick light brown oil was poured with pentane (40 ml) and kept in a refrigerator at –5 °C. The formed crystalline precipitate was filtered off and dried in vacuum (3.86 g). Additional crystallization from the filtrate yielded 1.11 g compound (**3b**). Yield is 4.97 g (78 %), m. p. 145-147 °C. Mass spectrum EI: *m/z*: 536.08 [M]$^+$. Calcd 536.08. Found, %: C, 51.23; H, 3.61; P, 5.24. $C_{20}H_{15}F_6O_6P$. Calcd, %: C, 51.50; H, 3.57; P, 5.77. IRS, cm^{-1} (nujol): 1710, 1602, 1593, 1494, 1397, 1375, 1359, 1280, 1260, 1223, 1173, 1160, 1147, 1125, 1103, 1086, 1063, 1034, 1000, 986, 969, 950, 934, 921, 900, 844, 813, 799, 780, 764, 756, 746, 737, 699, 682, 663, 640, 616, 609, 589, 567, 532, 509, 476, 449, 436, 414. IRS, cm^{-1} (pellet KBr): 3066, 2940, 2868, 1710, 1602, 1494, 1453, 1397, 1359, 1280, 1260, 1225, 1218, 1172, 1161, 1150, 1126, 1103, 1087, 1064, 1034, 1000, 988, 969, 951, 933, 921, 900, 843, 831, 789, 800, 779, 764, 756, 746, 737,700, 683, 664, 640, 609, 589, 567, 531, 510, 477, 451, 436, 414. ^{1}H NMR spectrum (400 MHz, CH_2Cl_2/C_6D_6 = 1 : 1, δ ppm, *J* Hz): 7.52 br. s (H^{17}, H^{21}, 2H), 7.28 m (H$^{18\text{-}20}$, 3H), 6.93 d. d. d (H^{15}, 1H, $^3J_{HH}$ 8.0, $^4J_{HH}$ 1.4, $^4J_{POCCH}$ 1.4), 6.87 d. d. d. d (H^{14}, 1H, $^3J_{HH}$ 8.0, $^3J_{HH}$ 7.2, $^4J_{HH}$ 1.7, $^5J_{POCCCH}$ 1.7), 6.79 br. d. d (H^{13}, 1H, $^3J_{HH}$ 7.9-8.0, $^3J_{HH}$ 7.3), 6.72 d. d (H^{12}, 1H, $^3J_{HH}$ 8.0, $^4J_{HH}$ 1.7), 2.61 br. d (Cy, 1H, $^2J_{HH}$ 10.6), 1.58-1.68 m (Cy, 6H), 1.39 m (Cy, 1H), 0.89 m (Cy, 1H), 0.67 t. d (Cy, 1H, $^2J_{HH}$ 13.3-13.4, $^3J_{HH}$ 4.5). ^{1}H NMR spectrum (400 MHz, $CDCl_3$ + 40% CH_2Cl_2, δ ppm, *J* Hz): 7.72 br. s (H^{17,21}, 2H), 7.49 br. s (H$^{18\text{-}20}$, 3H), 7.13 br. d (H^{15}, 1H, $^3J_{HH}$ 8.0), 7.08 d. d. d. d (H^{14}, 1H, $^3J_{HH}$ 8.0, $^3J_{HH}$ 7.2, $^4J_{HH}$ 1.7, $^5J_{POCCCH}$ 1.7), 6.98 br. d. d (H^{13}, 1H, $^3J_{HH}$ 8.0, $^3J_{HH}$ 7.3), 6.89 d. d (H^{12}, 1H, $^3J_{HH}$ 8.0, $^4J_{HH}$ 1.6), 2.79 br. d (Cy, 1H, $^2J_{HH}$ 10.9), 1.86 and 1.78 two m (Cy, 6H), 1.62 m (Cy, 1H), 1.12 m (Cy, 1H), 0.88 t. d (Cy, 1H, $^2J_{HH}$ 13.5, $^3J_{HH}$ 4.3). ^{1}H NMR spectrum (600 MHz, $CDCl_3$, δ ppm, *J* Hz): 7.62 br. s (H^{17}, H^{21}, 2H), 7.42 m (H$^{18\text{-}20}$, 3H), 7.08 br. d (H^{15}, 1H, $^3J_{HH}$ 8.0), 7.06 br. m (H^{14}, 1H, $^3J_{HH}$ 8.0, $^3J_{HH}$ 7.2, $^6J_{PH}$ 1.5-1.6, $^4J_{HH}$ 1.6), 6.94 br. d. d (H^{13}, 1H, $^3J_{HH}$ 8.0, $^3J_{HH}$ 7.3), 6.78 d. d (H^{12}, 1H, $^3J_{HH}$ 8.0, $^4J_{HH}$ 1.6), 2.68 br. d (Cy, 1H, $^2J_{HH}$ 13.3), 1.80 m (Cy, 2H), 1.72 m (Cy, 3H), 1.62 m (Cy, 1H), 1.55 m (Cy, 1H), 1.07 m (Cy, 1H), 0.77 t. d (Cy, 1H, $^2J_{HH}$ 13.6, $^3J_{HH}$ 4.4). ^{1}H NMR spectrum (400 MHz, acetone-d_6, δ ppm, *J* Hz): 7.66 br. s (H^{17}, H^{21}, 2H), 7.49 m (H$^{18\text{-}20}$, 3H), 7.17 m (H^{15}, 1H, $^3J_{HH}$ 8.0, $^4J_{HH}$ 1.5, $^5J_{PH}$ 1.3), 7.14 d. d. d. d (H^{14}, 1H, $^3J_{HH}$ 8.0, $^3J_{HH}$ 7.2, $^5J_{PH}$ 1.5-1.6, $^4J_{HH}$ 1.5), 7.05 d. d. d. d (H^{13}, 1H, $^3J_{HH}$ 8.0, $^3J_{HH}$ 7.3, $^4J_{HH}$ 1.5, $^5J_{PH}$ 1.3), 6.90 d. d (H^{12}, 1H, $^3J_{HH}$ 8.0, $^4J_{HH}$ 1.6), 2.65 br. d (Cy, 1H, $^2J_{HH}$ 13.5), 1.81 m (Cy, 3H), 1.69 m (Cy, 2H), 1.56-1.58 m (Cy, 2H), 1.09 m (Cy, 1H, $^3J_{HH}$ 13.5, $^3J_{HH}$ 12.8, $^3J_{HH}$ 4.5), 1.07 m (Cy, 1H, $^3J_{HH}$ 13.5, $^3J_{HH}$ 12.8, $^3J_{HH}$ 4.5), 0.80 d. d. d (Cy, 1H, $^2J_{HH}$ 13.6, $^3J_{HH}$ 12.8, $^3J_{HH}$ 4.4). ^{13}C NMR spectrum (150.9 MHz, $CDCl_3$, δ_C ppm, *J* Hz): 142.0 m (d) (C^3, $^3J_{HC^{13}CC}$ 9.0, $^3J_{HC^{15}CC}$ 6.5-7.0, $^2J_{POC}$ 3.5), 147.79 m (d) (C^4, $^3J_{HC^{14}CC}$ 8.5-9.0, $^3J_{POC^3C}$ 9.7, $^3J_{HC^{12}CC}$ 6.5-7.0, $^2J_{HC^{15}C}$ 5.0), 108.11 m (d) (C^6,

$^{2}J_{POC}$ 3.2), 90.10 br. s (s) (C^{7}), 125.49 q. d. q (q. d. q) (C^{8}, $^{2}J_{FC^{10}C}$ 44.5, $^{2}J_{POC}$ 4.8, $^{3}J_{FC^{11}C^{9}C}$ 3.4), 133.69 q. d. q (q. d. q) (C^{9}, $^{2}J_{FC^{11}C}$ 43.6, $^{2}J_{POC}$ 6.4, $^{3}J_{FC^{10}C^{8}C}$ 3.0), 118.79 q. d (q. d) (C^{10}, $^{1}J_{FC}$ 270.5, $^{3}J_{POCC}$ 18.8), 118.98 q. d (q. d) (C^{11}, $^{1}J_{FC}$ 268.2, $^{3}J_{POCC}$ 19.9), 119.91 d. d. d (d) (C^{12}, $^{1}J_{HC}$ 162.8, $^{3}J_{POCC}$ 10.5, $^{3}J_{HC^{14}CC}$ 9.6), 125.67 d. d (s) (C^{13}, $^{1}J_{HC}$ 163.4, $^{3}J_{HC^{15}CC}$ 7.7-7.8), 125.62 d. d (s) (C^{14}, $^{1}J_{HC}$ 163.3, $^{3}J_{HC^{12}CC}$ 7.7-7.8), 123.75 d. d (s) (C^{15}, $^{1}J_{HC}$ 164.8, $^{3}J_{HC^{13}CC}$ 8.7), 134.36 d. d. d (d) (C^{16}, $^{3}J_{POCC}$ 14.1, $^{3}J_{HC^{18}CC}$ 6.8-7.0, $^{3}J_{HC^{20}CC}$ 6.8-7.0), 126.90 br. d. m (br. s) ($C^{17,21}$, $^{1}J_{HC}$ 159.6), 128.41 d. d (s) ($C^{18,20}$, $^{1}J_{HC}$ 160.3, $^{3}J_{HC^{20,18}CC}$ 8.2), 129.73 d. t (s) (C^{19}, $^{1}J_{HC}$ 160.3, $^{3}J_{HC^{17,21}CC}$ 7.6), 33.99 br. t. m (s) (C^{22}, $^{1}J_{HC}$ 126.5), 28.58 br. t. m (d) (C^{26}, $^{1}J_{HC}$ 127.5, $^{3}J_{POCC}$ 10.1), 24.95 br. t. m (s) (C^{23}, $^{1}J_{HC}$ 127.9), 22.26 br. t. m (s) (C^{24}, $^{1}J_{HC}$ 128.5), 21.32 br. t. m (s) (C^{25}, $^{1}J_{HC}$ 128.5). ^{13}C NMR spectrum (100.9 MHz, acetone-d_6, δ_C ppm, J Hz): 142.69 m (d) (C^{3}, $^{3}J_{HC^{13}CC}$ 9.5, $^{3}J_{HC^{15}CC}$ 6.5, $^{2}J_{HCC}$ 4.3, $^{2}J_{POC}$ 3.5, $^{4}J_{HCCCC}$ 1.3), 148.48 m (d) (C^{4}, $^{3}J_{HC^{14}CC}$ 9.8, $^{3}J_{POC^{3}C}$ 9.7, $^{3}J_{HC^{12}CC}$ 7.5, $^{2}J_{HC^{15}C}$ 3.2, $^{4}J_{HCCCC}$ 1.3), 108.30 m (d) (C^{6}, $^{2}J_{POC}$ 3.3), 91.10 m (s) (C^{7}, $^{2}J_{HCC}$ 6.5), 126.06 q. d. q (q. d. q) (C^{8}, $^{2}J_{FC^{10}C}$ 44.5, $^{2}J_{POC}$ 5.2, $^{3}J_{FC^{11}C^{9}C}$ 3.5), 134.05 q. d. q (q. d. q) (C^{9}, $^{2}J_{FC^{11}C}$ 43.3, $^{2}J_{POC}$ 6.7, $^{3}J_{FC^{10}C^{8}C}$ 3.3), 119.58 q. d. q (q. d. q) (C^{10}, $^{1}J_{FC}$ 271.0, $^{3}J_{POCC}$ 18.2, $^{3}J_{FCCC}$ 1.3), 119.75 q. d. q (q. d. q) (C^{11}, $^{1}J_{FC}$ 267.6, $^{3}J_{POCC}$ 20.2, $^{3}J_{FCCC}$ 1.5), 120.70 d. d. d. d. d (d) (C^{12}, $^{1}J_{HC}$ 163.8, $^{3}J_{POCC}$ 10.6, $^{3}J_{HC^{14}CC}$ 8.8, $^{2}J_{HCC}$ 1.3, $^{4}J_{HCCCC}$ 1.3), 125.82 d. d (s) (C^{13}, $^{1}J_{HC}$ 164.0, $^{3}J_{HC^{15}CC}$ 8.6), 126.74 br. d. d (d) (C^{14}, $^{1}J_{HC}$ 162.8, $^{3}J_{HC^{12}CC}$ 7.8, $^{5}J_{POCCCC}$ 1.3), 124.64 br. d. d (d) (C^{15}, $^{1}J_{HC}$ 163.5, $^{3}J_{HC^{13}CC}$ 9.0, $^{4}J_{POCCC}$ 1.4), 134.83 d. d. d (d) (C^{16}, $^{3}J_{POCC}$ 14.0, $^{3}J_{HC^{18}CC}$ 7.3, $^{3}J_{HC^{20}CC}$ 6.5), 127.70 br. d. d. d (s) ($C^{17,21}$, $^{1}J_{HC}$ 162.0, $^{3}J_{FCCC}$ 6.8-7.0, $^{3}J_{FCCC}$ 5.8-6.0), 129.37 d. m (s) ($C^{18,20}$, $^{1}J_{HC}$ 162.3, $^{3}J_{HC^{20,18}CC}$ 7.4-7.6), 130.68 d. t (s) (C^{19}, $^{1}J_{HC}$ 161.2, $^{3}J_{HC^{17,21}CC}$ 7.5), 34.56 br. t. m (s) (C^{22}, $^{1}J_{HC}$ 129.4), 29.15 br. t. m (d) (C^{26}, $^{1}J_{HC}$ 124.0, $^{3}J_{POCC}$ 10.2), 25.47 br. t. m (s) (C^{23}, $^{1}J_{HC}$ 127.7), 22.98 br. t. m (s) (C^{24}, $^{1}J_{HC}$ 129.3), 21.95 br. t. m (s) (C^{25}, $^{1}J_{HC}$ 129.4). ^{19}F NMR spectrum (376.5 MHz, CH_2Cl_2/C_6D_6 = 1/1, δ_F ppm, J Hz): –65.61 br. q (CF_3, 3F, $^{5}J_{FF}$ 9.4), –64.25 q. d (CF_3, 3F, $^{5}J_{FF}$ 9.4, $^{4}J_{POCCF}$ 0.9). ^{19}F NMR spectrum (376.5 MHz, $CDCl_3$, δ_F ppm, J Hz): –65.39 q (CF_3, 3F, $^{5}J_{FF}$ 9.4), –64.04 q (CF_3, 3F, $^{5}J_{FF}$ 9.4). ^{19}F NMR spectrum (376.5 MHz, acetone-d_6, δ_F ppm, J Hz): –64.63 br. q (CF_3, 3F, $^{5}J_{FF}$ 9.6), –64.04 q (CF_3, 3F, $^{5}J_{FF}$ 9.6). ^{31}P-{^{1}H} NMR spectrum (δ_P ppm): –39.4 (242.94 MHz, CH_2Cl_2/C_6D_6 = 1 : 1), –39.3 (242.94 MHz, $CDCl_3$), –39.5 (162.0 MHz, acetone-d_6).

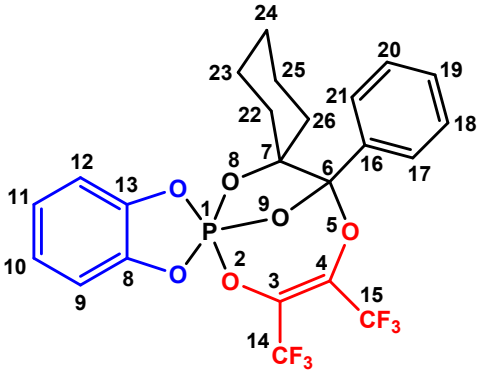

6'-Phenyl-3',4'-bis(trifluoromethyl)-2',5',8',9'-tetraoxa-2λ^{5}-phosphadispiro[benzo[d][1,3,2] dioxaphosphole-2,1'-bicyclo[4.2.1]nonane-7',1''-cyclohexan]-3'-ene (**5b**). ^{1}H NMR spectrum (400 MHz, CD_2Cl_2, 5°C, δ ppm, J Hz): 7.56 br. m ($H^{17,21}$, 2H), 7.38 br. m (H^{18-20}, 3H), 7.11 br. d (H^{12}, 1H, $^{3}J_{HH}$ 7.8), 6.99 m ($H^{8,9}$, 2H), 6.88 br. d. d (H^{11}, 1H, $^{3}J_{HH}$ 7.8, $^{3}J_{HH}$ 7.3), 2.58 br. m (Cy, 1H), 1.59-1.62 br. m (Cy, 4H), 1.43 br. m (Cy, 2H), 1.30 br. m (Cy, 1H), 0.96 br. m (Cy, 1H), 0.68 br. m (Cy, 1H). ^{13}C NMR spectrum (100.6 MHz, 5°C, CD_2Cl_2, δ_C ppm, J Hz): 145.32 m (d) (C^{13}, $^{3}J_{HC^{13}CC}$ 7.6-7.8, $^{3}J_{HC^{15}CC}$ 7.6-7.8, $^{2}J_{POC}$ 7.4), 142.25 m (d) (C^{8}, $^{3}J_{HC^{10}CC}$ 10.0, $^{2}J_{POC}$ 7.2, $^{3}J_{HC^{12}CC}$ 7.2, $^{2}J_{HC^{9}C}$ 5.0), 138.43 q. d. t (q. d. t) (C^{4}, $^{2}J_{FC^{15}C}$ 40.4, $^{3}J_{POC^{3}C}$ 15.6, $^{3}J_{FC^{14}CC}$ 3.1), 134.58 m (d) (C^{16}, $^{3}J_{POCC}$ 12.6, $^{3}J_{HC^{18,20}CC}$ 7.2, $^{4}J_{FC^{25}COC}$ 3.0-3.2), 133.34 q. d. q (q. d. q) (C^{3}, $^{2}J_{FC^{14}C}$ 40.4, $^{2}J_{POC}$ 5.5-5.6, $^{3}J_{FC^{15}C^{4}C}$ 2.5-2.6), 130.93 d. t (s) (C^{19}, $^{1}J_{HC}$ 161.7, $^{3}J_{HC^{17,21}CC}$ 7.1), 128.20 br. d. m (br. m) ($C^{18,20}$, $^{1}J_{HC}$ 162.5), 127.17 and 127.36 two br. d. m (two br. s) ($C^{17,21}$, $^{1}J_{HC}$ 161.6 and 161.8), 124.99 d. d (s) (C^{10}, $^{1}J_{HC}$ 162.9, $^{3}J_{HC^{12}CC}$ 7.6), 121.96 d. d (s) (C^{11}, $^{1}J_{HC}$ 164.8, $^{3}J_{HC^{9}CC}$ 7.0), 120.53 q (q) (C^{15}, $^{1}J_{FC}$ 274.3), 120.02 q. d (q. d) (C^{14}, $^{1}J_{FC}$ 273.0, $^{3}J_{POCC}$ 10.6), 112.77 m (d) (C^{6}, $^{2}J_{POC}$ 2.6), 89.58 s (m) (C^{7}), 111.47 d. d. d (d) (C^{12}, $^{1}J_{HC}$ 163.7, $^{3}J_{POCC}$ 16.4, $^{3}J_{HC^{10}CC}$ 8.5), 112.22 d. d. d (d) (C^{9}, $^{1}J_{HC}$ 162.6, $^{3}J_{POCC}$ 18.2, $^{3}J_{HC^{11}CC}$ 6.7), 34.97 br. t. m (s) (C^{26}, $^{1}J_{HC}$ 129.1), 29.20 br. t. m (d) (C^{22}, $^{1}J_{HC}$ 129.3, $^{3}J_{POCC}$ 9.8), 25.57 br. t. m (s) (C^{25}, $^{1}J_{HC}$ 126.0), 23.01 br. t. m (s) (C^{24}, $^{1}J_{HC}$ 126.0), 22.01 br. t. m (s) (C^{25}, $^{1}J_{HC}$ 126.7). ^{19}F NMR spectrum (376.5 MHz, 5°C, CD_2Cl_2, δ_F ppm, J Hz): –64.39 br. q (CF_3, 3F, $^{5}J_{FF}$ 11.6), –65.99 q (CF_3, 3F, $^{5}J_{FF}$ 11.6). ^{19}F NMR spectrum (376.5 MHz, 25°C, CH_2Cl_2 + 30% C_6D_6, δ_F ppm, J Hz): –64.25 q. d (CF_3, 3F, $^{5}J_{FF}$ 11.8, $^{4}J_{PF}$ 2.4), –65.68 q (CF_3, 3F, $^{5}J_{FF}$ 9.4). ^{31}P-{^{1}H}

NMR spectrum (162.0 MHz, 5°C, CD_2Cl_2, δ_P ppm): –40.7 (CD_2Cl_2). ^{31}P-{^1H} NMR spectrum (162.0 MHz, 25°C, CD_2Cl_2, δ_P ppm): –40.2. ^{31}P-{^1H} NMR spectrum (162.0 MHz, 25°C, CH_2Cl_2 + 30% C_6D_6, δ_P ppm): –40.7 q ($^4J_{FP}$ 2.3).

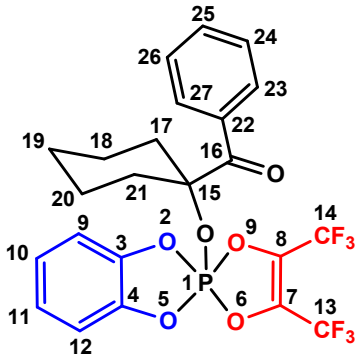

(1-((4',5'-Bis(trifluoromethyl)-2λ^5-spiro[benzo[d][1,3,2]dioxaphosphole-2,2'-[1,3,2]dioxaphosphol]-2-yl)oxy) cyclohexyl)(phenyl)methanone (**4b**). ^1H NMR spectrum (400 MHz, $CDCl_3$, 25°C, δ ppm, *J* Hz): 8.11 br. d (H^{17}, H^{23}, 2H, $^3J_{HH}$ 8.1), 7.59 br. t (H^{25}, 1H, $^3J_{HH}$ 7.5), 7.41 br. d. d ($H^{24,26}$, 2H, $^3J_{HH}$ 8.1, $^3J_{HH}$ 7.5), 6.84 m ($H^{9\text{-}12}$, 4H), 2.40 br. d (Cy, 1H, $^2J_{HH}$ 13.5), 2.07 br. m (Cy, 1H), 1.68-1.78 br. m (Cy, 8H). ^1H NMR spectrum (400 MHz, CD_2Cl_2, 5°C, δ ppm, *J* Hz): 8.01 br. d (H^{17}, H^{23}, 2H, $^3J_{HH}$ 8.1), 7.52 br. t (H^{25}, 1H, $^3J_{HH}$ 7.5), 7.33 br. d. d ($H^{24,26}$, 2H, $^3J_{HH}$ 8.1, $^3J_{HH}$ 7.5), 6.75 m ($H^{9\text{-}12}$, 4H), 2.28 br. m (Cy, 1H), 1.94 br. m (Cy, 1H), 1.68-1.70 br m (Cy, 8H). ^{13}C NMR spectrum (100.6 MHz, 5°C, CD_2Cl_2, δ_C ppm, *J* Hz): 143.80 m (d) ($C^{3,4}$, $^3J_{HCCC}$ 7.0-7.5, $^3J_{HCCC}$ 6.5-7.8, $^2J_{POC}$ 6.0), 130.40 br. q. d (br. q. d) ($C^{7,8}$, $^2J_{FC^{14}C}$ 45.2, $^2J_{POC}$ 4.0-5.0), 111.45 d. d. d (d) ($C^{9,12}$, $^1J_{HC}$ 164.2, $^3J_{POCC}$ 17.3, $^3J_{HC^{11,10}CC}$ 8.0), 122.95 d. d (br. s) ($C^{10,11}$, $^1J_{HC}$ 162.7, $^3J_{HC^{12,9}CC}$ 7.2), 119.77 br. q (br. q) ($C^{13,14}$, $^1J_{FC}$ 270.4, $^3J_{POCC}$ 19.6), 89.95 br m (br. s) (C^{15}), 203.55 br. m (br. s) (C^{16}), 35.48 br. t. m (s) ($C^{17,21}$, $^1J_{HC}$ 127.0, $^3J_{POCC}$ 8.2), 22.04 br. t. m (s) ($C^{18,20}$, $^1J_{HC}$ 128.7), 25.50 br. t. m (d) (C^{19}, $^1J_{HC}$ 127.0), 131.01 br. m (br. s) (C^{22}), 132.03 br. d. m (br. s) ($C^{23,27}$, $^1J_{HC}$ 161.7), 129.50 br. d. d (br. s) ($C^{24,26}$, $^1J_{HC}$ 165.2, $^3J_{HC^{26,24}CC}$ 7.0), 136.40 br. d. m (br. s) (C^{25}, $^1J_{HC}$ 162.5). ^{13}C NMR spectrum (150.6 MHz, 25°C, $CDCl_3$, δ_C ppm, *J* Hz): 143.07 m (d) ($C^{3,4}$, $^3J_{HCCC}$ 7.0-7.5, $^3J_{HCCC}$ 6.8-7.0, $^2J_{POC}$ 6.2), 129.49 br. q. d (br. q. d) ($C^{7,8}$, $^2J_{FC^{14}C}$ 45.4, $^2J_{POC}$ 4.5), 110.90 d. d. d (d) ($C^{9,12}$, $^1J_{HC}$ 164.9, $^3J_{POCC}$ 17.2, $^3J_{HC^{11,10}CC}$ 8.6), 122.38 d. d (s) ($C^{10,11}$, $^1J_{HC}$ 162.8, $^3J_{HC^{12,9}CC}$ 7.6), 118.96 br. q (br. q) ($C^{13,14}$, $^1J_{FC}$ 269.6, $^3J_{POCC}$ 19.4), 89.63 m (d) (C^{15}, $^2J_{POC}$ 11.7), 201.57 br. m (br. s) (C^{16}), 35.30 br. t. m (d) ($C^{17,21}$, $^1J_{HC}$ 127.0, $^3J_{POCC}$ 6.7), 21.45 br. t. m (s) ($C^{18,20}$, $^1J_{HC}$ 128.0), 24.92 br. t. m (d) (C^{19}, $^1J_{HC}$ 129.0), 130.76 m (br. s) (C^{22}, $^3J_{HCCC}$ 8.0), 131.10 d. d. d (s) ($C^{23,27}$, $^1J_{HC}$ 162.2, $^3J_{HC^{27,23}CC}$ 7.3, $^3J_{HC^{25}CC}$ 6.6), 128.70 d. d (s) ($C^{24,26}$, $^1J_{HC}$ 164.1, $^3J_{HC^{26,24}CC}$ 7.7), 135.22 d. t (s) (C^{25}, $^1J_{HC}$ 161.7, $^3J_{HCCC}$ 7.4). ^{19}F NMR spectrum (376.5 MHz, 25°C, CD_2Cl_2, δ_F ppm, *J* Hz): –66.11 br. s ($2CF_3$, 6F). ^{19}F NMR spectrum (376.5 MHz, 25°C, CH_2Cl_2 + 30% C_6D_6, δ_F ppm, *J* Hz): –64.95 d ($2CF_3$, 6F, $^4J_{PF}$ 0.9). ^{19}F NMR spectrum (376.5 MHz, 25°C, $CDCl_3$, δ_F ppm): –64.74 br. s. ^{31}P-{^1H} NMR spectrum (162.0 MHz, 25°C, CD_2Cl_2, δ_P ppm): –48.4 br. s. ^{31}P-{^1H} NMR spectrum (162.0 MHz, 5°C, CD_2Cl_2, δ_P ppm): –45.0 very br. s. ^{31}P-{^1H} NMR spectrum (162.0 MHz, 25°C, CH_2Cl_2 + 30% C_6D_6, δ_P ppm): –45.7 br. s. ^{31}P-{^1H} NMR spectrum (162.0 MHz, 25°C, $CDCl_3$, δ_P ppm): –41.7 br. s. ^{31}P-{^1H} NMR spectrum (162.0 MHz, 25°C, pentane, δ_P ppm): –32.8 br. s.

Crystallographic data for (3a) and (3b)

X-Ray Crystallography. Crystallographic data of compound (**3a**) were measured on a Bruker Kappa Apex II CCD diffractometer using graphite monochromatic MoKα (λ = 0.71073 Å) radiation and ω- and φ-scan rotation at 100 K. Crystal (**3a**) is twin. Cell parameters were determined by program CELL_NOW. Data collection images were indexed, integrated, and scaled using the APEX2 data reduction package as two component twin[1] and corrected for absorption using TWINABS-2012/1 (Bruker, 2012).[2] The structure was solved by direct methods and refined using SHELX[3] program, final refinements was made by OLEX2 programs.[4] All non-hydrogen atoms were refined anisotropically, H atoms were calculated on idealized positions and refined as riding atoms.

Crystallographic data of compound (**3b**) were measured on a XtaLAB Synergy, Single source at home/near, HyPix diffractometer (RIGAKU). The crystal was kept at 100.0(1) K during data collection using graphite monochromatic CuKα (λ = 1.54184 Å) radiation and ω- and φ-scan rotation. Using Olex2[4], the structure was solved with the ShelXT[5] structure solution program using Intrinsic Phasing and refined with the ShelXL[6] refinement package using Least Squares minimization. All non-hydrogen atoms were refined anisotropically, H atoms were calculated on idealized positions and refined as riding atoms. Crystal Data and Refinement Details are presented in Table 1. CCDC 2085033 (**3a**), 2085034 (**3b**) contain the supplementary crystallographic data for this paper. These data can be obtained free of charge via www.ccdc.cam.ac.uk/conts/retrieving.html or from the Cambridge Crystallographic Data Centre, 12 Union Road, CambridgeCB2 1EZ, UK; fax: +44) 1223-336-033; or deposit@ccdc.cam.uk).

1. APEX2 Version 2.1), SAINTPlus. Data Reduction and Correction Program Version 7.31A, Bruker Advanced X-ray Solutions, Bruker AXS Inc., Madison, Wisconsin, USA, 2006.
2. TWINABS-2012/1 (Bruker, 2012).
3. G. M. Sheldrick, *Acta Cryst.*, 2015, **A71**, 3−8
4. O. V. Dolomanov, L. J. Bourhis, R. J. Gildea, J. A. K. Howard and H. Puschmann, *J. Appl. Cryst.*, 2009, **42**, 339−341.
5. G. M. Sheldrick, *Acta Cryst*., 2008, **A64**, 112−122.
6. G. M.Sheldrick, *Acta Cryst*. 2015, **C71**, 3−8.

Table 1. Crystal Data and Refinement Details for compounds (**3a**) and (**3b**).

	3a	**3b**
Chemical formula	$C_{20}H_{15}F_6O_6P$	$C_{23}H_{19}F_6O_6P$
fw	496.29	536.35
temp.	100(2) K	100.0(2) K
radiation	MoKα, 0.71073	CuKα (λ = 1.54184)
cryst syst	Triclinic	Monoclinic
space group	P-1	I2/a
unit cell parametrs		
a (Å)	10.223(2)	10.1241(1)
b (Å)	13.603(3)	13.5556(2)
c (Å)	15.047(3)	34.2865(4)
α(deg)	104.000(7)	90
β(deg)	97.928(6)	98.111(1)
γ(deg)	90.021(7)	90
vol ($Å^3$)	2009.7(7)	4658.35(10)
Z (Z')	4 (2)	8 (1)
density (calcd) (Mg/m^3)	1.640	1.530
abs coeff (mm-1)	0.230	1.850
F(000)	1008	2192
Crystal habit, color	Prism, colorless	Plate, orange
cryst size (mm)	0.21 × 0.37 × 0.48	0.146 × 0.124 × 0.083
θ range (deg)	1.5, 28.8	2.6 to 76.46°
index ranges	–13 : 13; –18 : 17; 0 : 20	12: 12, –14 : 17, –43 : 21
reflns collected	48041	16879
Independent, observed (I≥2σ), (Rint)	16754, 10189, (0.0810)	4739, 4367, (0.0274)
data/restraints/parameters	16754/0/597	4367/0 / 272
final R indices (observed data), R1 and wR2	0.0453 and 0.1253	0.0350 and 0.0910.
R indices (all data), R1 and wR2	0.0636 and 0.1545,	0.0377 and 0.0928
goodness-of-fit on F2	1.036	1.056
largest difference peak and hole (e $Å^{-3}$)	–0.525, 0.561	–0.441, 0.494

In crystal **3a**, two independent molecules **A** and **B** were observed. Both have the same conformation and all the geometric parameters of these molecules coincide within the experimental errors, and then the averaged geometric parameters of two independent molecules are discussed below. The geometry of the molecules **3a**, **b** in the crystal is shown in fig. 1, 3. The phosphorus atom has almost undistorted trigonal-bipyramidal configuration in both molecules. The sum of the bond angles in the equatorial plane is 359.8(2)° in both molecules, the bond angle between the apical O^1 and O^9 atoms is 176.1(1)° in the molecules **3a** and 176.21(5)° in the molecule **3b**. The deviations of the phosphorus atom from the equatorial atoms plane (O^2–O^3–O^8) does not exceed 0.046 Å. The lengths of the P^1–O^1 and P^1–O^9 axial bonds in the molecules coincide within the experimental errors and are equal to 1.708(3) and 1.663(3) Å (in molecules **3a**), and 1.713(1) and 1.664(1) Å (in molecule **3b**). The lengths of the equatorial bonds are noticeably shorter and vary from 1.574(3) to 1.635(1) Å in molecules **3a** and **3b**, they are also the same within the experimental errors. Dioxaphosphole rings are planar within ±0.031(6) Å in both molecules. Dioxaphospholane heterocycle in the bicyclononane scaffold has the C^6-*envelope* conformation (the deviation of the C^6 atom from the plane of four atoms is equal to 0.605(5) Å), a seven-membered 1,3,5,2-trioxaphosphepine heterocycle has an asymmetric *boat* conformation. The fused with the benzene ring $O^2C^3C^4O^5$ fragment is planar, the P^1, C^6, and O^9 atoms deviate from this plane on one side at different distances (0.937, 1.265, and 1.846(5) Å, respectively), and the O^9 atom is most deflected. The bond lengths and bond angles are usual in molecules **3a** and **3b**.

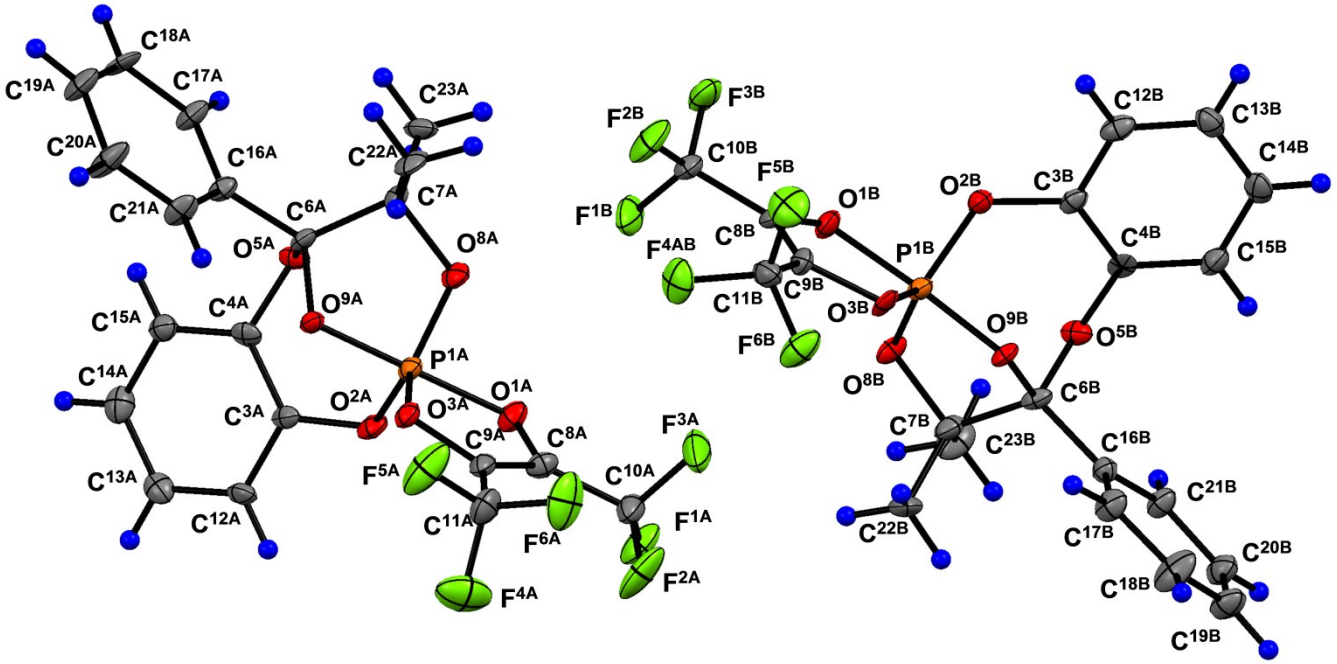

Figure 1. Independent part of the crystal (**3a**), there are two molecules **A** and **B** in the crystal cell. Non-hydrogen atoms are shown in view of thermal ellipsoids with a probability of 50%.

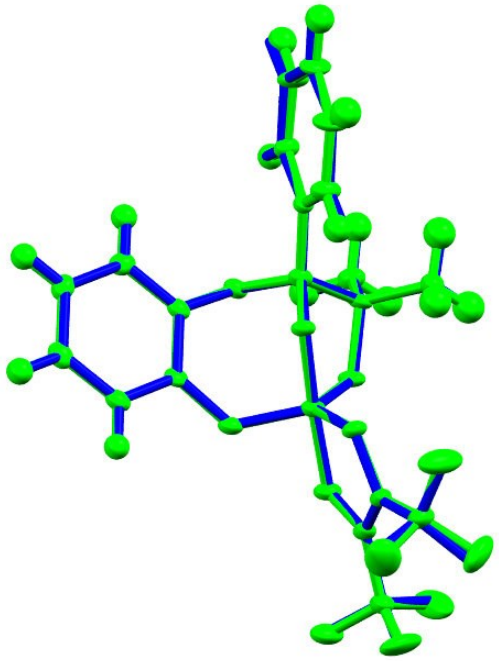

Figure 2. Overlap of independent molecules **A** and **B** of the crystal (**3a**).

Molecules (**3a**) contain two chiral centers – P^1 and C^6 atoms, and during the synthesis one could expect the formation of 4 diastereoisomers, 2 enantiomeric pairs ($P^1_S C^6_S$ / $P^1_R C^6_R$) and ($P^1_S C^6_R$ / $P^1_R C^6_S$). There are four molecules for the centrosymmetric triclinic crystal (**3a**) in the cell, and all four diastereoisomers could be obtained. However the independent molecules have the same absolute configuration $P^1_R C^6_S$ (Fig. 1) in the crystal of (**3a**), that is, one diastereoisomeric pair is realized in it. Moreover, independent molecules in the crystal have the same conformation and their geometric parameters coincide within the experimental errors. When the molecules are superimposed, they almost completely match (Fig. 2), including trifluoromethyl substituents and hydrogen atoms.

There are eight molecules in the cell of the centrosymmetric monoclinic crystal (**3b**), but the independent part of the crystal is one molecule, which has the same absolute configuration $P^1_R C^6_S$ (Fig. 3), as in crystal (**3a**), that is, the same diastereoisomeric pair. Fig. 4 demonstrates the superposition of molecules (**3a**) and (**3b**), showing almost complete coincidence of their conformations and geometric parameters, which coincide within the experimental errors.

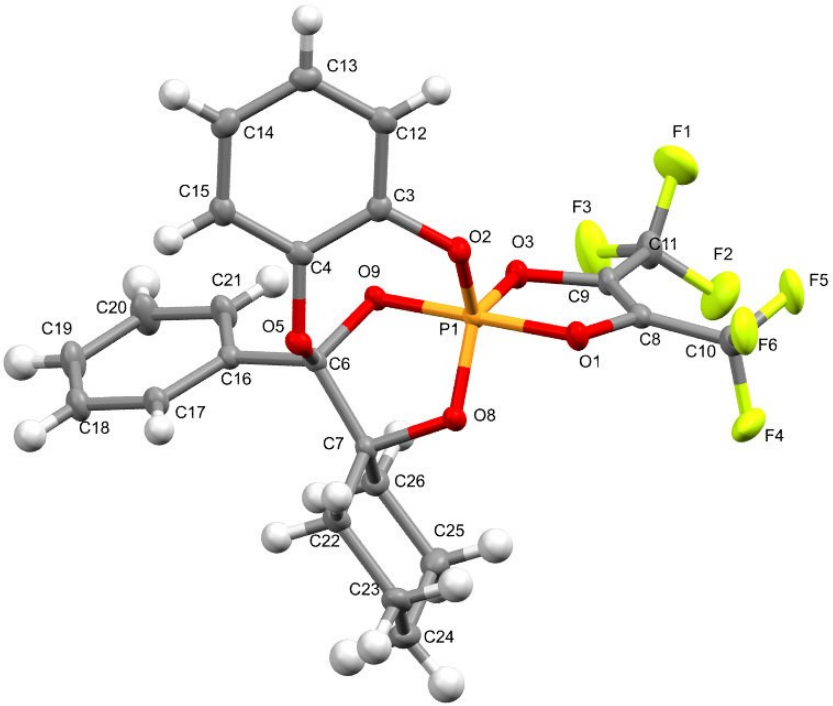

Figure 3. Molecular structure of (**3b**) and atom numbering scheme. Displacement ellipsoids are drawn at the 50% probability level.

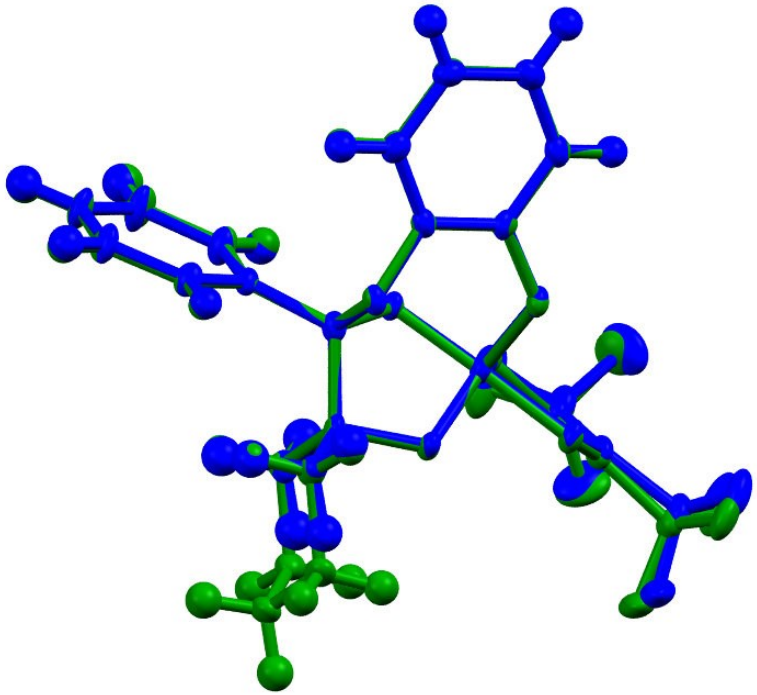

Figure 4. Overlap of molecules (**3a**) and (**3b**).

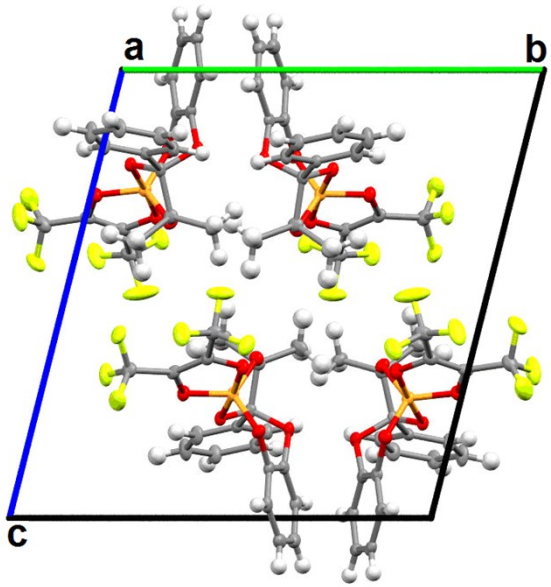

Figure 5. Crystal packing of **3a**. Projection along the ***a*** axis. Displacement ellipsoids are drawn at the 50% probability level.

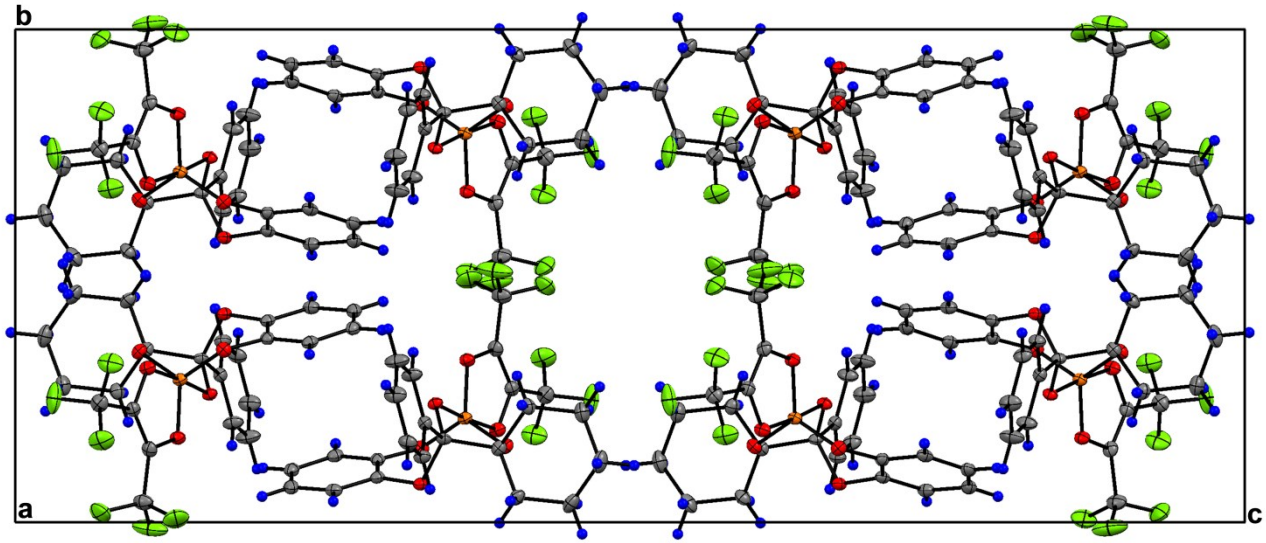

Figure 6. Crystal packing of (**3b**). Projection along the ***a*** axis. Displacement ellipsoids are drawn at the 50% probability level.

The packing of molecules in crystals (**3a**) and (**3b**) is determined by van der Waals interactions (Fig. 5 and 6). It should be noted that the packing of monoclinic crystal (**3b**) is less dense than that of crystal 3a (the calculated densities of crystals (**3a**) and (**3b**) are 1.640 and 1.530 g / cm^3). In this case, the parameters of crystal (**3b**) in the triclinic setup (a = 10.124, b = 13.556, c = 18.465 Å, α = 111.53, β = 98.23, γ = 90.00°, V = 2329 Å^3) are close to the parameters of crystal (**3a**) (a = 10.223 (2), b = 13.603 (3), c = 15.047 (3) Å, α = 104.000 (7), β = 97.928 (6), γ = 90.021 (7)°, V = 2009.7 (7) Å^3). Triclinic crystal (**3a**) does not convert to a monoclinic setup. In this regard, it can be assumed that compounds (**3a**) and (**3b**) can have both triclinic and monoclinic polymorphic modifications.

Table 2. Bond lengths and bond angles for molecule (**3a**).

bond length	***d*, Å**	**bond length**	***d*, Å**	**bond length**	***d*, Å**	**bond length**	***d*, Å**
P^{1A}–O^{1A}	1.713(6)	O^{9A}–C^{6A}	1.42(1)	F^{5A}–C^{11A}	1.32(1)	C^{7A}–C^{22A}	1.51(1)
P^{1A}–O^{2A}	1.604(6)	O^{1B}–C^{8B}	1.33(1)	F^{6A}–C^{11A}	1.32(1)	C^{8A}–C^{9A}	1.35(1)
P^{1A}–O^{3A}	1.625(6)	O^{2B}–C^{3B}	1.393(9)	F^{1B}–C^{10B}	1.32(1)	C^{8A}–C^{10A}	1.48(1)
P^{1A}–O^{8A}	1.571(6)	O^{3B}–C^{9B}	1.41(1)	F^{2B}–C^{10B}	1.33(1)	C^{9A}–C^{11A}	1.49(1)
P^{1A}–O^{9A}	1.666(6)	O^{5B}–C^{4B}	1.386(9)	F^{3B}–C^{10B}	1.32(1)	C^{12A}–C^{13A}	1.39(1)
P^{1B}–O^{3B}	1.634(6)	O^{5B}–C^{6B}	1.45(1)	F^{4B}–C^{11B}	1.33(1)	C^{13A}–C^{14A}	1.40(1)
P^{1B}–O^{1B}	1.712(6)	O^{8B}–C^{7B}	1.47(1)	F^{5B}–C^{11B}	1.33(1)	C^{14A}–C^{15A}	1.38(1)
P^{1B}–O^{2B}	1.599(6)	O^{9B}–C^{6B}	1.41(1)	F^{6B}–C^{11B}	1.34(1)	C^{16A}–C^{21A}	1.39(1)
P^{1B}–O^{8B}	1.584(6)	C^{3A}–C^{4A}	1.40(1)	O^{1A}–C^{8A}	1.35(1)	C^{16A}–C^{17A}	1.39(1)
P^{1B}–O^{9B}	1.650(6)	C^{3A}–C^{12A}	1.37(1)	O^{2A}–C^{3A}	1.40(1)	C^{17A}–C^{18A}	1.39(1)
F^{1A}–C^{10A}	1.32(1)	C^{4A}–C^{15A}	1.38(1)	O^{3A}–C^{9A}	1.38(1)	C^{18A}–C^{19A}	1.37(1)
F^{2A}–C^{10A}	1.32(1)	C^{6A}–C^{16A}	1.51(1)	O^{5A}–C^{6A}	1.437(1)	C^{19A}–C^{20A}	1.39(1)
F^{3A}–C^{10A}	1.32(1)	C^{6A}–C^{7A}	1.52(1)	O^{5A}–C^{4A}	1.386(9)	C^{20A}–C^{21A}	1.38(1)
F^{4A}–C^{11A}	1.34(1)	C^{7A}–C^{23A}	1.51(1)	O^{8A}–C^{7A}	1.473(9		
bond angle	**φ, deg.**	**bond angle**	**φ, deg.**	**bond angle**	**φ, deg.**	**bond angle**	**φ, deg.**
O^{1A}–P^{1A}–O^{2A}	87.0(3)	P^{1B}–O^{3B}–C^{9B}	112.9(5)	O^{2B}–P^{1B}–O^{8B}	120.3(3)	C^{7A}–C^{6A}–C^{16A}	118.1(6)
O^{1A}–P^{1A}–O^{3A}	90.4(3)	C^{4B}–O^{5B}–C^{6B}	113.1(6)	O^{2B}–P^{1B}–O^{9B}	95.6(3)	O^{5A}–C^{6A}–C^{16A}	110.4(6)
O^{1A}–P^{1A}–O^{8A}	87.6(3)	P^{1B}–O^{8B}–C^{7B}	115.4(5)	O^{1B}–P^{1B}–O^{2B}	87.7(3)	O^{8A}–C^{7A}–C^{22A}	107.1(6)
O^{1A}–P^{1A}–O^{9A}	176.4(3)	P^{1B}–O^{9B}–C^{6B}	110.1(5)	O^{1B}–P^{1B}–O^{3B}	90.2(3)	O^{8A}–C^{7A}–C^{23A}	108.1(6)
O^{2A}–P^{1A}–O^{3A}	116.6(3)	O^{2A}–C^{3A}–C^{12A}	117.1(7)	O^{3B}–P^{1B}–O^{9B}	86.6(3)	O^{8A}–C^{7A}–C^{6A}	101.5(6)
O^{2A}–P^{1A}–O^{8A}	120.1(3)	C^{4A}–C^{3A}–C^{12A}	119.9(8)	O^{3B}–P^{1B}–O^{8B}	124.2(3)	C^{22A}–C^{7A}–C^{23A}	112.0(7)
O^{2A}–P^{1A}–O^{9A}	96.0(3)	O^{2A}–C^{3A}–C^{4A}	122.9(7)	P^{1A}–O^{1A}–C^{8A}	111.9(5)	C^{6A}–C^{7A}–C^{22A}	112.7(7)
O^{3A}–P^{1A}–O^{8A}	123.1(3)	O^{5A}–C^{4A}–C^{3A}	118.6(7)	P^{1A}–O^{2A}–C^{3A}	123.9(5)	C^{6A}–C^{7A}–C^{23A}	114.6(7)
O^{3A}–P^{1A}–O^{9A}	86.3(3)	O^{5A}–C^{4A}–C^{15A}	120.5(7)	P^{1A}–O^{3A}–C^{9A}	113.6(5)	C^{9A}–C^{8A}–C^{10A}	131.2(8)
O^{8A}–P^{1A}–O^{9A}	92.7(3)	C^{3A}–C^{4A}–C^{15A}	120.8(7)	C^{4A}–O^{5A}–C^{6A}	115.4(6)	O^{1A}–C^{8A}–C^{9A}	112.2(7)
O^{8B}–P^{1B}–O^{9B}	92.4(3)	O^{5A}–C^{6A}–O^{9A}	108.3(6)	P^{1A}–O^{8A}–C^{7A}	115.2(5)	O^{1A}–C^{8A}–C^{10A}	116.6(8)
O^{1B}–P^{1B}–O^{8B}	87.6(3)	O^{5A}–C^{6A}–C^{7A}	106.4(6)	P^{1A}–O^{9A}–C^{6A}	108.9(5)	O^{3A}–C^{9A}–C^{8A}	111.9(8)
O^{1B}–P^{1B}–O^{9B}	176.2(3)	O^{9A}–C^{6A}–C^{7A}	102.8(6)	P^{1B}–O^{1B}–C^{8B}	112.1(5)	O^{3A}–C^{9A}–C^{11A}	115.8(7)
O^{2B}–P^{1B}–O^{3B}	115.3(3)	O^{9A}–C^{6A}–C^{16A}	110.2(6)	P^{1B}–O^{2B}–C^{3B}	124.7(5)	C^{8A}–C^{9A}–C^{11A}	132.3(8)

Table 3. Torsion bond angles for molecule (**3a**).

torsion angle	τ, deg.	torsion angle	τ, deg.	torsion angle	τ, deg.	torsion angle	τ, deg.
O^{2A}–P^{1A}–O^{1A}–C^{8A}	–118.0(6)	C^{10B}–C^{8B}–C^{9B}–O^{3B}	177.2(7)	P^{1A}–O^{8A}–C^{7A}–C^{6A}	–22.8(7)	C^{7A}–C^{6A}–C^{16A}–C^{21A}	–73.6(7)
O^{3A}–P^{1A}–O^{1A}–C^{8A}	–1.4(6)	O^{1B}–C^{8B}–C^{9B}–O^{3B}	1.2(9)	P^{1A}–O^{8A}–C^{7A}–C^{22A}	95.5(6)	O^{5A}–C^{6A}–C^{7A}–O^{8A}	172.1(6)
O^{8A}–P^{1A}–O^{1A}–C^{8A}	121.7(6)	O^{1B}–C^{8B}–C^{9B}–C^{11B}	179.1(8)	P^{1A}–O^{9A}–C^{6A}–C^{16A}	–171.0(5)	O^{5A}–C^{6A}–C^{7A}–C^{22A}	75(1)
O^{1A}–P^{1A}–O^{2A}–C^{3A}	–172.2(6)	O^{1B}–P^{1B}–$O^{2B}C^{3B}$	–172.8(6)	P^{1A}–O^{9A}–C^{6A}–O^{5A}	68.2(6)	C^{7A}–C^{6A}–C^{16A}–C^{17A}	48(1)
O^{3A}–P^{1A}–O^{2A}–C^{3A}	98.9(6)	O^{3B}–P^{1B}–O^{2B}–C^{3B}	98.0(6)	P^{1A}–O^{9A}–C^{6A}–C^{7A}	–44.2(6)	C^{16A}–C^{6A}–C^{7A}–C^{22A}	17(1)
O^{8A}–P^{1A}–O^{2A}–C^{3A}	–86.7(7)	O^{8B}–P^{1B}–O^{2B}–C^{3B}	–86.8(7)	P^{1B}–O^{1B}–C^{8B}–C^{9B}	0.2(8)	O^{9A}–C^{6A}–C^{16A}–C^{21A}	40.1(7)
O^{9A}–P^{1A}–O^{2A}–C^{3A}	10.0(6)	O^{9B}–P^{1B}–O^{2B}–C^{3B}	9.2(6)	P^{1B}–O^{1B}–C^{8B}–C^{10B}	–176.5(5)	O^{9A}–C^{6A}–C^{7A}–O^{8A}	–74.1(7)
O^{1A}–P^{1A}–O^{3A}–C^{9A}	1.1(5)	O^{1B}–P^{1B}–O^{3B}–C^{9B}	1.9(5)	P^{1B}–O^{2B}–C^{3B}–C^{4B}	43(1)	O^{9A}–C^{6A}–C^{7A}–C^{22A}	–82.1(9)
O^{2A}–P^{1A}–O^{3A}–C^{9A}	87.9(6)	O^{2B}–P^{1B}–O^{3B}–C^{9B}	89.5(5)	P^{1B}–O^{2B}–C^{3B}–C^{12B}	–141.4(6)	C^{16A}–C^{6A}–C^{7A}–C^{23A}	156.3(6)
O^{8A}–P^{1A}–O^{3A}–C^{9A}	–86.3(6)	O^{8B}–P^{1B}–O^{3B}–C^{9B}	–85.4(6)	P^{1B}–O^{3B}–C^{9B}–C^{8B}	–2.2(8)	O^{9A}–C^{6A}–C^{7A}–C^{23A}	161.7(7)
O^{9A}–P^{1A}–O^{3A}–C^{9A}	–177.2(5)	O^{9B}–P^{1B}–O^{3B}–C^{9B}	–176.0(5)	P^{1B}–O^{3B}–C^{9B}–C^{11B}	179.5(5)	C^{16A}–C^{6A}–C^{7A}–O^{8A}	–178.3(8)
O^{1A}–P^{1A}–O^{8A}–C^{7A}	–177.8(5)	O^{8B}–P^{1B}–O^{9B}–C^{6B}	28.5(5)	C^{4B}–O^{5B}–C^{6B}–O^{9B}	36.9(8)	O^{1A}–C^{8A}–C^{9A}–C^{11A}	–3(1)
O^{2A}–P^{1A}–O^{8A}–C^{7A}	97.1(5)	O^{2B}–P^{1B}–O^{9B}–C^{6B}	–92.2(5)	C^{6B}–O^{5B}–C^{4B}–C^{15B}	110.1(8)	C^{3B}–C^{4B}–C^{15B}–C^{14B}	50(1)
O^{3A}–P^{1A}–O^{8A}–C^{7A}	–88.8(6)	O^{3B}–P^{1B}–O^{9B}–C^{6B}	152.7(5)	C^{4B}–O^{5B}–C^{6B}–C^{16B}	–85.9(8)	C^{16B}–C^{6B}–C^{7B}–C^{22B}	154.6(7)
O^{9A}–P^{1A}–O^{8A}–C^{7A}	–1.4(5)	P^{1A}–O^{1A}–C^{8A}–C^{10A}	–179.4(6)	C^{6B}–O^{5B}–C^{4B}–C^{3B}	–73.9(9)	O^{9B}–C^{6B}–C^{7B}–C^{23B}	162.5(7)
O^{2A}–P^{1A}–O^{9A}–C^{6A}	–92.6(5)	P^{1A}–O^{1A}–C^{8A}–C^{9A}	1.3(9)	C^{4B}–O^{5B}–C^{6B}–C^{7B}	146.3(6)	C^{16B}–C^{6B}–C^{7B}–O^{8B}	–41.5(10)
O^{3A}–P^{1A}–O^{9A}–C^{6A}	151.1(5)	P^{1A}–O^{2A}–C^{3A}–C^{4A}	43.3(11)	P^{1B}–O^{8B}–C^{7B}–C^{23B}	–143.6(6)	O^{5B}–C^{6B}–C^{16B}–C^{21B}	19.2(11)
O^{8A}–P^{1A}–O^{9A}–C^{6A}	28.1(5)	P^{1A}–O^{2A}–C^{3A}–C^{12A}	–141.4(6)	P^{1B}–O^{8B}–C^{7B}–C^{6B}	–21.3(8)	O^{9B}–C^{6B}–C^{16B}–C^{17B}	–162.1(7)
O^{1B}–P^{1B}–O^{8B}–C^{7B}	–178.4(6)	P^{1A}–O^{3A}–C^{9A}–C^{8A}	–0.6(8)	P^{1B}–O^{8B}–C^{7B}–C^{22B}	95.2(7)	O^{9B}–C^{6B}–C^{16B}–C^{21B}	–99.9(9)
O^{2B}–P^{1B}–O^{8B}–C^{7B}	95.6(6)	P^{1A}–O^{3A}–C^{9A}–C^{11A}	177.6(6)	P^{1B}–O^{9B}–C^{6B}–C^{16B}	–171.5(5)	C^{7B}–C^{6B}–C^{16B}–C^{17B}	78.8(10)
O^{3B}–P^{1B}–O^{8B}–C^{7B}	–89.7(6)	C^{4A}–O^{5A}–C^{6A}–C^{16A}	–85.3(7)	P^{1B}–O^{9B}–C^{6B}–C^{7B}	–43.8(7)	C^{7B}–C^{6B}–C^{16B}–C^{21B}	–82(1)
O^{9B}–P^{1B}–O^{8B}–C^{7B}	–2.2(6)	C^{6A}–O^{5A}–C^{4A}–C^{3A}	–72.0(9)	P^{1B}–O^{9B}–C^{6B}–O^{5B}	67.0(7)	C^{16B}–C^{6B}–C^{7B}–C^{23B}	139.8(7)
O^{2B}–P^{1B}–O^{1B}–C^{8B}	–116.6(5)	C^{4A}–O^{5A}–C^{6A}–C^{7A}	145.4(6)	O^{9A}–C^{6A}–C^{16A}–C^{17A}	–166.9(7)	O^{5B}–C^{6B}–C^{16B}–C^{17B}	41.3(9)
O^{3B}–P^{1B}–O^{1B}–C^{8B}	–1.2(5)	C^{4A}–O^{5A}–C^{6A}–O^{9A}	35.4(8)	O^{5A}–C^{6A}–C^{16A}–C^{17A}	–47.4(9)	O^{5B}–C^{6B}–C^{7B}–C^{23B}	38.6(8)
O^{8B}–P^{1B}–$O^{1B}C^{8B}$	123.0(5)	C^{6A}–O^{5A}–C^{4A}–C^{15A}	111.3(8)	O^{5A}–C^{6A}–C^{16A}–C^{21A}	136.4(7)	O^{9B}–C^{6B}–C^{7B}–O^{8B}	–74.1(8)
O^{5B}–C^{6B}–C^{7B}–O^{8B}	–74.7(7)	P^{1A}–O^{8A}–C^{7A}–C^{23A}	–143.7(5)	O^{5A}–C^{6A}–C^{7A}–C^{23A}	42.6(8)	O^{9B}–C^{6B}–C^{7B}–C^{22B}	–100.9(9)

Table 4. Bond lengths and bond angles for molecule (**3b**).

bond length	***d*, Å**	**bond length**	***d*, Å**	**bond length**	***d*, Å**	**bond length**	***d*, Å**
P^1–O^1	1.713(1)	F^4–C^{10}	1.328(2)	O^8–C^7	1.477(2)	C^{18}–C^{19}	1.381(2)
P^1–O^2	1.602(1)	F^5–C^{10}	1.323(2)	O^9–C^6	1.407(2)	C^{19}–C^{20}	1.386(2)
P^1–O^3	1.635(1)	F^6–C^{10}	1.334(2)	C^{12}–C^{13}	1.391(2)	C^{20}–C^{21}	1.393(2)
P^1–O^8	1.585(1)	O^1–C^8	1.345(2)	C^{13}–C^{14}	1.387(2)	C^{22}–C^{23}	1.531(2)
P^1–O^9	1.664(1)	O^2–C^3	1.405(2)	C^{14}–C^{15}	1.389(2)	C^{23}–C^{24}	1.529(2)
F^1–C^{11}	1.345(2)	O^3–C^9	1.387(2)	C^{16}–C^{17}	1.393(2)	C^{24}–C^{25}	1.528(2)
F^2–C^{11}	1.320(2)	O^5–C^4	1.381(2)	C^{16}–C^{21}	1.392(2)	C^{25}–C^{26}	1.528(2)
F^3–C^{11}	1.316(2)	O^5–C^6	1.450(2)	C^{17}–C^{18}	1.392(2)		
bond angle	**φ, deg.**	**bond angle**	**φ, deg.**	**bond angle**	**φ, deg.**	**bond angle**	**φ, deg.**
O^1–P^1–O^2	87.55(5)	P^1–O^8–C^7	115.23(8)	O^8–C^7–C^6	101.1(1)	F^4–C^{10}–C^8	111.1(1)
O^1–P^1–O^3	89.88(5)	P^1–O^9–C^6	109.46(8)	O^8–C^7–C^{22}	107.1(1)	F^5–C^{10}–F^6	107.6(1)
O^1–P^1–O^8	87.66(6)	O^2–C^3–C^4	121.2(1)	O^8–C^7–C^{26}	107.6(1)	F^5–C^{10}–C^8	112.0(1)
O^1–P^1–O^9	176.21(5)	O^2–C^3–C^{12}	117.7(1)	C^6–C^7–C^{22}	116.4(1)	F^6–C^{10}–C^8	110.6(1)
O^2–P^1–O^3	116.90(6)	C^4–C^3–C^{12}	121.0(1)	C^6–C^7–C^{26}	111.5(1)	F^1–C^{11}–F^2	106.0(1)
O^2–P^1–O^8	119.55(5)	O^5–C^4–C^3	119.8(1)	C^{22}–C^7–C^{26}	112.2(1)	F^1–C^{11}–F^3	105.7(1)
O^2–P^1–O^9	95.58(6)	O^5–C^4–C^{15}	120.4(1)	O^1–C^8–C^9	113.4(1)	F^1–C^{11}–C^9	111.8(1)
O^3–P^1–O^8	123.31(6)	C^3–C^4–C^{15}	119.7(1)	O^1–C^8–C^{10}	115.5(1)	F^2–C^{11}–F^3	109.6(1)
O^3–P^1–O^9	86.80(5)	O^5–C^6–O^9	108.7(1)	C^9–C^8–C^{10}	131.1(1)	F^2–C^{11}–C^9	112.1(1)
O^8–P^1–O^9	92.63(5)	O^5–C^6–C^7	106.0(1)	O^3–C^9–C^8	111.4(1)	F^3–C^{11}–C^9	111.2(1)
P^1–O^1–C^8	111.58(9)	O^5–C^6–C^{16}	110.5(1)	O^3–C^9–C^{11}	115.2(1)	C^3–C^{12}–C^{13}	119.1(1)
P^1–O^2–C^3	124.66(9)	O^9–C^6–C^7	103.2(1)	C^8–C^9–C^{11}	133.5(1)	C^{12}–C^{13}–C^{14}	120.2(1)
P^1–O^3–C^9	113.51(9)	O^9–C^6–C^{16}	111.4(1)	F^4–C^{10}–F^5	108.3(1)	C^{13}–C^{14}–C^{15}	120.5(1)
C^4–O^5–C^6	113.7(1)	C^7–C^6–C^{16}	116.7(1)	F^4–C^{10}–F^6	106.9(1)	C^4–C^{15}–C^{14}	119.5(1)

Table 5. Torsion angles for molecule (**3b**).

torsion angle	τ, deg.	torsion angle	τ, deg.	torsion angle	τ, deg.	torsion angle	τ, deg.
O^2–P^1–O^1–C^8	–121.95(9)	O^2–P^1–O^9–C^6	–91.55(9)	P^1–O^8–C^7–C^{22}	–144.02(9)	O^5–C^6–C^{16}–C^{17}	–47.6(2)
O^3–P^1–O^1–C^8	–5.0(1)	O^3–P^1–O^9–C^6	151.72(9)	P^1–O^8–C^7–C^{26}	95.2(1)	O^5–C^6–C^{16}–C^{21}	134.8(1)
O^8–P^1–O^1–C^8	118.33(9)	O^8–P^1–O^9–C^6	28.49(9)	P^1–O^9–C^6–O^5	68.1(1)	O^9–C^6–C^{16}–C^{17}	–168.42(12)
O^1–P^1–O^2–C^3	–174.6(1)	P^1–O^1–C^8–C^9	3.8(2)	P^1–O^9–C^6–C^7	–44.1(1)	O^9–C^6–C^{16}–C^{21}	13.9(2)
O^3–P^1–O^2–C^3	96.8(1)	P^1–O^1–C^8–C^{10}	–173.1(1)	P^1–O^9–C^6–C^{16}	–170.03(9)	C^7–C^6–C^{16}–C^{17}	73.5(2)
O^8–P^1–O^2–C^3	–88.7(1)	P^1–O^2–C^3–C^4	45.0(2)	O^2–C^3–C^4–O^5	0.3(2)	C^7–C^6–C^{16}–C^{21}	–104.2(2)
O^9–P^1–O^2–C^3	7.6(1)	P^1–O^2–C^3–C^{12}	–138.9(1)	O^5–C^6–C^7–O^8	–74.8(1)	O^8–C^7–C^{22}–C^{23}	–63.8(1)
O^1–P^1–O^3–C^9	5.0(1)	P^1–O^3–C^9–C^8	–3.9(2)	O^5–C^6–C^7–C^{22}	40.8(2)	C^6–C^7–C^{22}–C^{23}	–175.7(1)
O^2–P^1–O^3–C^9	92.2(1)	P^1–O^3–C^9–C^{11}	175.6(1)	O^5–C^6–C^7–C^{26}	171.2(1)	C^{26}–C^7–C^{22}–C^{23}	54.1(2)
O^8–P^1–O^3–C^9	–82.1(1)	C^6–O^5–C^4–C^3	–72.8(2)	O^9–C^6–C^7–O^8	39.4(1)	O^8–C^7–C^{26}–C^{25}	63.4(1)
O^9–P^1–O^3–C^9	–173.1(1)	C^6–O^5–C^4–C^{15}	110.6(1)	O^9–C^6–C^7–C^{22}	154.9(1)	C^6–C^7–C^{26}–C^{25}	173.3(1)
O^1–P^1–O^8–C^7	–178.05(9)	C^4–O^5–C^6–O^9	35.52(14)	O^9–C^6–C^7–C^{26}	–74.7(1)	C^{22}–C^7–C^{26}–C^{25}	–54.2(2)
O^2–P^1–O^8–C^7	96.10(9)	C^4–O^5–C^6–C^7	145.8(1)	C^{16}–C^6–C^7–O^8	161.8(1)	O^1–C^8–C^9–O^3	–0.1(2)
O^3–P^1–O^8–C^7	–89.7(1)	C^4–O^5–C^6–C^{16}	–86.9(1)	C^{16}–C^6–C^7–C^{22}	–82.7(2)	O^1–C^8–C^9–C^{11}	–179.4(2)
O^9–P^1–O^8–C^7	–1.83(9)	P^1–O^8–C^7–C^6	–21.8(1)	C^{16}–C^6–C^7–C^{26}	47.7(2)		

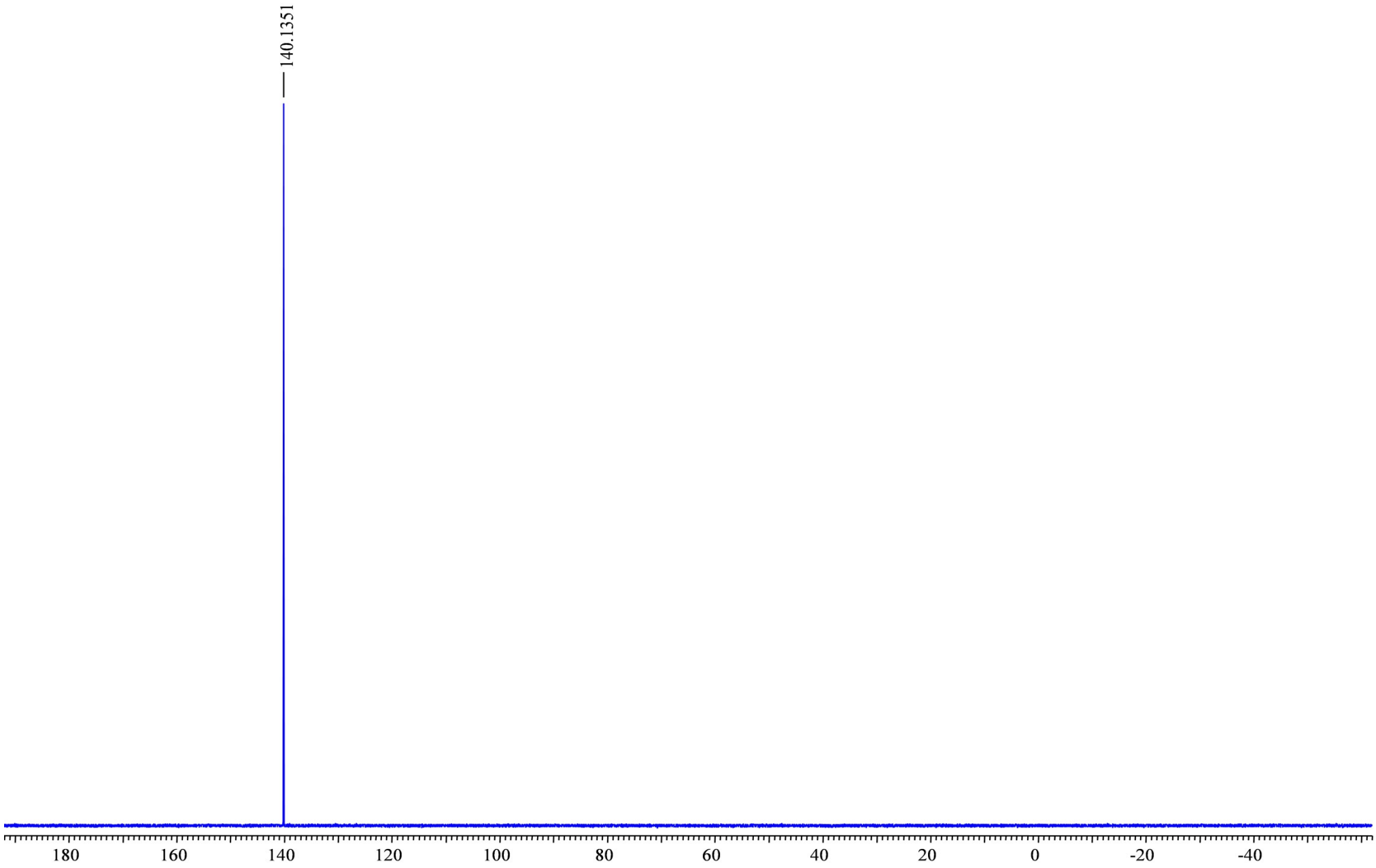

Figure 7. ^{31}P-{^{1}H} NMR spectrum (242.94 MHz, $CDCl_3$) of the initial phosphole (**1a**).

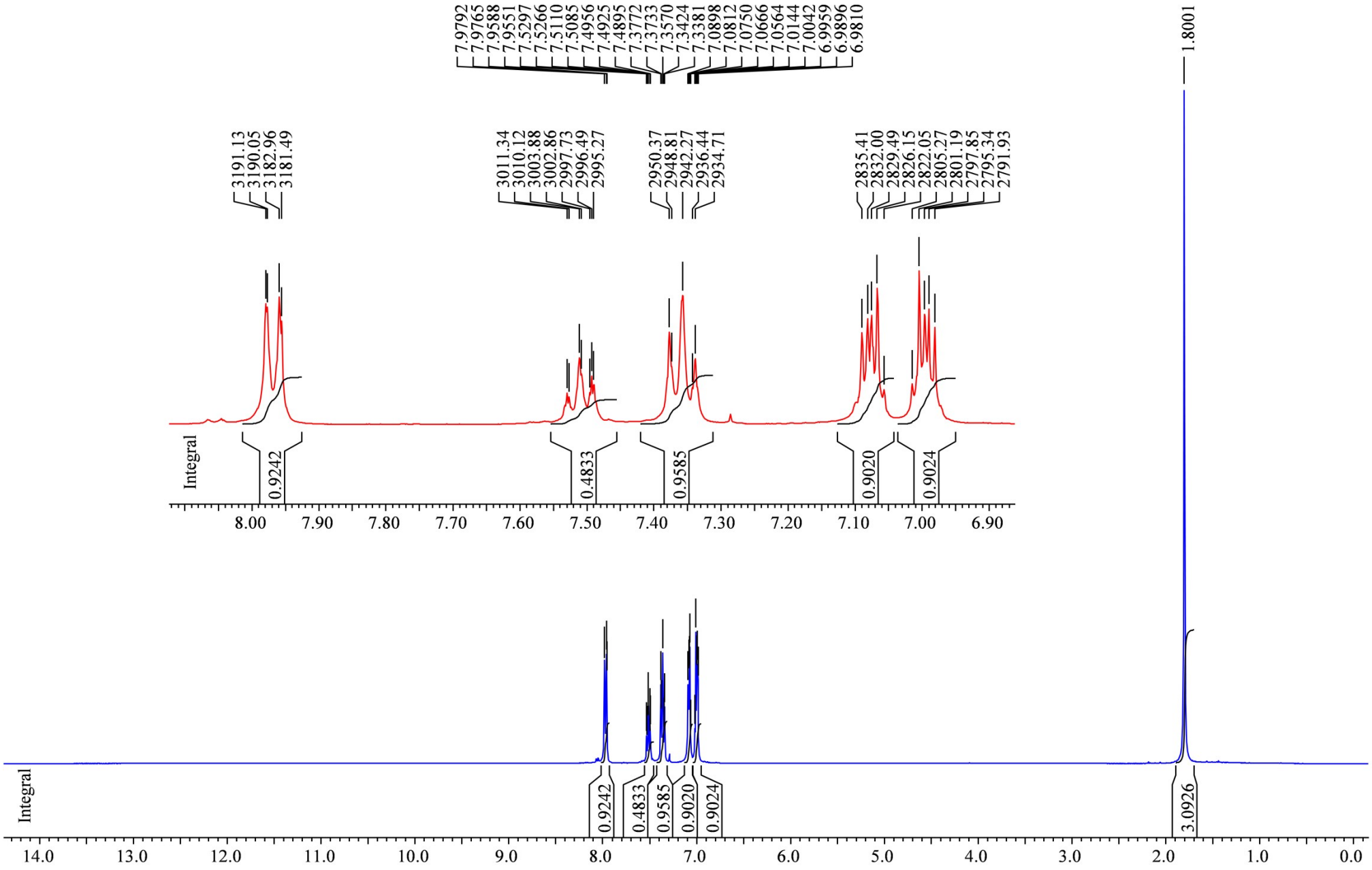

Figure 8. ^{1}H NMR spectrum (400.0 MHz, $CDCl_3$) of the initial phosphole (**1a**).

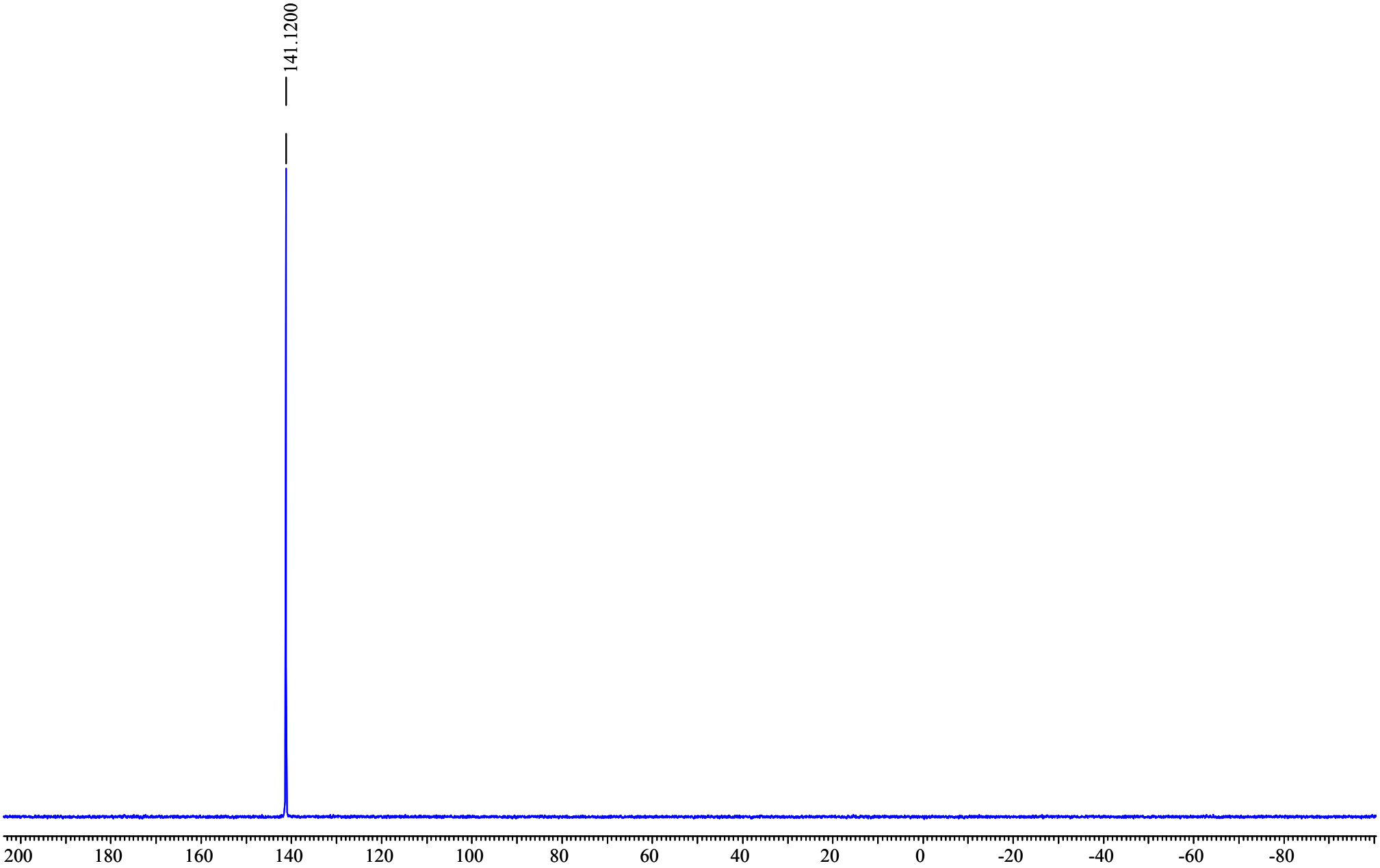

Figure 9. ^{31}P-{^{1}H} NMR spectrum (162.0 MHz, $CDCl_3$) of the initial phosphole (**1b**).

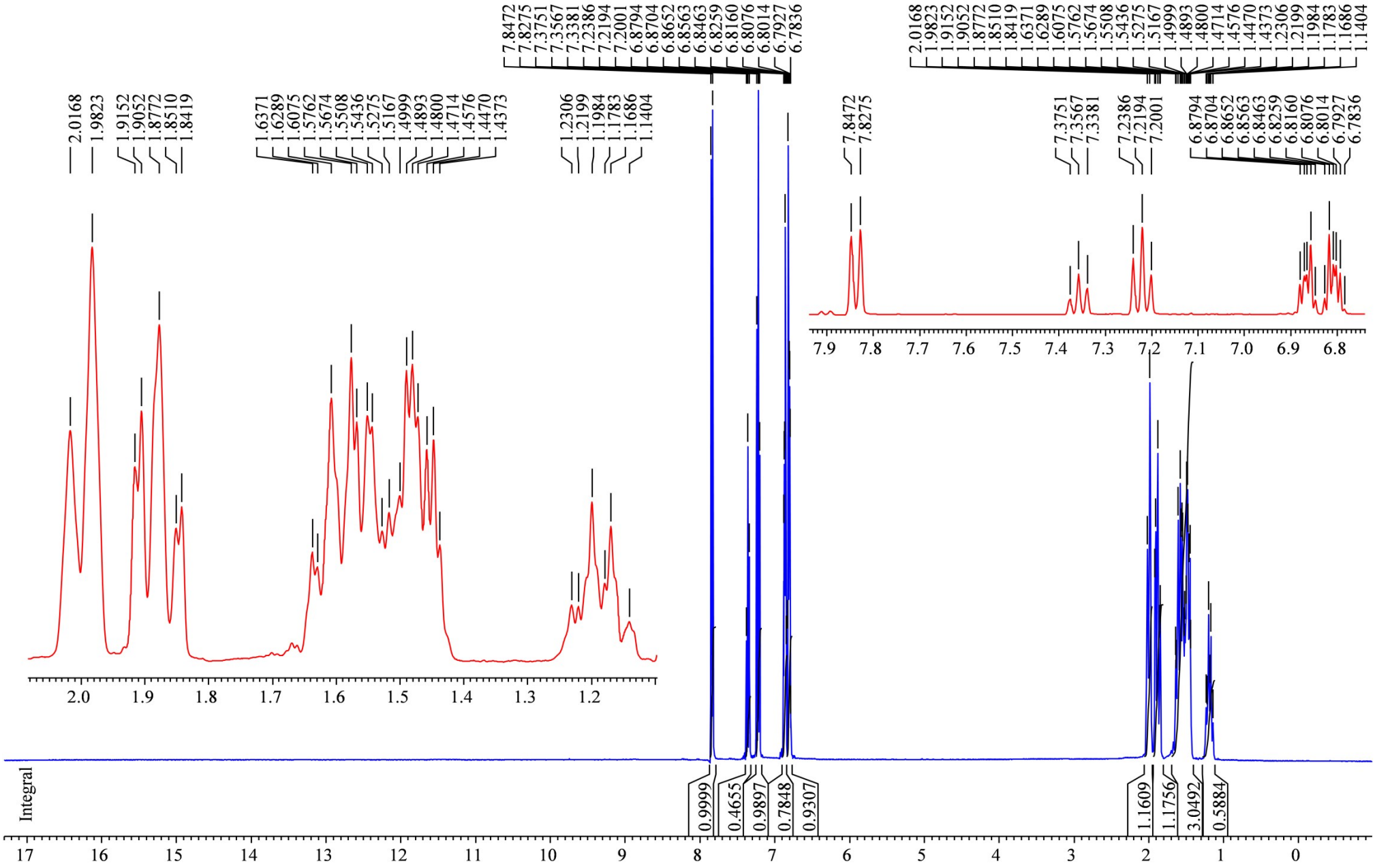

Figure 10. ^{1}H NMR spectrum (400.0 MHz, $CDCl_3$) of the initial phosphole (**1b**).

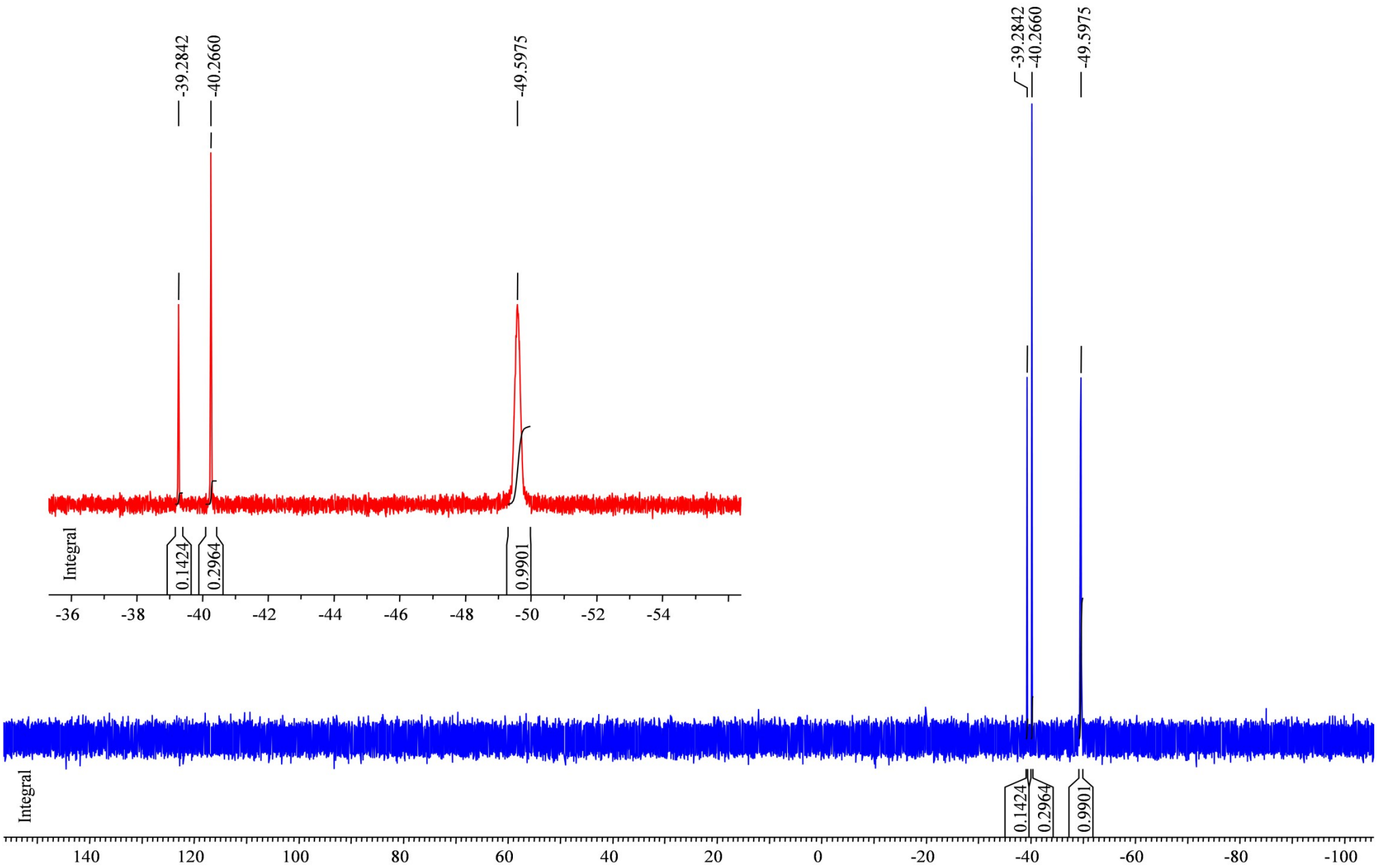

Figure 11. ^{31}P-{^{1}H} NMR spectrum (242.94 MHz, CH_2Cl_2) of the phosphole (**1a**) and perfluorodiacetyl reaction mixture after 2 h (compounds **3a-5a**).

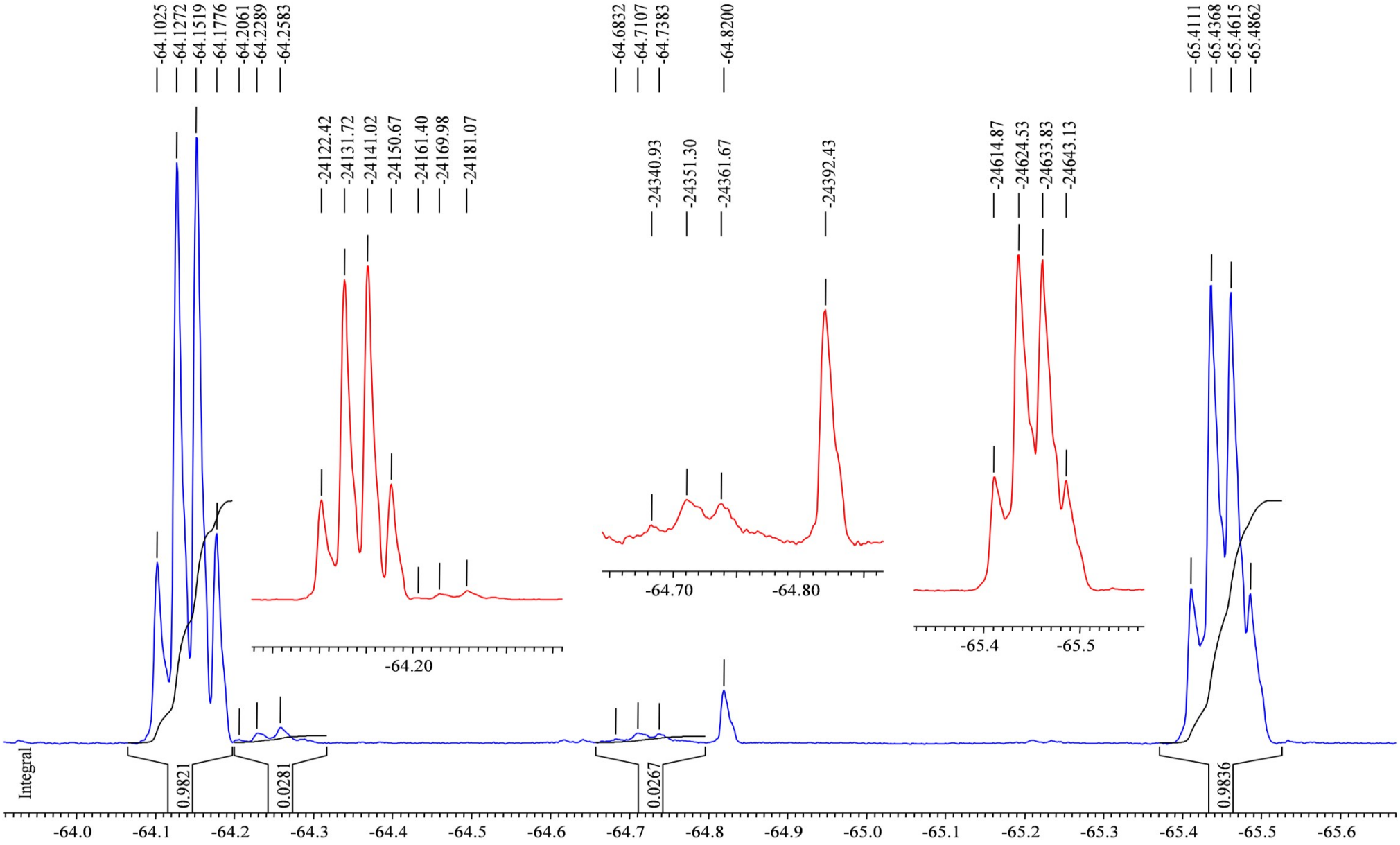

Figure 12. ^{19}F-{^{1}H} NMR spectrum (376.5 MHz, $CH_2Cl_2/CDCl_3$ = 1/2) of the phosphole (**1a**) and perfluorodiacetyl reaction mixture the next day.

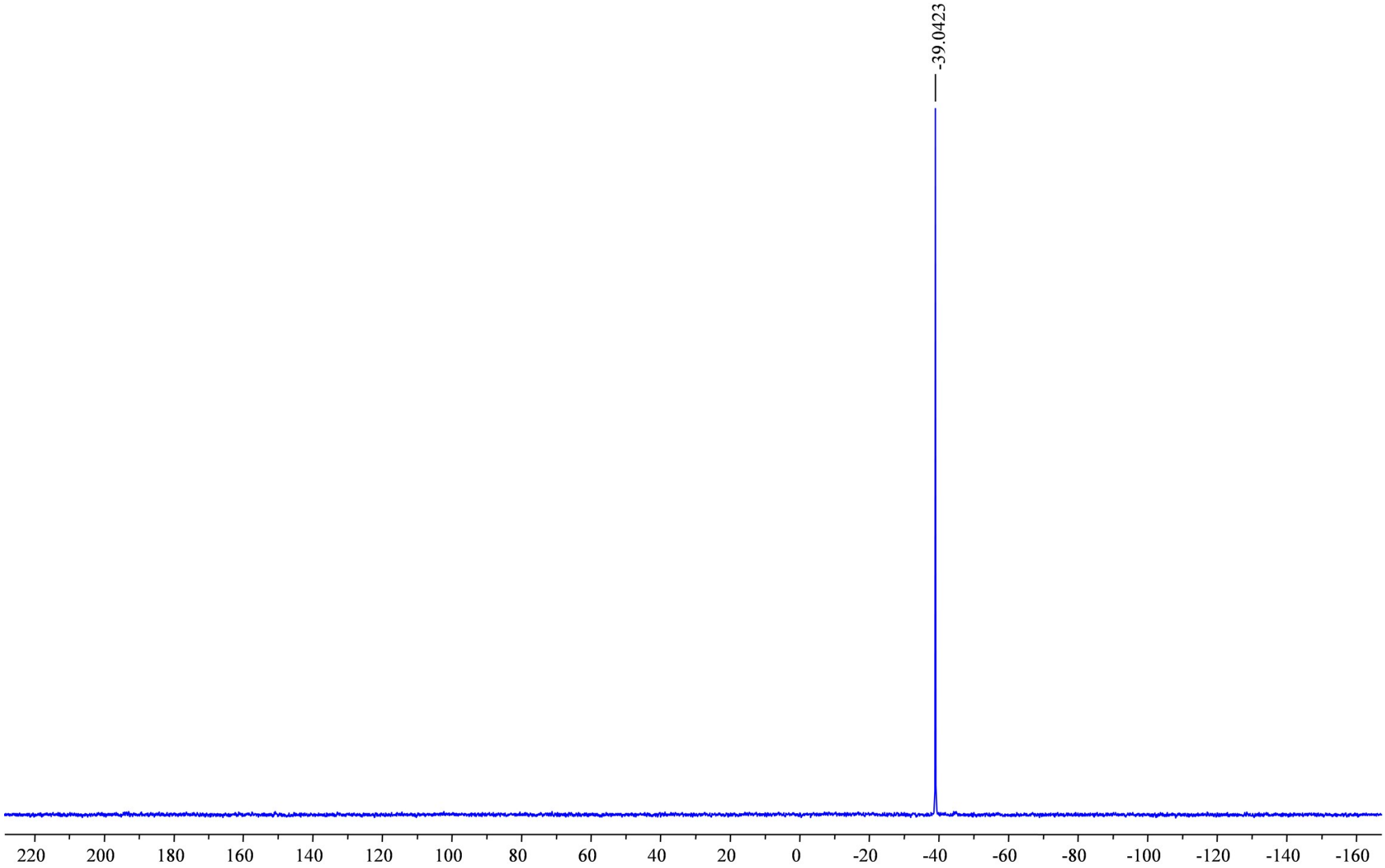

Figure 13. ^{31}P-{^{1}H} NMR spectrum (162.0 MHz, $CH_2Cl_2/CDCl_3$ = 1/2) of the phosphole (**1a**) and perfluorodiacetyl reaction mixture the next day.

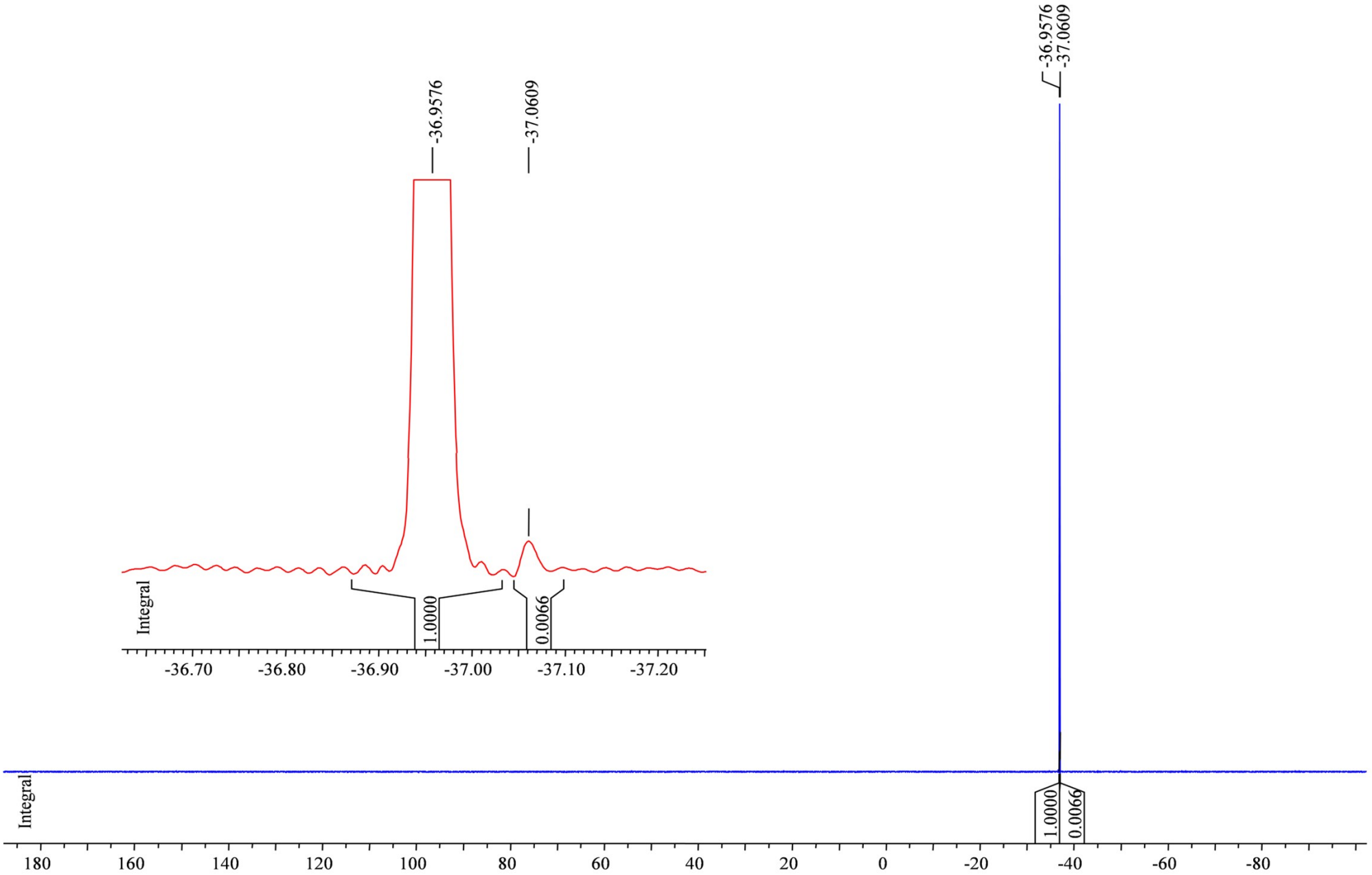

Figure 14. ^{31}P-{^{1}H} NMR spectrum (162.0 MHz, acetone-d_6) of phosphorane (**3a**).

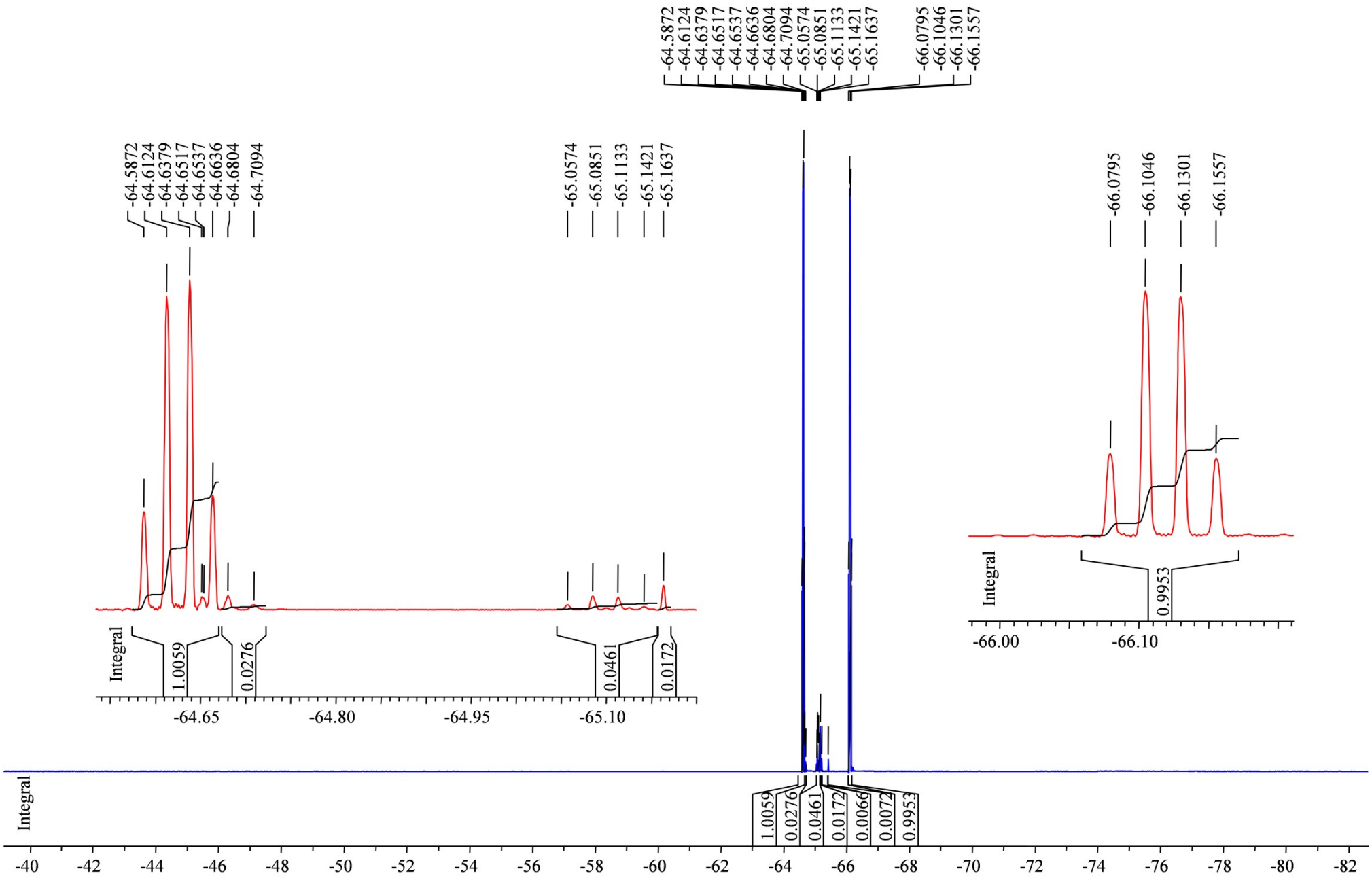

Figure 15. ^{19}F-{^{1}H} NMR spectrum (376.5 MHz, acetone-d_6) of phosphorane (**3a**) [minor quartets belong to phosphorane (**5a**)].

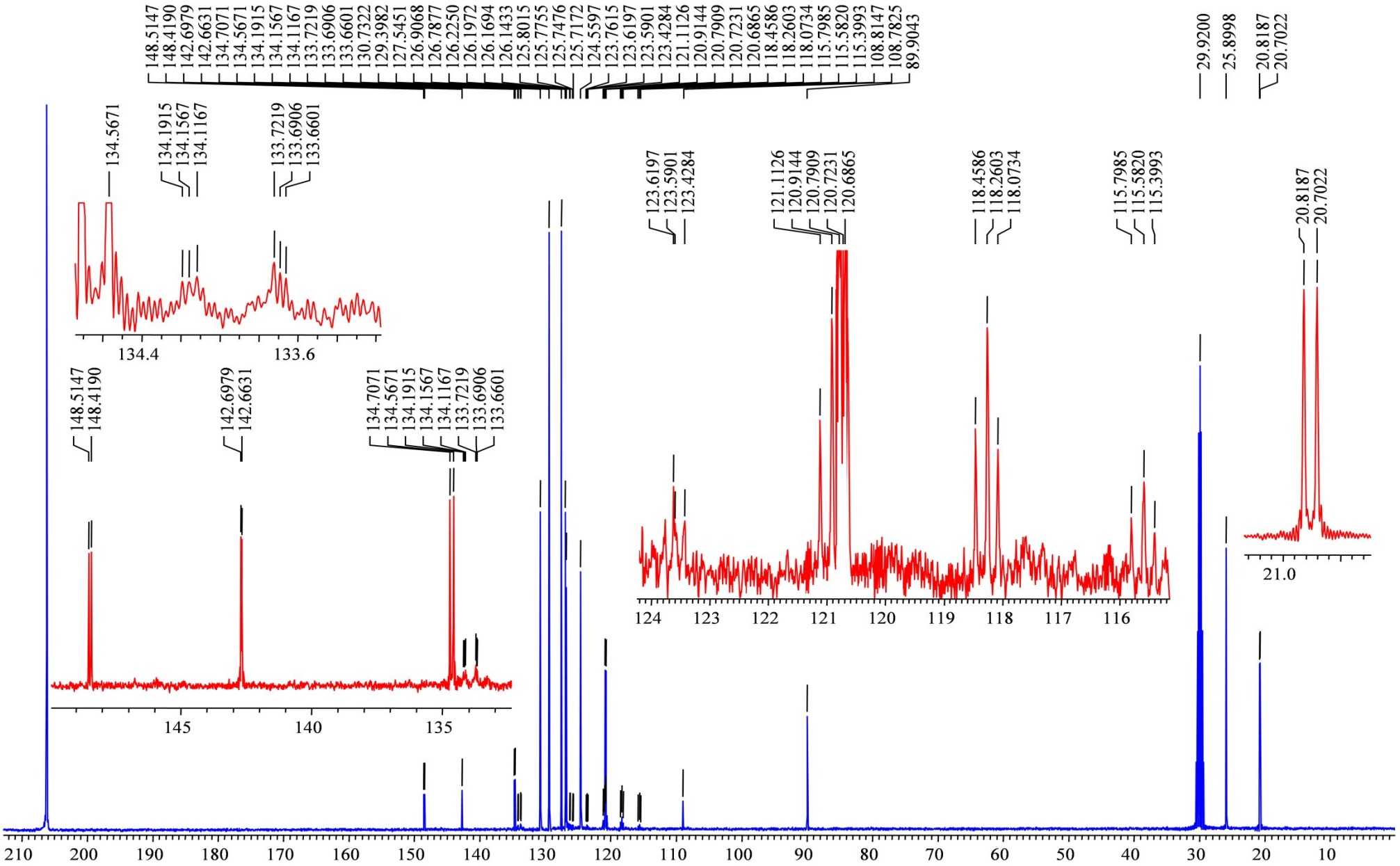

Figure 16. ^{13}C-{^{1}H} NMR spectrum (100.6 MHz, acetone-d_6) of phosphorane (**3a**).

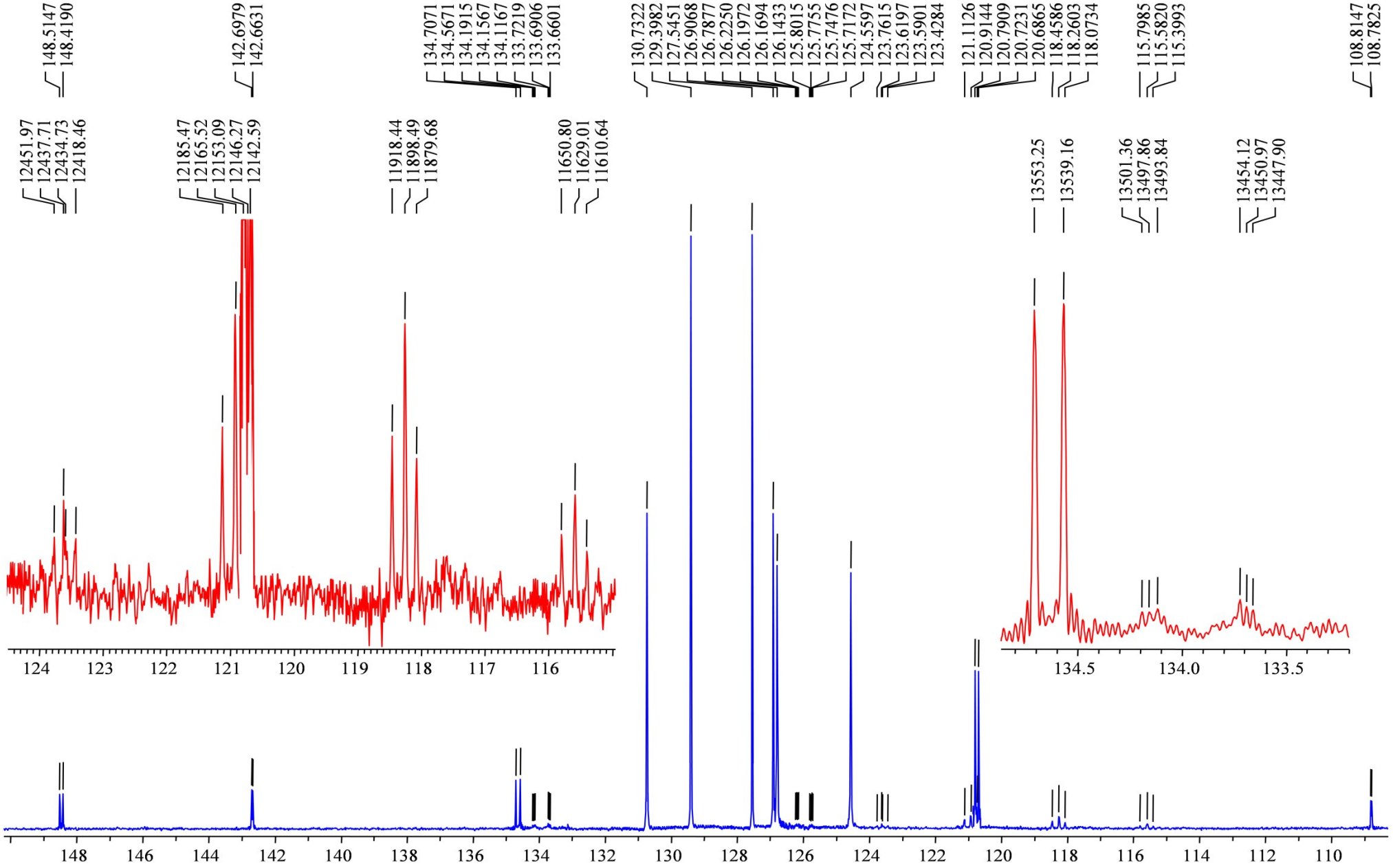

Figure 17. Low-field fragment of ^{13}C-{^{1}H} NMR spectrum (100.6 MHz, acetone-d_6) of phosphorane (**3a**).

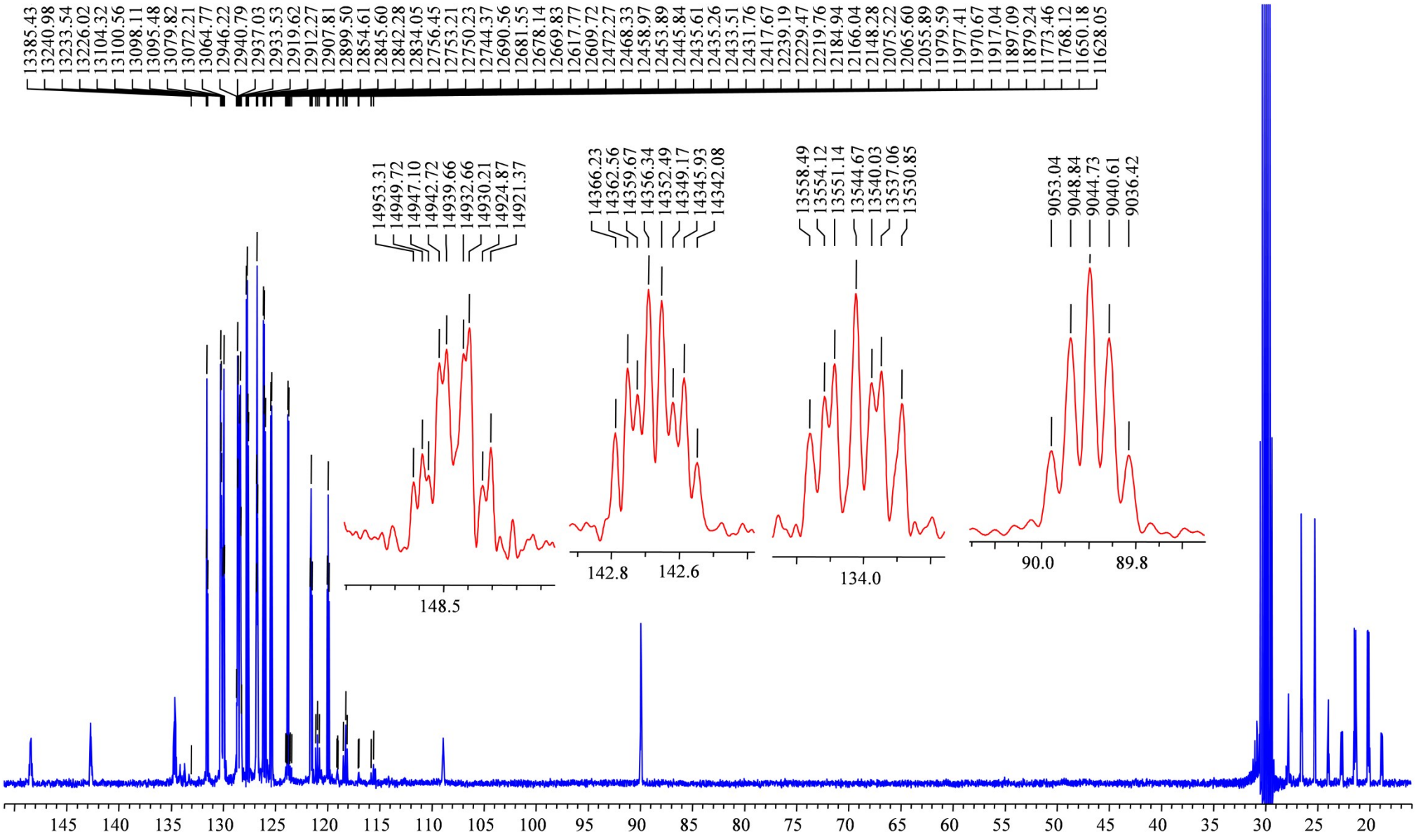

Figure 18. ^{13}C NMR spectrum (100.6 MHz, acetone-d_6) of phosphorane (**3a**).

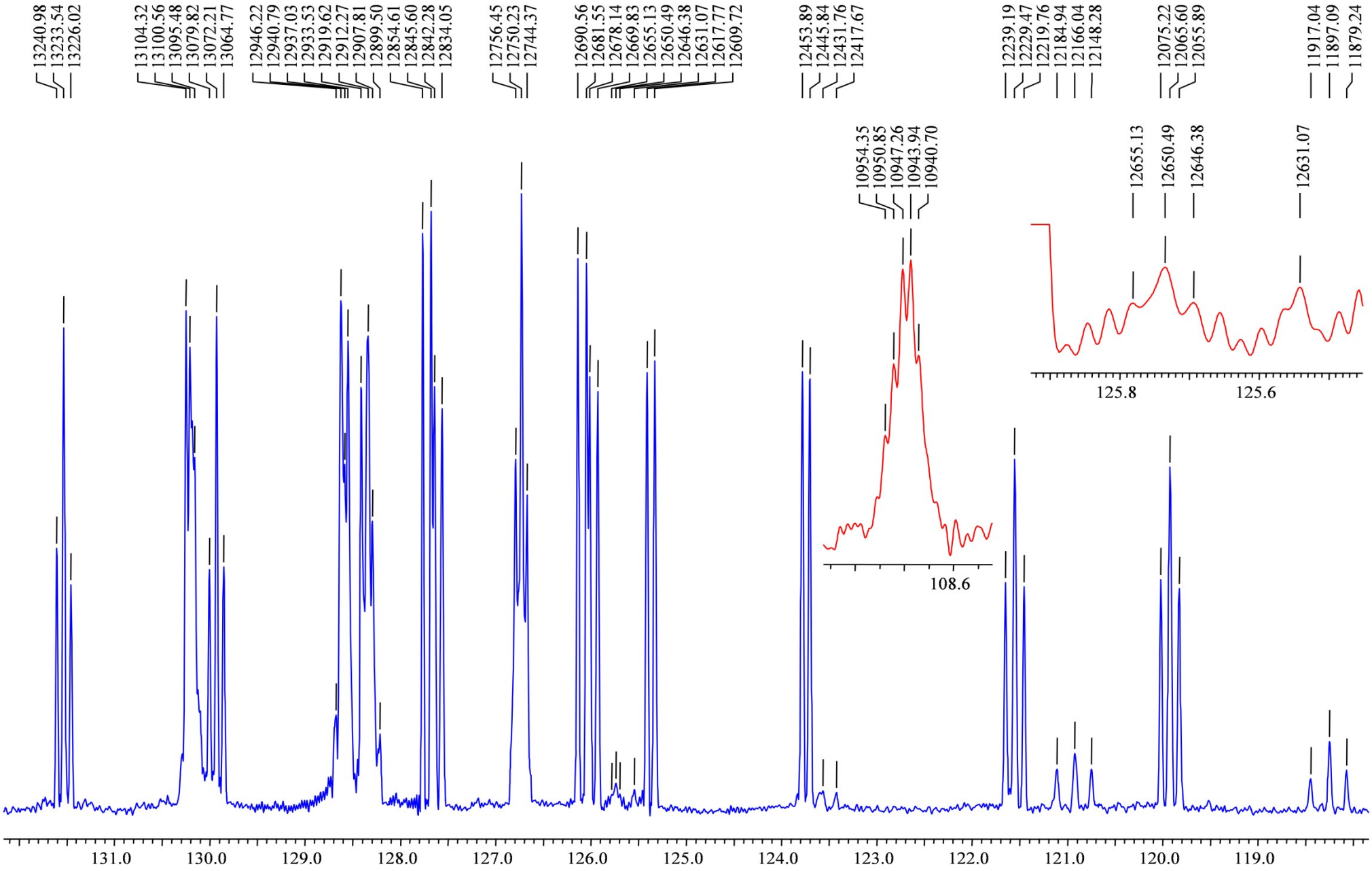

Figure 19. The aromatic carbons region of ^{13}C NMR spectrum (100.6 MHz, acetone-d_6) of phosphorane (**3a**).

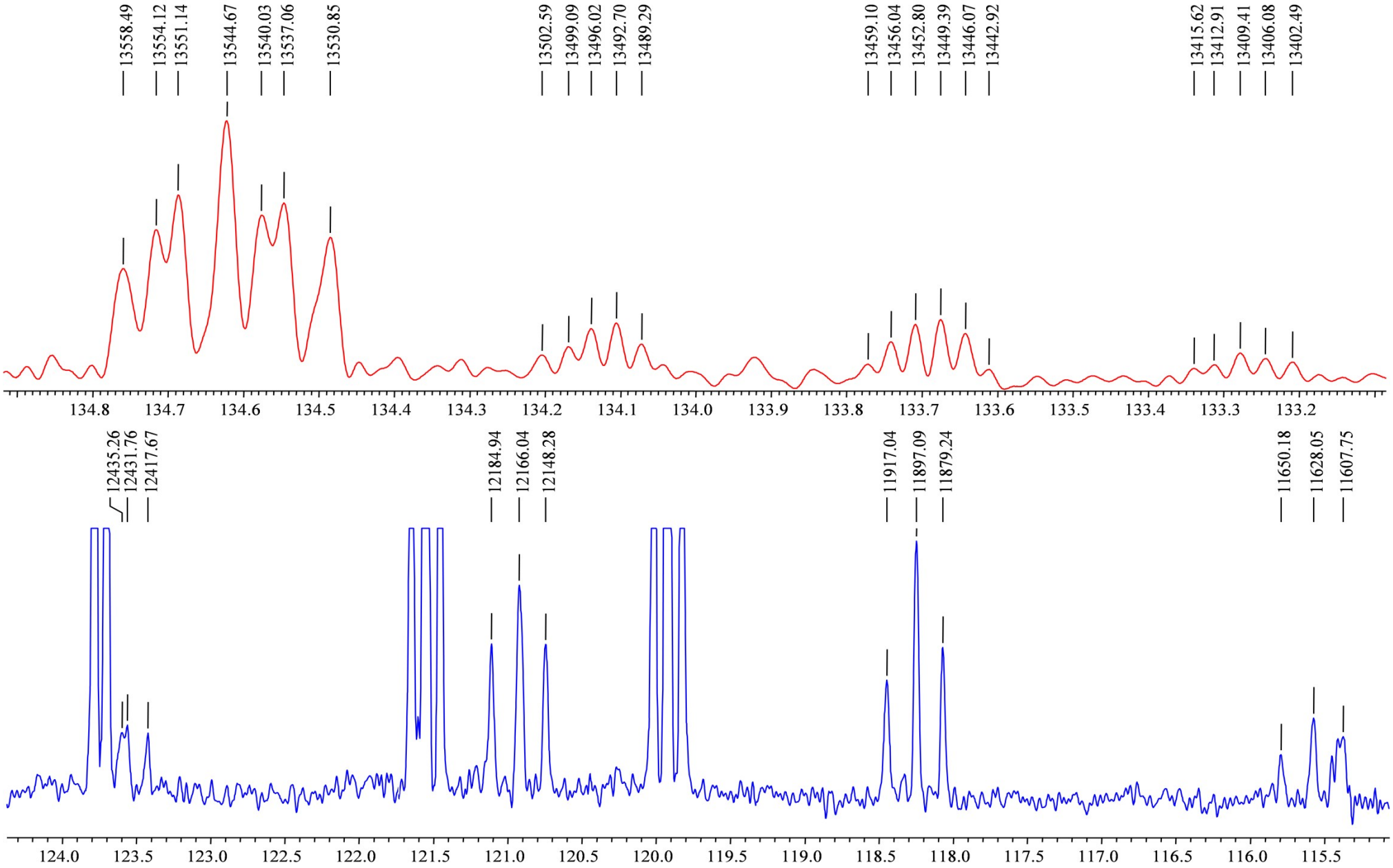

Figure 20. The 133-135 and 115-125 ppm regions of ^{13}C NMR spectrum (100.6 MHz, acetone-d_6) of phosphorane (**3a**).

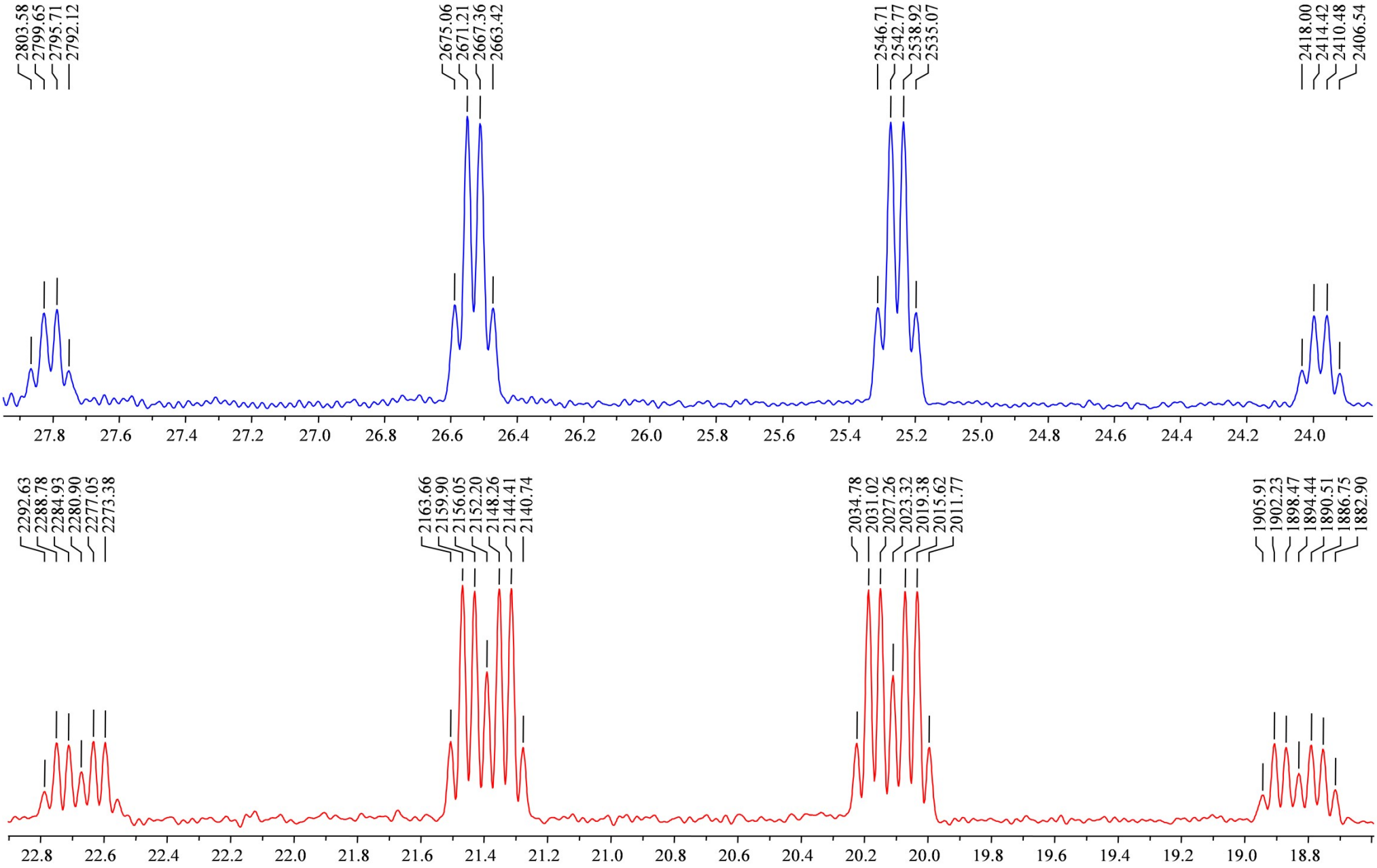

Figure 21. High-field regions of ^{13}C-{^{1}H} NMR spectrum (100.6 MHz, acetone-d_6) of phosphorane (**3a**).

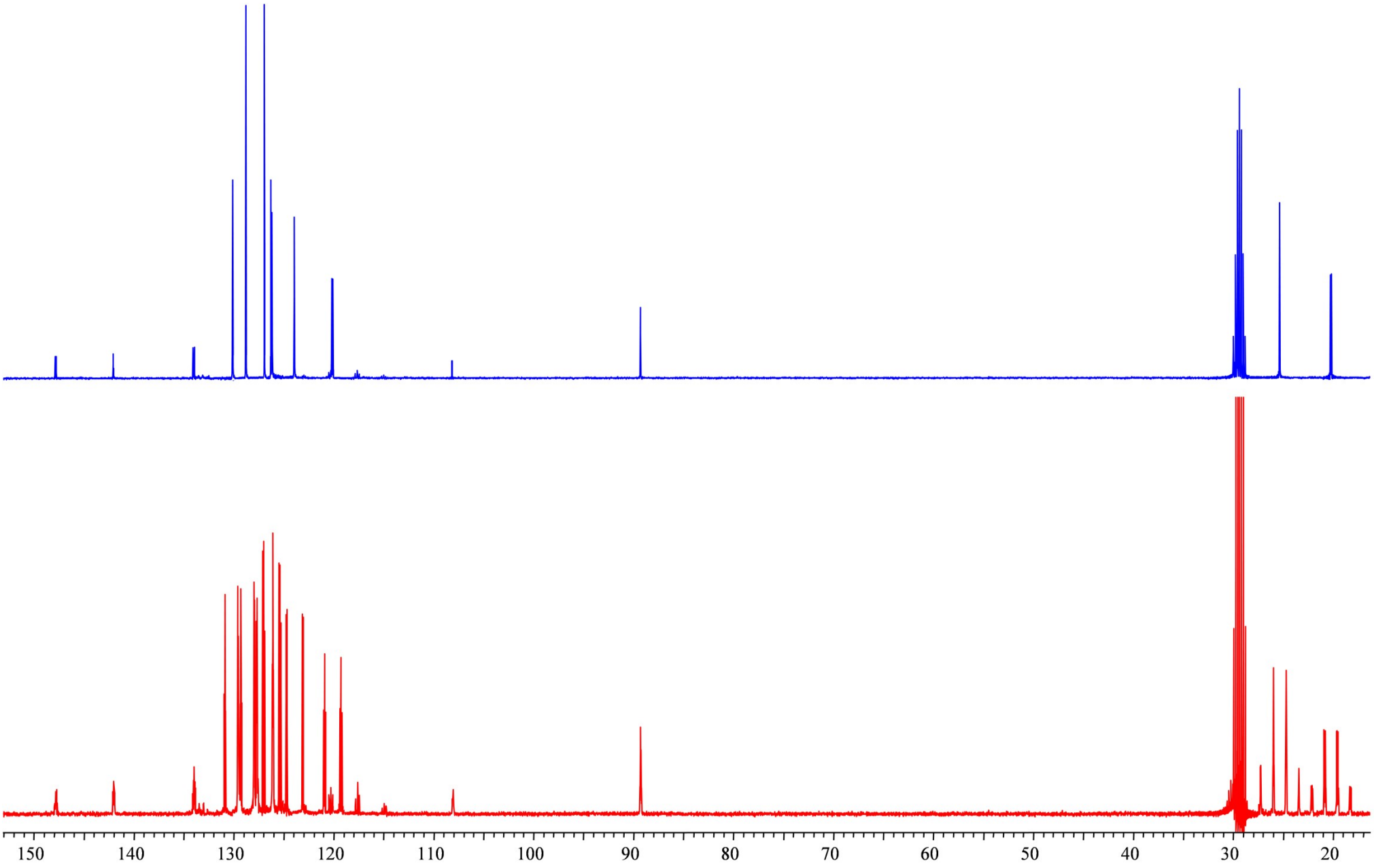

Figure 22. ^{13}C-{^{1}H} and ^{13}C NMR spectra (100.6 MHz, acetone-d_6) of phosphorane (**3a**).

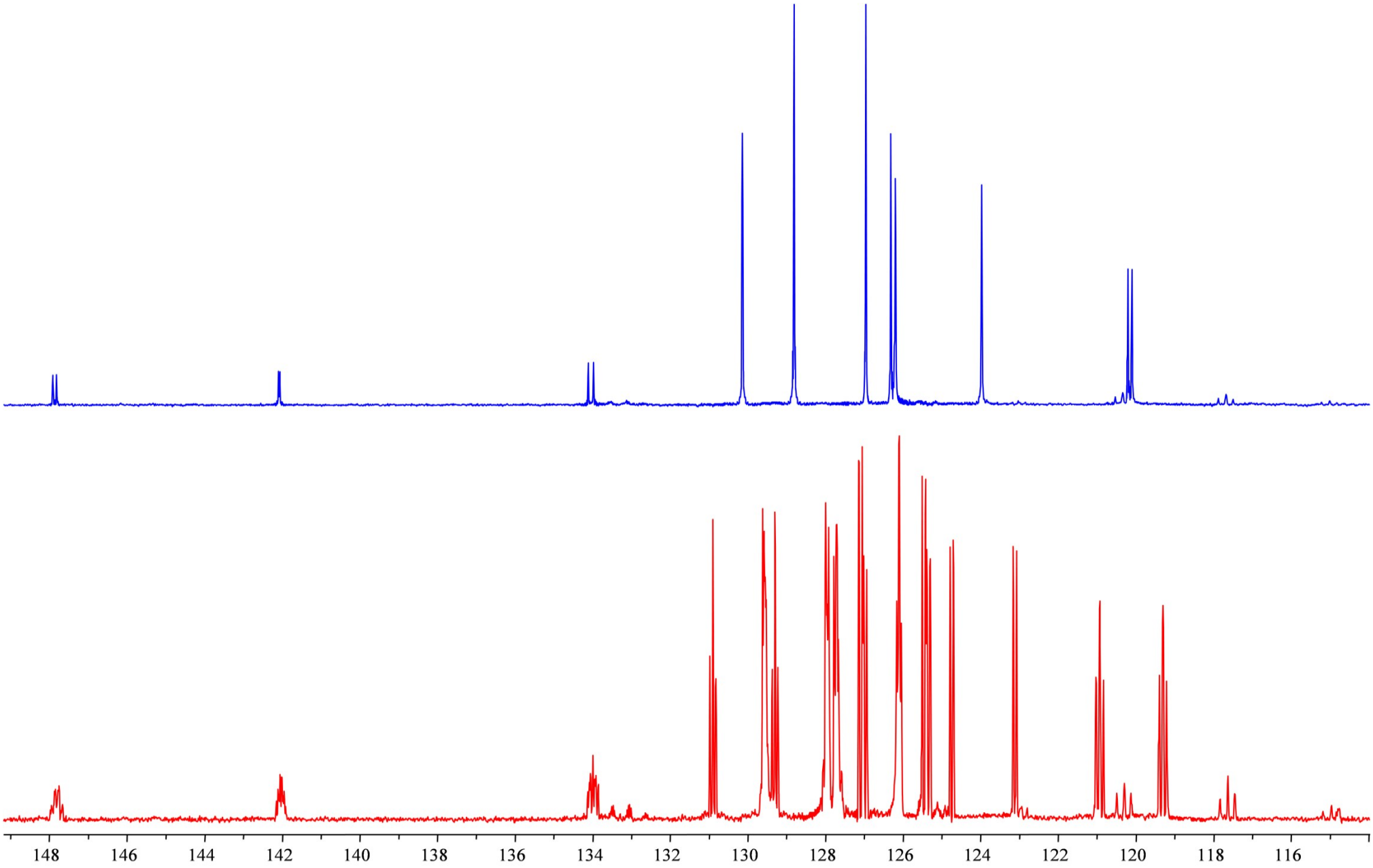

Figure 23. Low-field region of ^{13}C-{^{1}H} and ^{13}C NMR spectra (100.6 MHz, acetone-d_6) of phosphorane (**3a**).

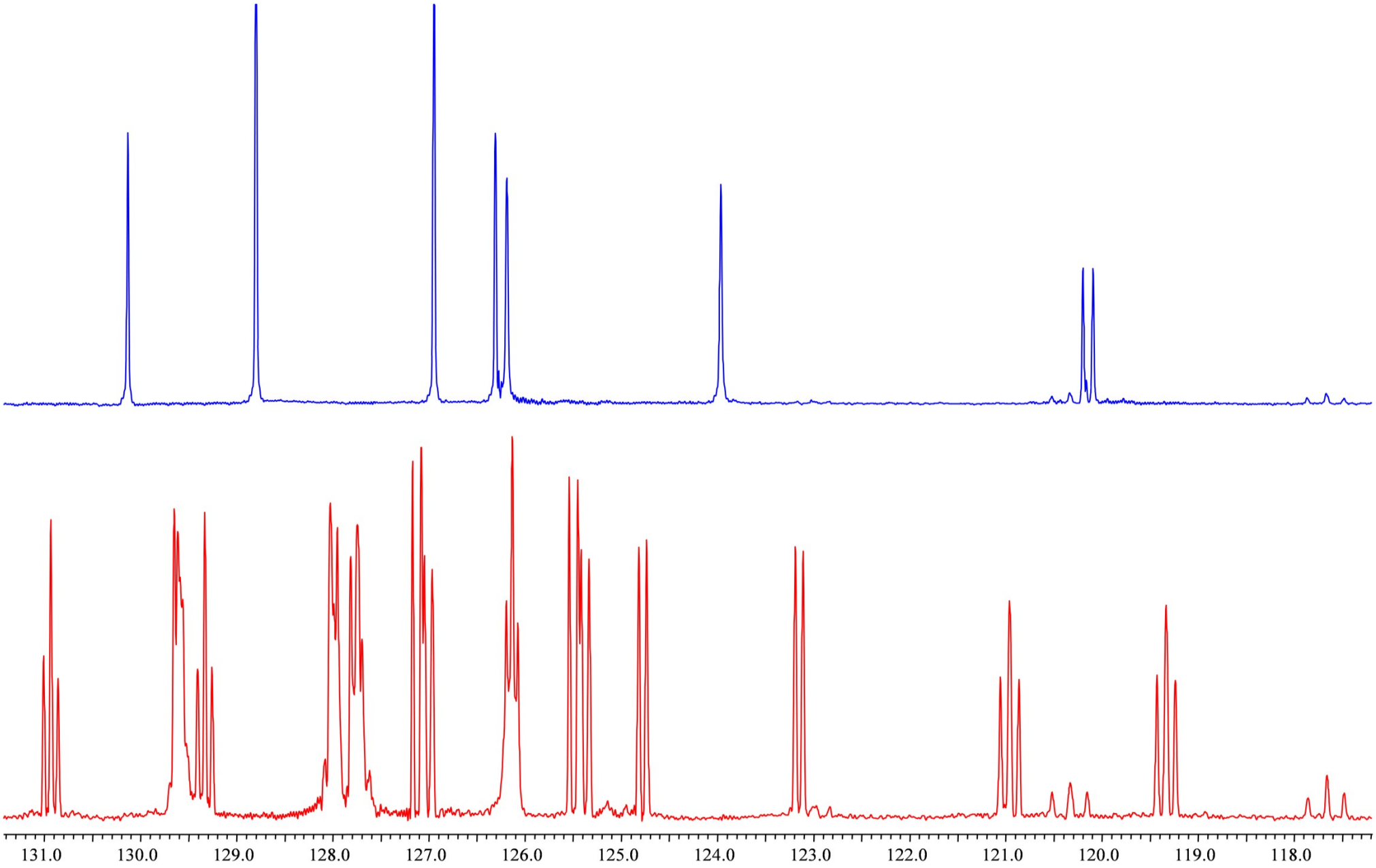

Figure 24. The aromatic carbons region of ^{13}C-{^{1}H} and ^{13}C NMR spectra (100.6 MHz, acetone-d_6) of phosphorane (**3a**).

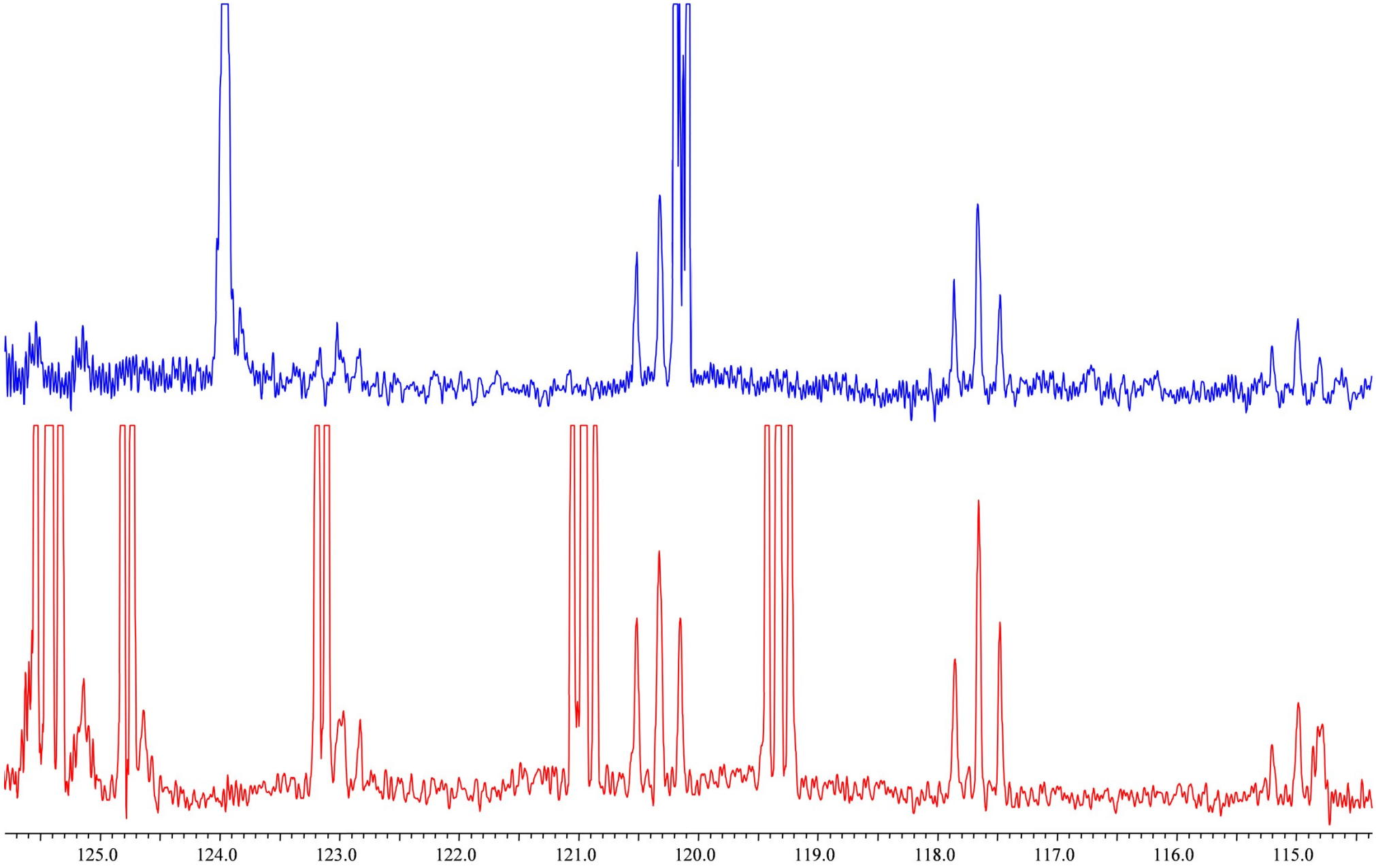

Figure 25. The 114-126 ppm region of ^{13}C-{^{1}H} and ^{13}C NMR spectra (100.6 MHz, acetone-d_6) of phosphorane (**3a**).

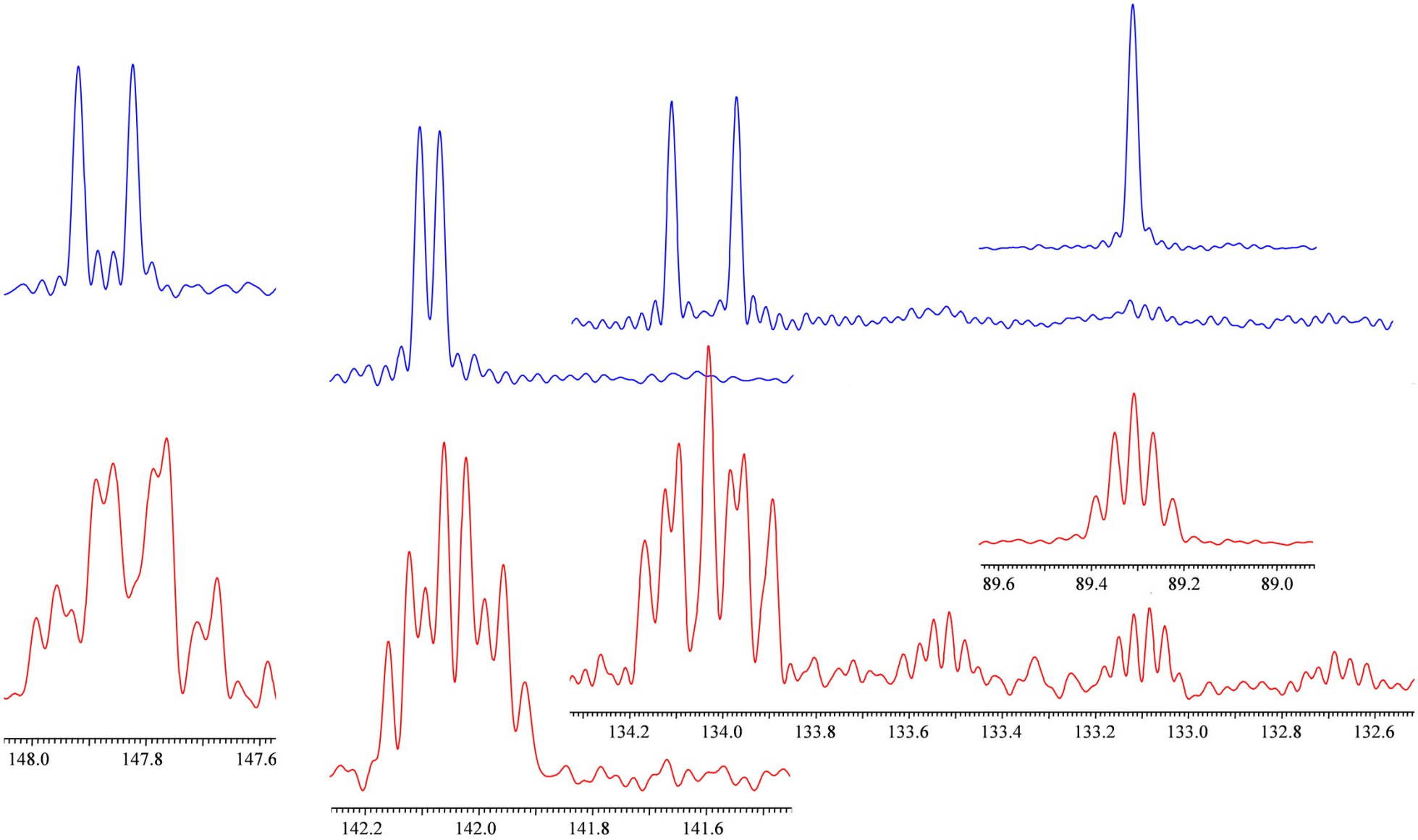

Figure 26. Low-field regions of ^{13}C-{^{1}H} and ^{13}C NMR spectra (100.6 MHz, acetone-d_6) of phosphorane (**3a**).

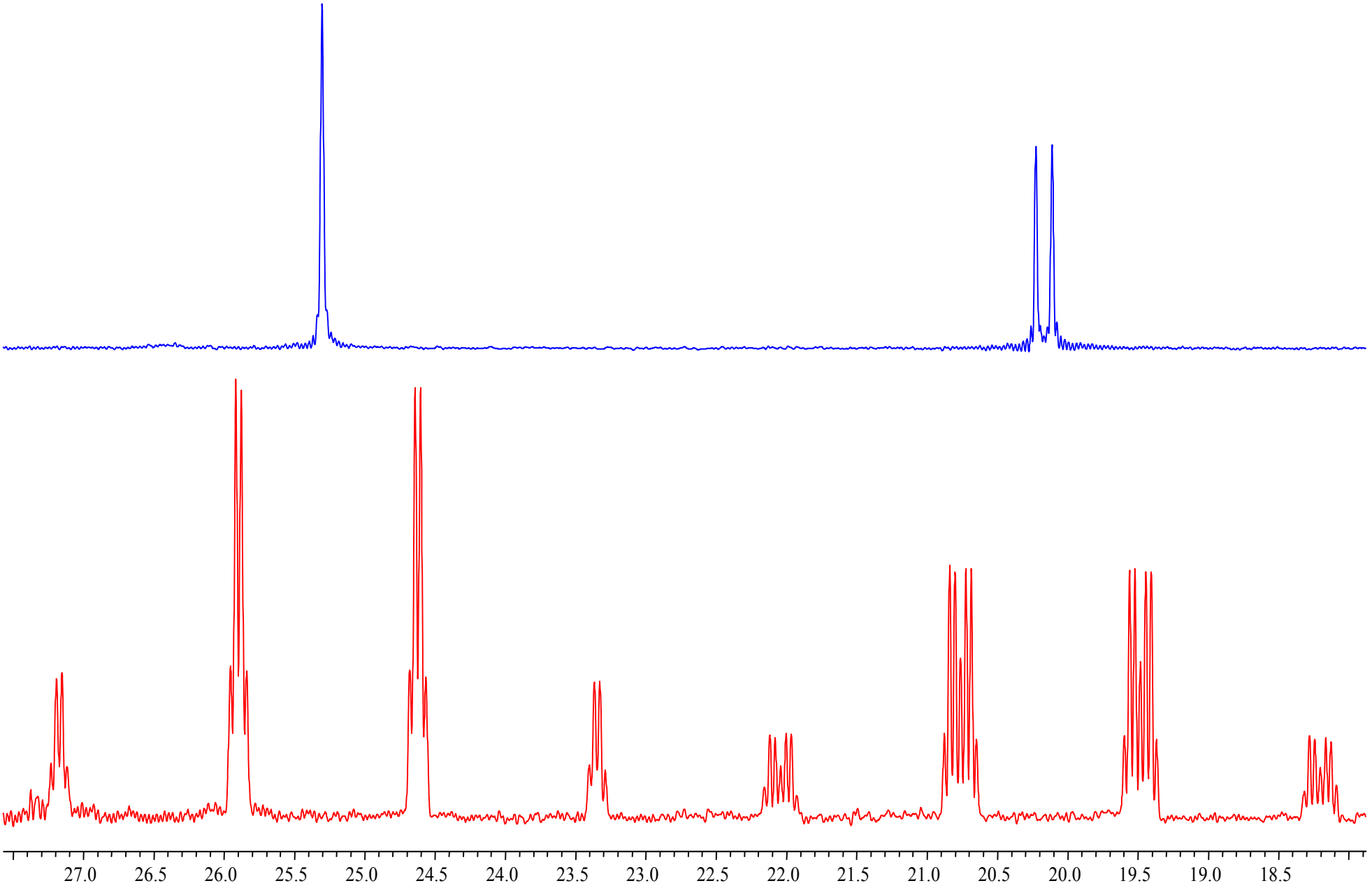

Figure 27. High-field region of ^{13}C-{^{1}H} and ^{13}C NMR spectra (100.6 MHz, acetone-d_6) of phosphorane (**3a**).

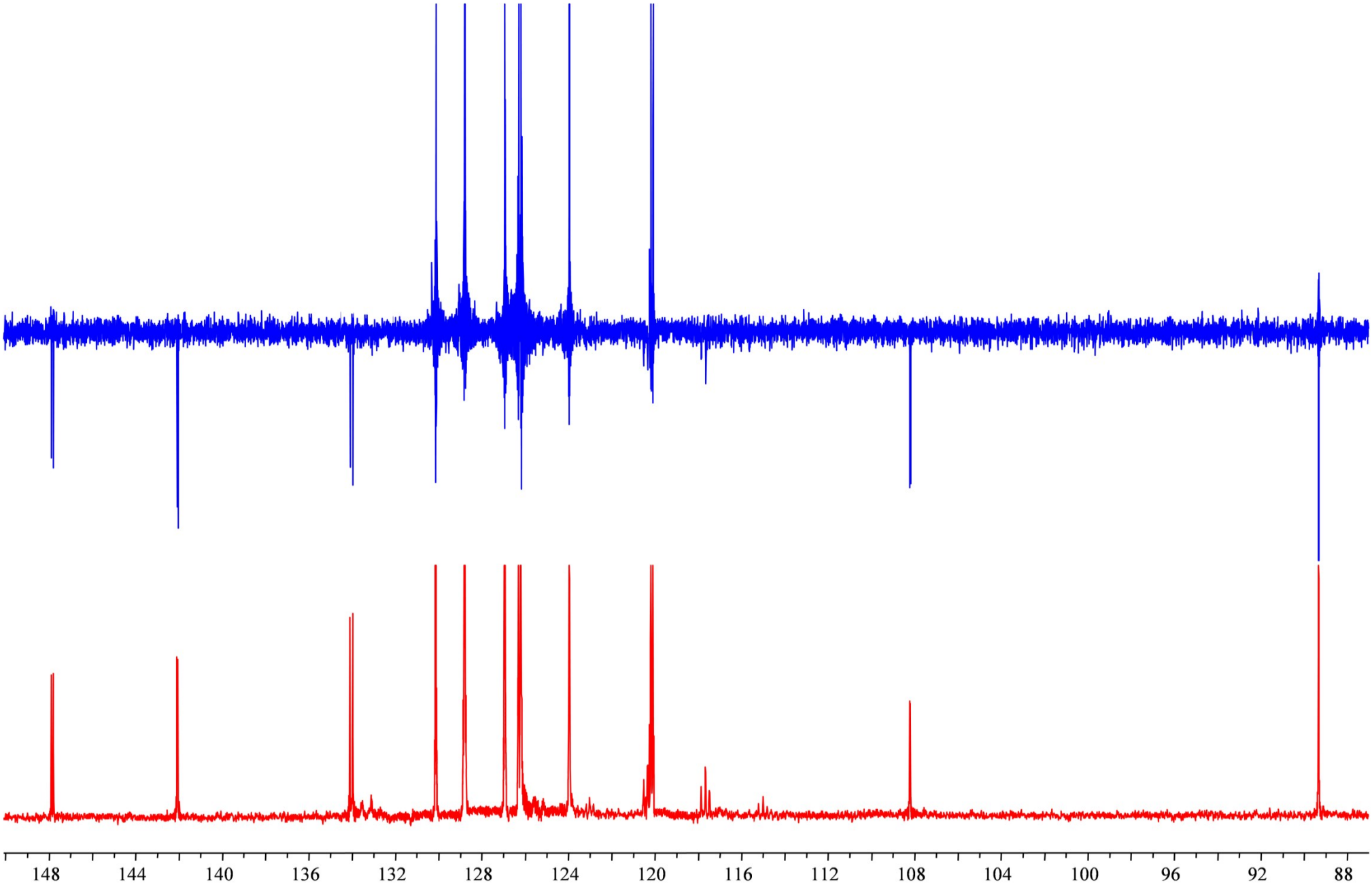

Figure 28. Fragment of ^{13}C-{^{1}H} and APT spectra (100.6 MHz, acetone-d_6) of phosphorane (**3a**).

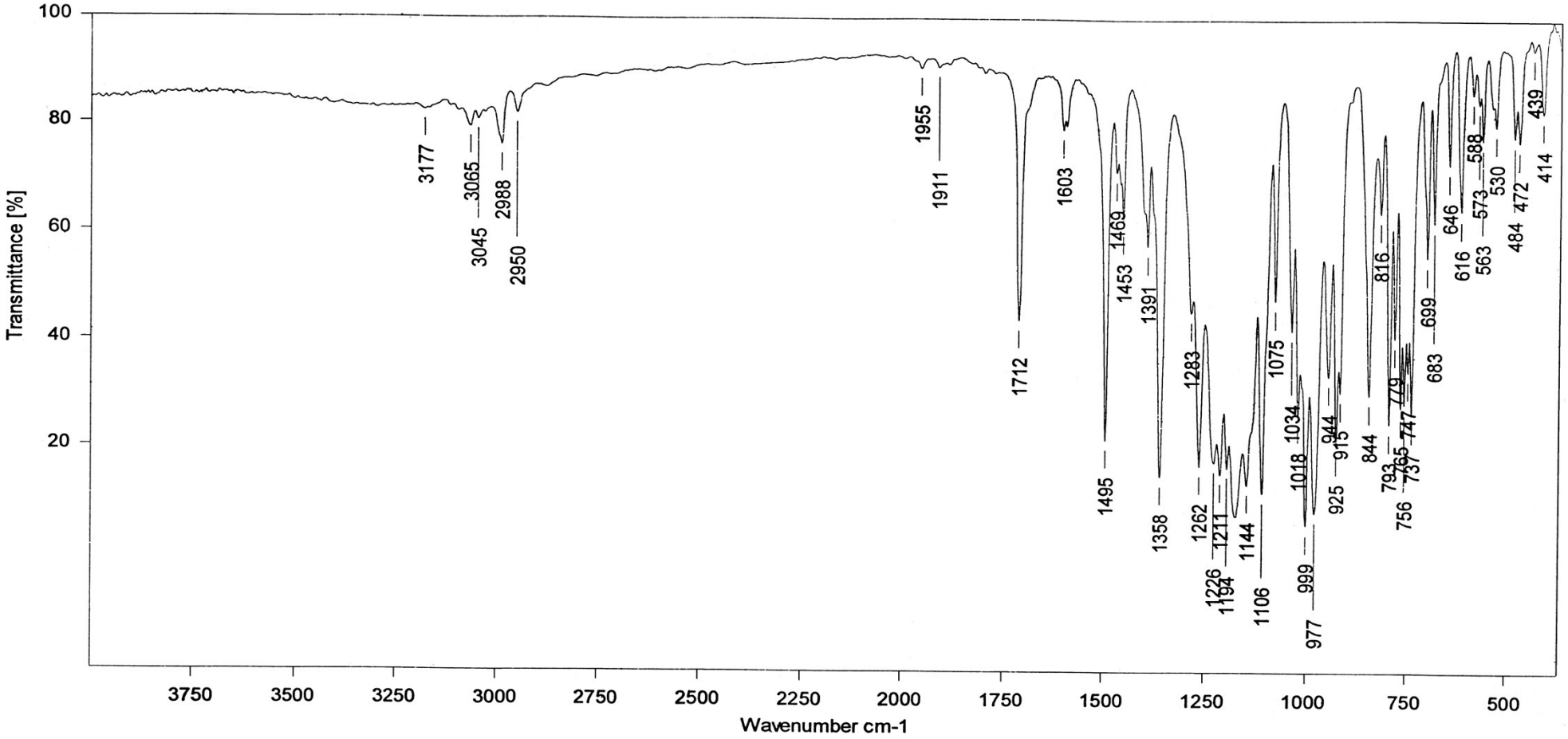

Sample Name MIR 410
Operator Name Sasha
Instrument Type Tensor 27
Resolution 4

Path of File E:\work\2019
Date of Measurement 17/04/2019
Sample Form KBr
Time of Measurement 11:50:58 AM

Filename MIR 410.3

Figure 29. IR spectrum (400-4000 cm^{-1}, KBr pellet) of phosphorane (**3a**).

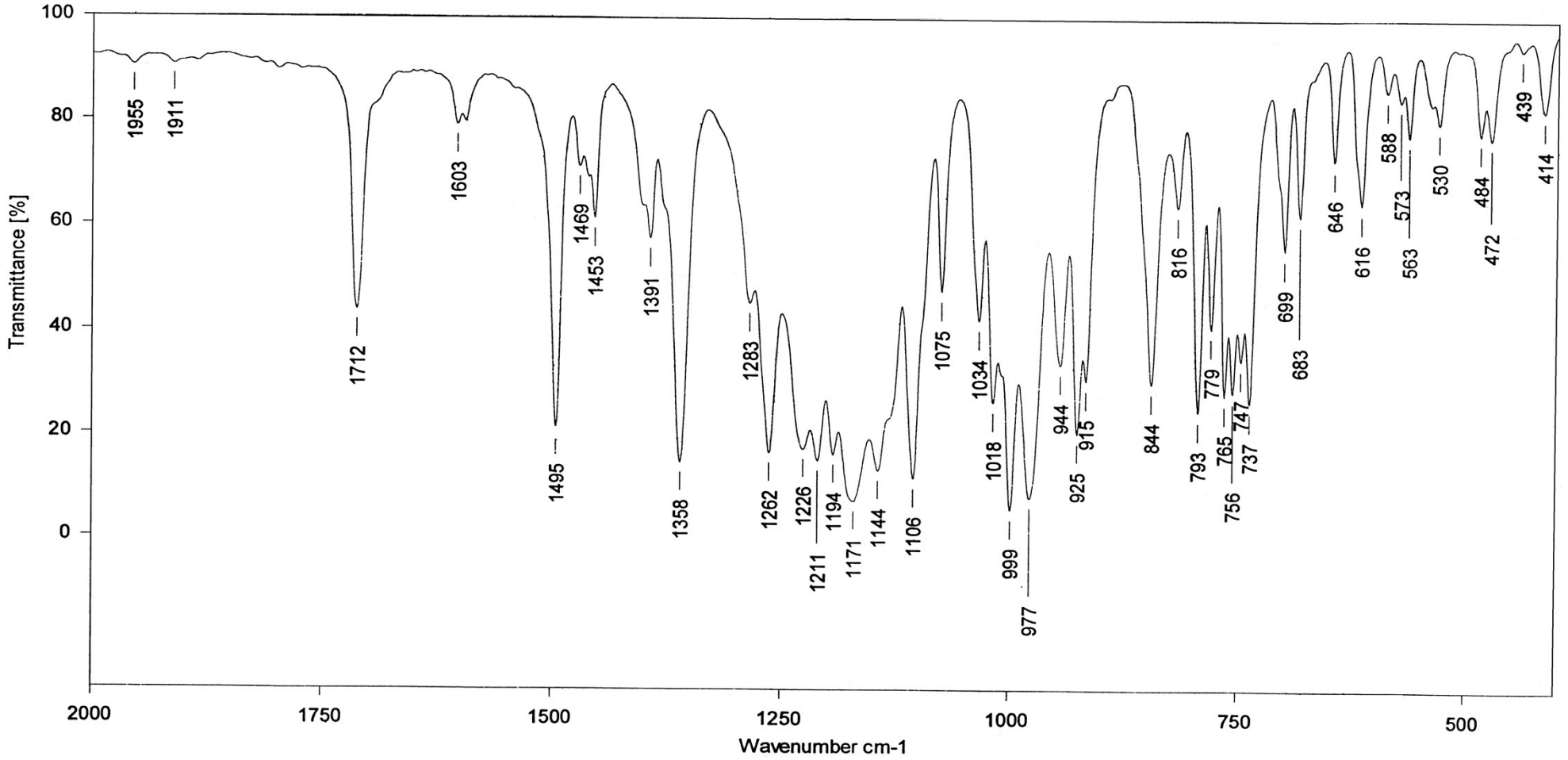

Sample Name MIR 410

Operator Name Sasha

Instrument Type Tensor 27

Resolution 4

Path of File E:\work\2019

Date of Measurement 17/04/2019

Sample Form KBr

Time of Measurement 11:50:58 AM

Filename MIR 410.3

Figure 30. The fragment (400-2000 cm^{-1}) of IR spectrum (KBr pellet) of phosphorane (**3a**).

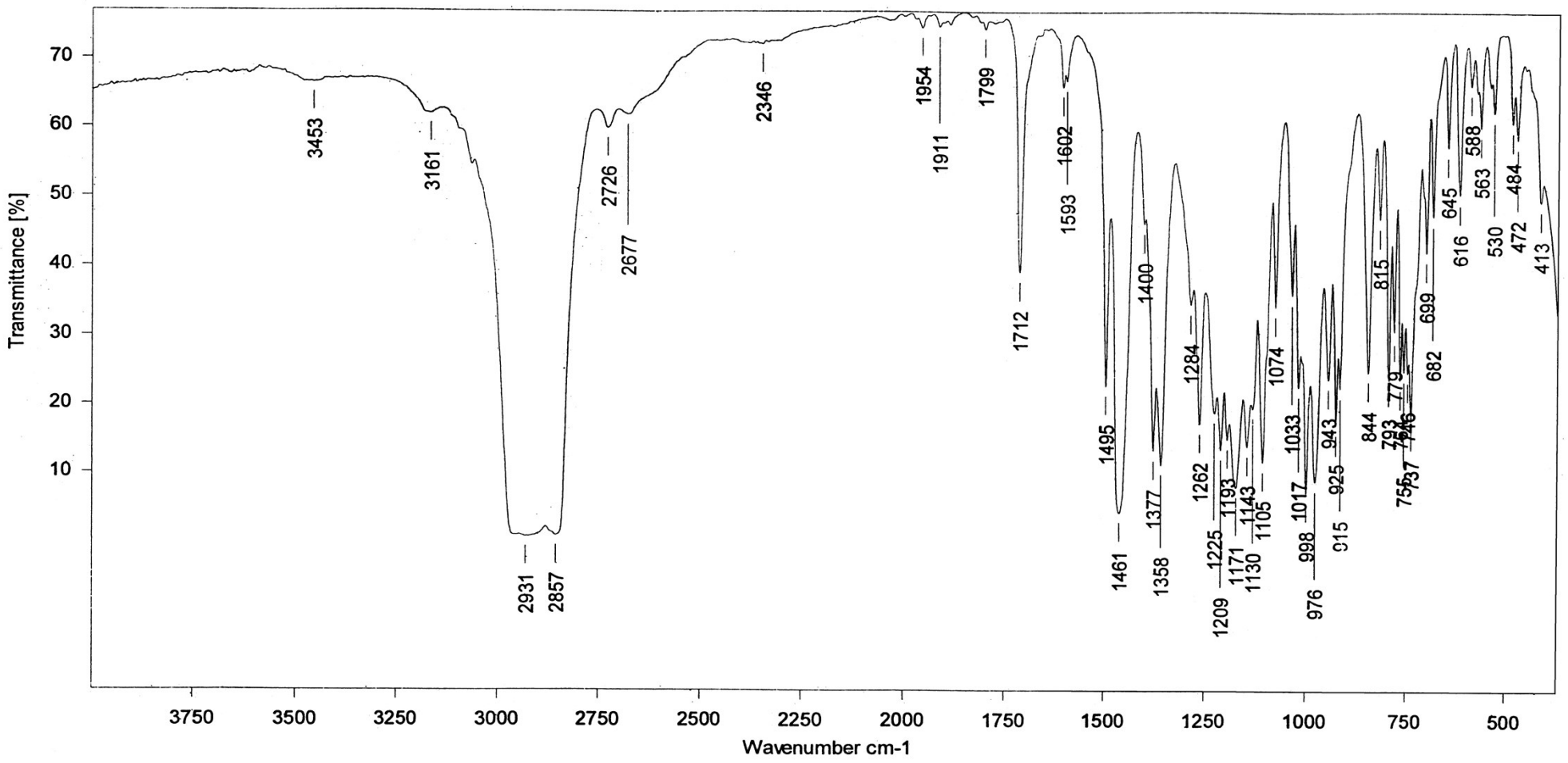

Sample Name MIR 410

Operator Name Sasha

Instrument Type Tensor 27

Resolution 4

Path of File E:\work\2019

Date of Measurement 17/04/2019

Sample Form vazelin

Time of Measurement 12:00:28 PM

Filename MIR 410.4

Figure 31. IR spectrum (400-4000 cm^{-1}, Vaseline oil) of phosphorane (**3a**).

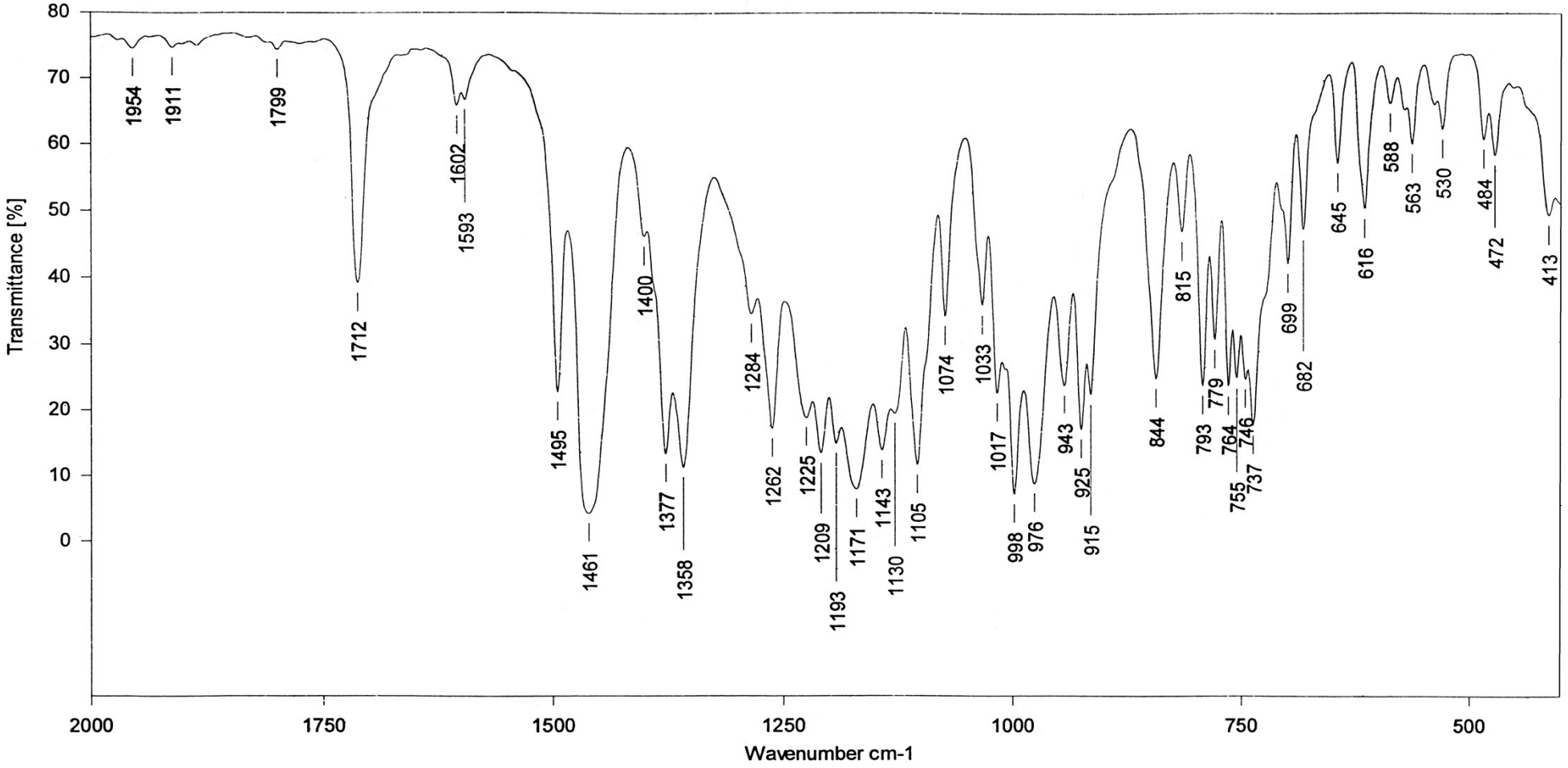

Figure 32. The fragment (400-2000 cm^{-1}) of IR spectrum (400-2000 cm^{-1}, Vaseline oil) of phosphorane (**3a**).

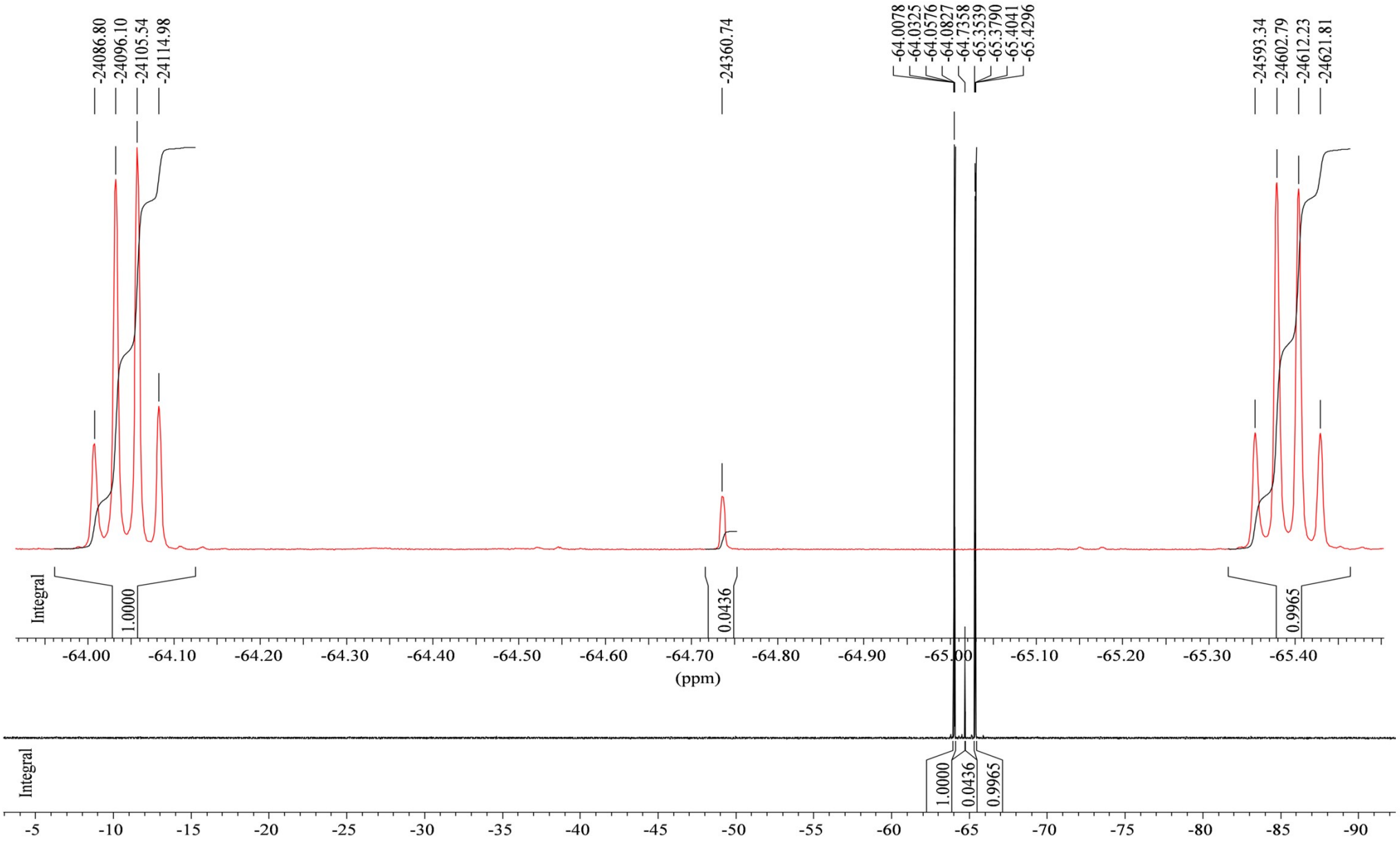

Figure 33. ^{19}F NMR spectrum (386.5 MHz, $CDCl_3$) of the phosphole (**3b**) and perfluorodiacetyl reaction mixture after heating at 60°C for 40 min and evaporation of dichloromethane in vacuo [compounds (**3b**) and (**4b**) in the ratio of 50 : 1].

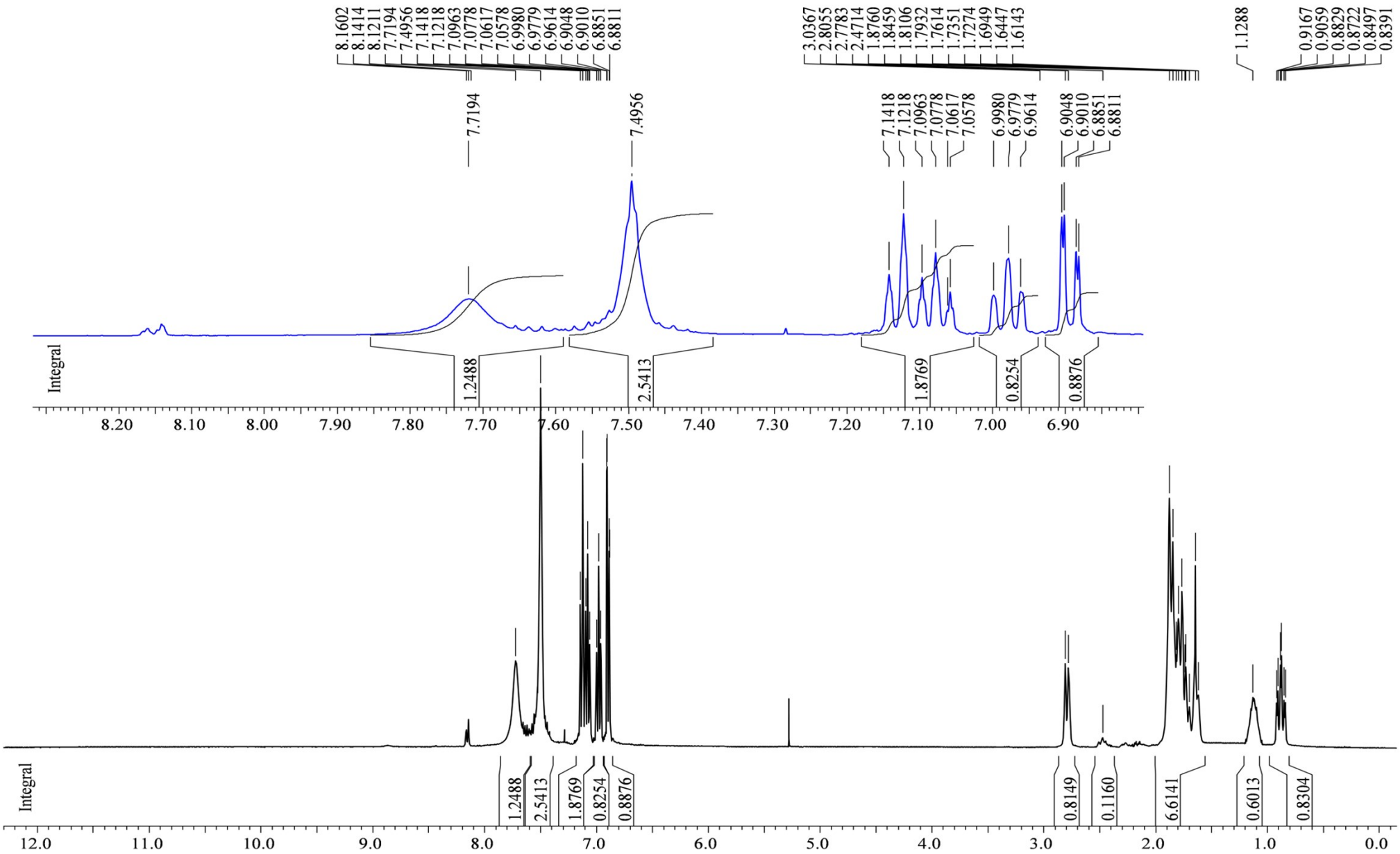

Figure 34. ^{1}H NMR spectrum (400 MHz, $CDCl_3$) of the phosphole (**1b**) and perfluorodiacetyl reaction mixture after heating at 60°C for 40 min and evaporation of dichloromethane in vacuo [compounds (**3b**) and (**4b**) in the ratio of 50 : 1].

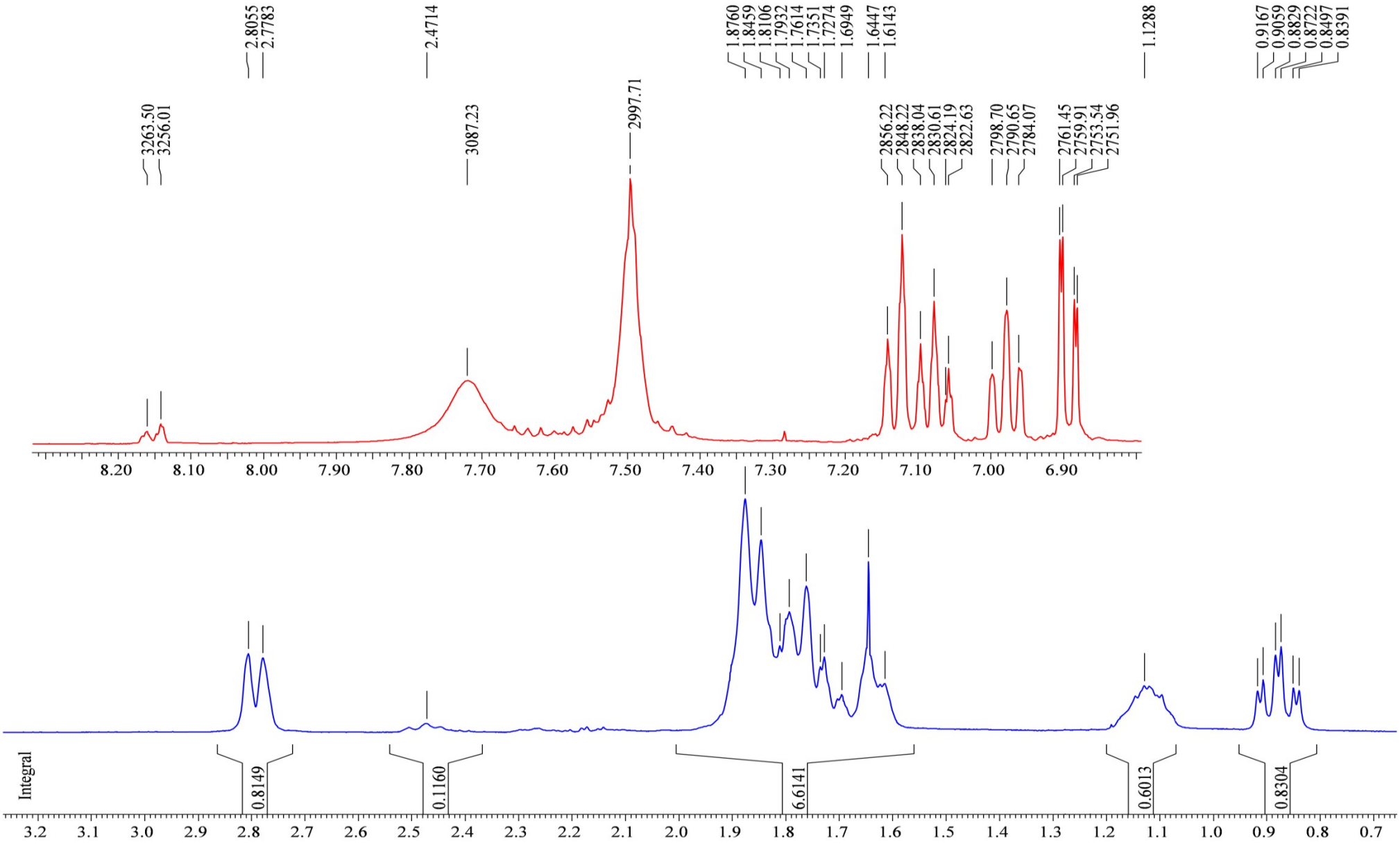

Figure 35. Fragment of ^{1}H NMR spectrum (400 MHz, $CDCl_3$) of the phosphole (**1b**) and perfluorodiacetyl reaction mixture after heating at 60°C for 40 min and evaporation of dichloromethane in vacuo [compounds (**3b**) and (**4b**) in the ratio of 50 : 1].

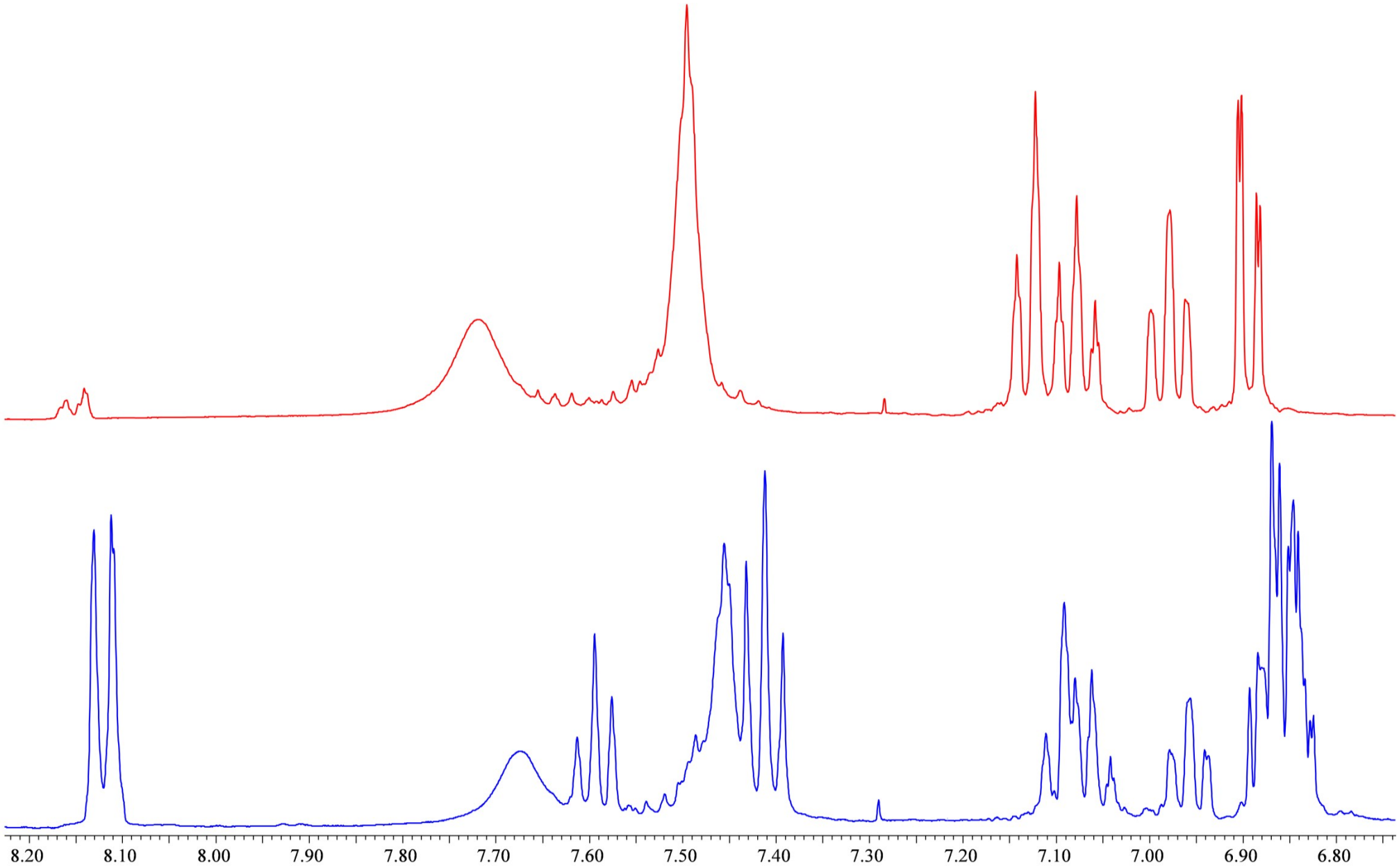

Figure 36. Low-field fragments of ^{1}H NMR spectra (400 MHz, $CDCl_3$) of the phosphole (**1b**) and perfluorodiacetyl reaction mixture after 11 days (blue) [compounds (**3b**) and (**4b**) in the ratio of 1 : 1] and after heating at 60°C for 40 min (red) [compounds (**3b**) and (**4b**) in the ratio of 50 : 1].

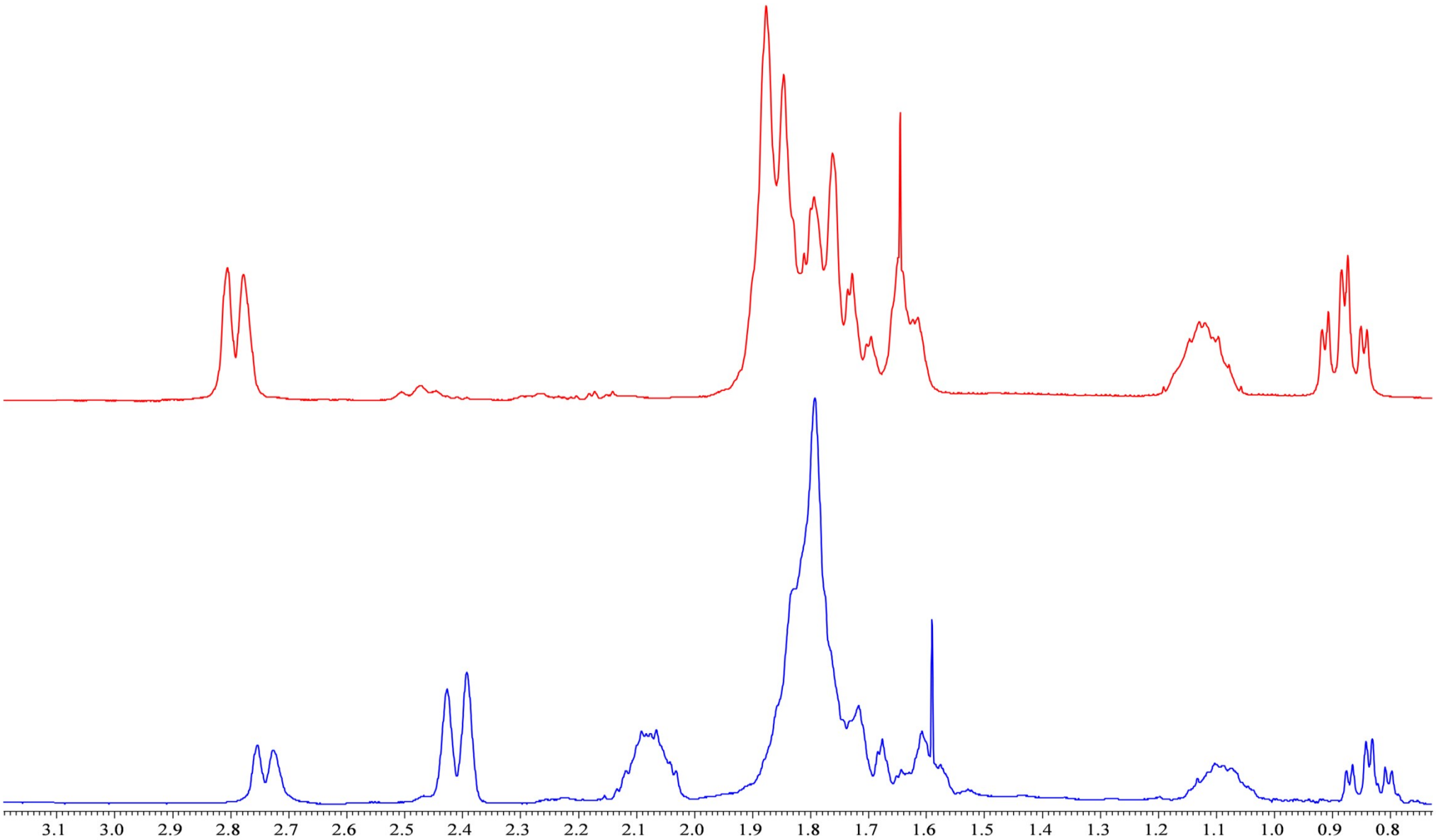

Figure 37. Up-field fragments of ^{1}H NMR spectra (400 MHz, $CDCl_3$) of the phosphole (**3b**) and perfluorodiacetyl reaction mixture after 11 days (blue) [compounds (**3b**) and (**4b**) in the ratio of 1 : 1] and after heating at 60°C for 40 min (red) [compounds (**3b**) and (**4b**) in the ratio of 50 : 1].

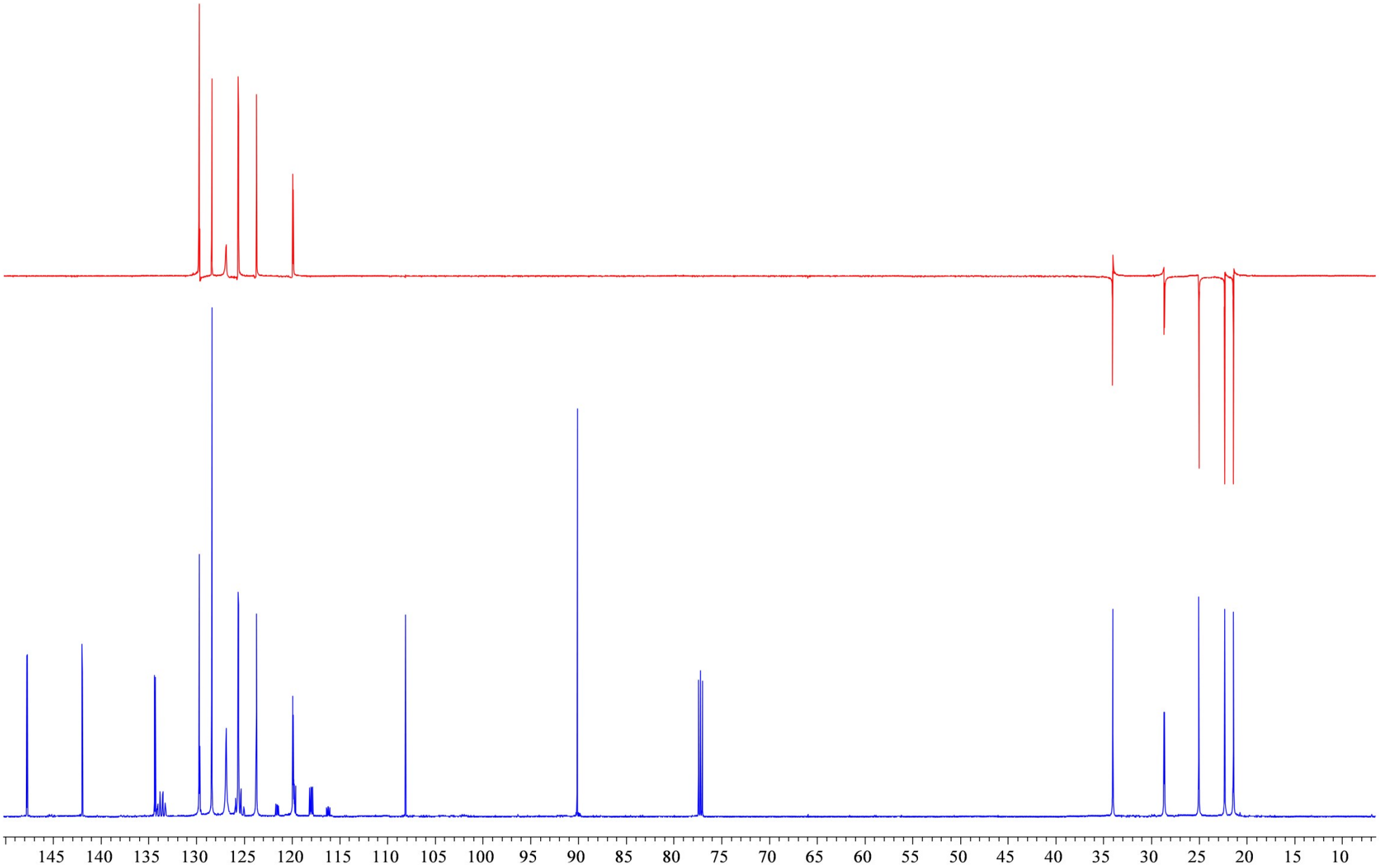

Figure 38. ^{13}C-{^{1}H} and ^{13}C-{^{1}H}-dept NMR spectra (100.6 MHz, $CDCl_3$) of compound (**3b**).

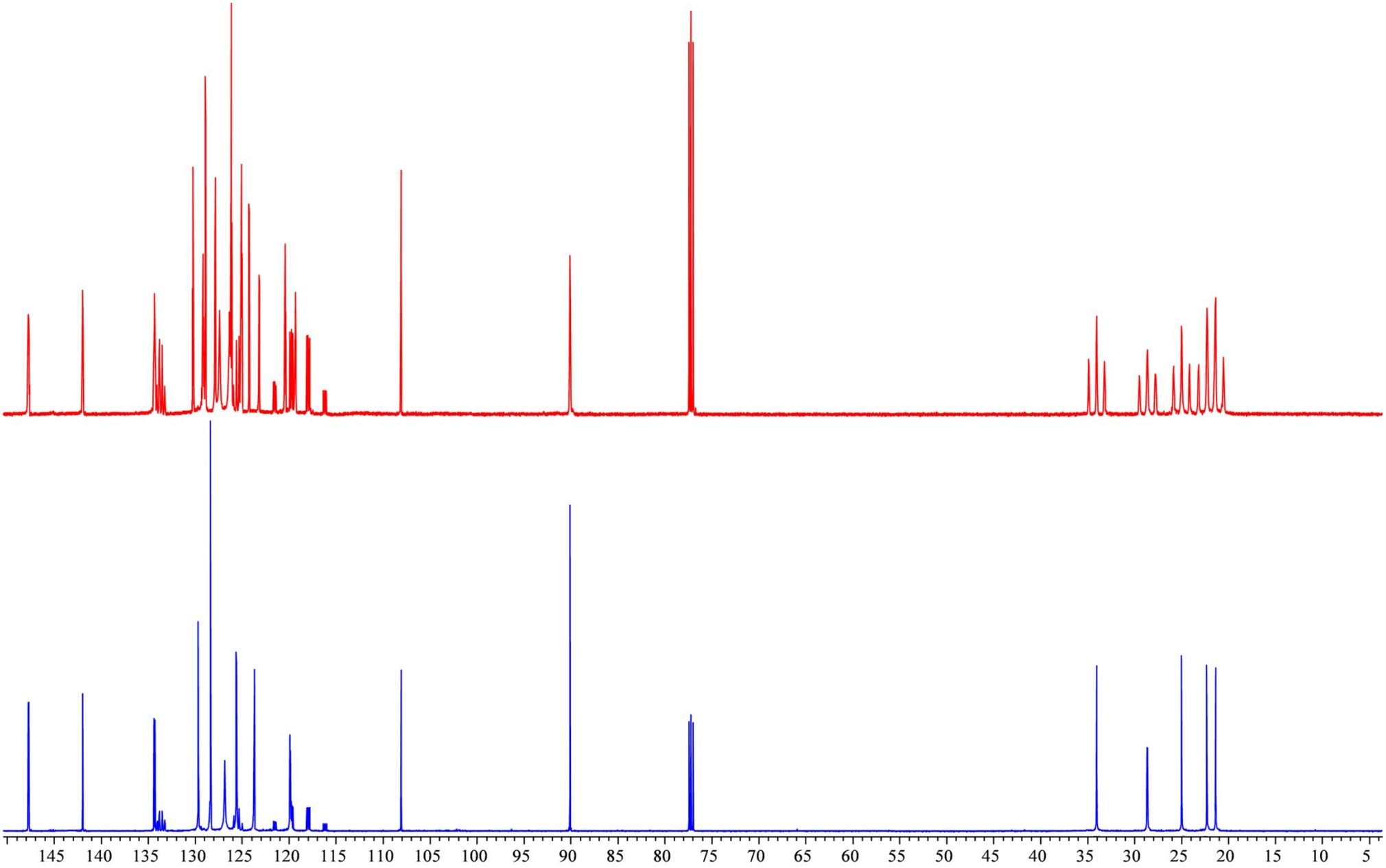

Figure 39. ^{13}C-{^{1}H} and ^{13}C NMR spectra (100.6 MHz, $CDCl_3$) of compound (**3b**).

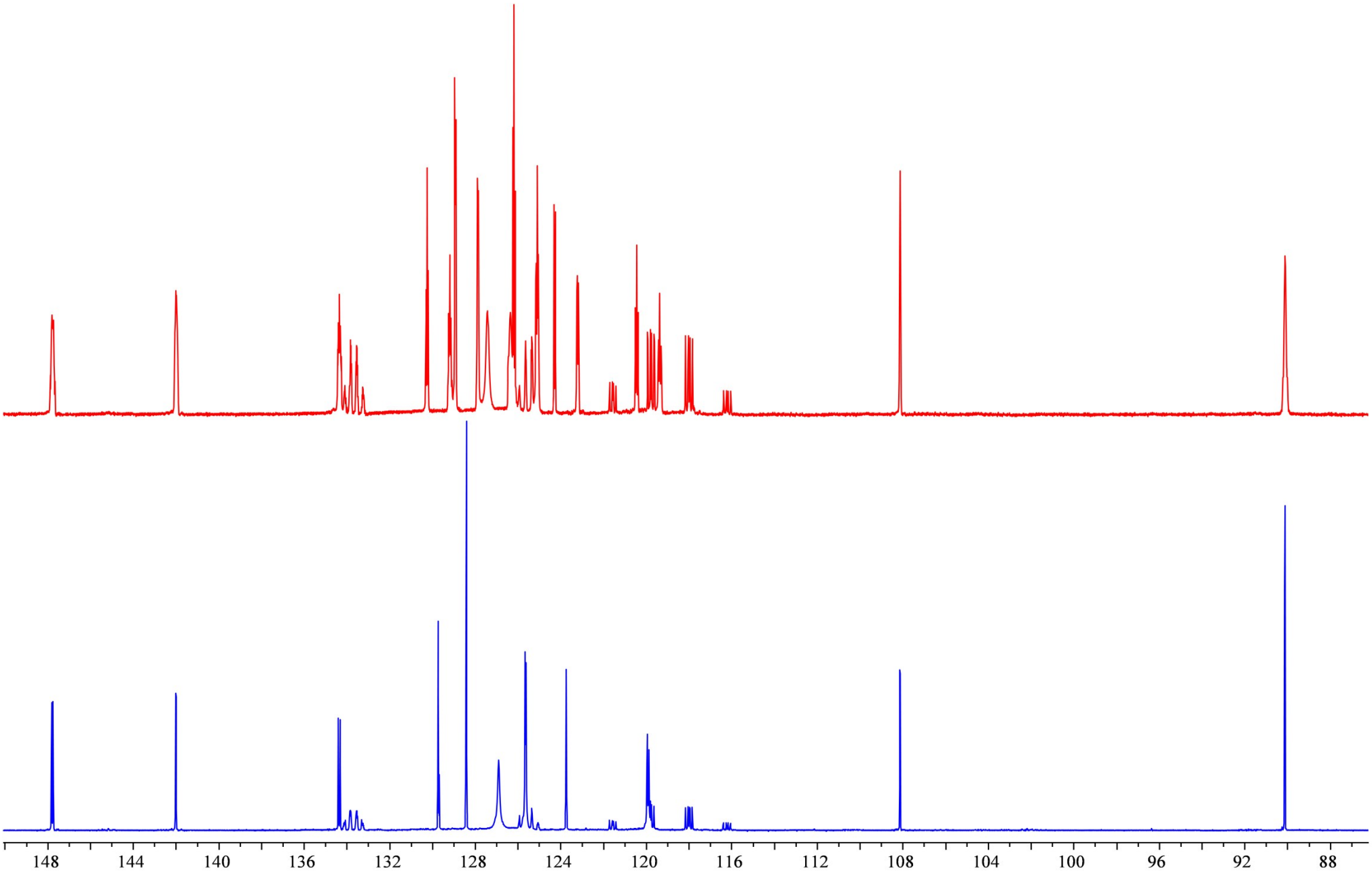

Figure 40. Fragments of ^{13}C-{^{1}H} and ^{13}C NMR spectra (100.6 MHz, $CDCl_3$) of compound (**3b**), the 88-149 ppm region is shown.

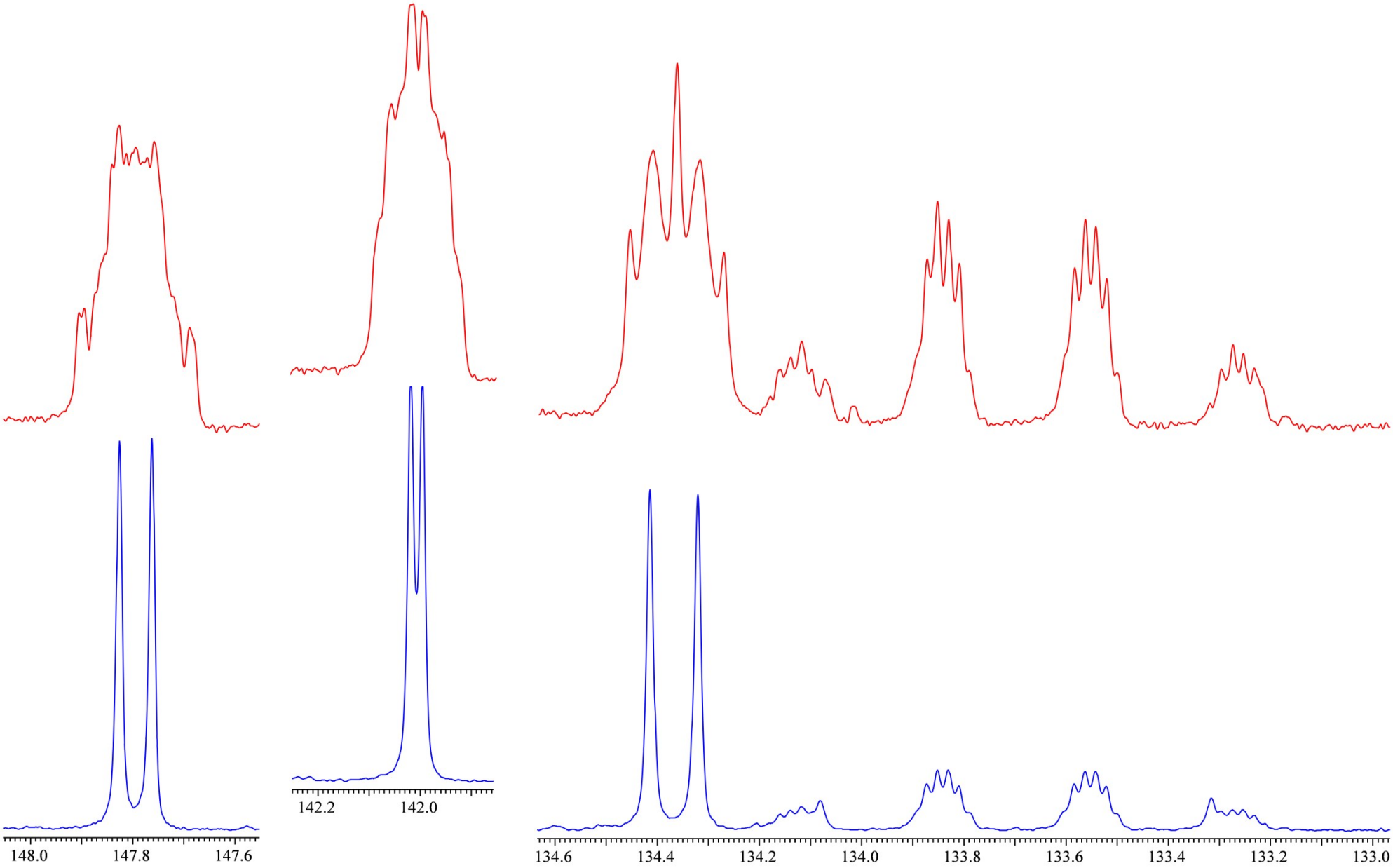

Figure 41. Fragments of ^{13}C-{^{1}H} and ^{13}C NMR spectra (100.6 MHz, $CDCl_3$) of compound (**3b**), the 147, 142 137-145 ppm regions are shown.

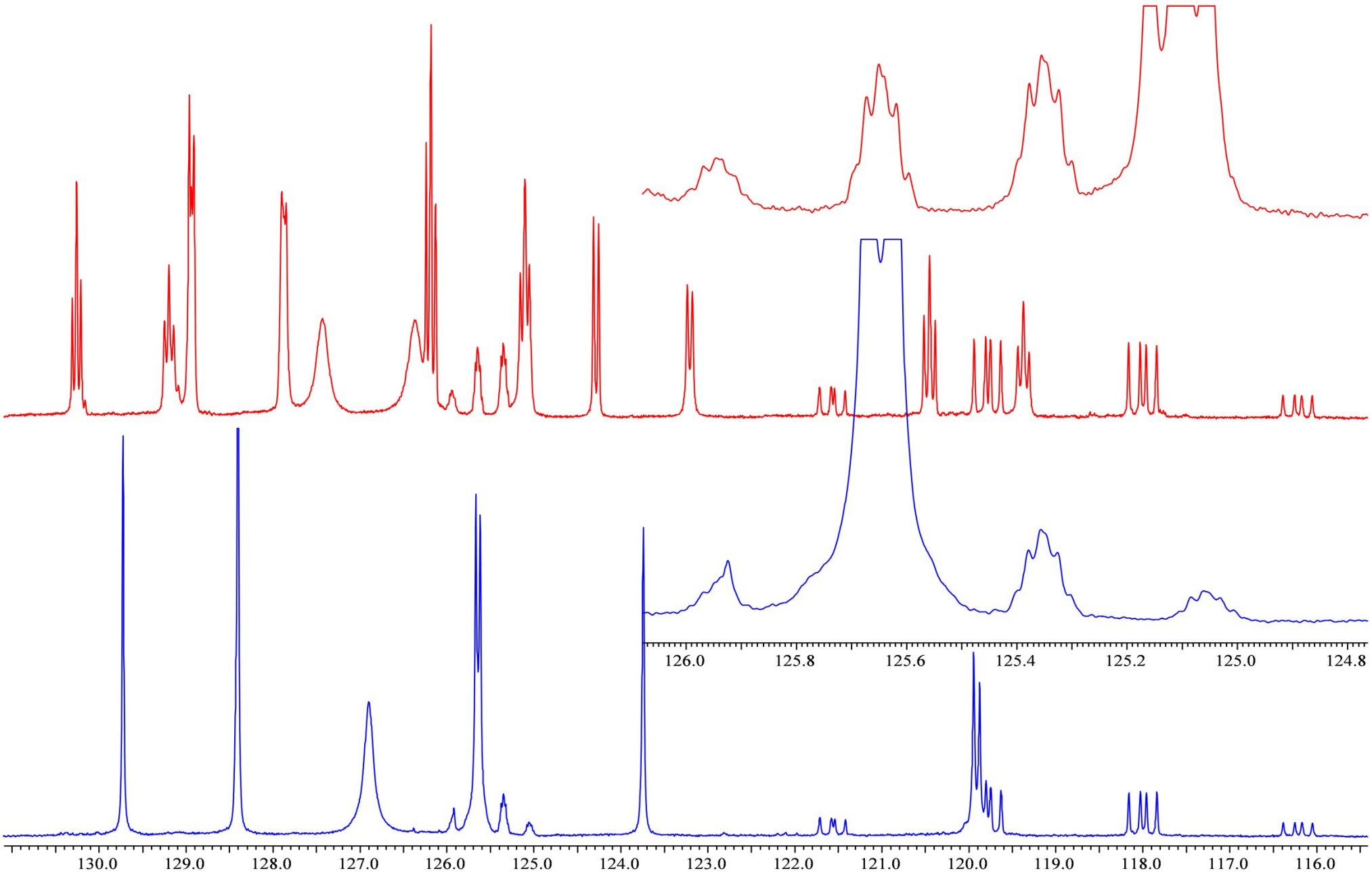

Figure 42. Fragments of ^{13}C-{^{1}H} and ^{13}C NMR spectra (100.6 MHz, $CDCl_3$) of compound (**3b**), aromatic carbon region is shown.

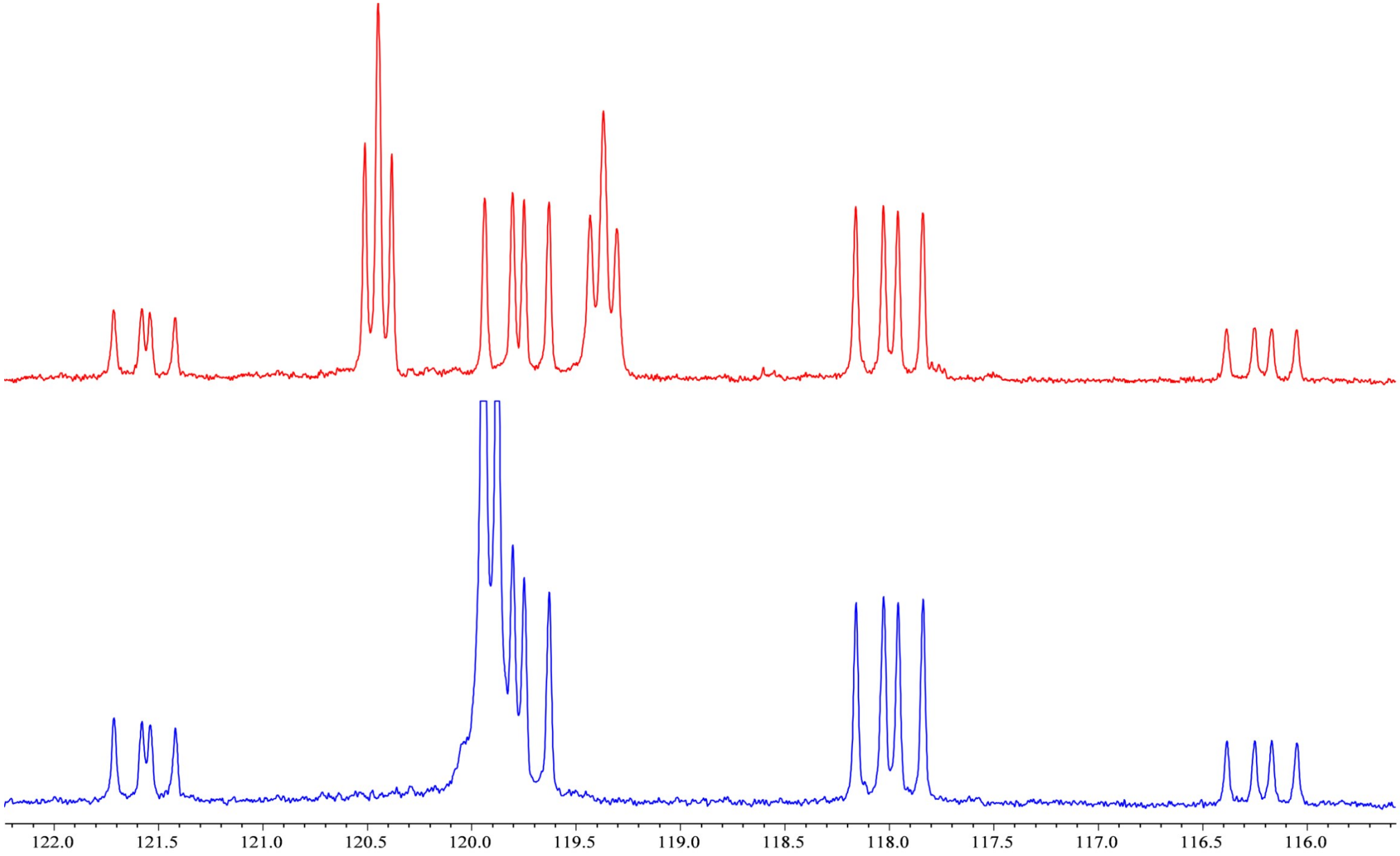

Figure 43. Fragments of ^{13}C-{^{1}H} and ^{13}C NMR spectra (100.6 MHz, $CDCl_3$) of compound (**3b**), trifluoromethyl groups region is shown.

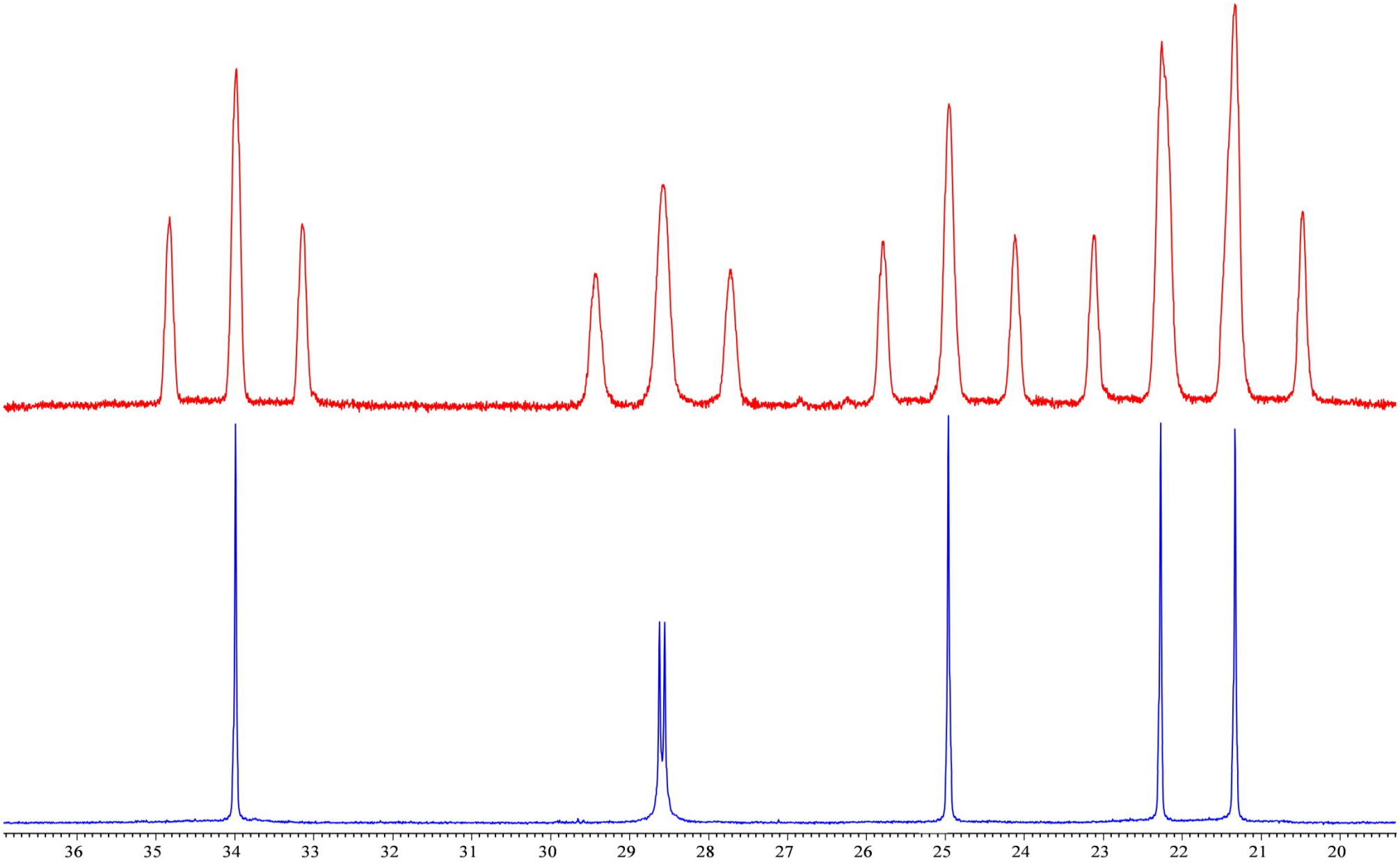

Figure 44. Up-field fragment of ^{13}C-{^{1}H} and ^{13}C NMR spectra (100.6 MHz, $CDCl_3$) of compound (**3b**).

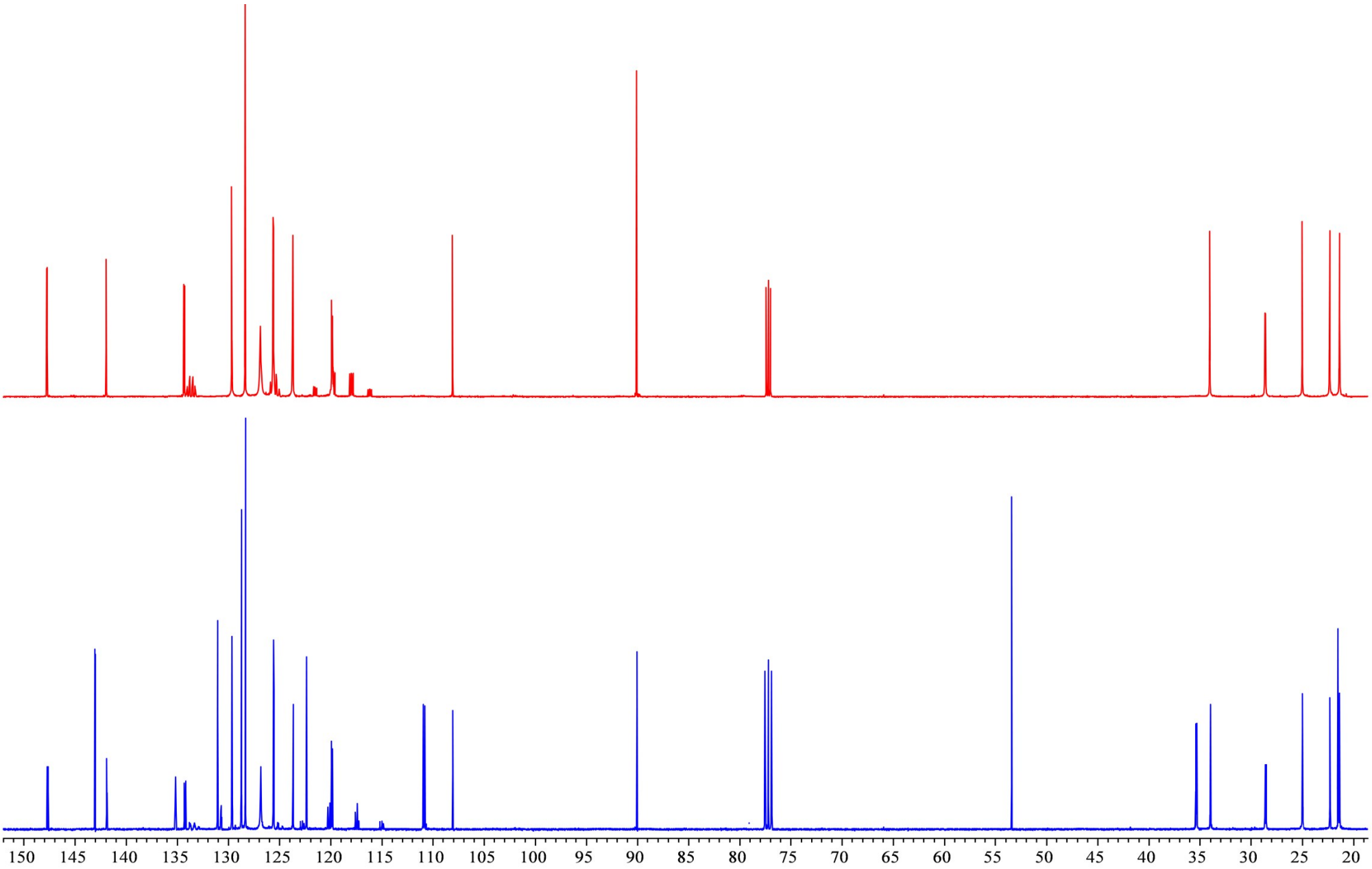

Figure 45. ^{13}C-{^{1}H} NMR spectra (100.6 MHz, $CDCl_3$, red; 150.9 MHz, $CH_2Cl_2/CDCl_3$, blue) of compound (**3b**, red) and its mixture with phosphorane (**4b**) in the ratio of 1 : 1 (10 days after the start of the reaction).

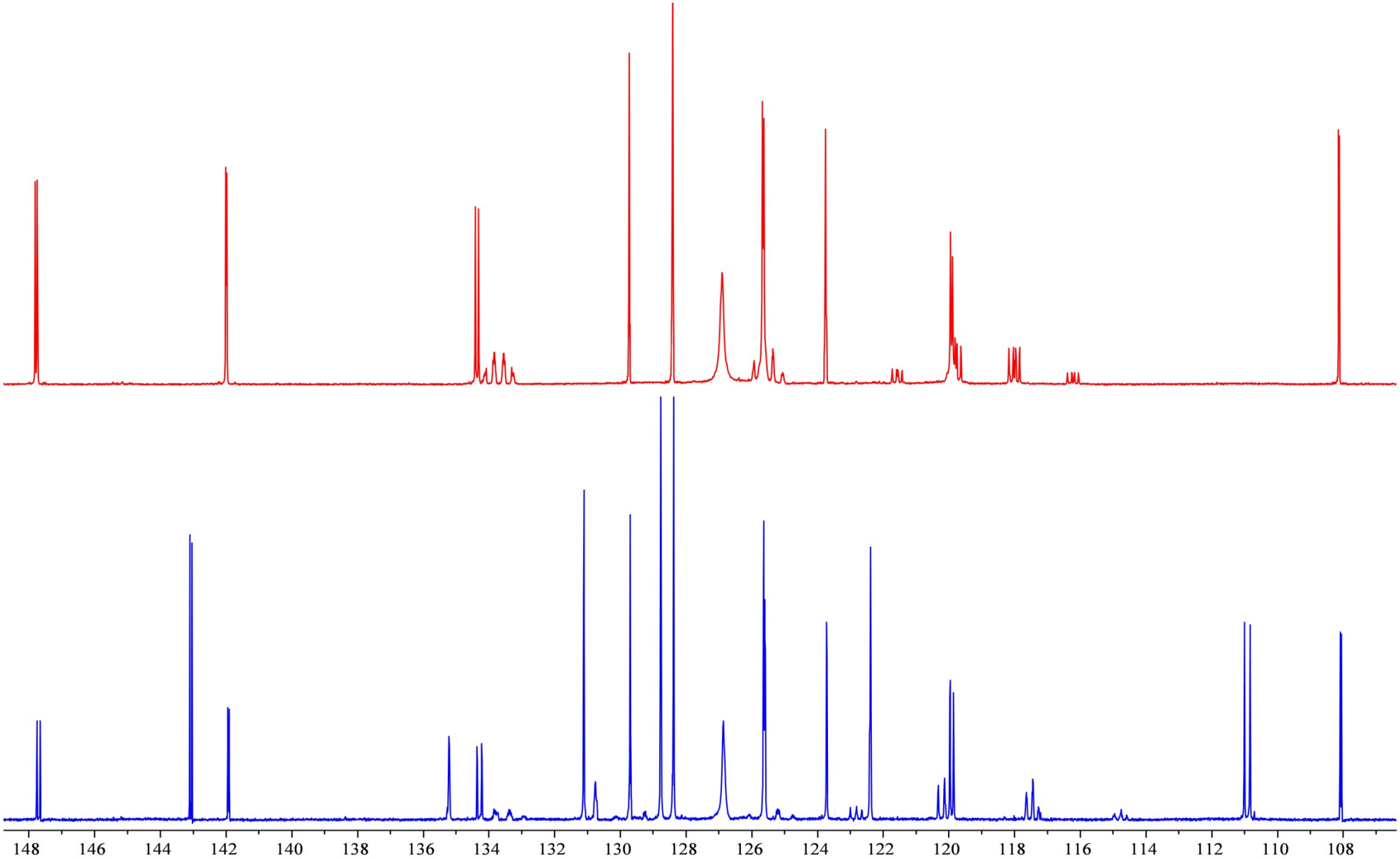

Figure 46. Fragments of ^{13}C-{^{1}H} NMR spectra (100.6 MHz, $CDCl_3$, red; 150.9 MHz, $CH_2Cl_2/CDCl_3$, blue) of compound (**3b**, red) and its mixture with phosphorane (**4b**) in the ratio of 1 : 1 (10 days after the start of the reaction).

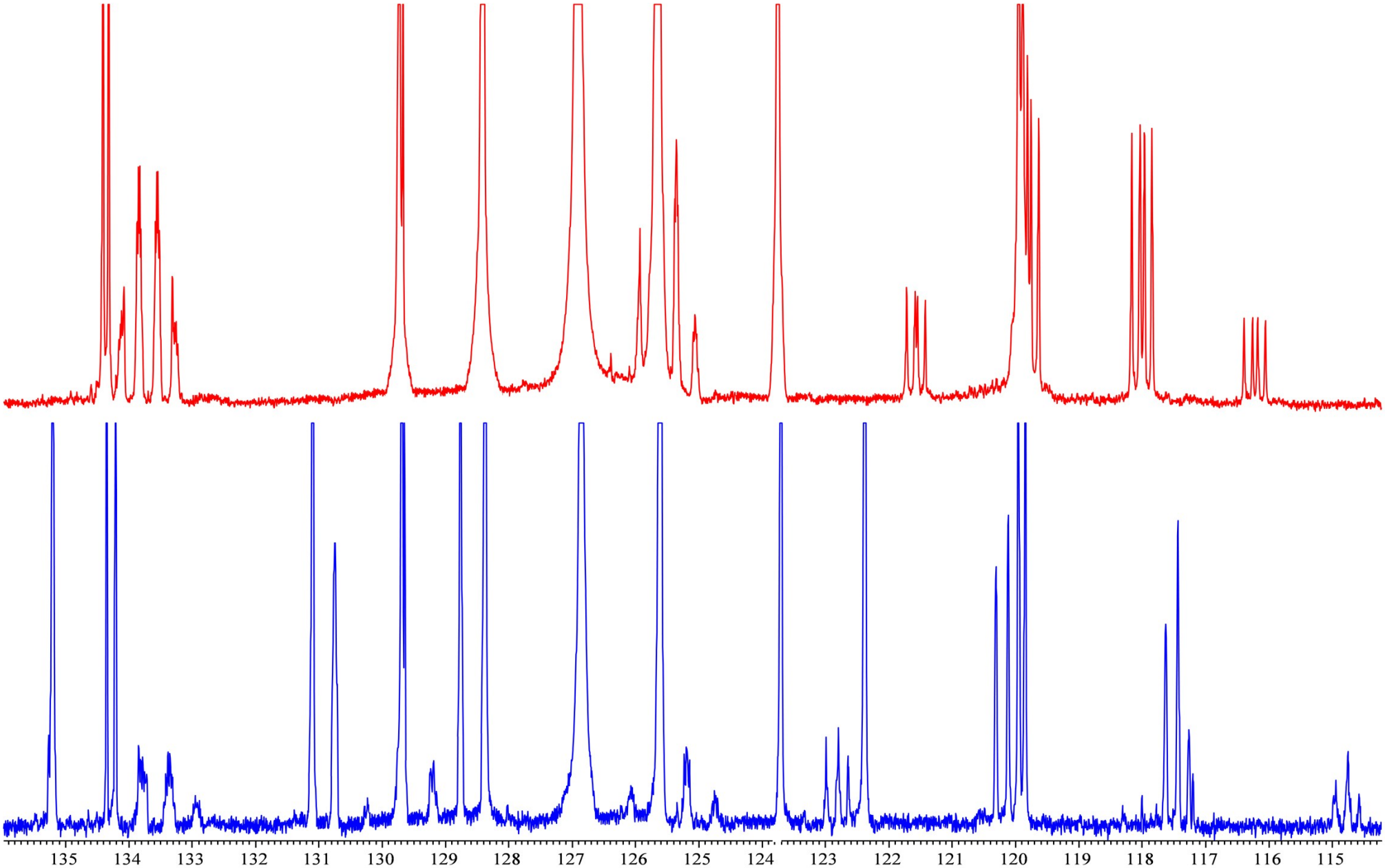

Figure 47. Fragments of ^{13}C-{^{1}H} NMR spectra (100.6 MHz, $CDCl_3$, red; 150.9 MHz, $CH_2Cl_2/CDCl_3$, blue) of compound (**3b**, red) and its mixture with phosphorane (**4b**) in the ratio of 1 : 1 (10 days after the start of the reaction), the 114-136 ppm region is shown.

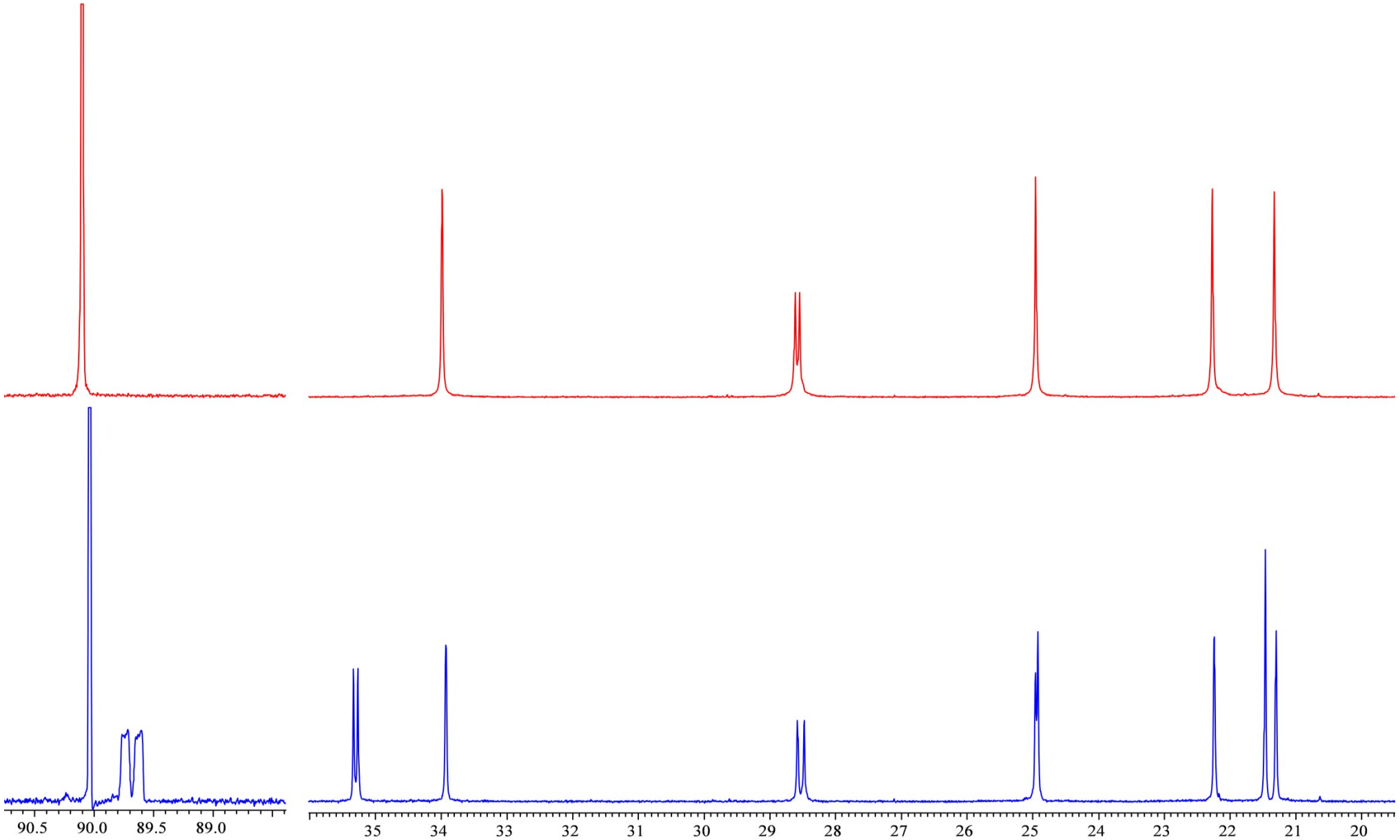

Figure 48. Up-field fragments of ^{13}C-{^{1}H} NMR spectra (100.6 MHz, $CDCl_3$, red; 150.9 MHz, $CH_2Cl_2/CDCl_3$, blue) of compound (**3b**, red) and its mixture with phosphorane (**4b**) in the ratio of 1 : 1 (10 days after the start of the reaction).

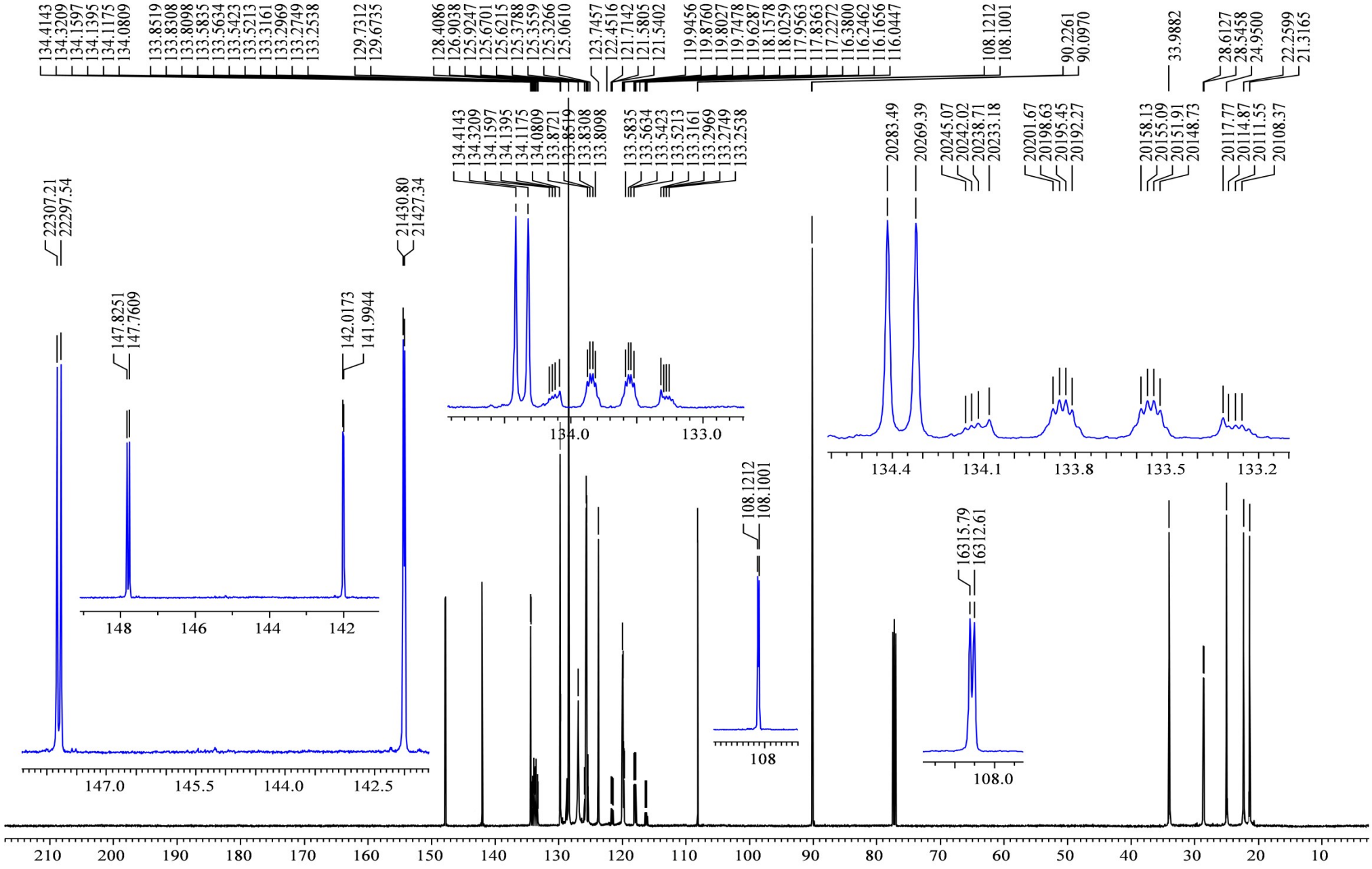

Figure 49. ^{13}C-{^{1}H} NMR spectrum (100.6 MHz, $CDCl_3$) of compound (**3b**).

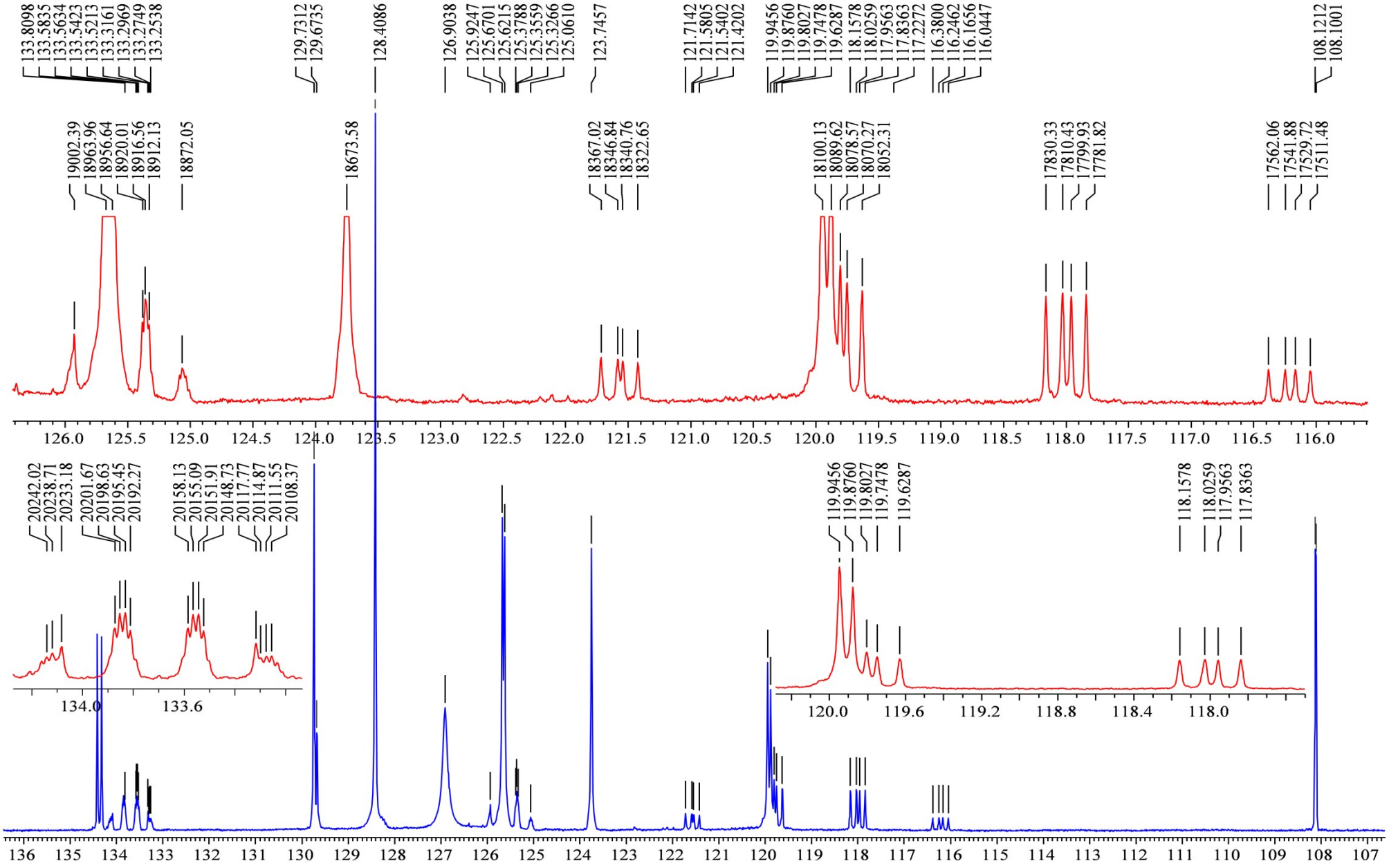

Figure 50. Fragment of ^{13}C-{^{1}H} NMR spectrum (100.6 MHz, $CDCl_3$) of compound (**3b**), the 107-136 ppm region is shown.

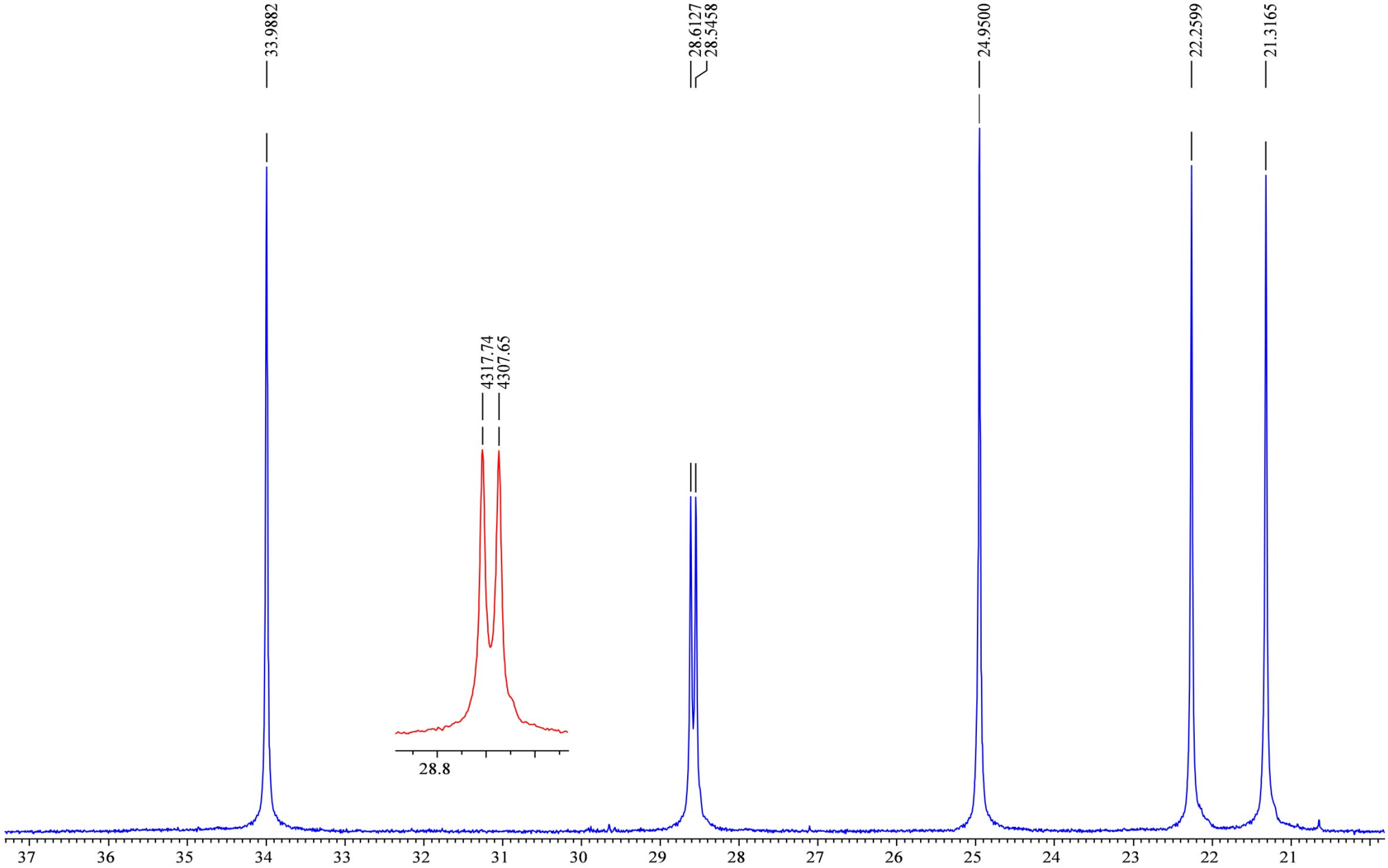

Figure 51. Up-field fragment of ^{13}C-{^{1}H} NMR spectrum (100.6 MHz, $CDCl_3$) of compound (**3b**).

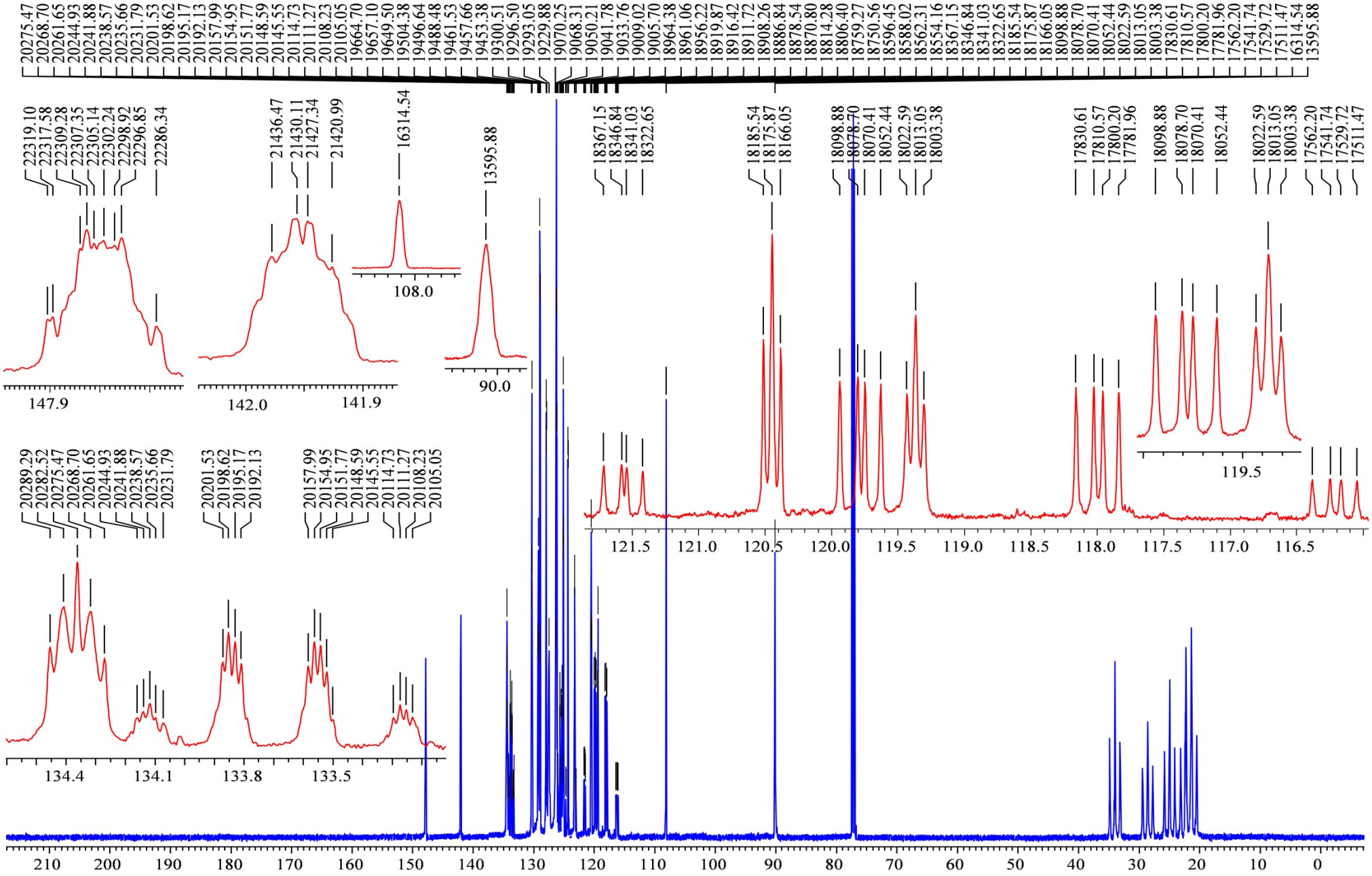

Figure 52. ^{13}C NMR spectrum (100.6 MHz, $CDCl_3$) of compound (**3b**).

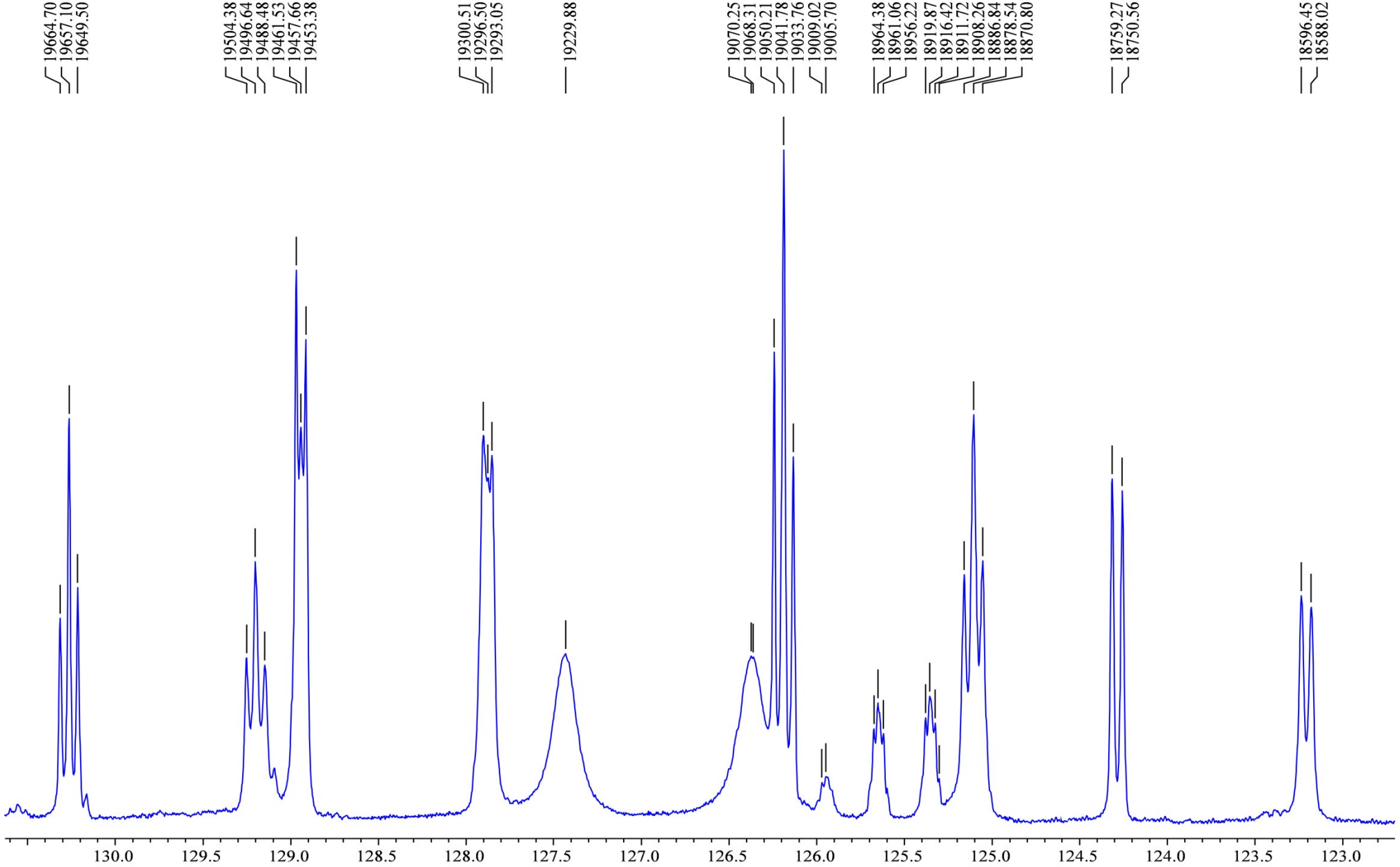

Figure 53. Fragment of ^{13}C NMR spectrum (100.6 MHz, $CDCl_3$) of compound (**3b**), the 122-131 ppm region is shown.

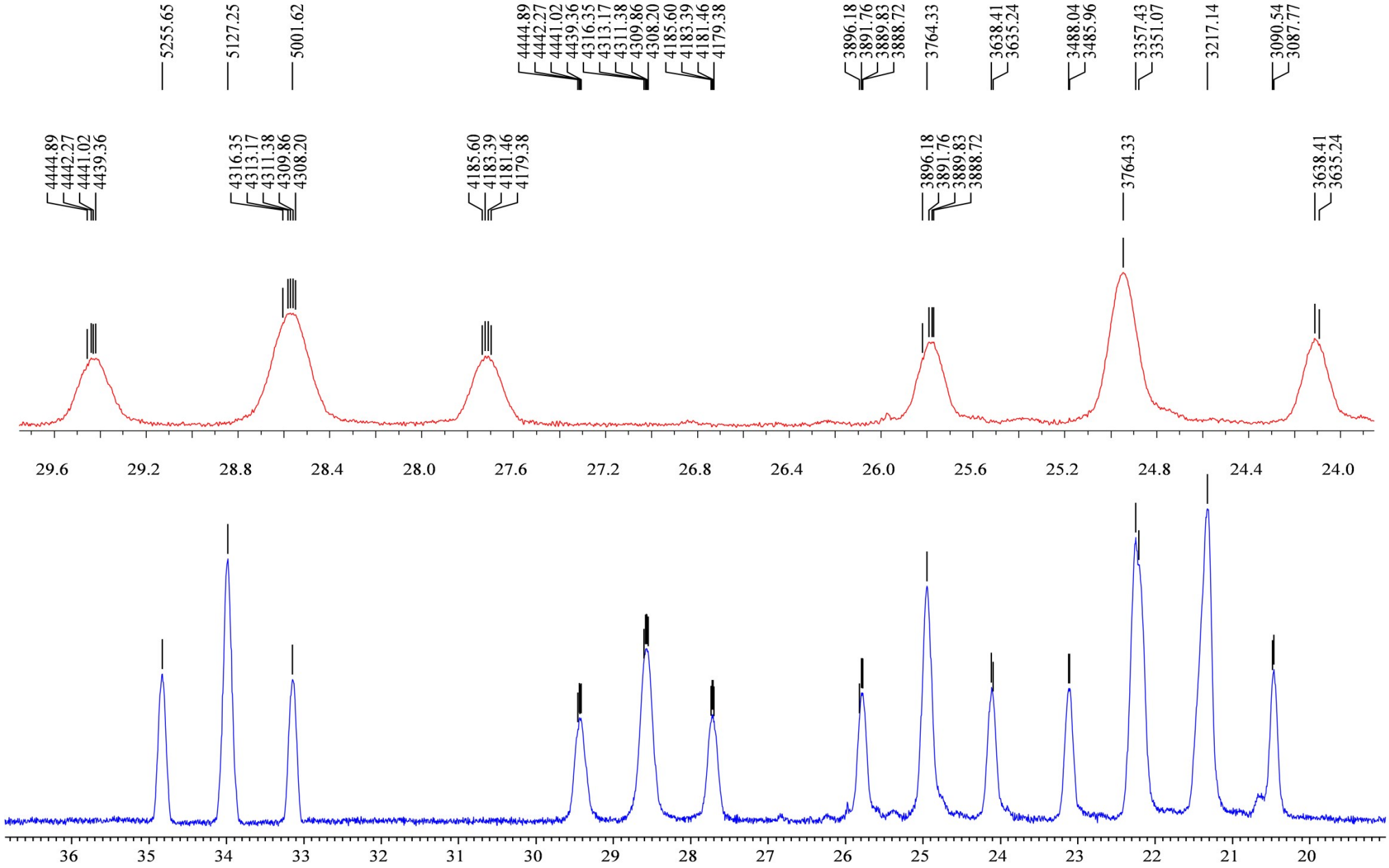

Figure 54. Up-field fragments of ^{13}C NMR spectrum (100.6 MHz, $CDCl_3$) of compound (**3b**).

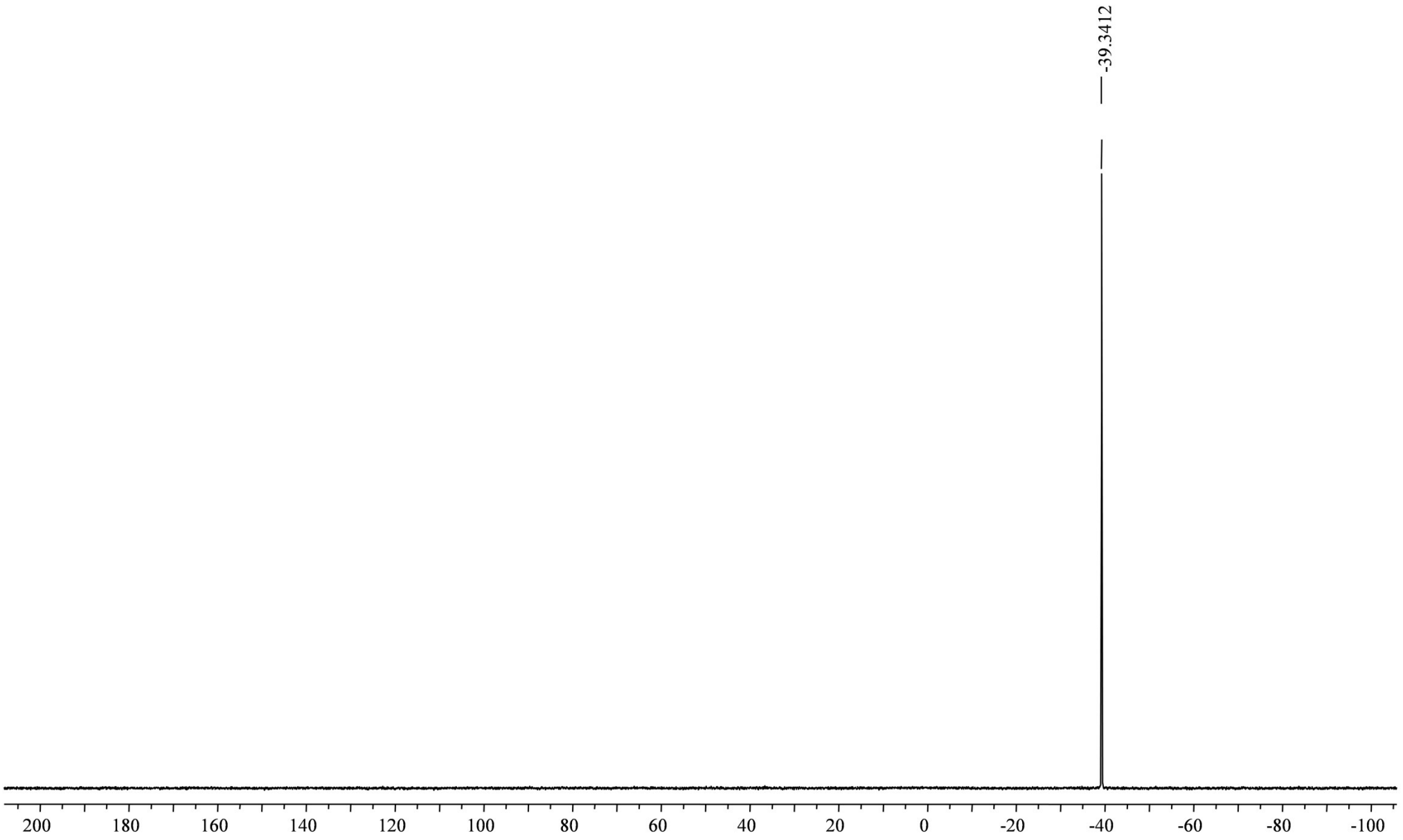

Figure 55. ^{31}P-{^{1}H} NMR spectrum (242.94 MHz, acetone-d_6) of compound (**3b**).

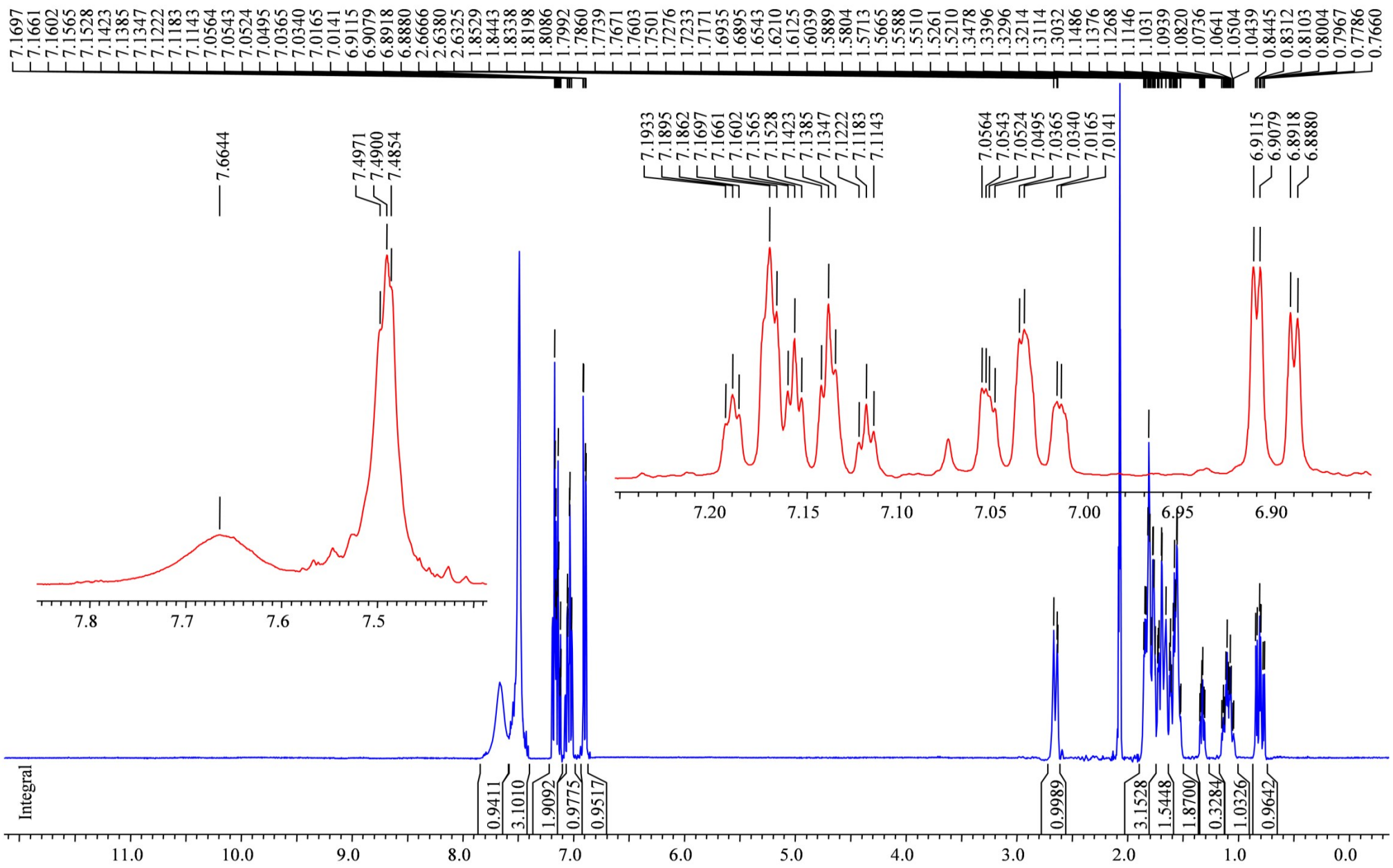

Figure 56. ^{1}H NMR spectrum (600 MHz, acetone-d_6) of compound (**3b**).

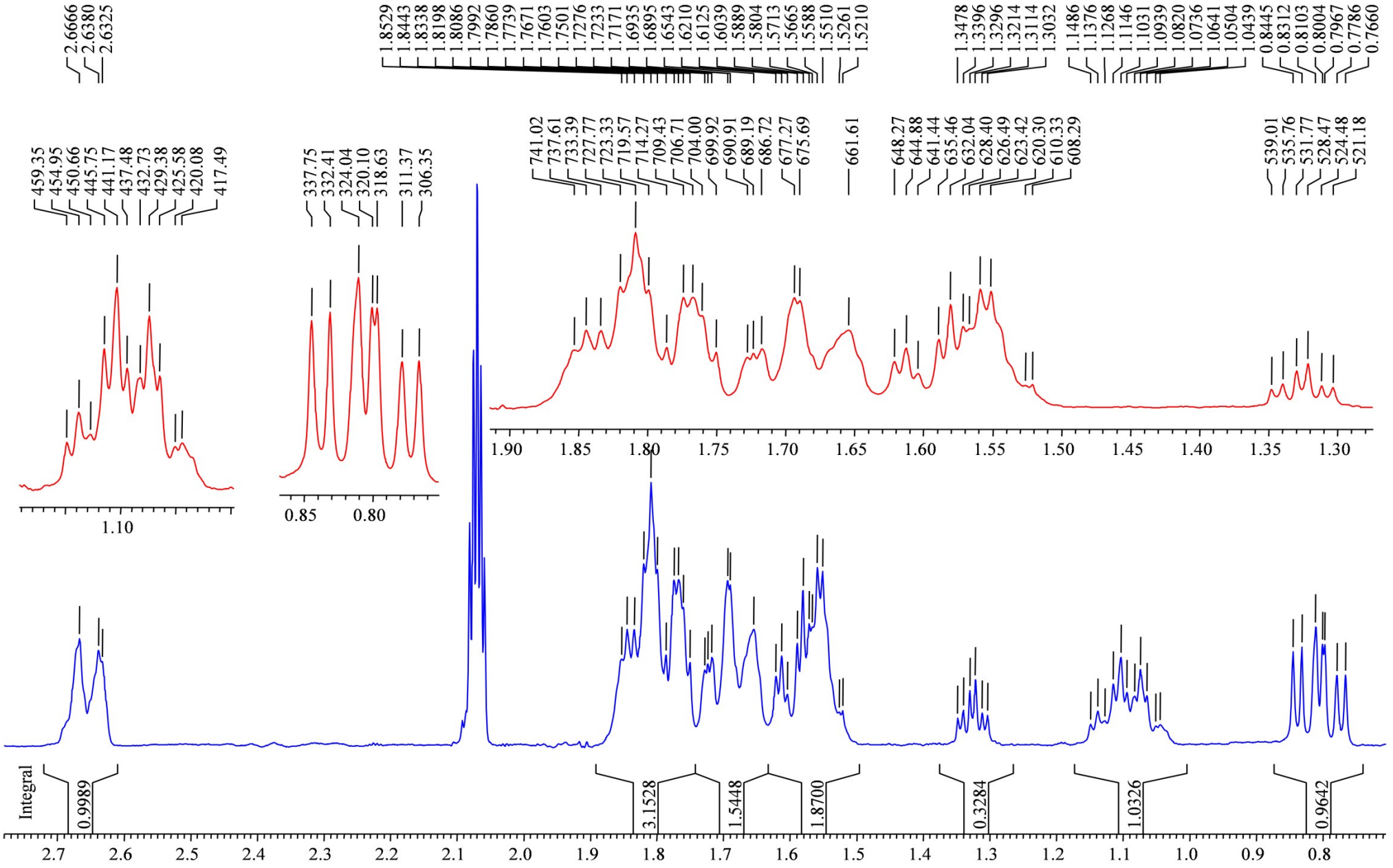

Figure 57. Fragments of ^{1}H NMR spectrum (600 MHz, acetone-d_6) of compound (**3b**).

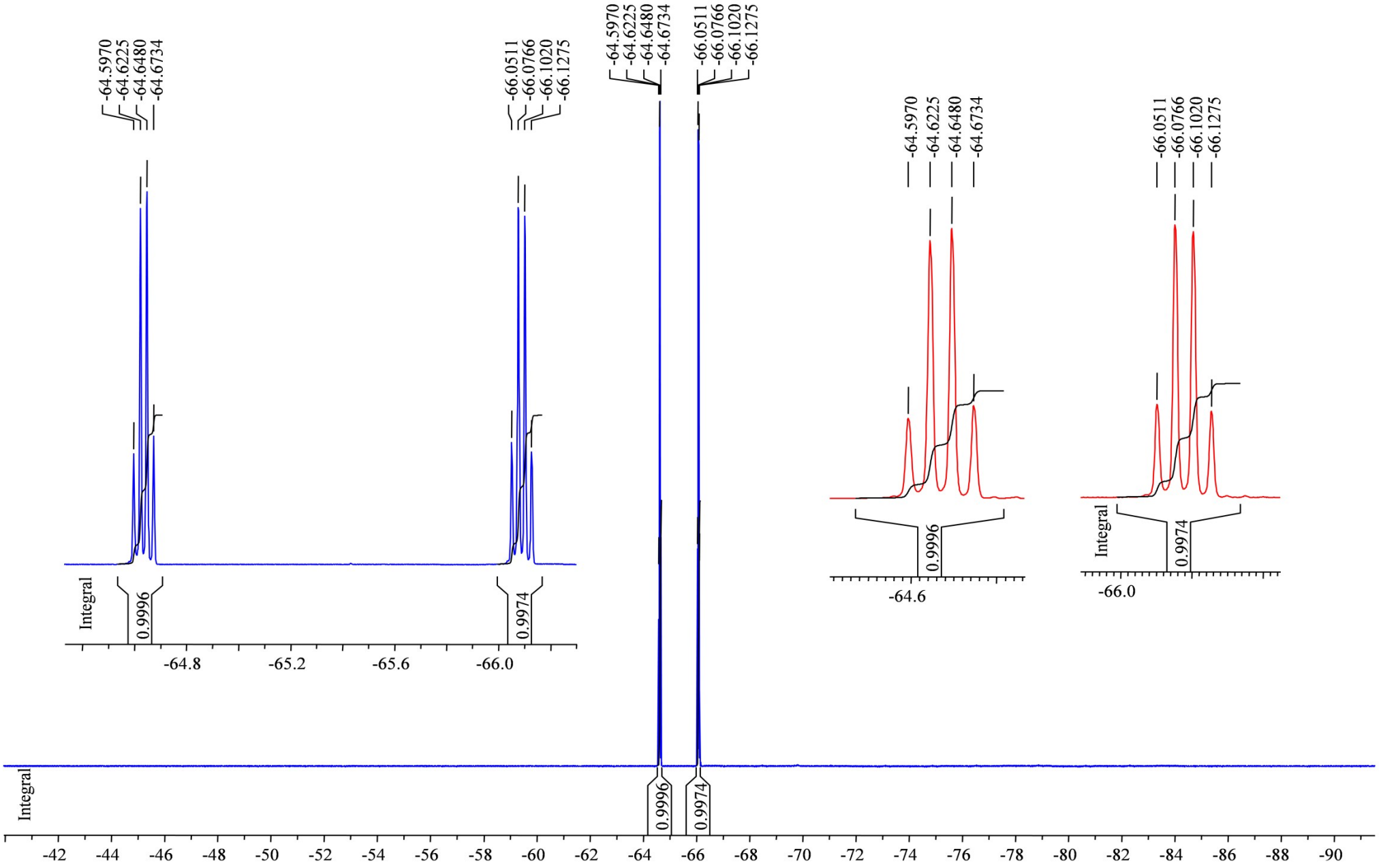

Figure 58. ^{19}F NMR spectrum (376.3 MHz, acetone-d_6) of compound (**3b**).

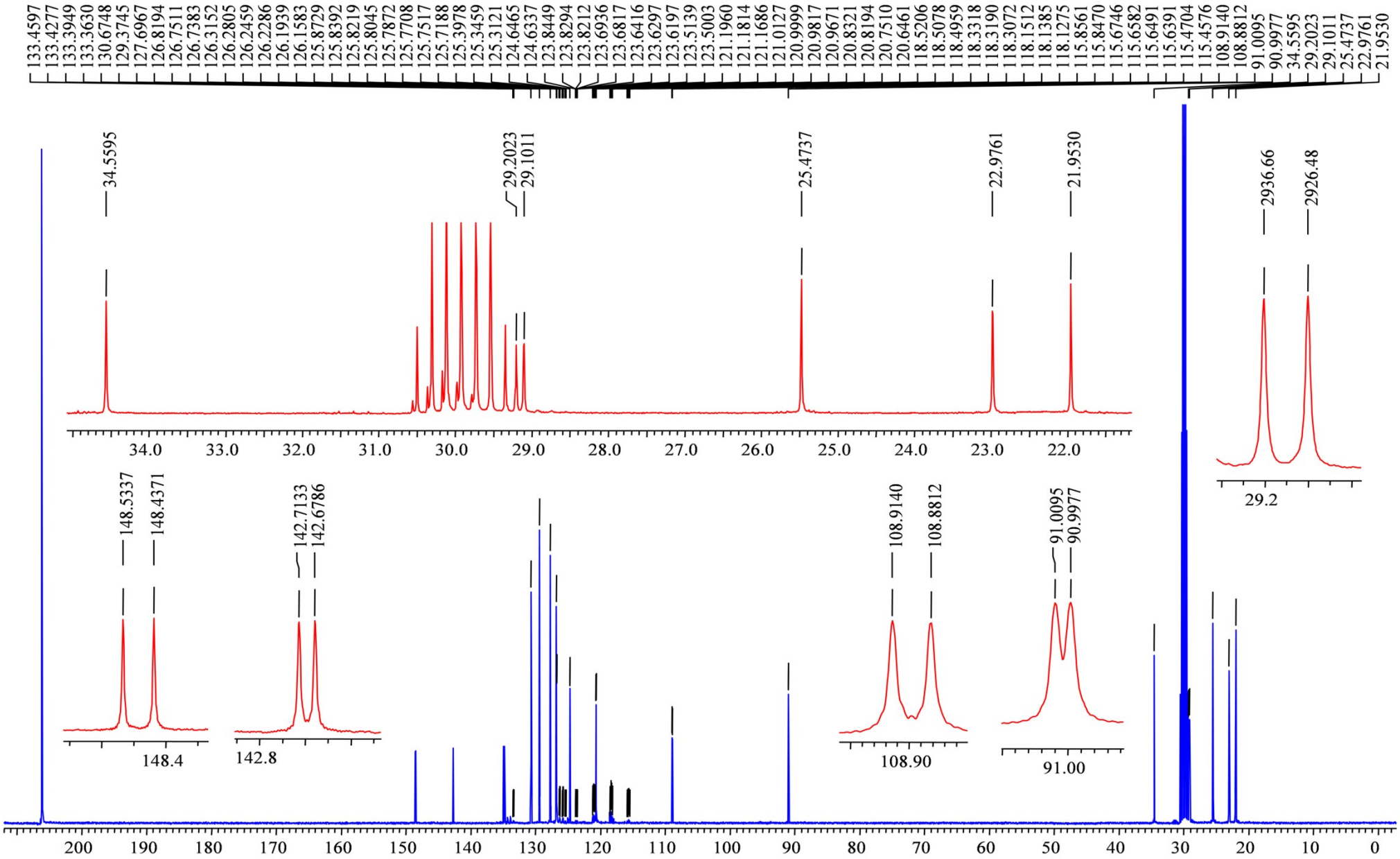

Figure 59. ^{13}C-{^{1}H} NMR spectrum (100.6 MHz, acetone-d_6) of compound (**3b**).

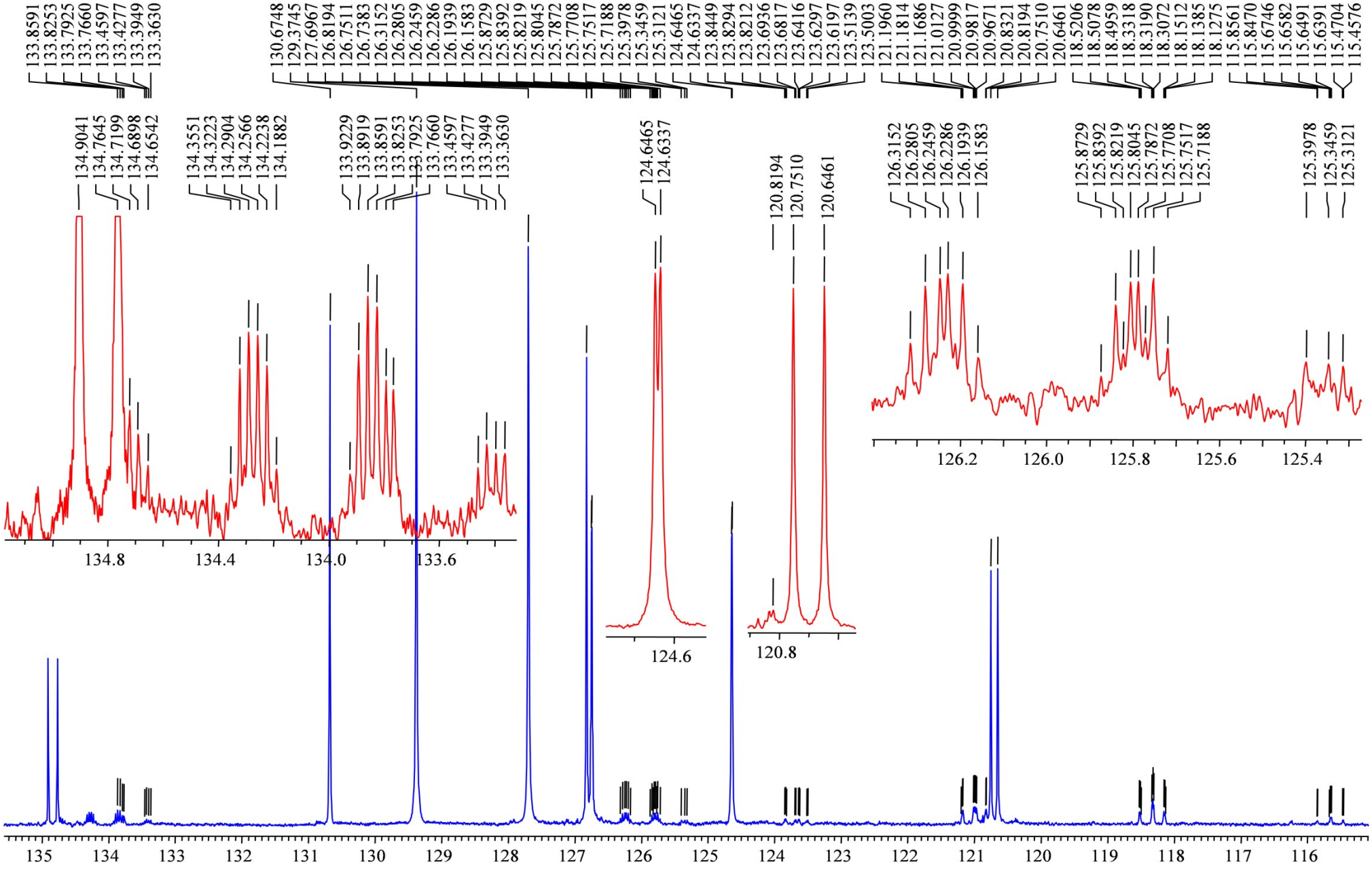

Figure 60. Fragment of ^{13}C-{^{1}H} NMR spectrum (100.6 MHz, acetone-d_6) of compound (**3b**), aromatic carbons region is shown.

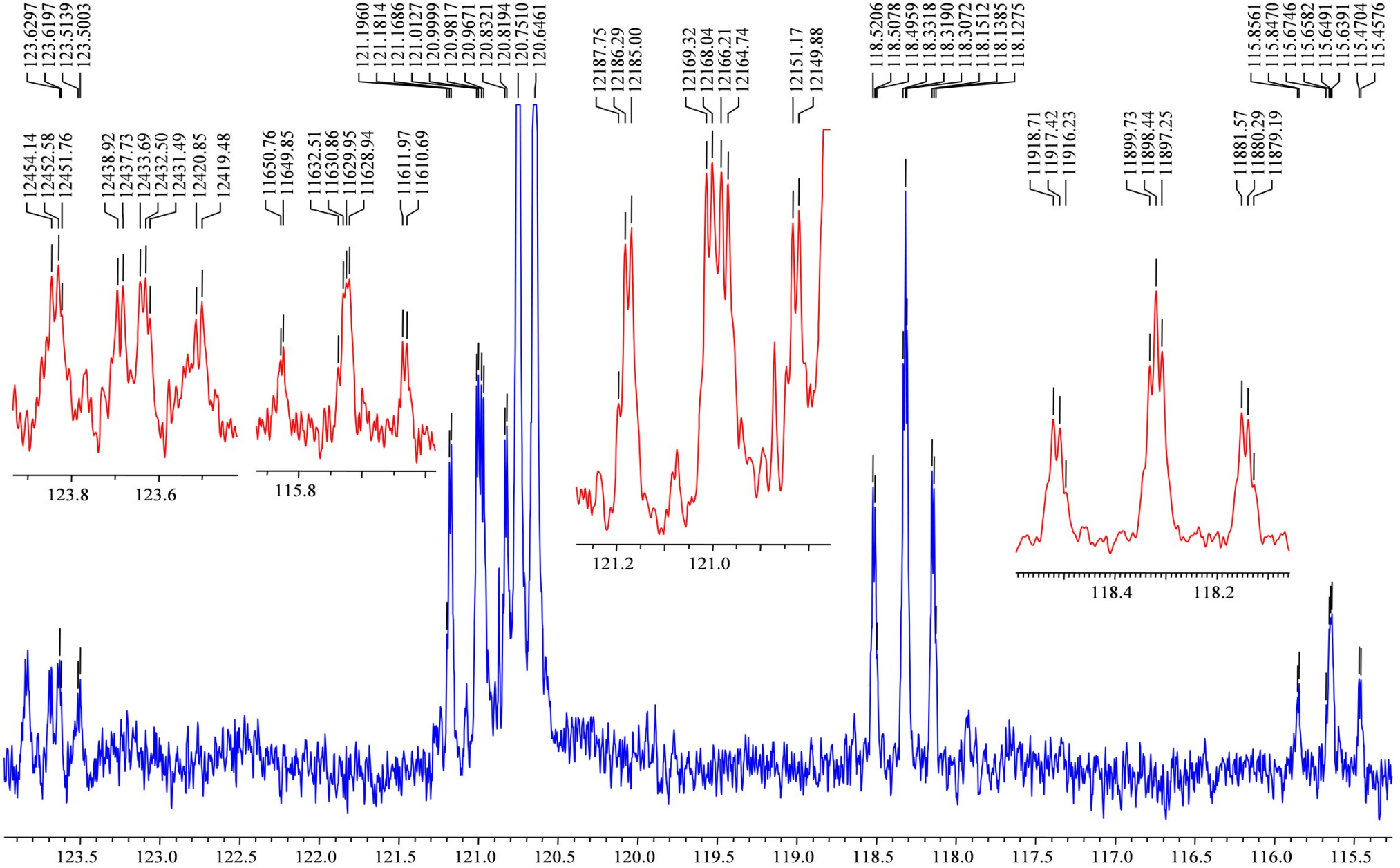

Figure 61. Fragment of ^{13}C-{^{1}H} NMR spectrum (100.6 MHz, acetone-d_6) of compound (**3b**), trifluoromethyl groups region is shown.

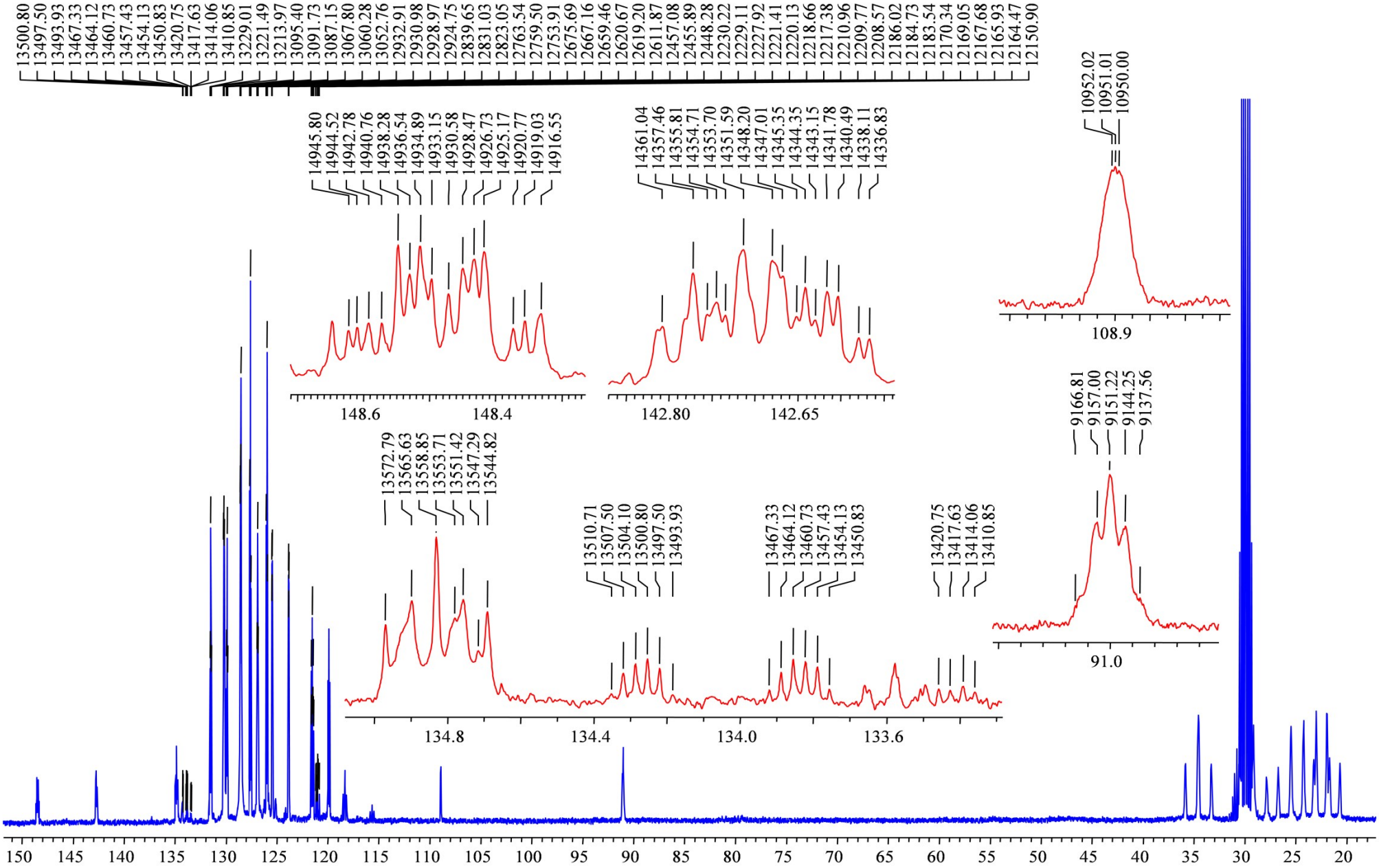

Figure 62. ^{13}C NMR spectrum (100.6 MHz, acetone-d_6) of compound (**3b**).

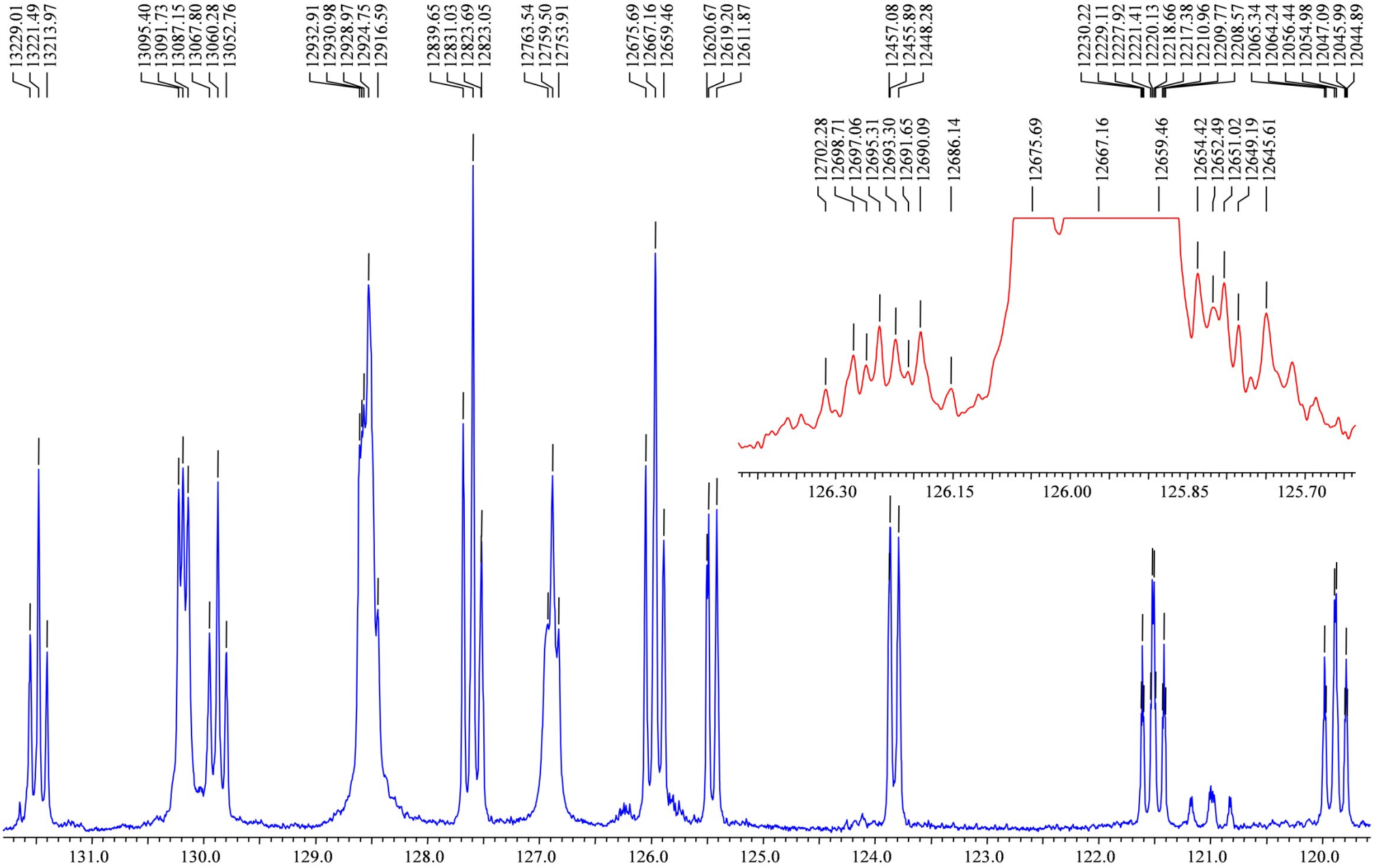

Figure 63. Fragment of ^{13}C NMR spectrum (100.6 MHz, acetone-d_6) of compound (**3b**), aromatic carbons region is shown.

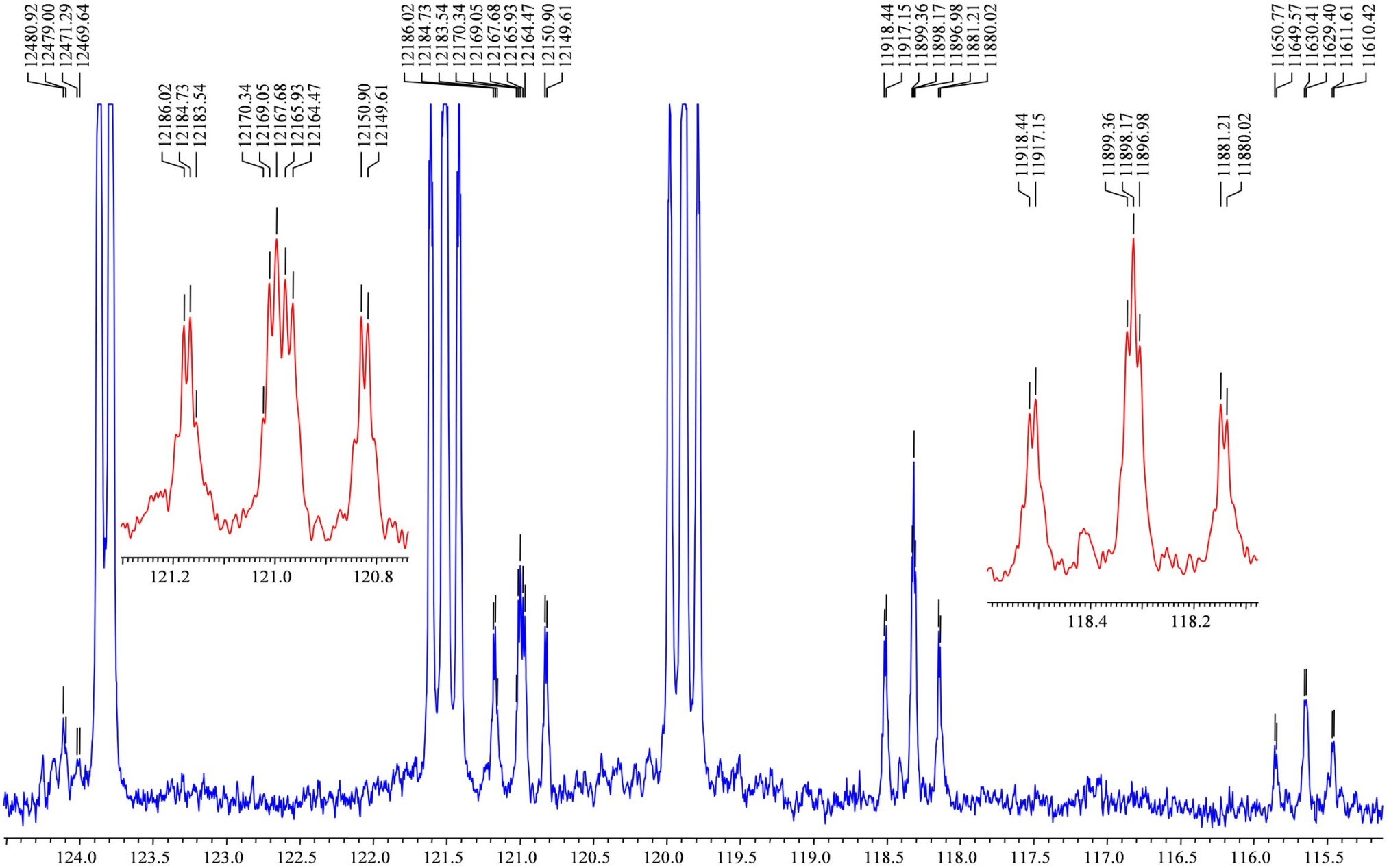

Figure 64. Fragment of ^{13}C NMR spectrum (100.6 MHz, acetone-d_6) of compound (**3b**), trifluoromethyl groups region is shown.

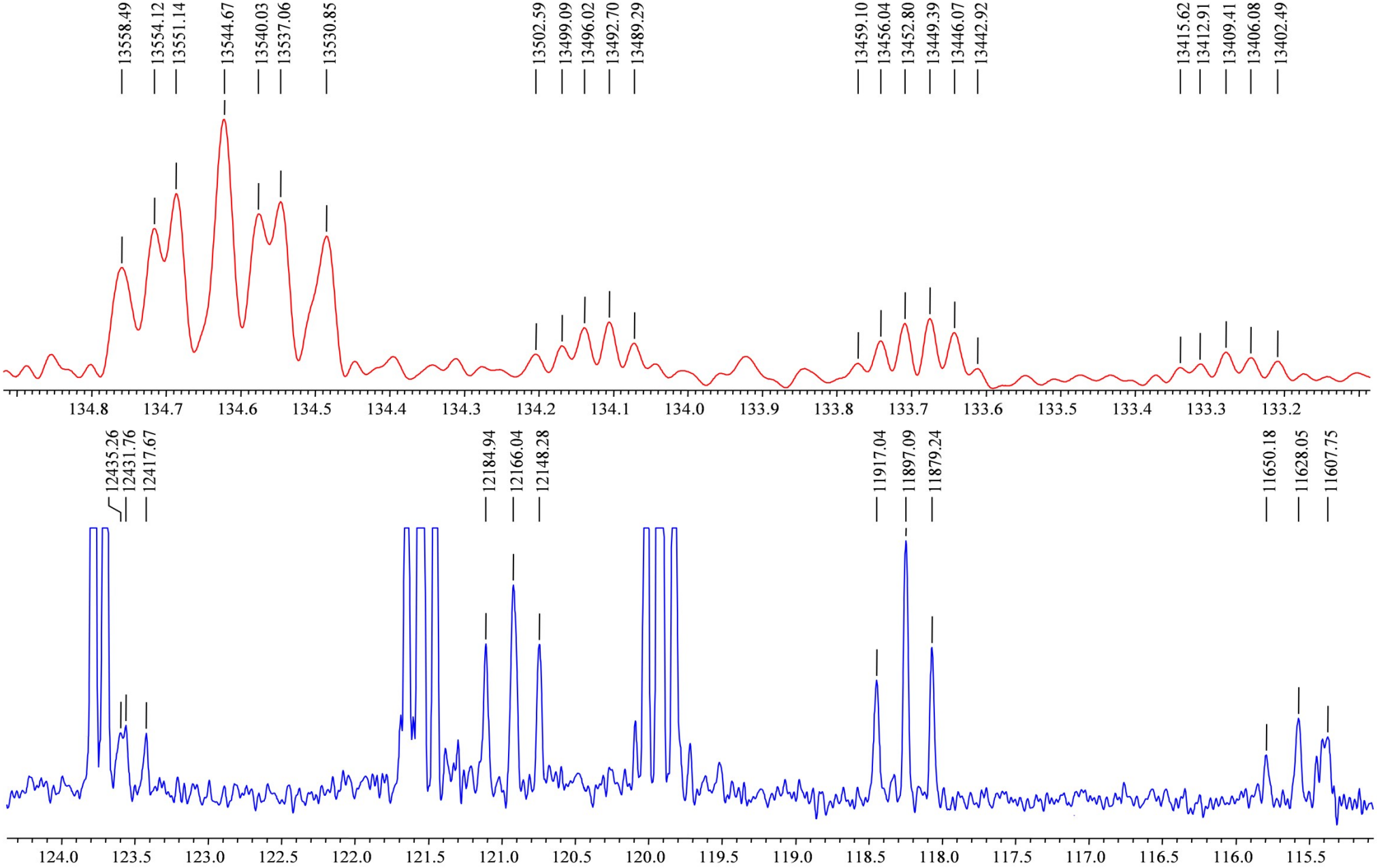

Figure 65. Fragments of ^{13}C NMR spectrum (100.6 MHz, acetone-d_6) of compound (**3b**), the 133-135 and 115-124 ppm regions are shown.

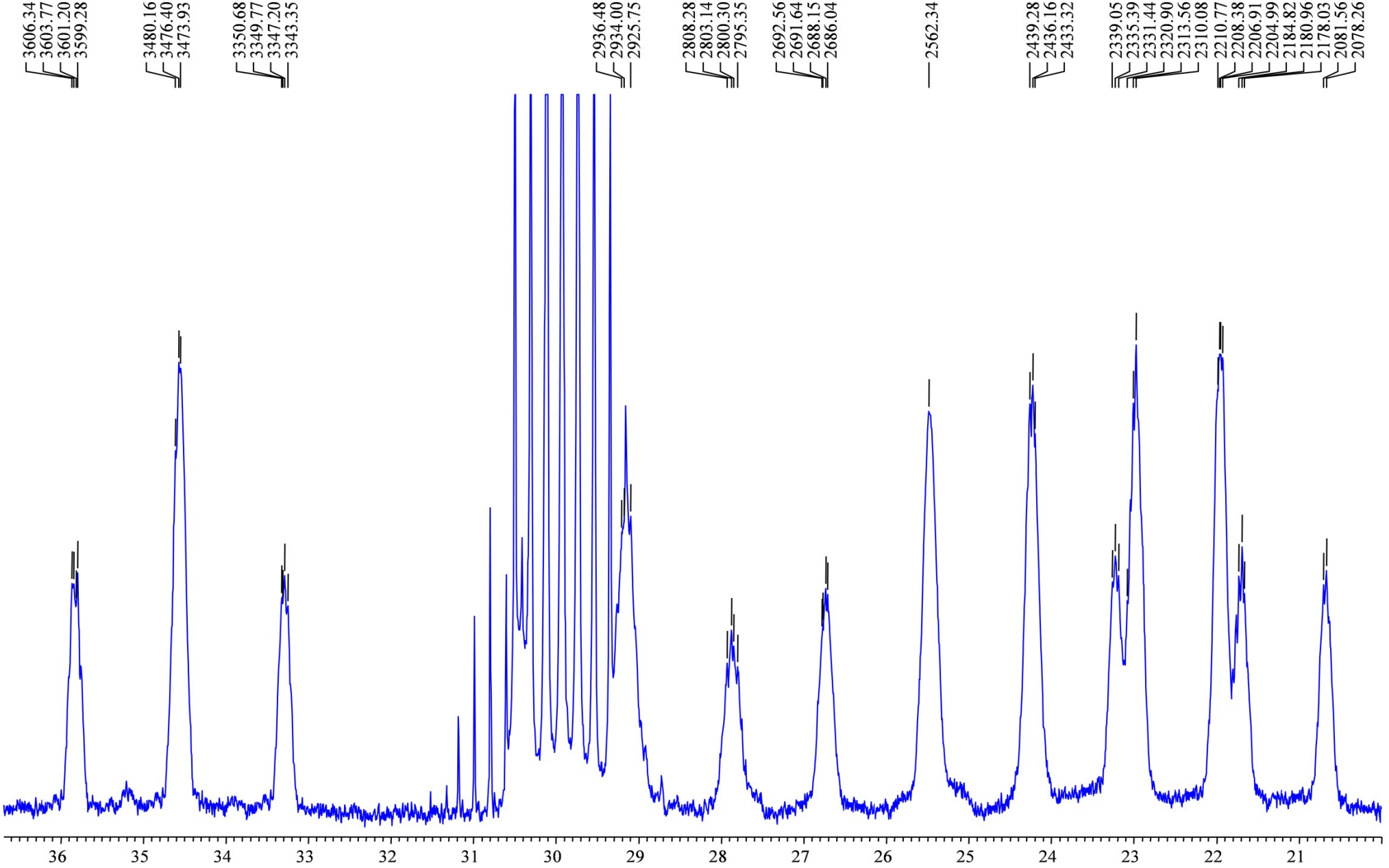

Figure 66. Up-field region of ^{13}C NMR spectrum (100.6 MHz, acetone-d_6) of compound (**3b**).

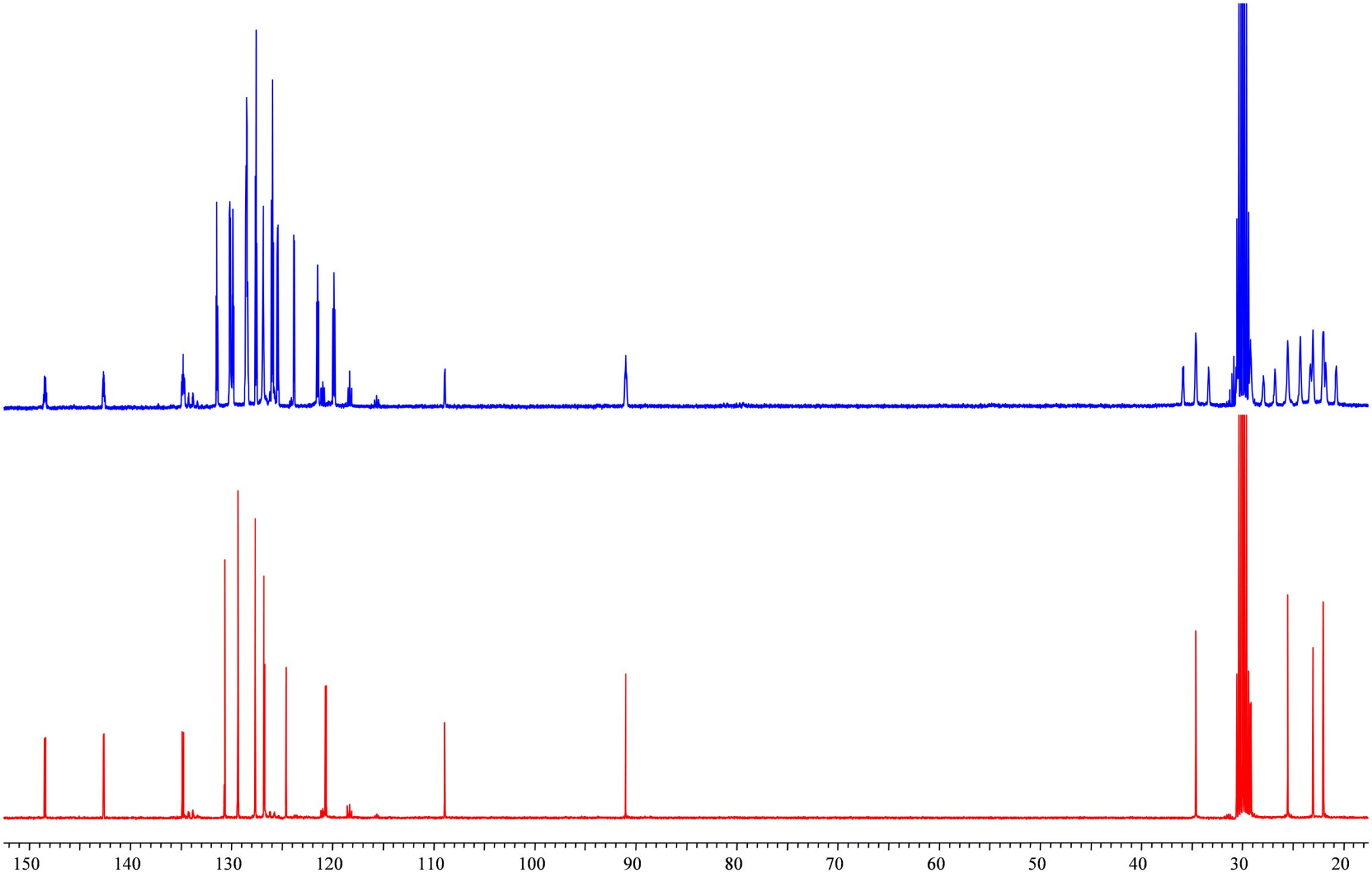

Figure 67. ^{13}C-{^{1}H} and ^{13}C NMR spectra (100.6 MHz, acetone-d_6) of compound (**3b**).

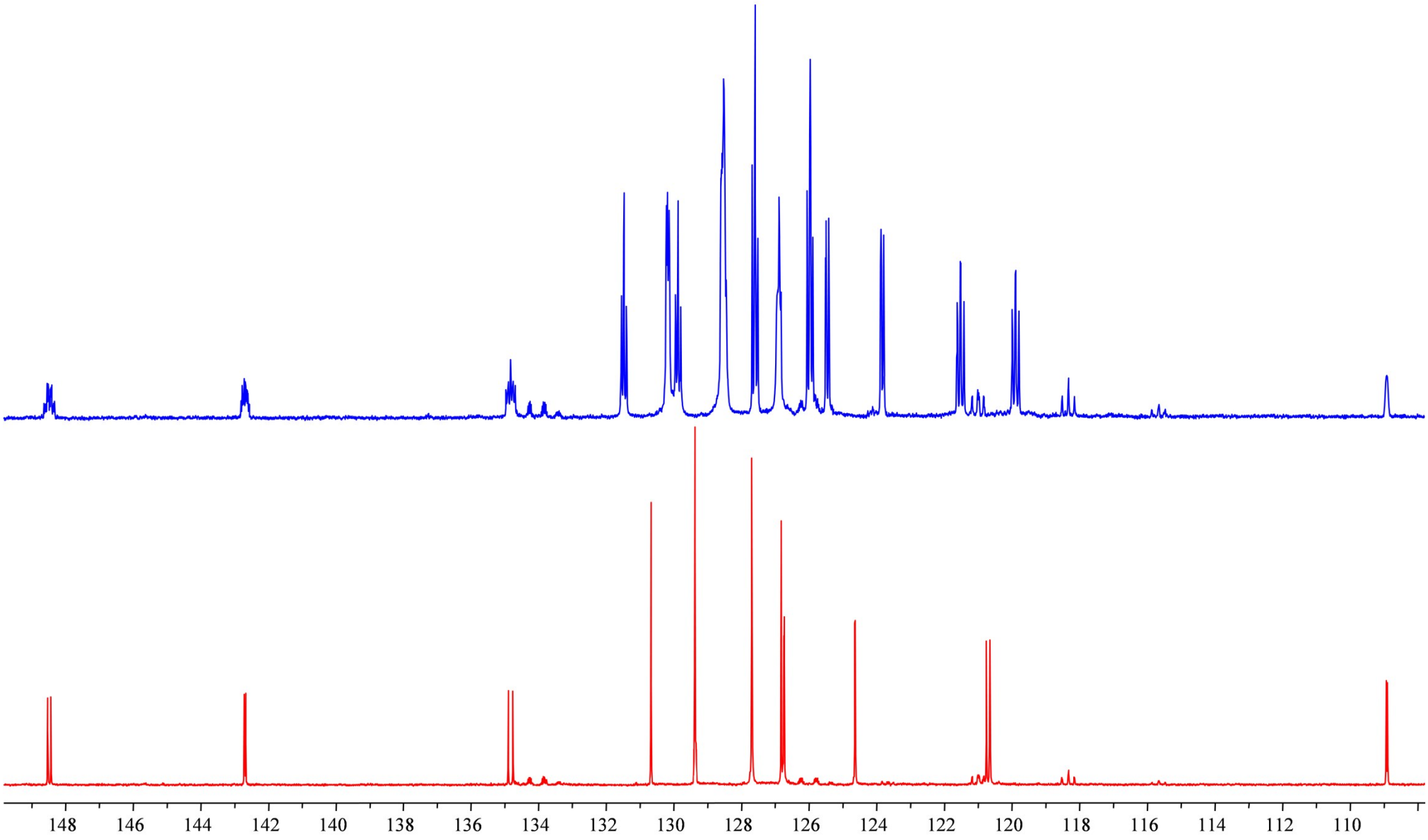

Figure 68. ^{13}C-{^{1}H} and ^{13}C NMR spectra (100.6 MHz, acetone-d_6) of compound (**3b**), aromatic carbons region is shown.

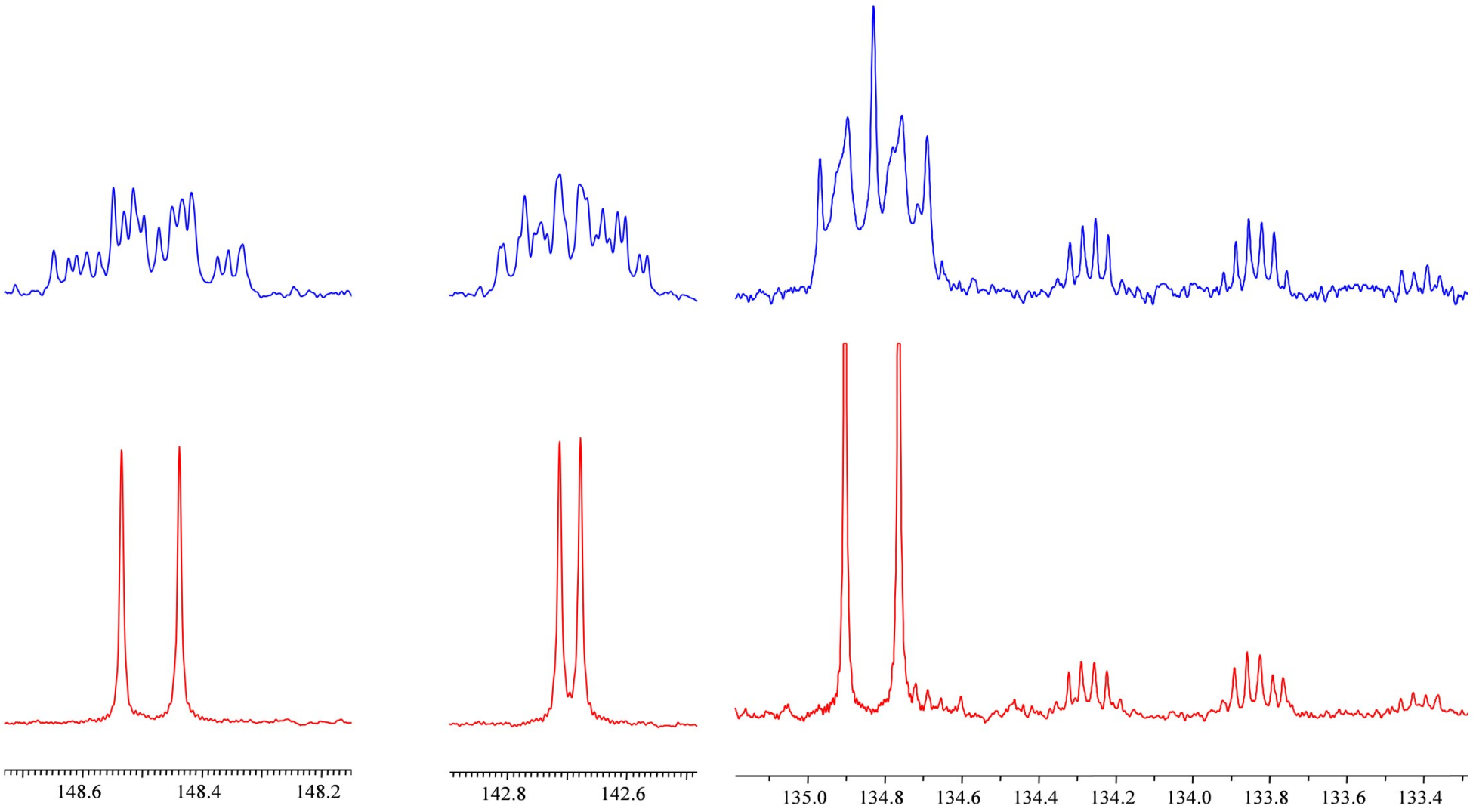

Figure 69. Fragments of ^{13}C-{^{1}H} and ^{13}C NMR spectra (100.6 MHz, acetone-d_6) of compound (**3b**), the 148, 142 and 133-135 ppm regions are shown.

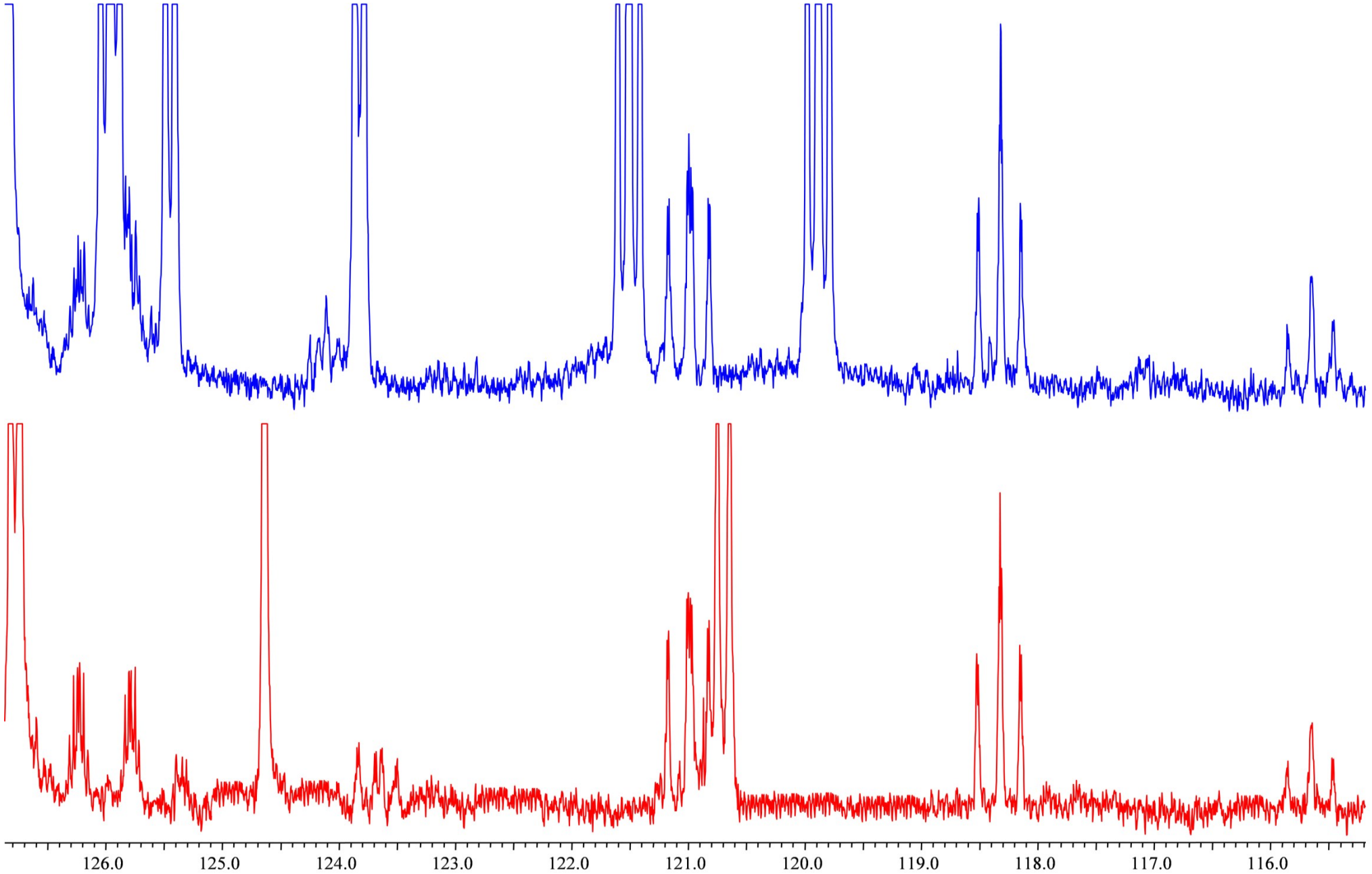

Figure 70. Fragments of ^{13}C-{^{1}H} and ^{13}C NMR spectra (100.6 MHz, acetone-d_6) of compound (**3b**), trifluoromethyl groups region is shown.

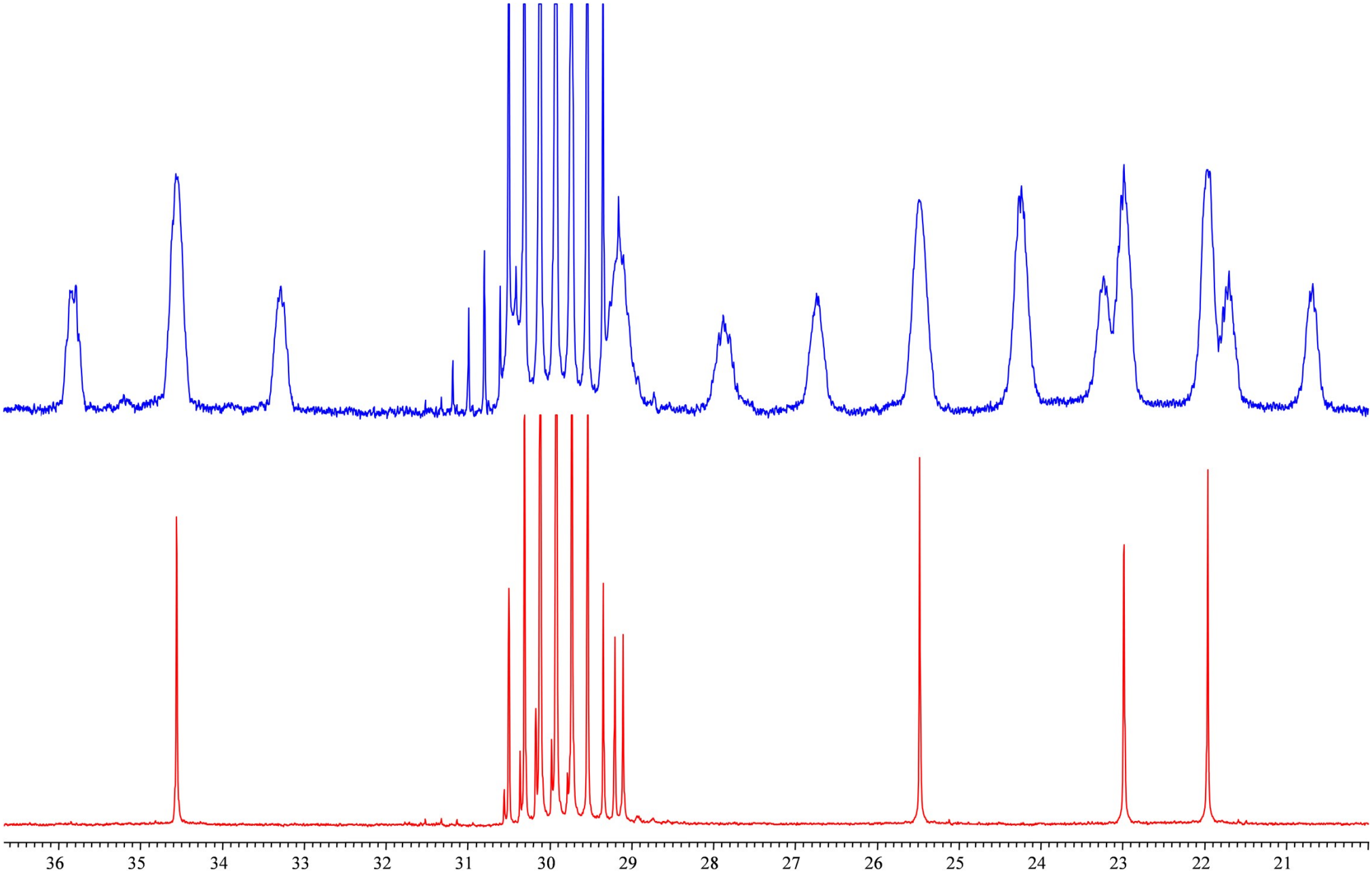

Figure 71. Up-field fragments of ^{13}C-{^{1}H} and ^{13}C NMR spectra (100.6 MHz, acetone-d_6) of compound (**3b**).

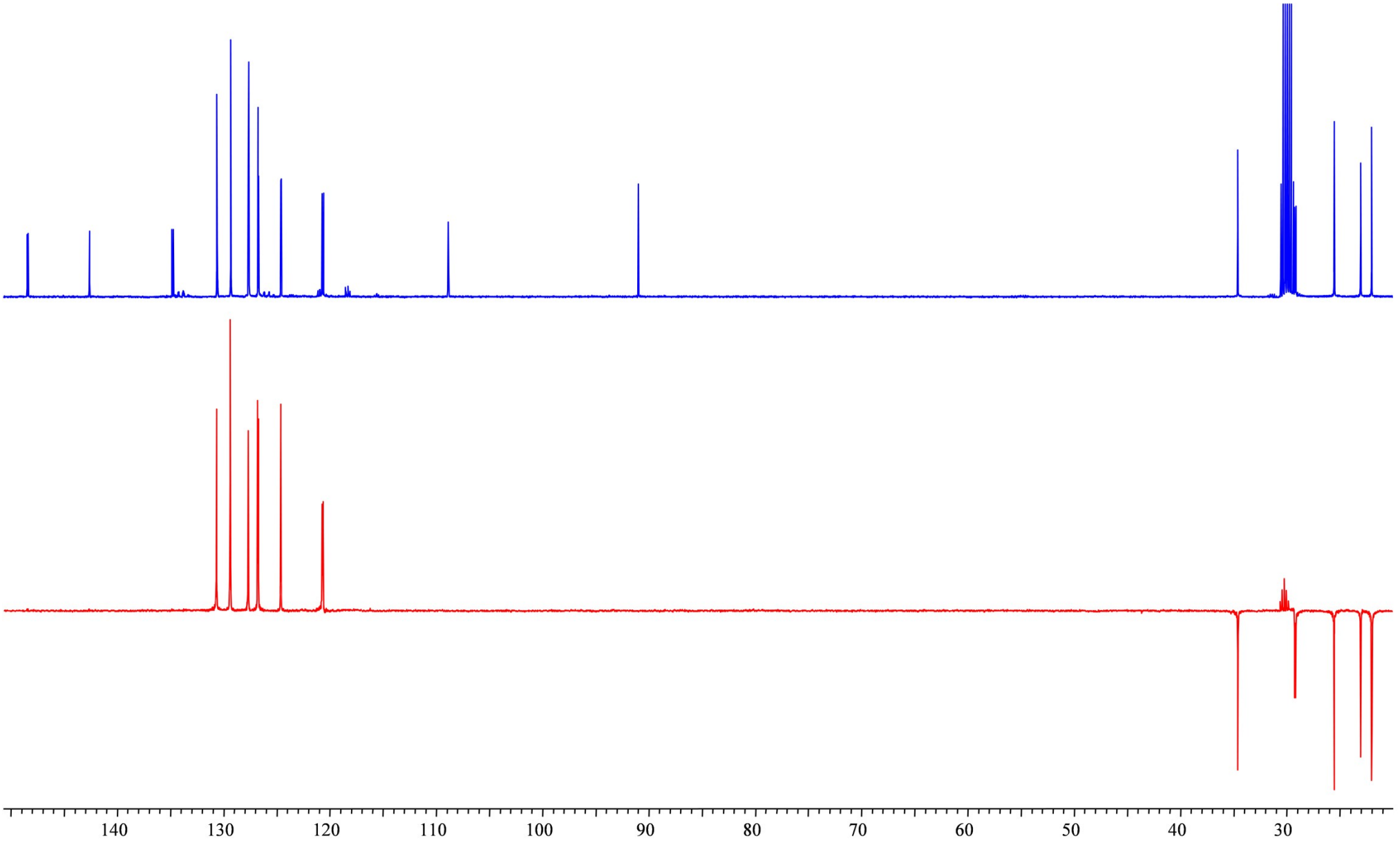

Figure 72. ^{13}C-{^{1}H} and ^{13}C-{^{1}H}-dept NMR spectra (100.6 MHz, acetone-d_6) of compound (**3b**).

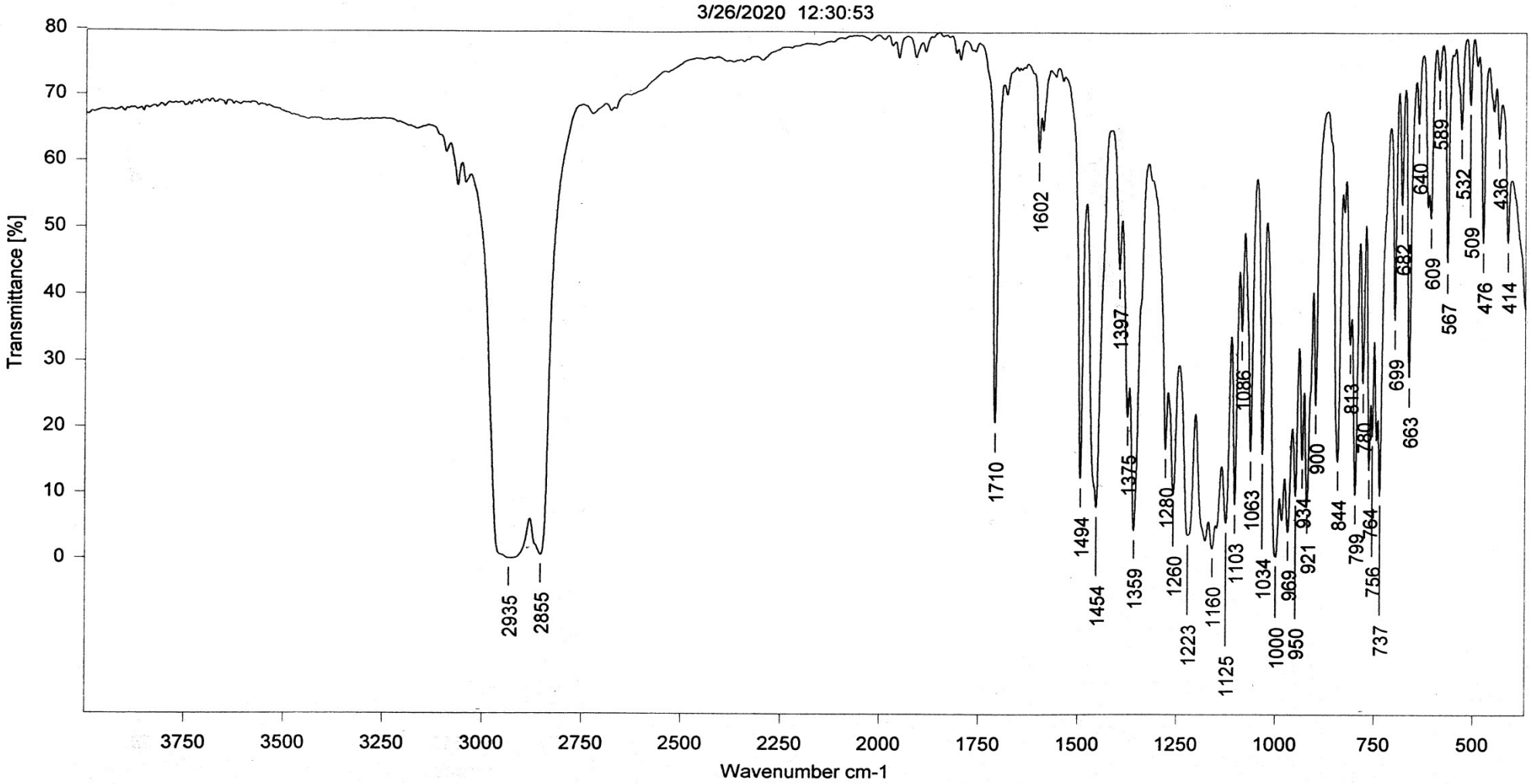

Figure 73. IR spectrum (400-4000 cm^{-1}, Vaseline oil) of phosphorane (**3b**).

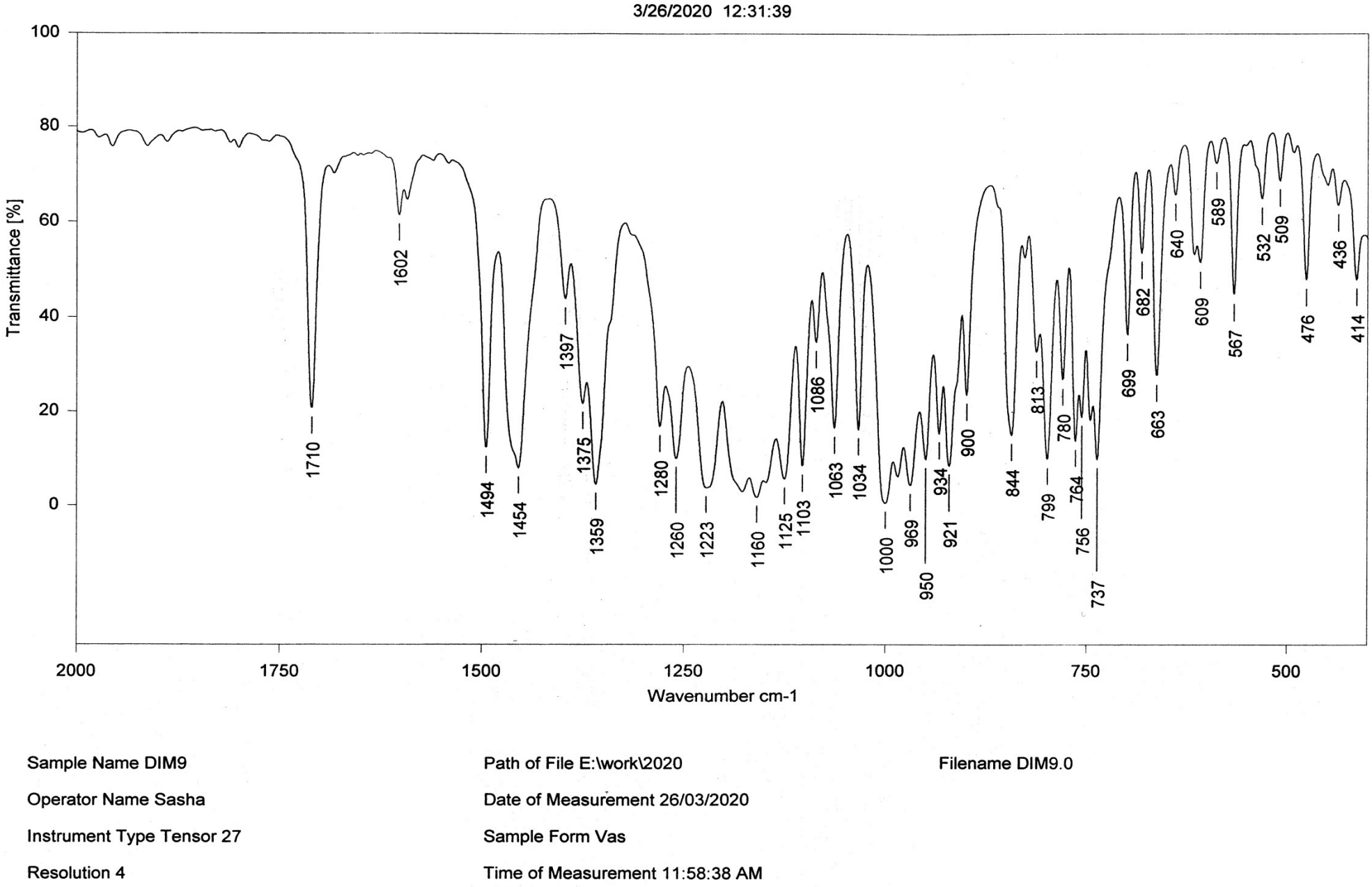

Figure 74. The fragment (400-2000 cm^{-1}) of IR spectrum (400-2000 cm^{-1}, Vaseline oil) of phosphorane (**3a**).

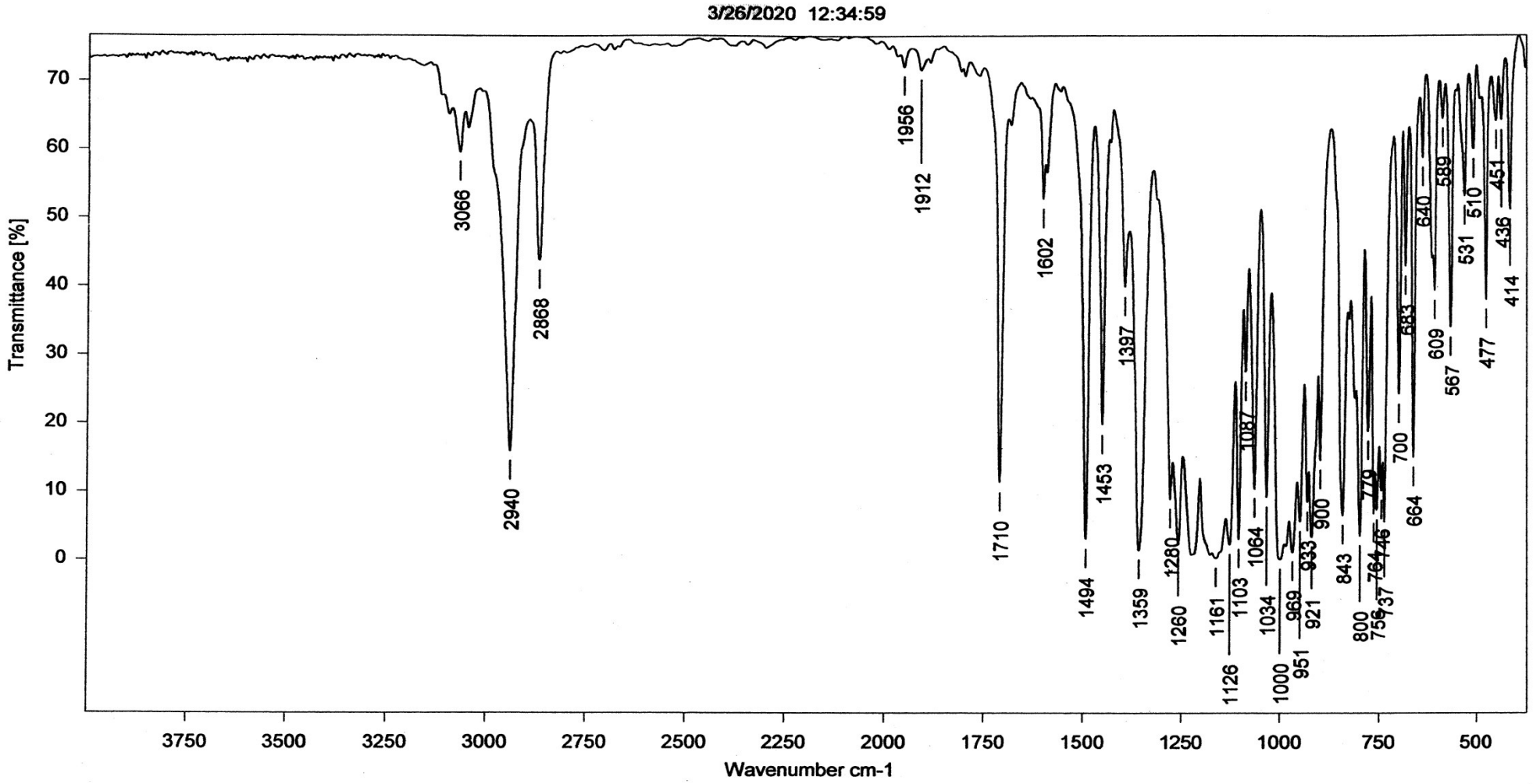

Sample Name DIM9	Path of File E:\work\2020	Filename DIM9.7
Operator Name Sasha	Date of Measurement 26/03/2020	
Instrument Type Tensor 27	Sample Form KBr	
Resolution 4	Time of Measurement 12:29:00 PM	

Figure 75. IR spectrum (400-4000 cm^{-1}, KBr pellet) of phosphorane (**3b**).

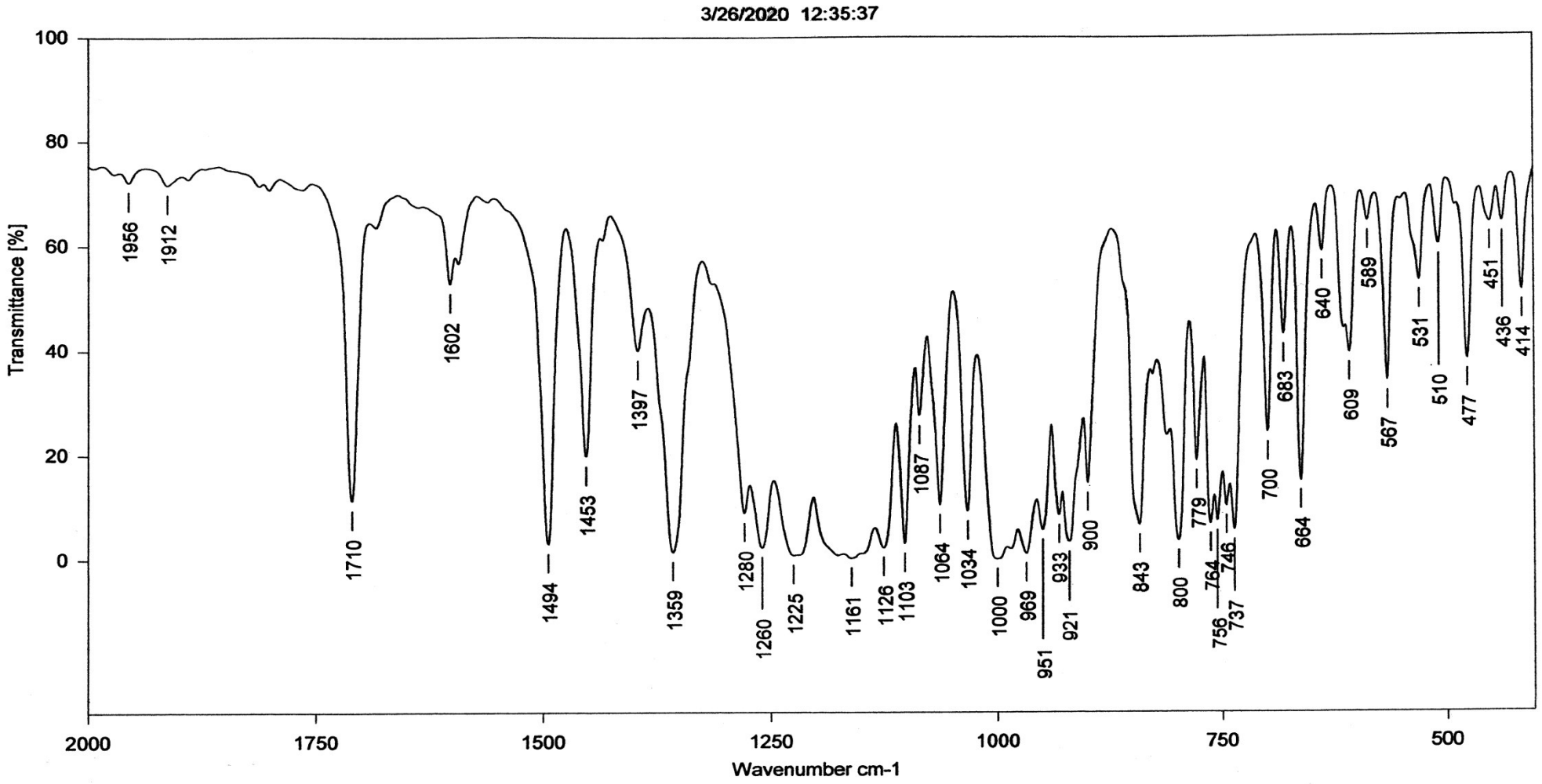

Sample Name DIM9 | Path of File E:\work\2020 | Filename DIM9.7

Operator Name Sasha | Date of Measurement 26/03/2020

Instrument Type Tensor 27 | Sample Form KBr

Resolution 4 | Time of Measurement 12:29:00 PM

Figure 76. The fragment (400-2000 cm^{-1}) of IR spectrum (KBr pellet) of phosphorane (**3b**).

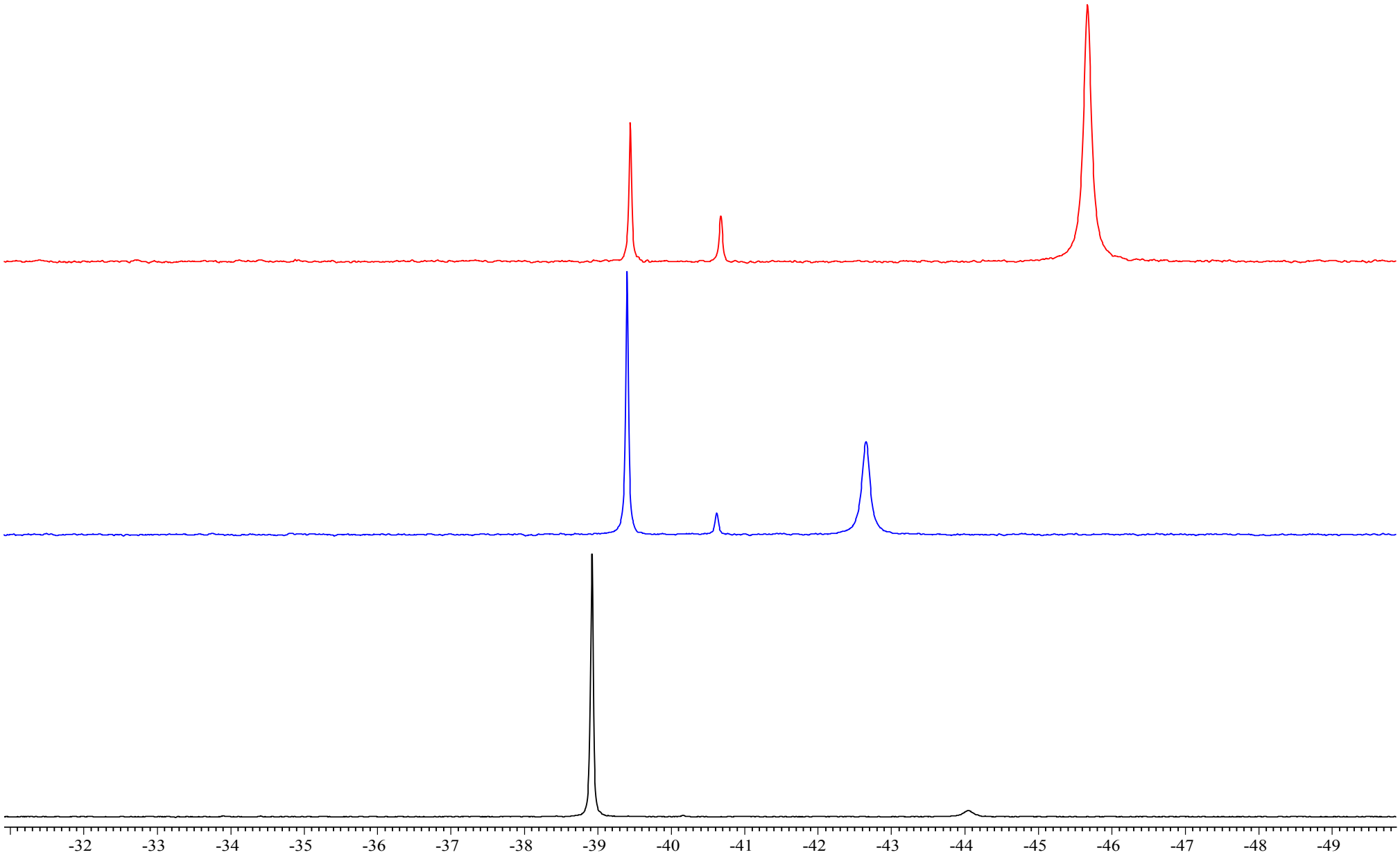

Figure 77. ^{13}P-{^{1}H} NMR spectra (162.0 MHz, CH_2Cl_2/C_6D_6) of the phosphole (**1b**) and perfluorodiacetyl reaction mixture in 5 days at 25°C (red), in 11 days at 25°C (blue) and after heating for 40 min at 60°C and evaporation of dichloromethane in vacuo (black, $CDCl_3$).

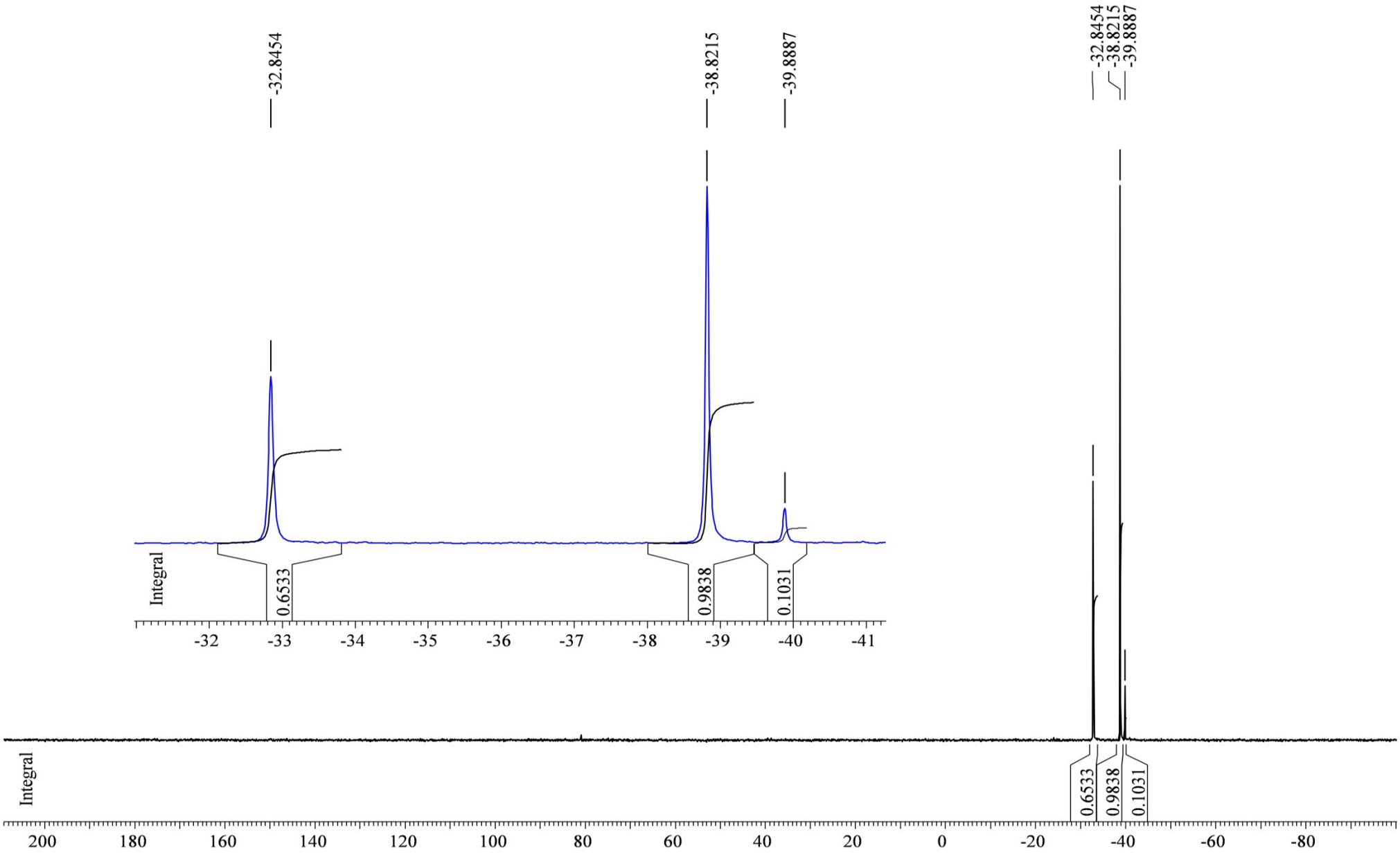

Figure 78. ^{13}P-{^{1}H} NMR spectrum (162.0 MHz, pentane) of the phosphole (**1b**) and perfluorodiacetyl reaction mixture after 11 days and evaporation of dichloromethane in vacuo [compounds (**3b**), (**4b**) and (**5b**)].

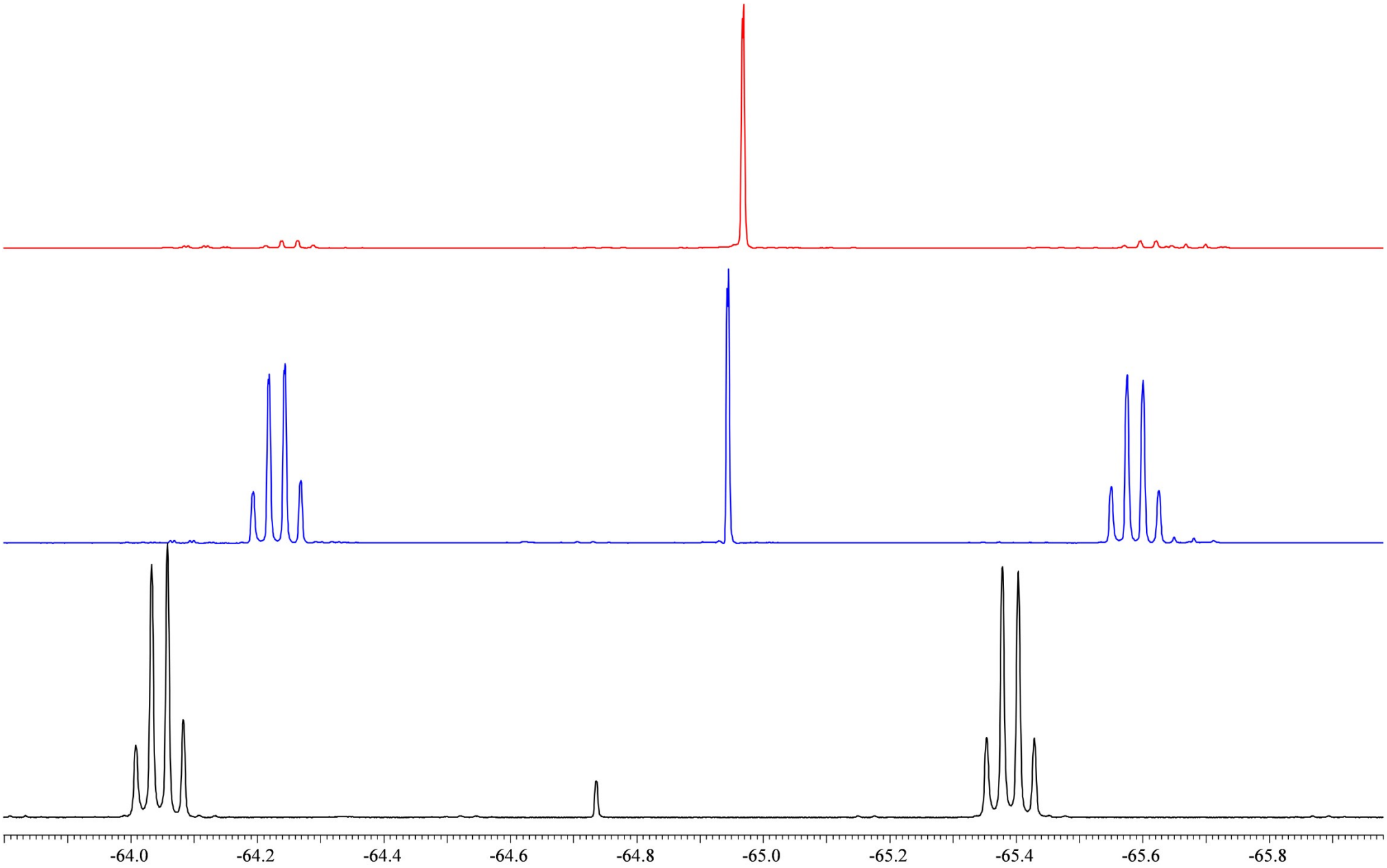

Figure 79. ^{19}F NMR spectra (376.5 MHz, CH_2Cl_2/C_6D_6) of the phosphole (**1b**) and perfluorodiacetyl reaction mixture after two hours at 25°C (red), 12 days (blue) and after heating at 60°C for 40 min and evaporation of dichloromethane in vacuo (black, $CDCl_3$).

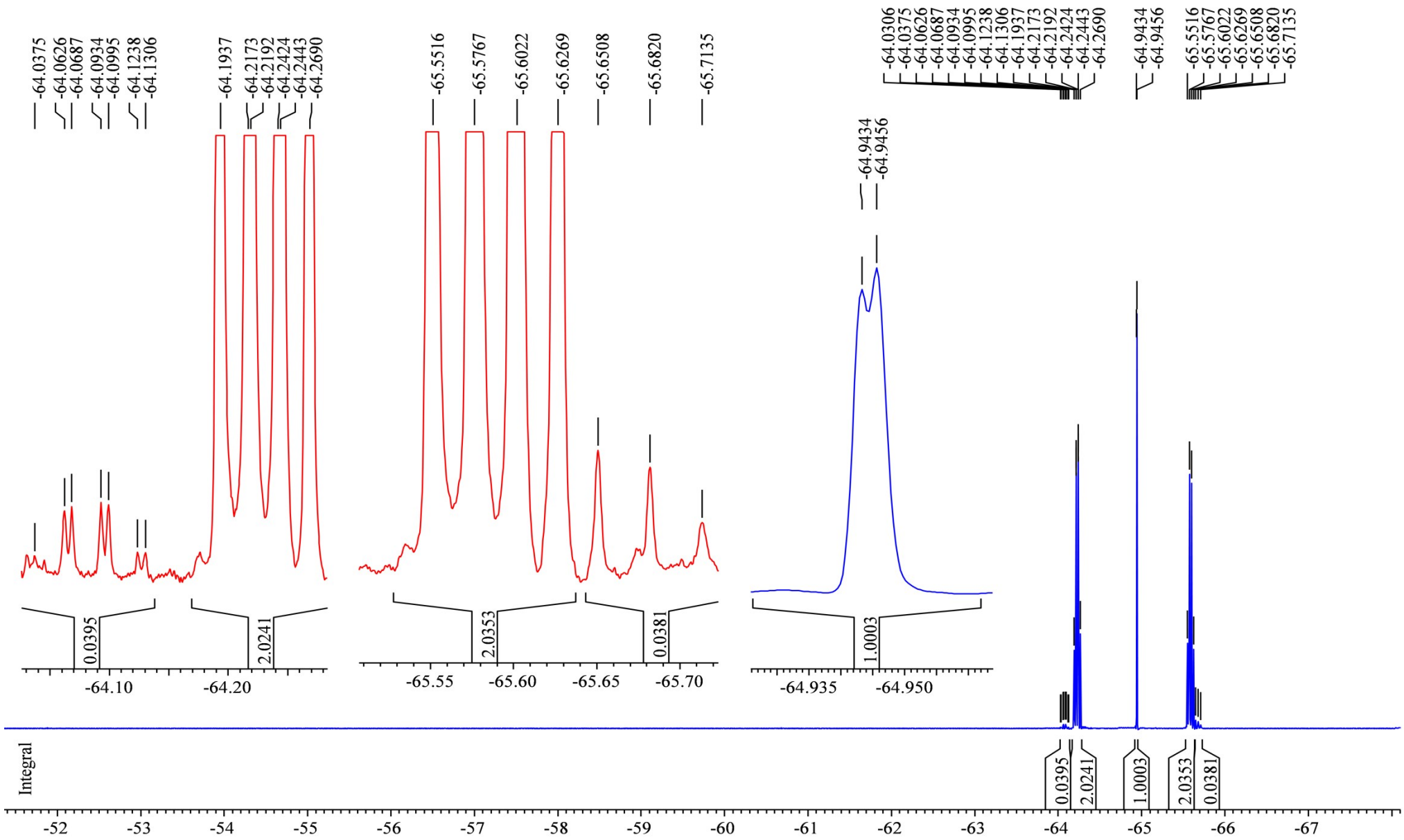

Figure 80. ^{19}F NMR spectrum (386.5 MHz, CH_2Cl_2/C_6D_6) of the phosphole (**3b**) and perfluorodiacetyl reaction mixture after 12 days at 25°C [compounds (**3b**), (**4b**) and (**5b**)].

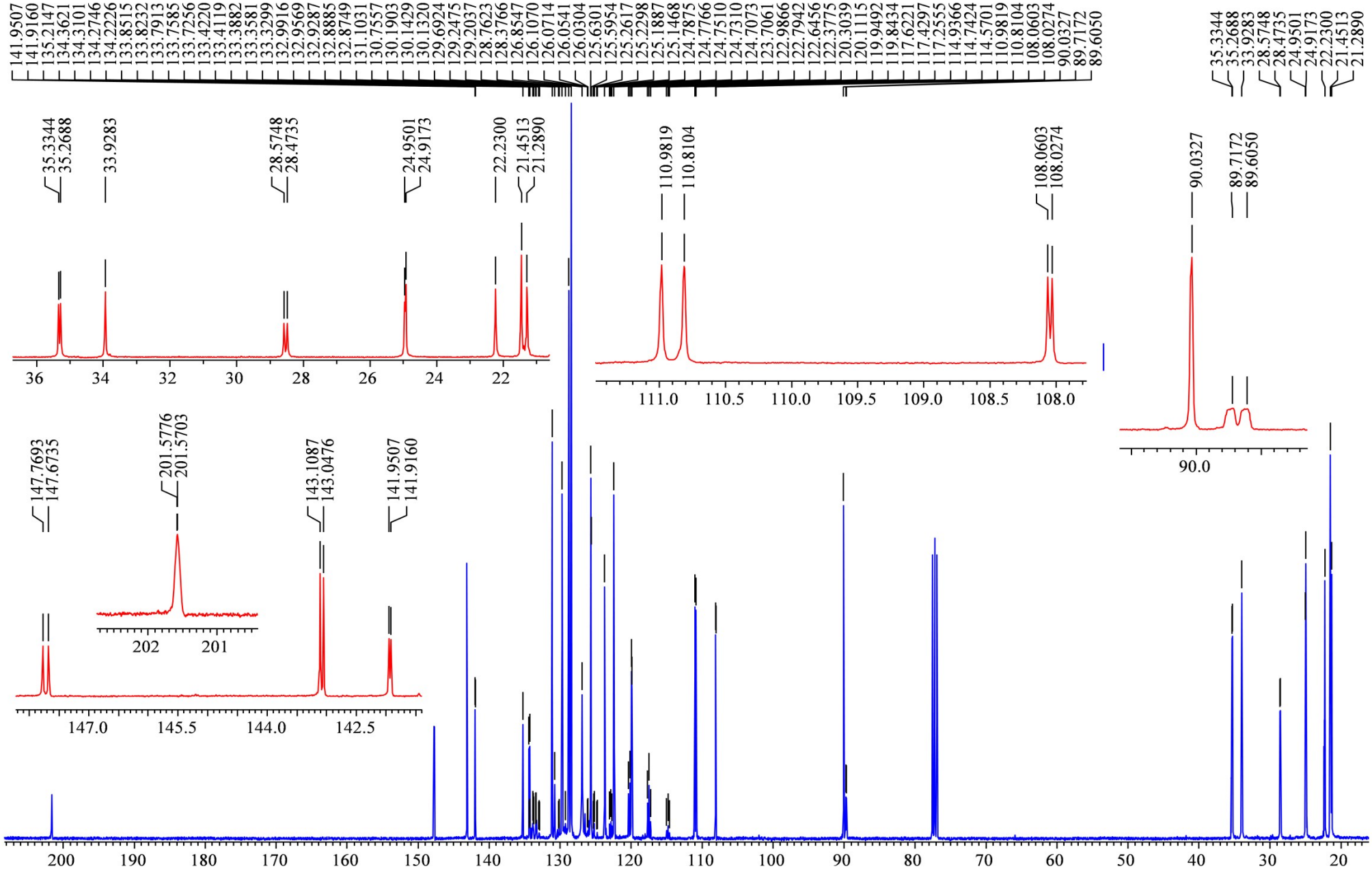

Figure 81. ^{13}C-{^{1}H} NMR spectrum (150.9 MHz, $CDCl_3$) of the compounds (**3b**) and (**4b**) mixture (1 : 1).

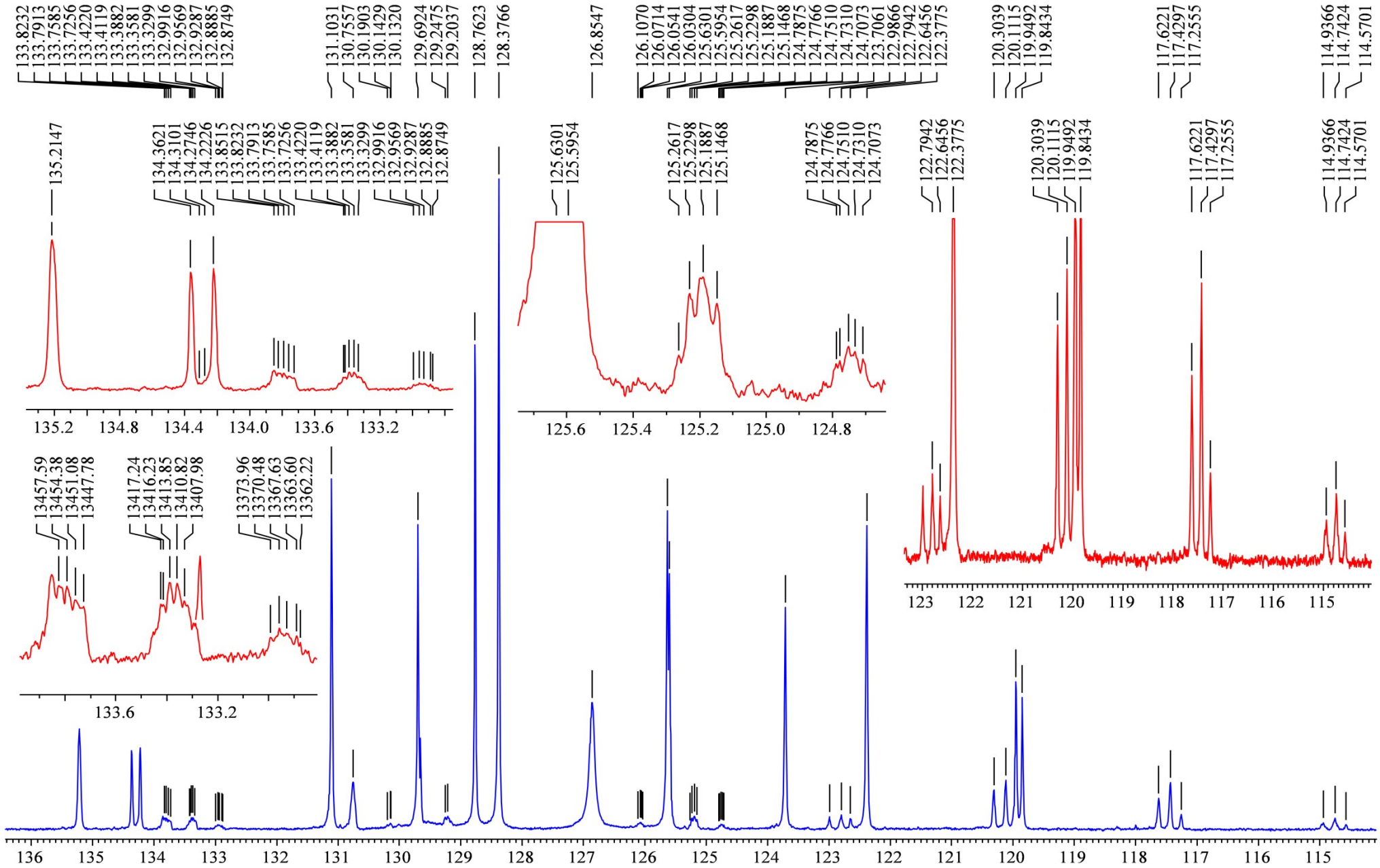

Figure 82. The 114-136 ppm region of ^{13}C-{^{1}H} NMR spectrum (150.9 MHz, $CDCl_3$) of the compounds (**3b**) and (**4b**) mixture (1 : 1).

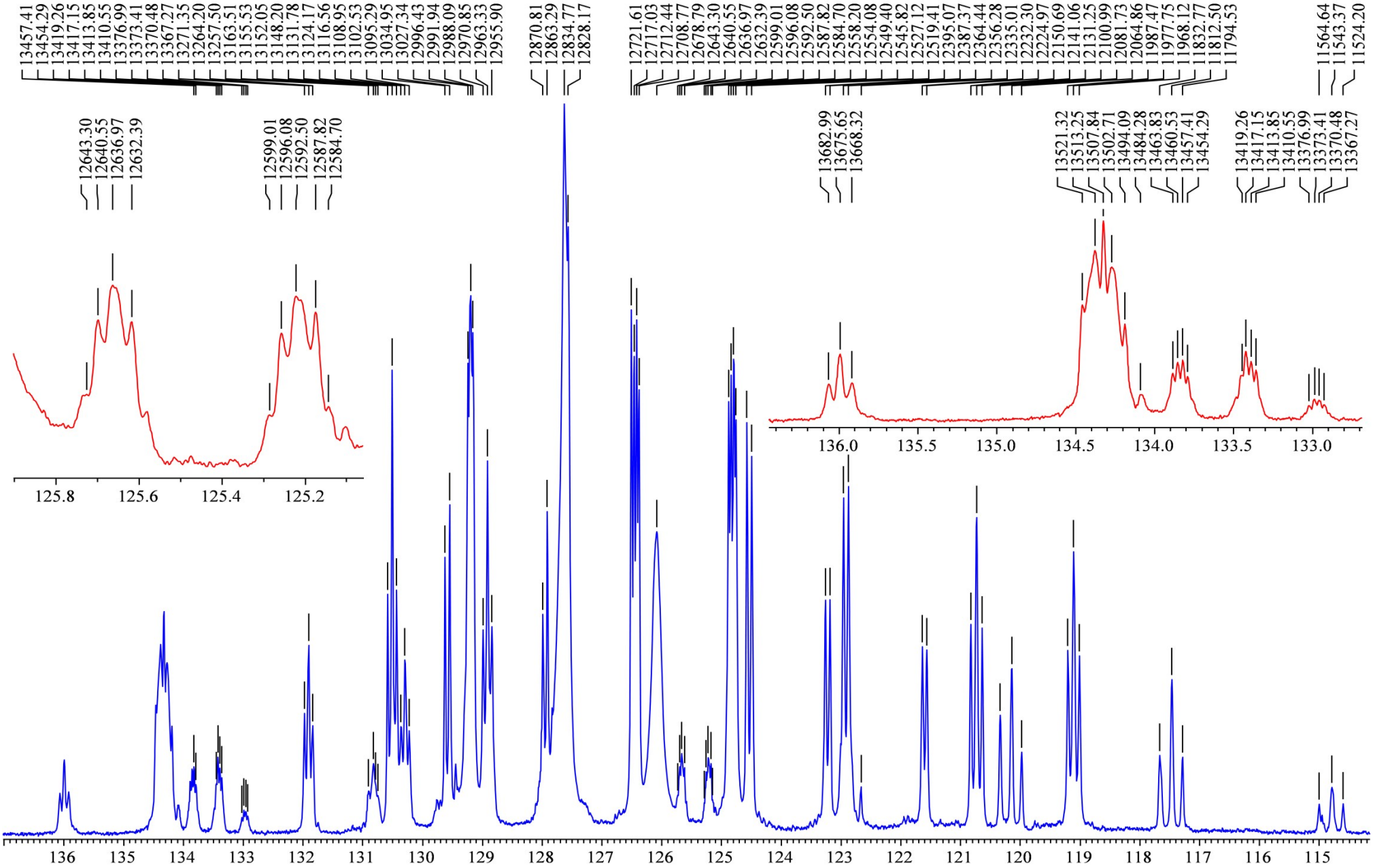

Figure 83. The 114-136 ppm region of ^{13}C NMR spectrum (150.9 MHz, $CDCl_3$) of the compounds (**3b**) and (**4b**) mixture (1 : 1).

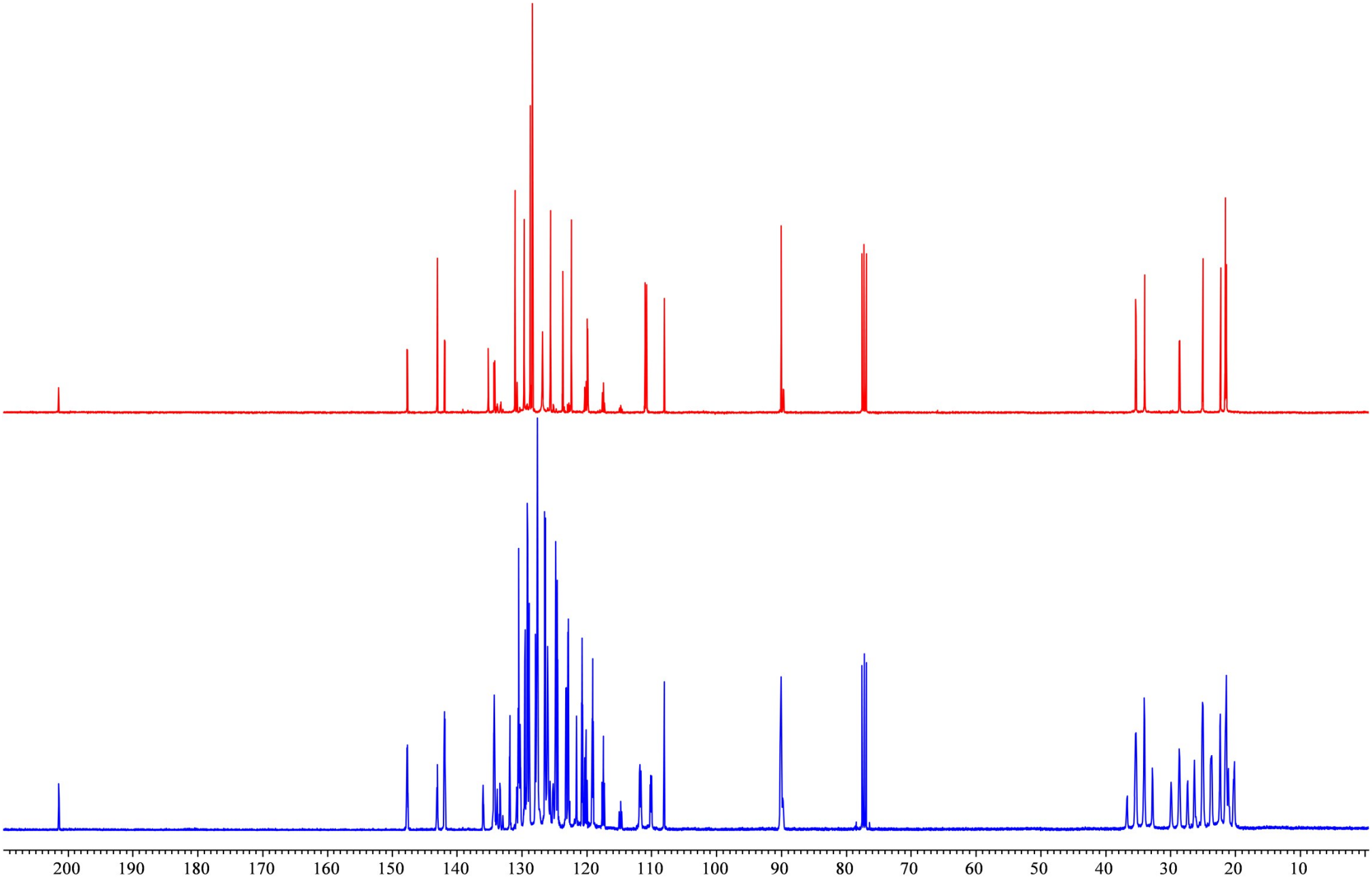

Figure 84. ^{13}C-{^{1}H} and ^{13}C NMR spectra (150.9 MHz, $CDCl_3$) of the compounds (**3b**) and (**4b**) mixture (1 : 1).

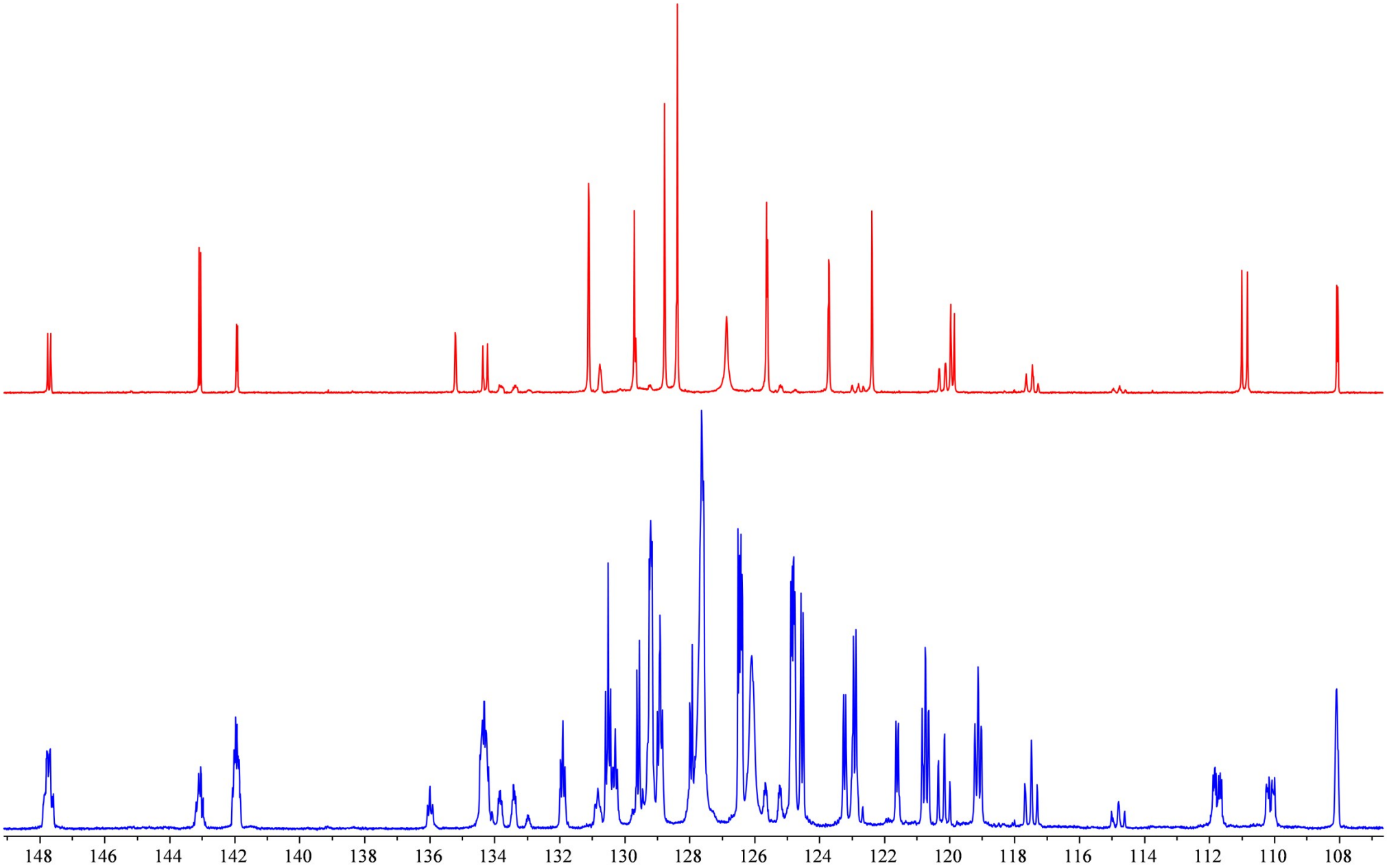

Figure 85. The 107-149 ppm region of ^{13}C-{^{1}H} and ^{13}C NMR spectra (150.9 MHz, $CDCl_3$) of the compounds (**3b**) and (**4b**) mixture (1 : 1).

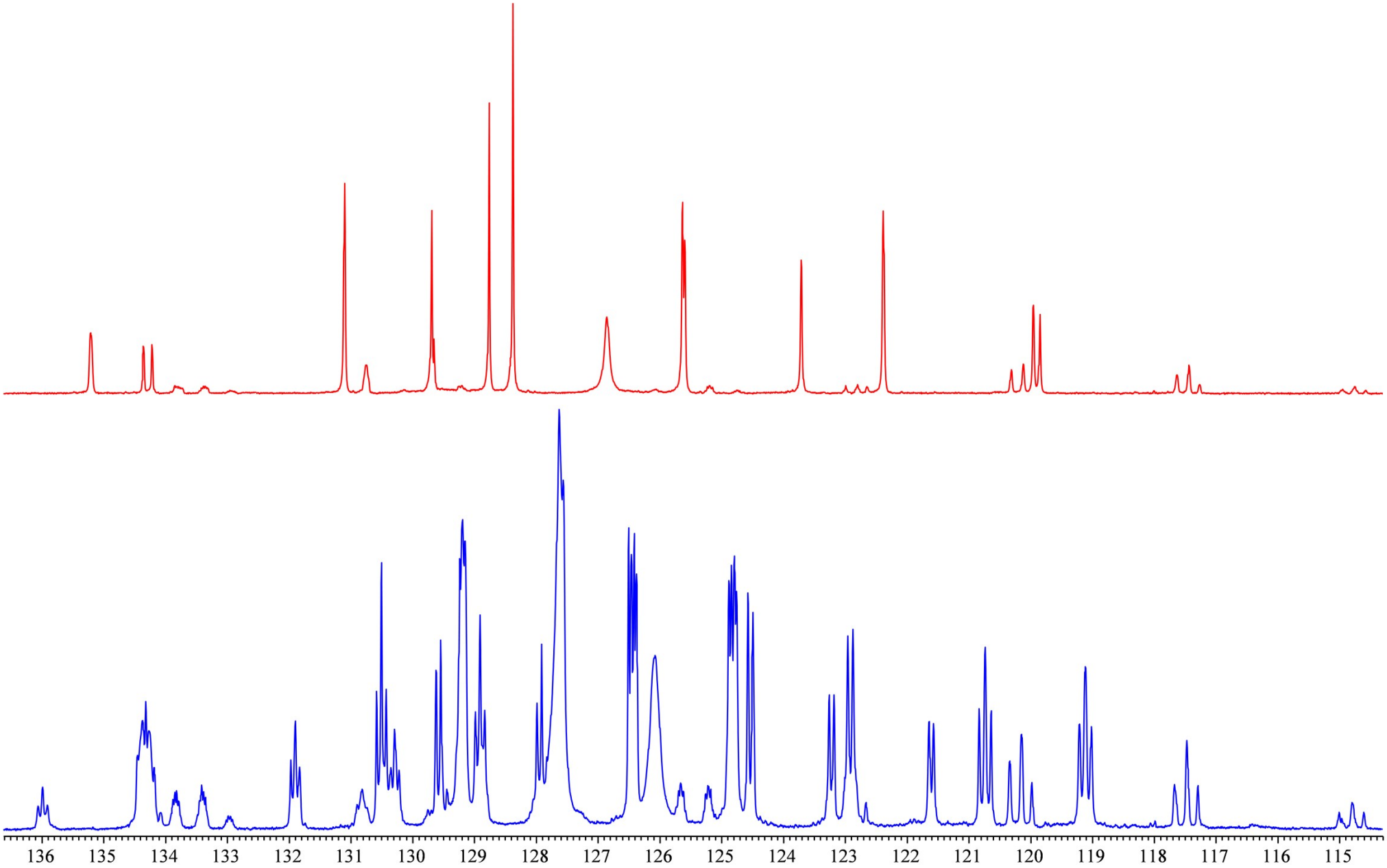

Figure 86. The 114-137 ppm region of ^{13}C-{^{1}H} and ^{13}C NMR spectra (150.9 MHz, $CDCl_3$) of the compounds (**3b**) and (**4b**) mixture (1 : 1).

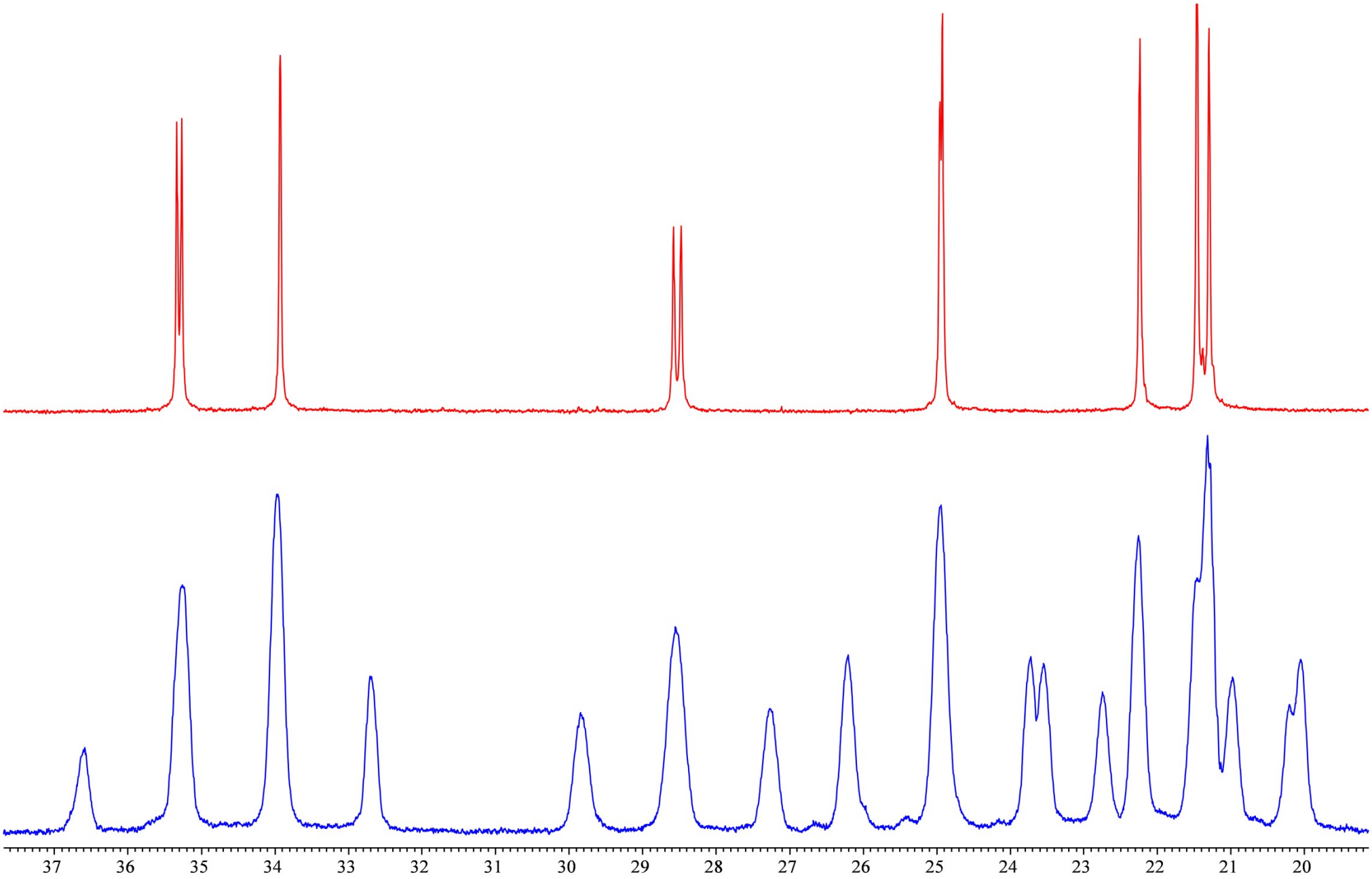

Figure 87. High-field region of ^{13}C-{^{1}H} and ^{13}C NMR spectra (150.9 MHz, $CDCl_3$) of the compounds (**3b**) and (**4b**) mixture (1 : 1).

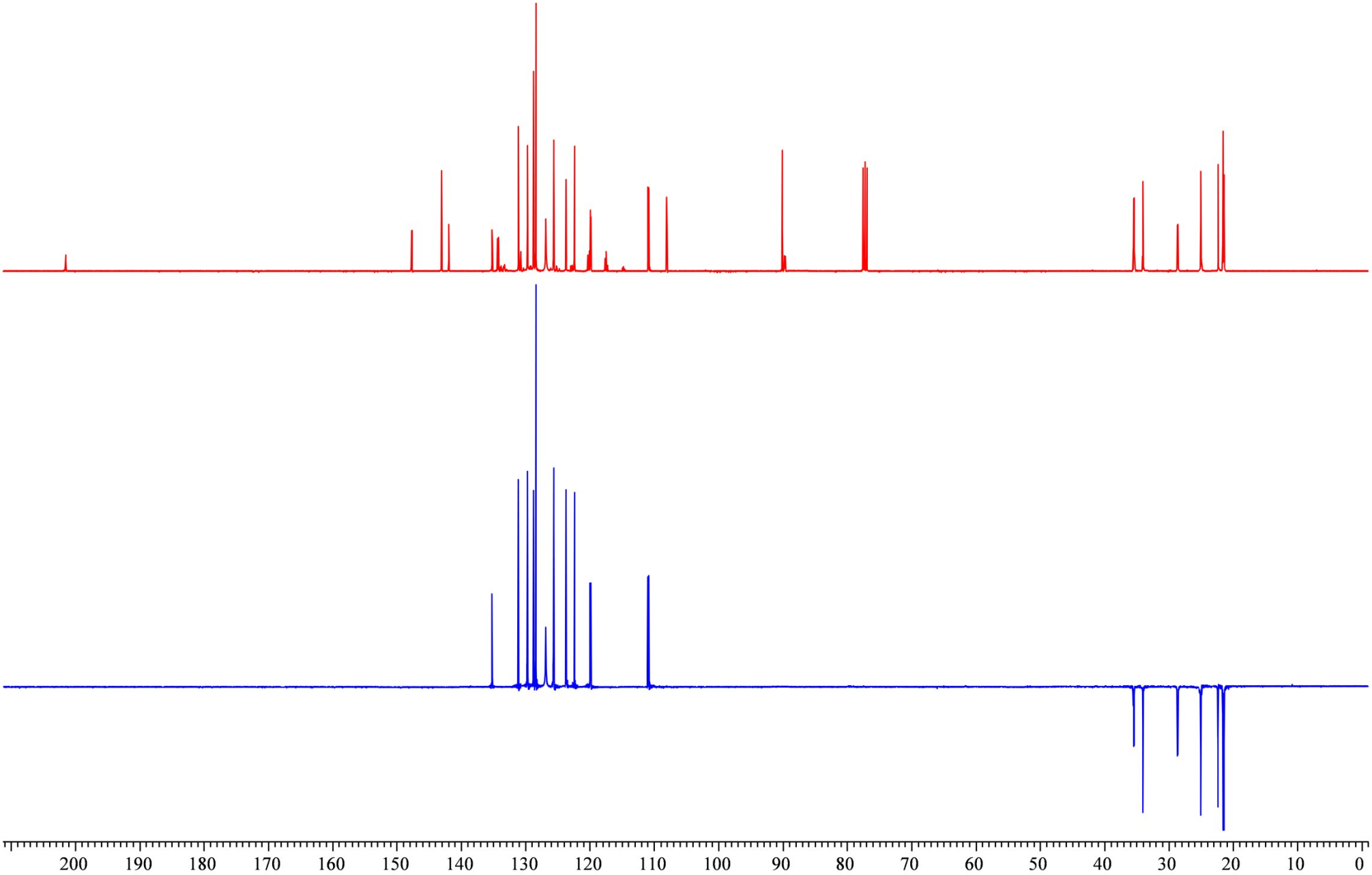

Figure 88. ^{13}C-{^{1}H} and ^{13}C-{^{1}H}-dept NMR spectra (150.9 MHz, $CDCl_3$) of the compounds (**3b**) and (**4b**) mixture (1 : 1).

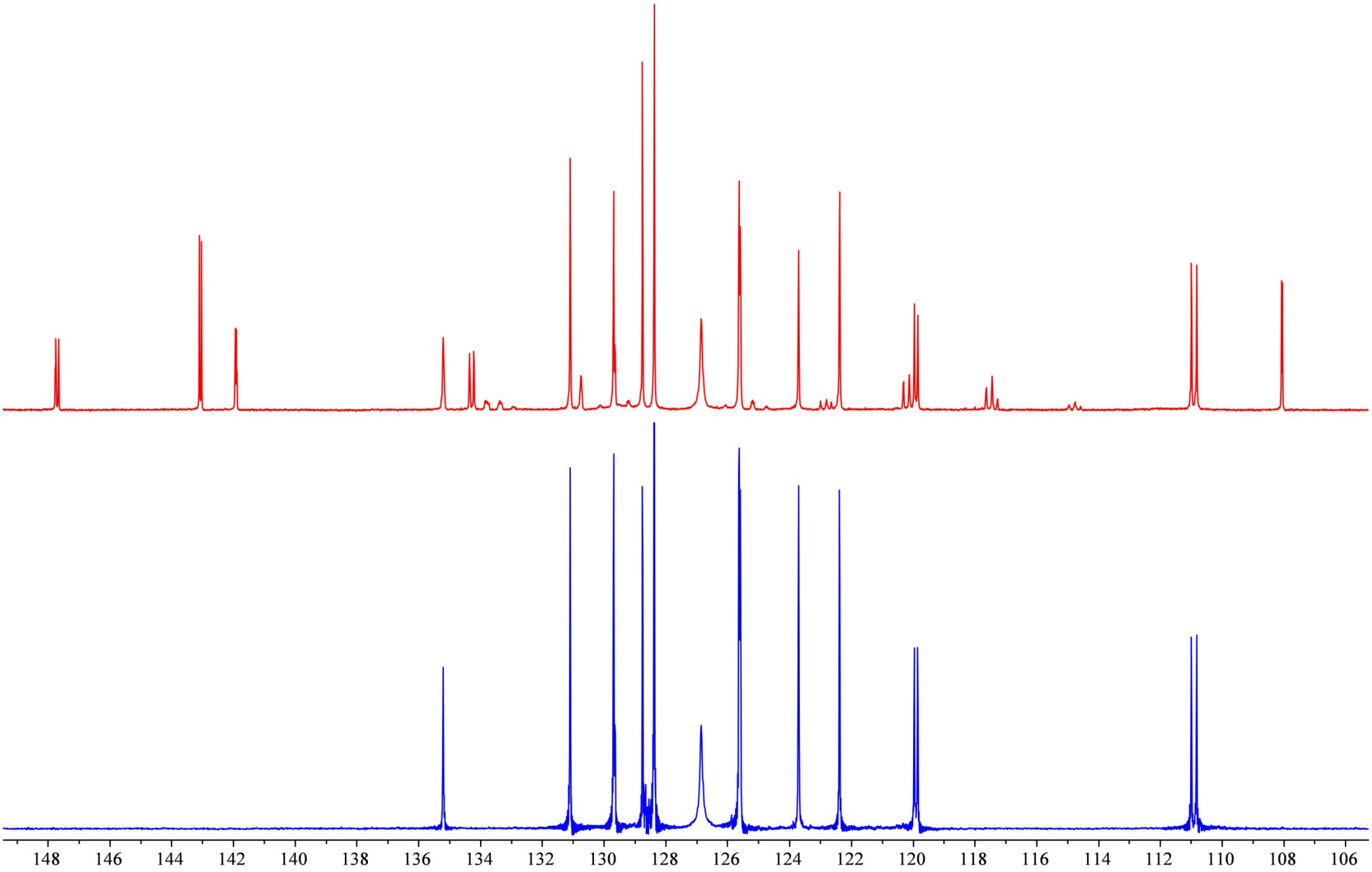

Figure 89. Low-field region of ^{13}C-{^{1}H} and ^{13}C-{^{1}H}-dept NMR spectra (150.9 MHz, $CDCl_3$) of the compounds (**3b**) and (**4b**) mixture (1 : 1).

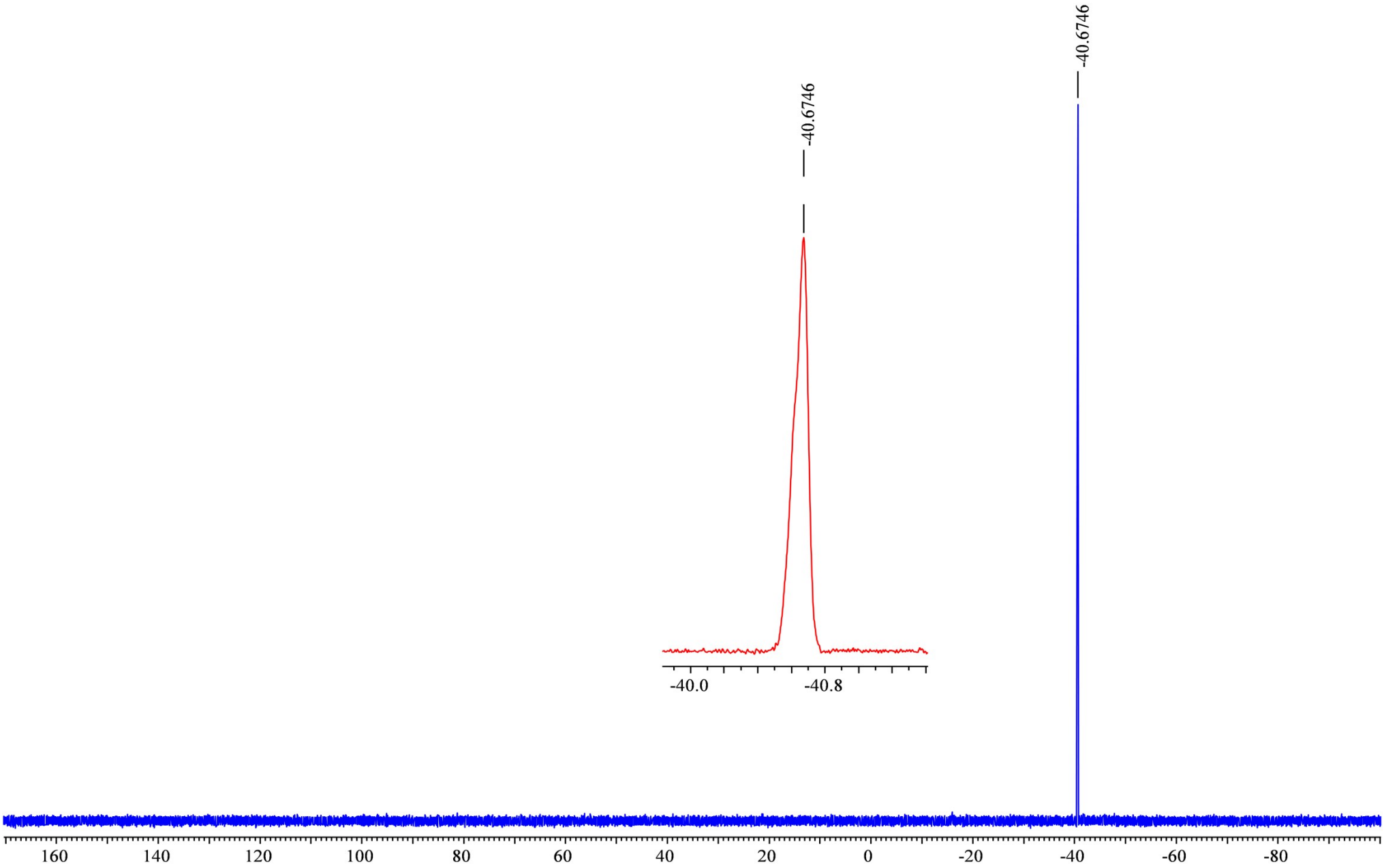

Figure 90. ^{31}P-{^{1}H} NMR spectrum (242.94 MHz, CD_2Cl_2, –5°C) of compound (**5b**), 15 min after mixing the reagents (**1b**) and (**2**).

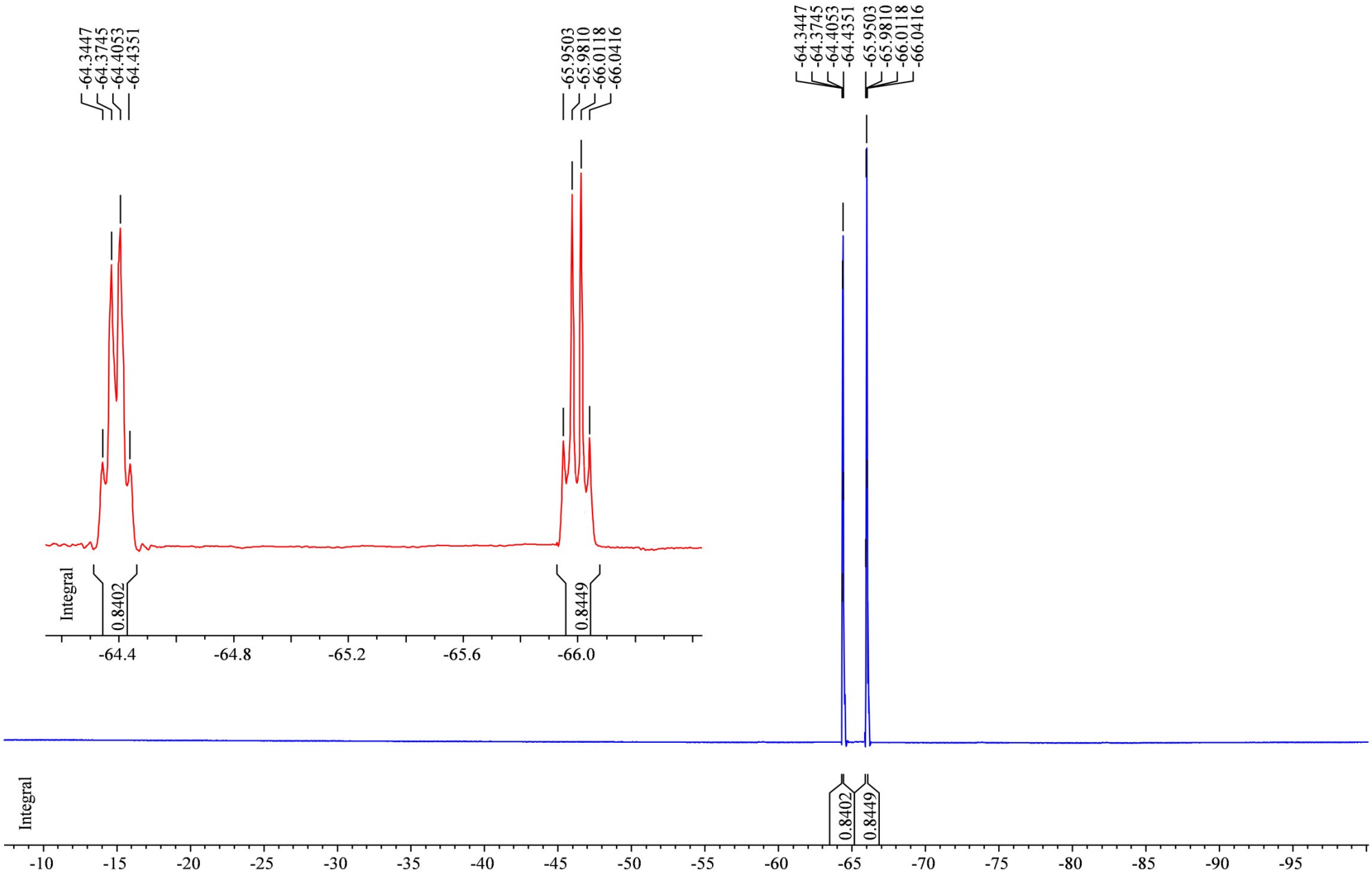

Figure 91. ^{19}F NMR spectrum (376.3 MHz, CD_2Cl_2, –5°C) of compound (**5b**), 15 min after mixing the reagents (**1b**) and (**2**).

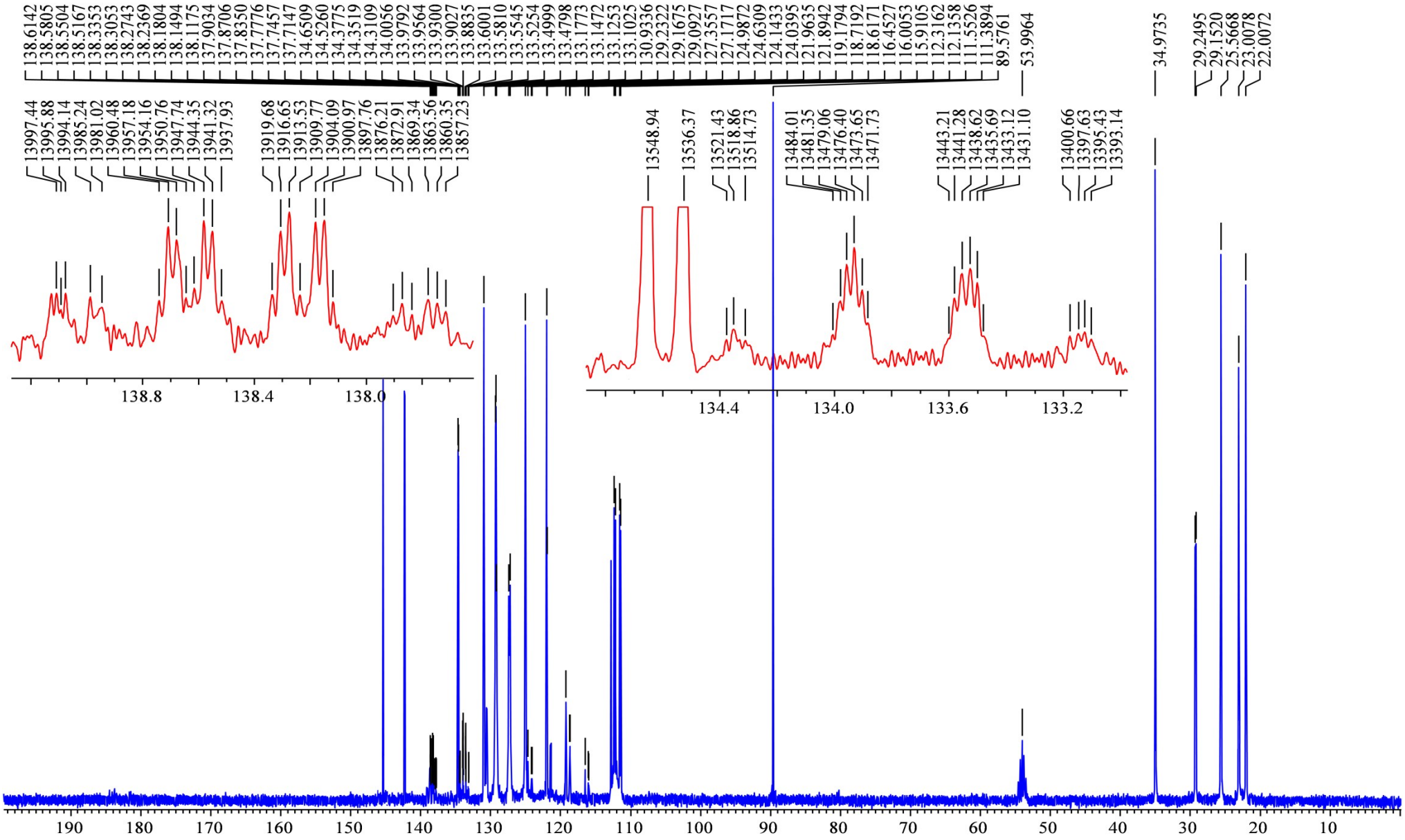

Figure 92. ^{13}C-{^{1}H} NMR spectrum (100.6 MHz, CD_2Cl_2, –5°C) of compound (**5b**).

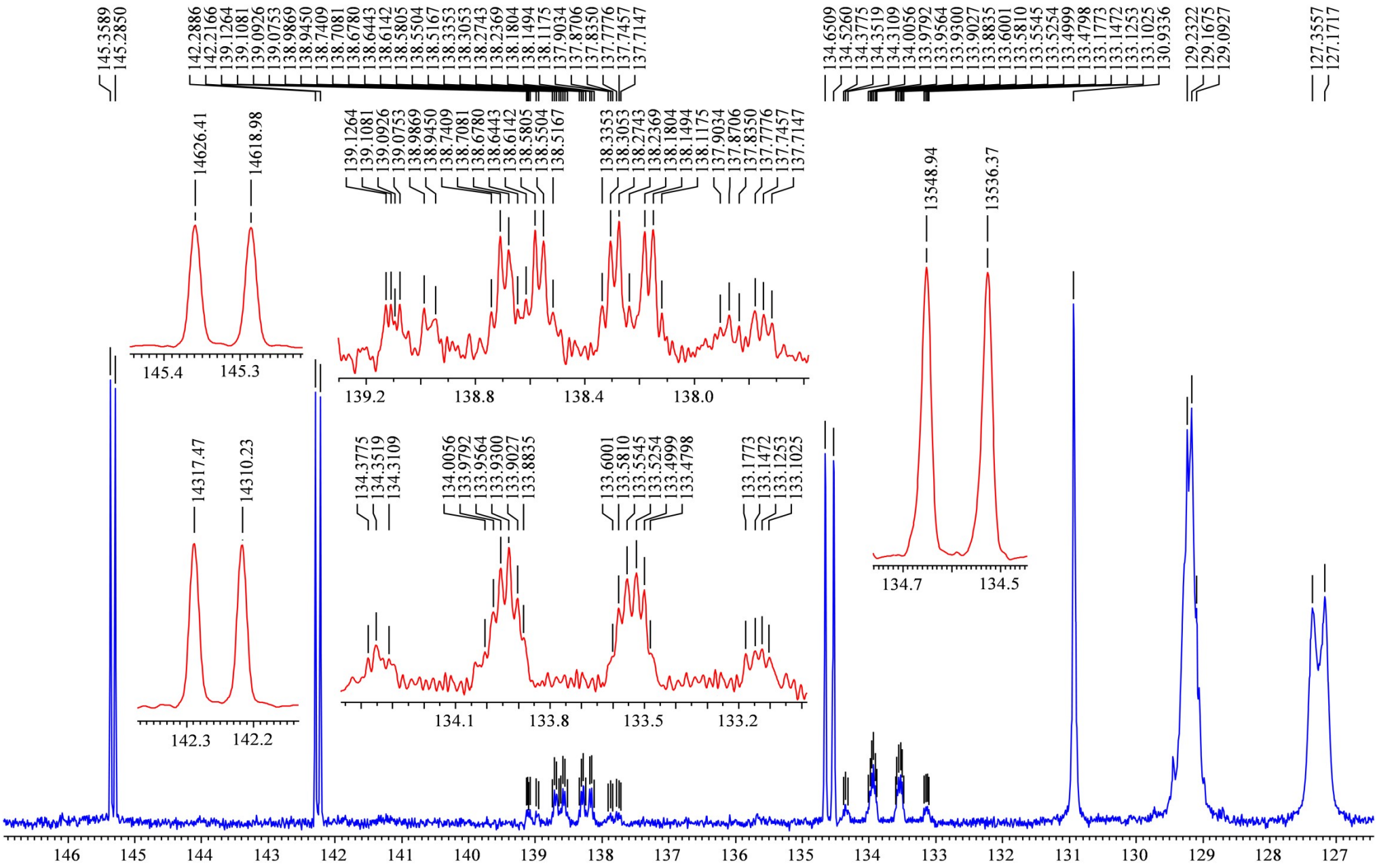

Figure 93. Low-field fragment of ^{13}C-{^{1}H} NMR spectrum (100.6 MHz, CD_2Cl_2, –5°C) of compound (**5b**).

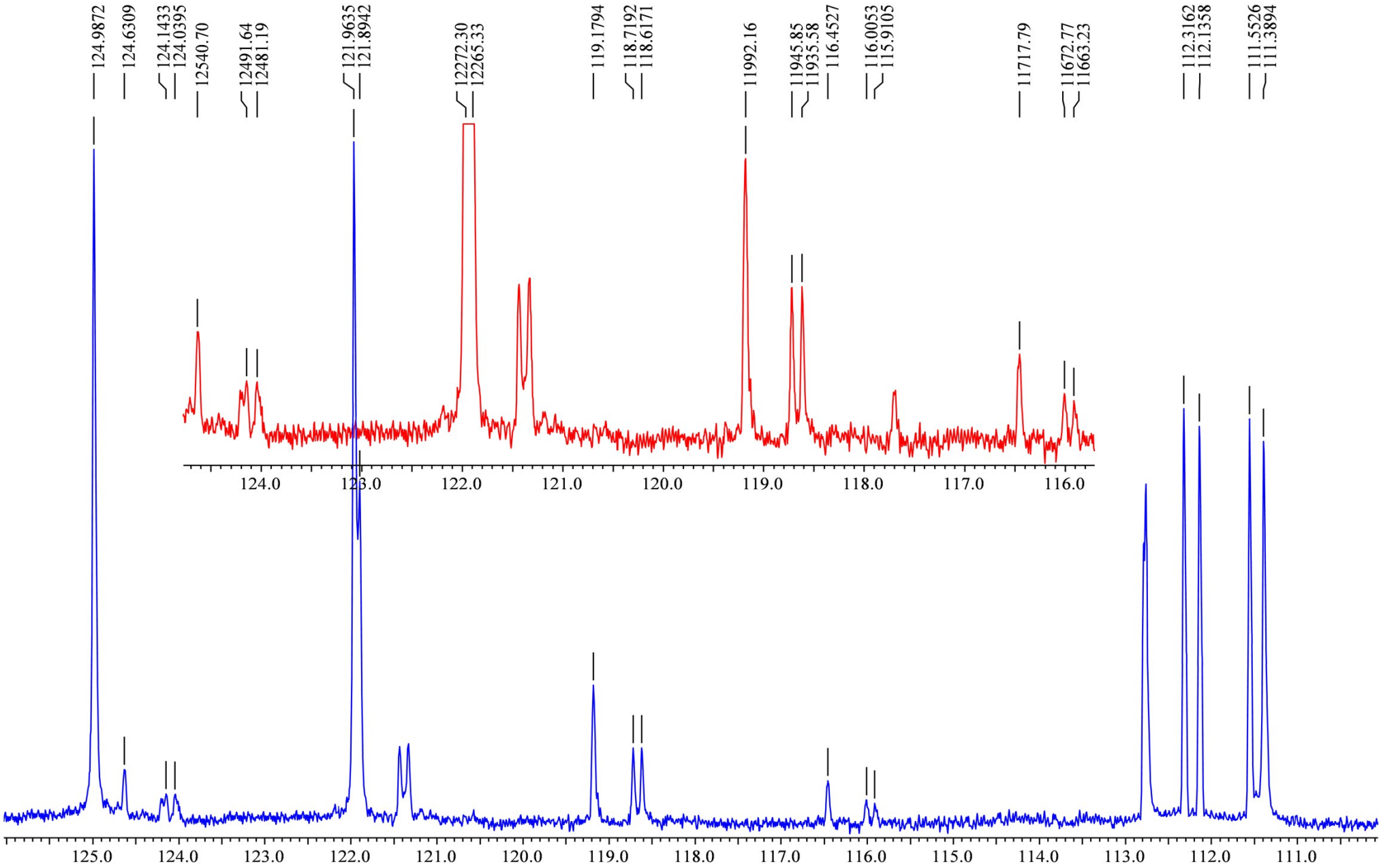

Figure 94. The 110-126 ppm region of ^{13}C-{^{1}H} NMR spectrum (100.6 MHz, CD_2Cl_2, –5°C) of compound (**5b**).

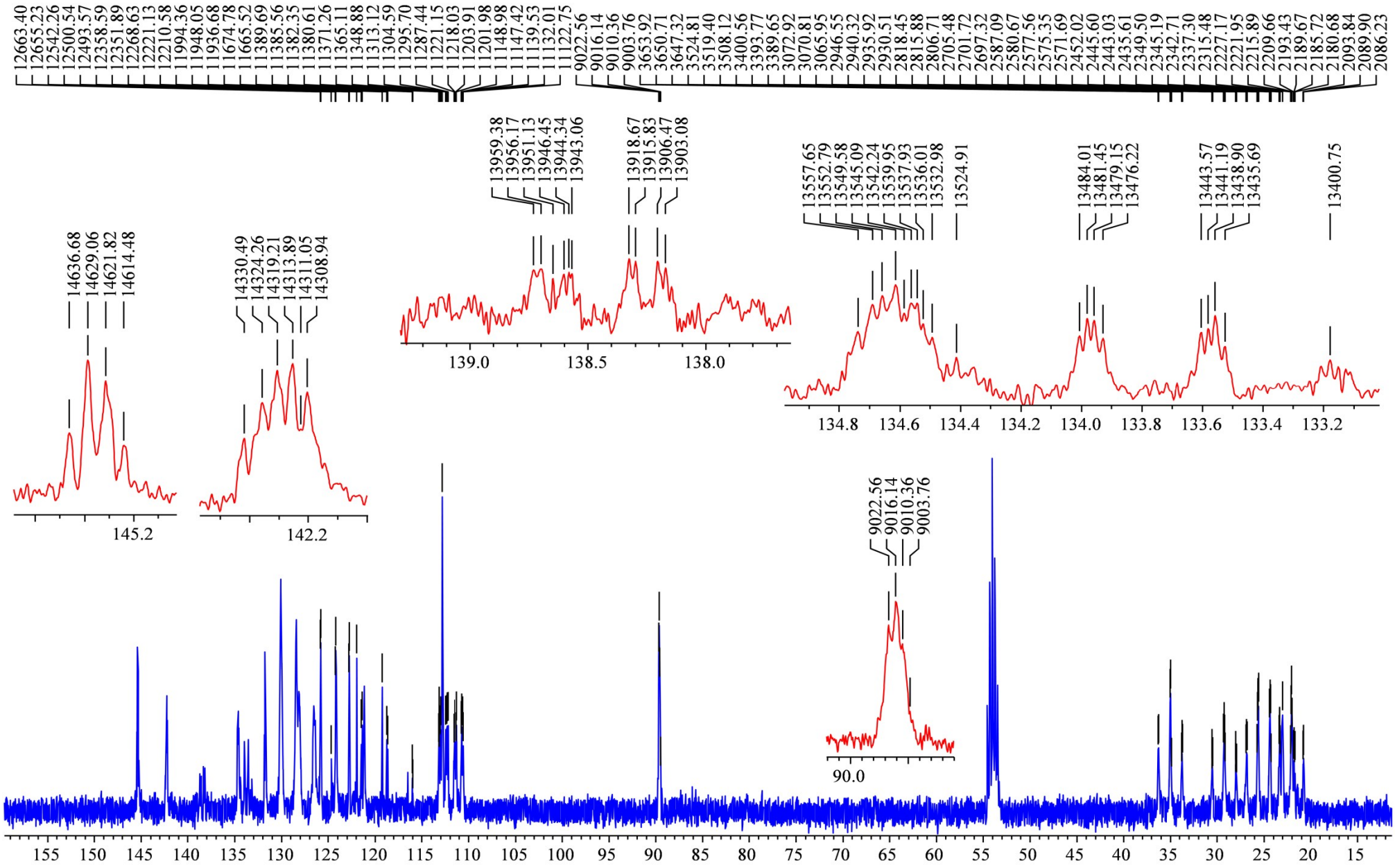

Figure 95. ^{13}C NMR spectrum (100.6 MHz, CD_2Cl_2, –5°C) of compound (**5b**).

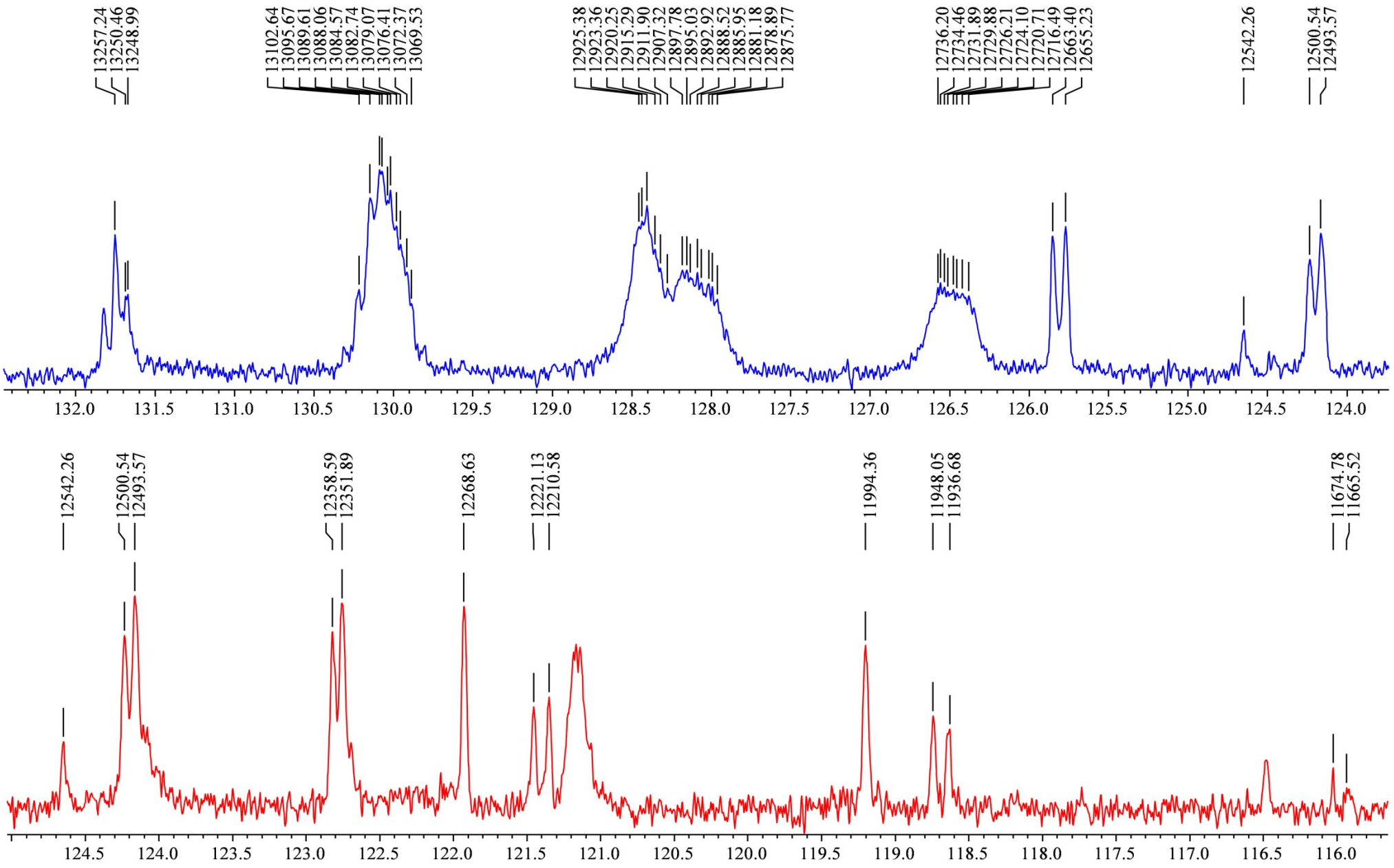

Figure 96. The 115-125 ppm region of ^{13}C NMR spectrum (100.6 MHz, CD_2Cl_2, –5°C) of compound (**5b**).

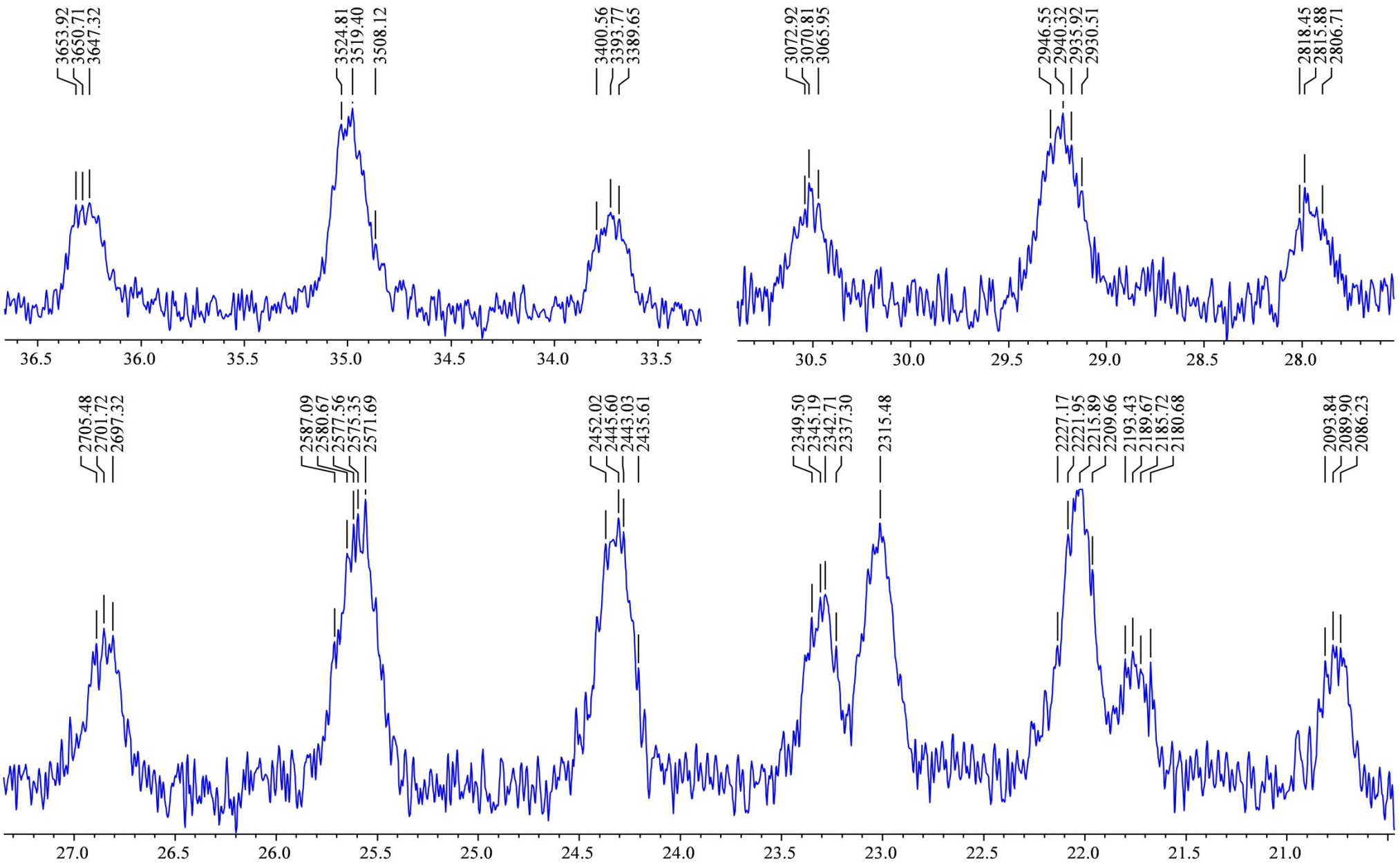

Figure 97. High-field fragments of ^{13}C-{^{1}H} NMR spectrum (100.6 MHz, CD_2Cl_2, –5°C) of compound (**5b**).

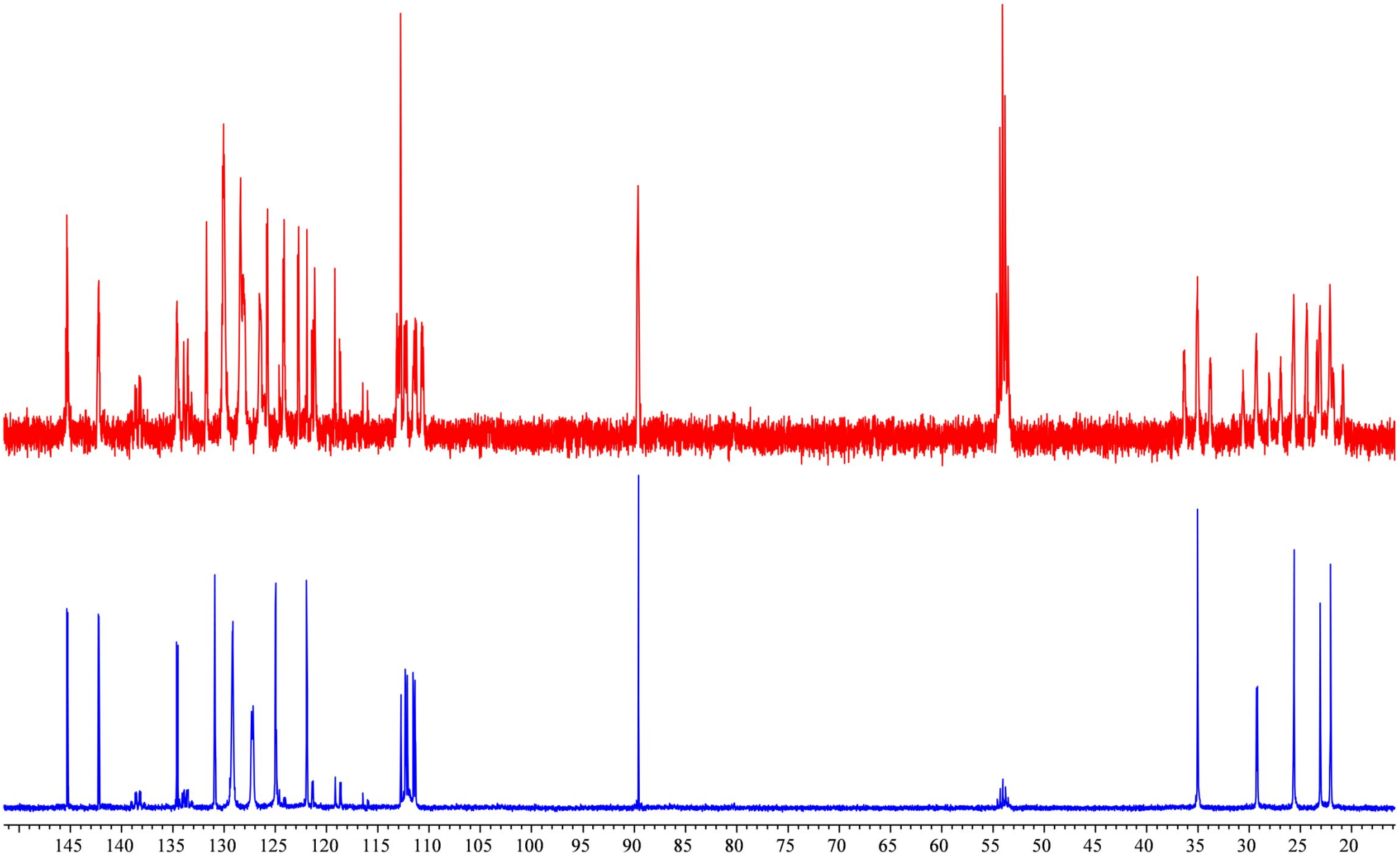

Figure 98. ^{13}C-{^{1}H} and ^{13}C NMR spectra (100.6 MHz, CD_2Cl_2, –5°C) of compound (**5b**).

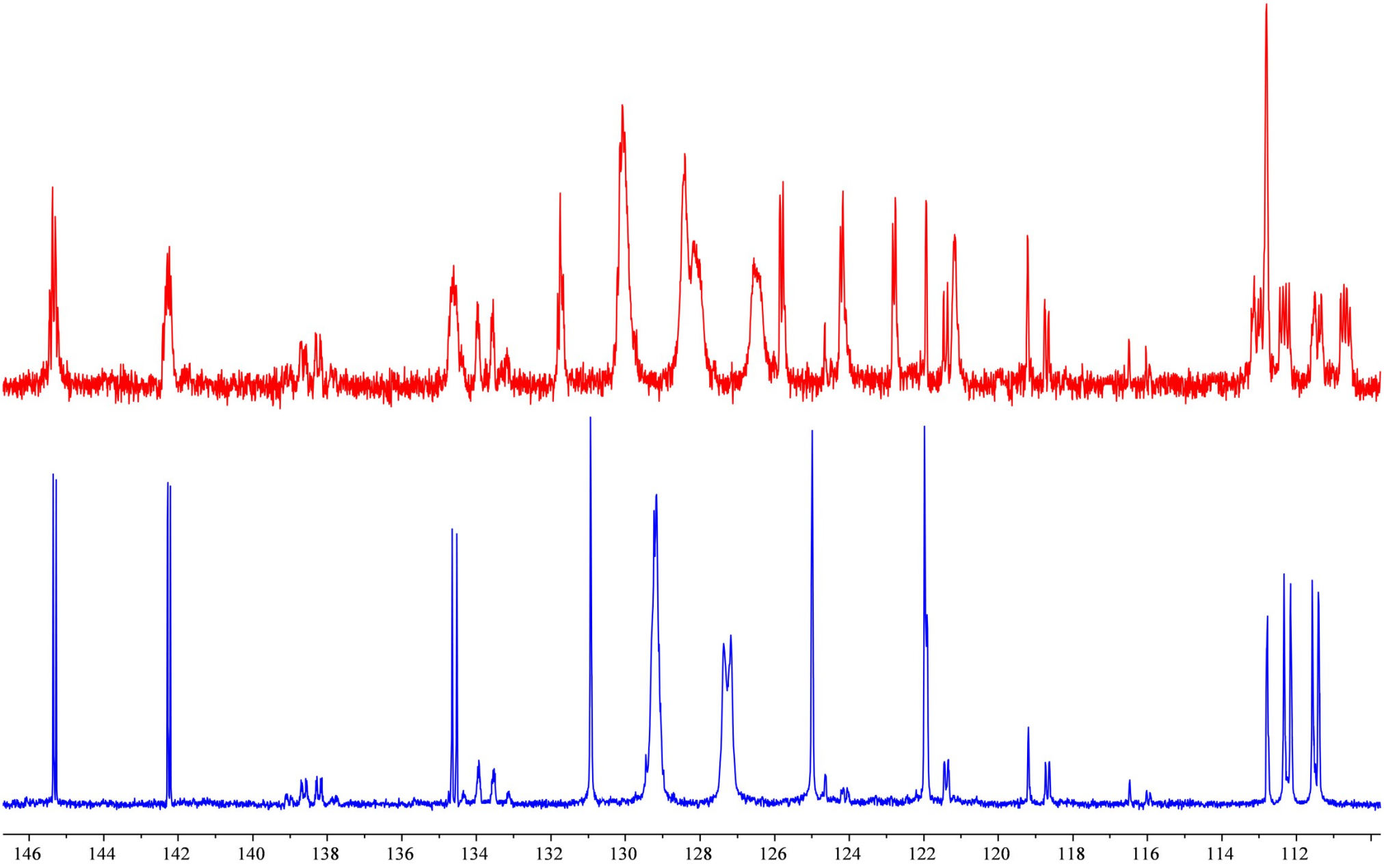

Figure 99. Low-field fragments of ^{13}C-{^{1}H} and ^{13}C NMR spectra (100.6 MHz, CD_2Cl_2, –5°C) of compound (**5b**).

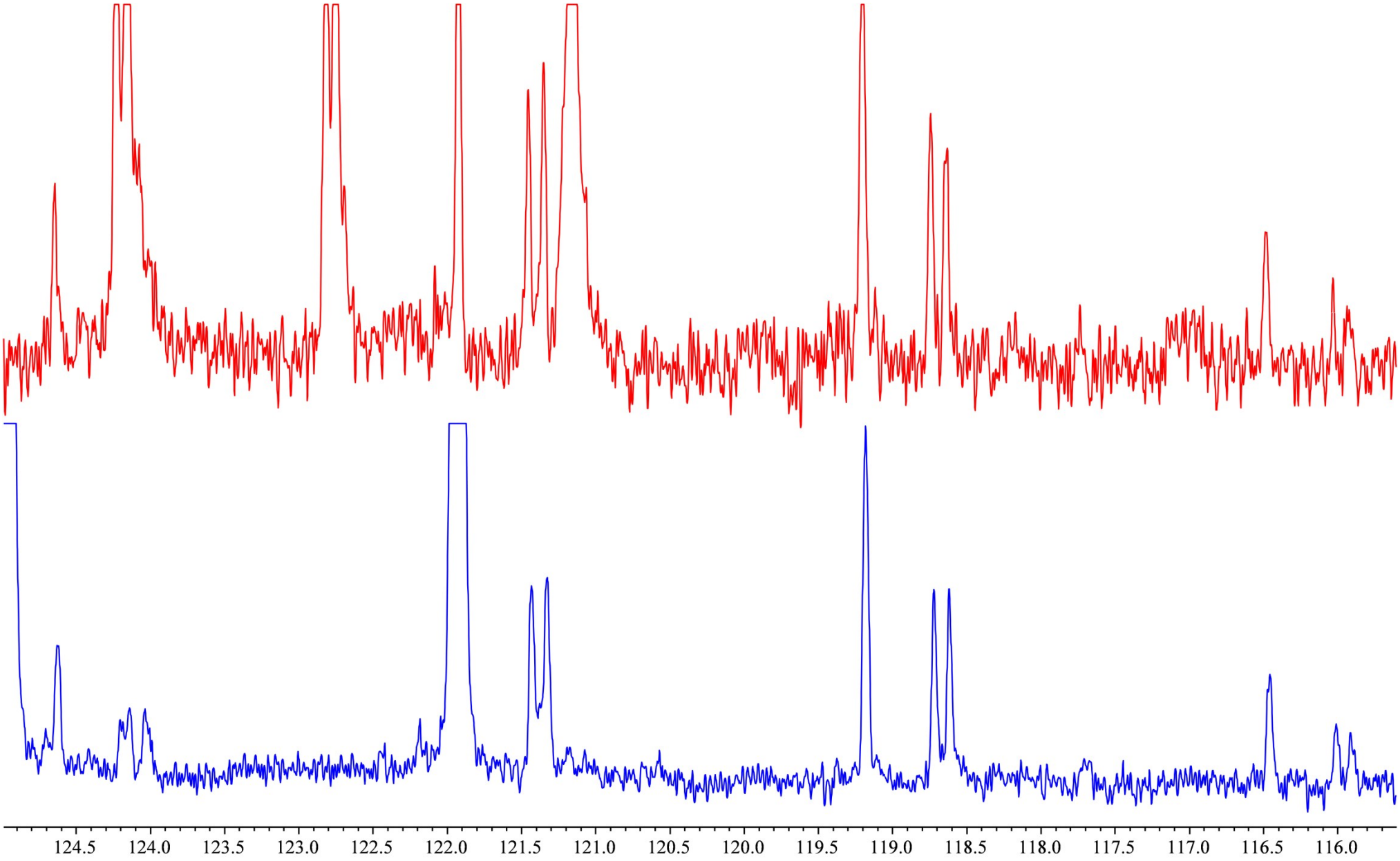

Figure 100. The 115-125 ppm region of ^{13}C-{^{1}H} and ^{13}C NMR spectra (100.6 MHz, CD_2Cl_2, –5°C) of compound (**5b**).

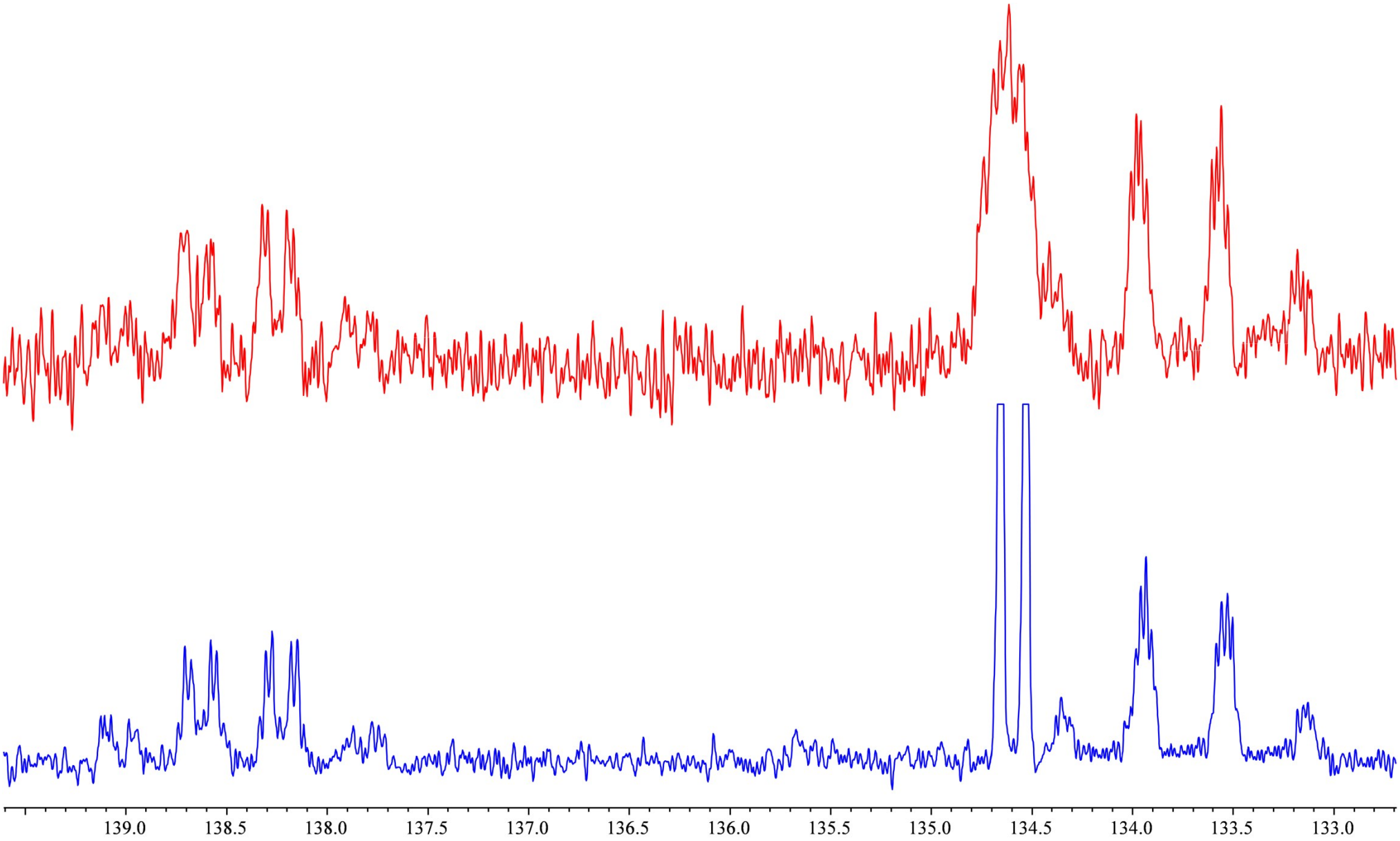

Figure 101. The 132-140 ppm region of ^{13}C-{^{1}H} and ^{13}C NMR spectra (100.6 MHz, CD_2Cl_2, –5°C) of compound (**5b**).

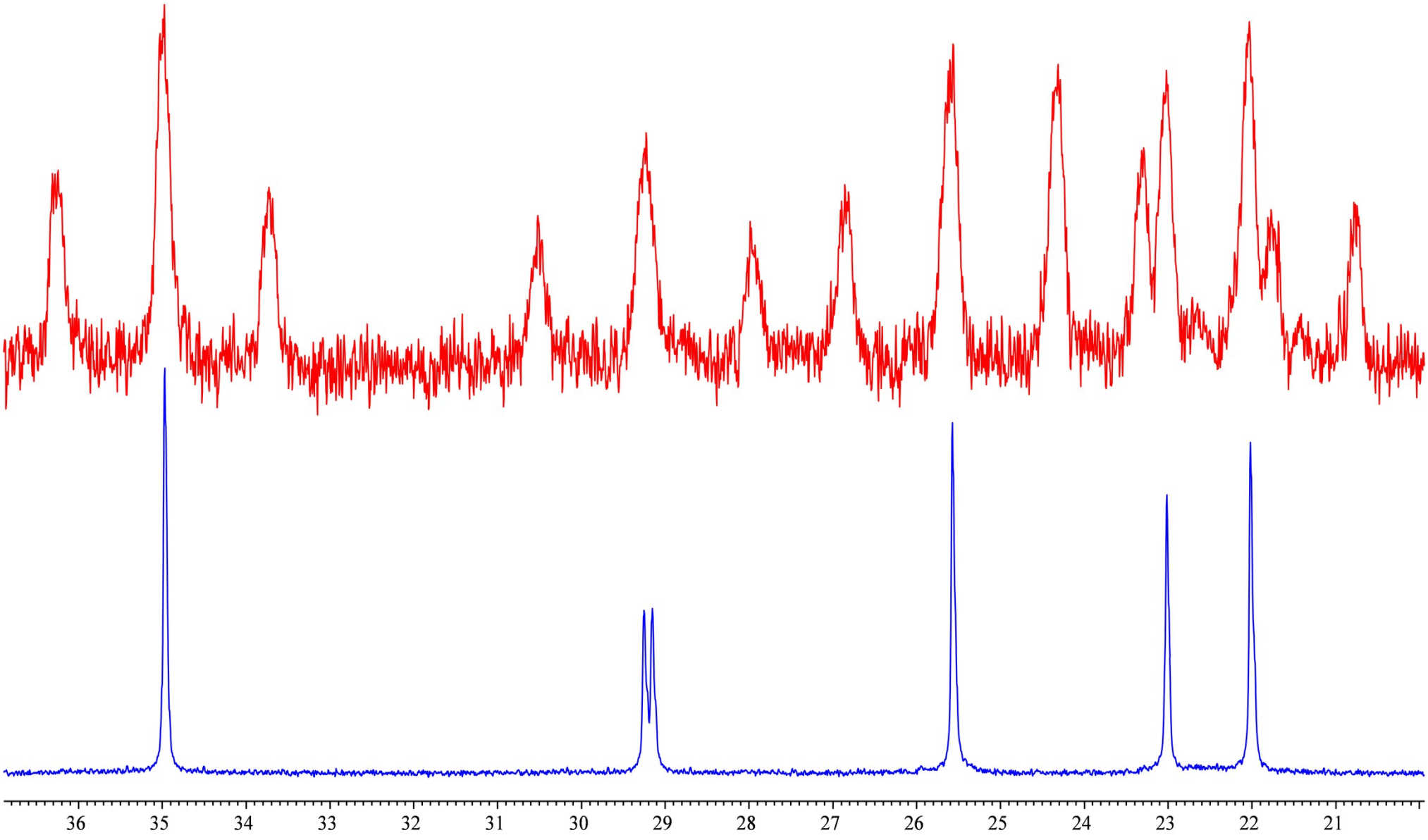

Figure 102. High-field fragments of ^{13}C-{^{1}H} and ^{13}C NMR spectra (100.6 MHz, CD_2Cl_2, –5°C) of compound (**5b**).

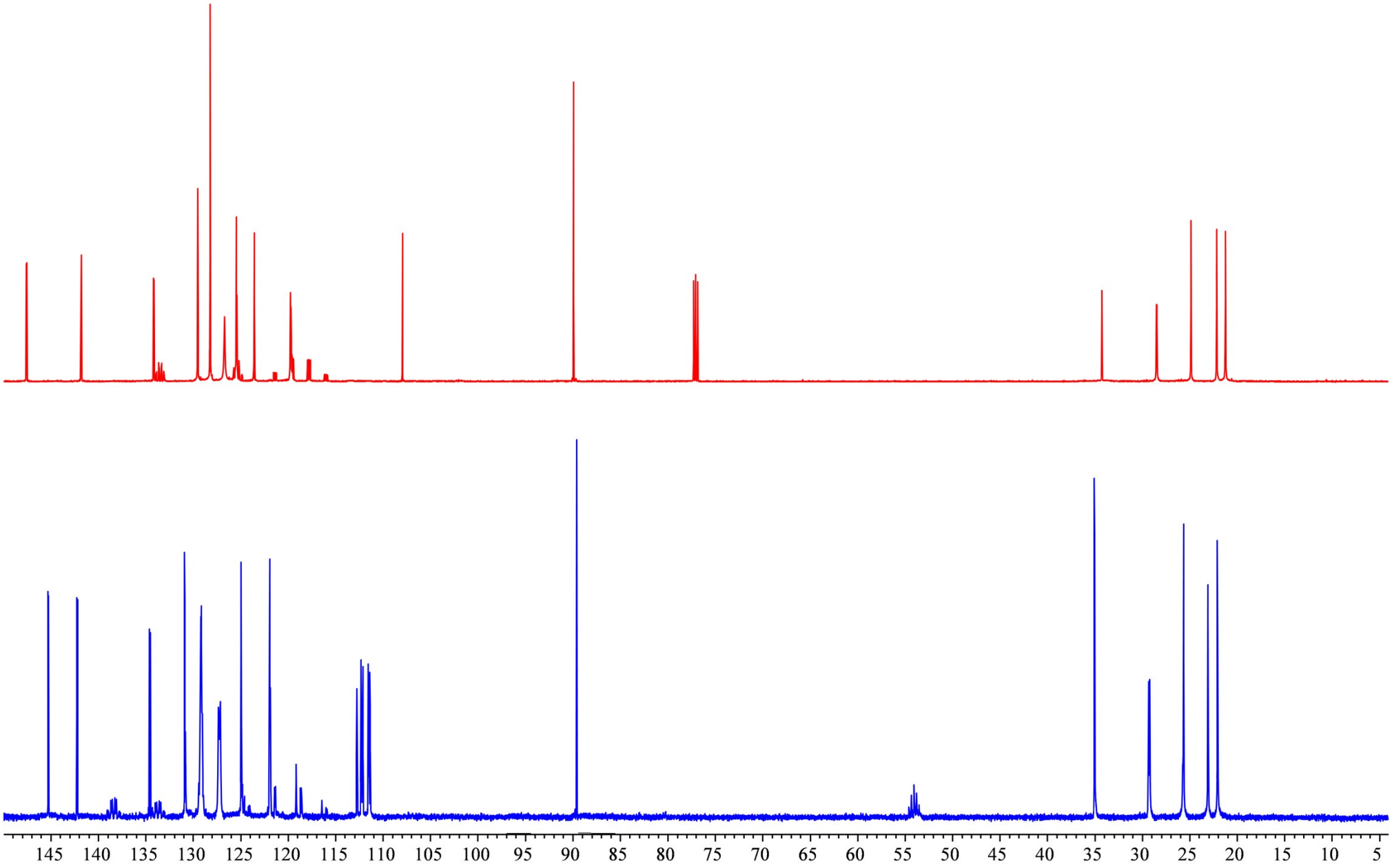

Figure 103. ^{13}C-{^{1}H} NMR spectra (100.6 MHz, $CDCl_3$, 25°C, red; 100.6 MHz, CD_2Cl_2, –5°C, blue) of compounds (**3b**, red) and (**5b**, blue).

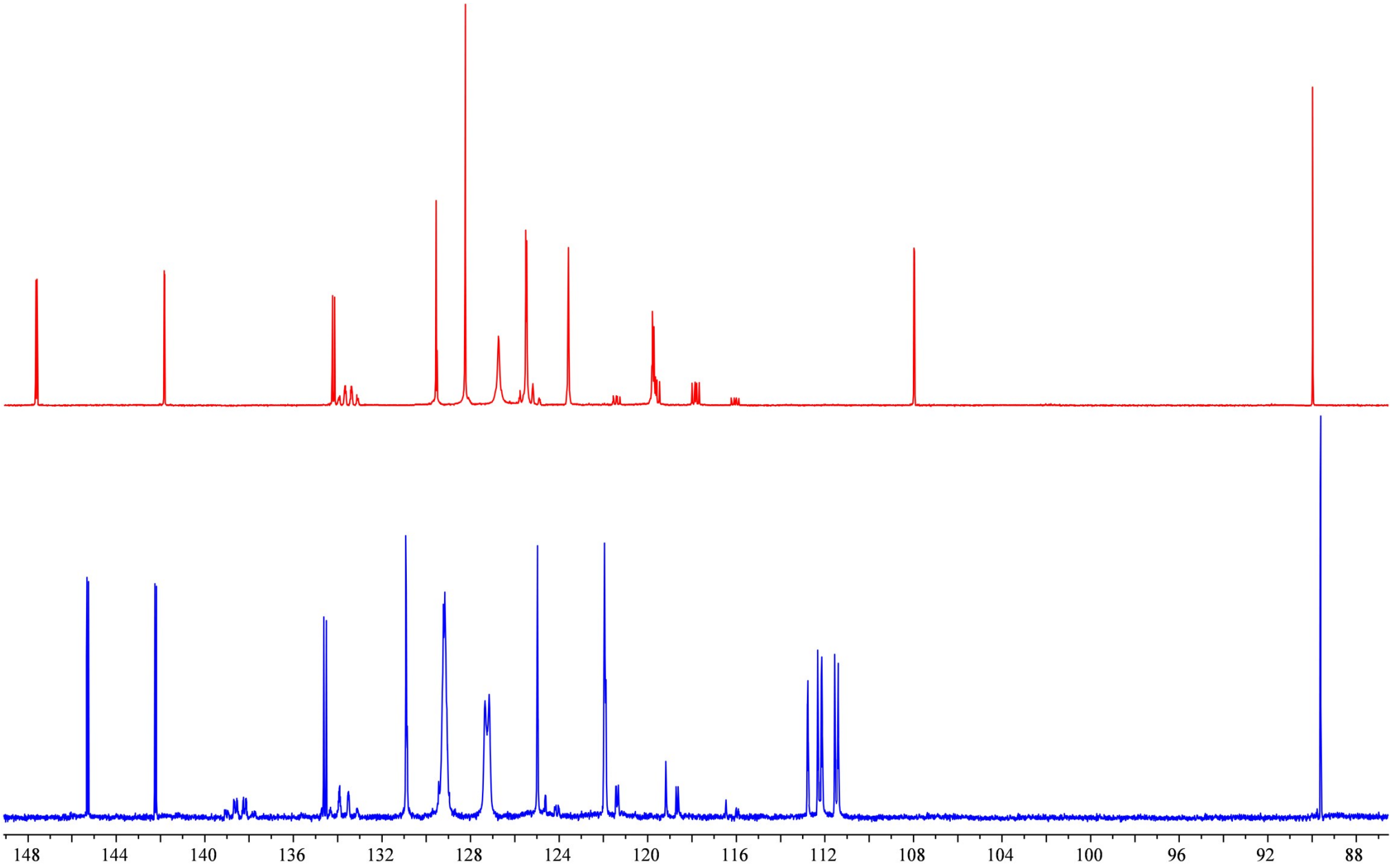

Figure 104. Fragments of ^{13}C-{^{1}H} NMR spectra (100.6 MHz, $CDCl_3$, 25°C, red; 100.6 MHz, CD_2Cl_2, –5°C, blue) of compounds (**3b**, red) and (**5b**, blue).

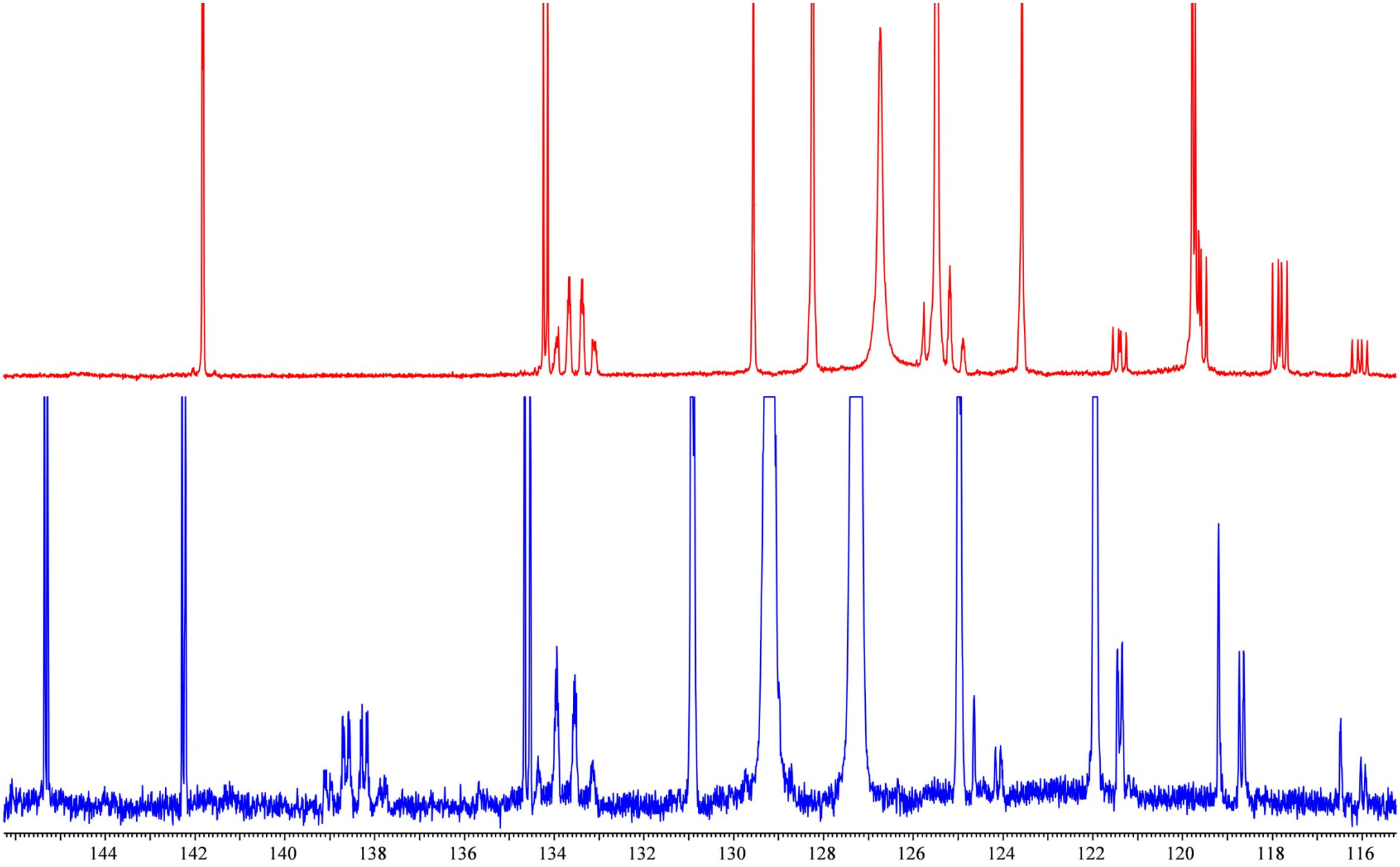

Figure 105. The 115-145 ppm region of ^{13}C-{^{1}H} NMR spectra (100.6 MHz, $CDCl_3$, 25°C, red; 100.6 MHz, CD_2Cl_2, –5°C, blue) of compounds (**3b**, red) and (**5b**, blue).

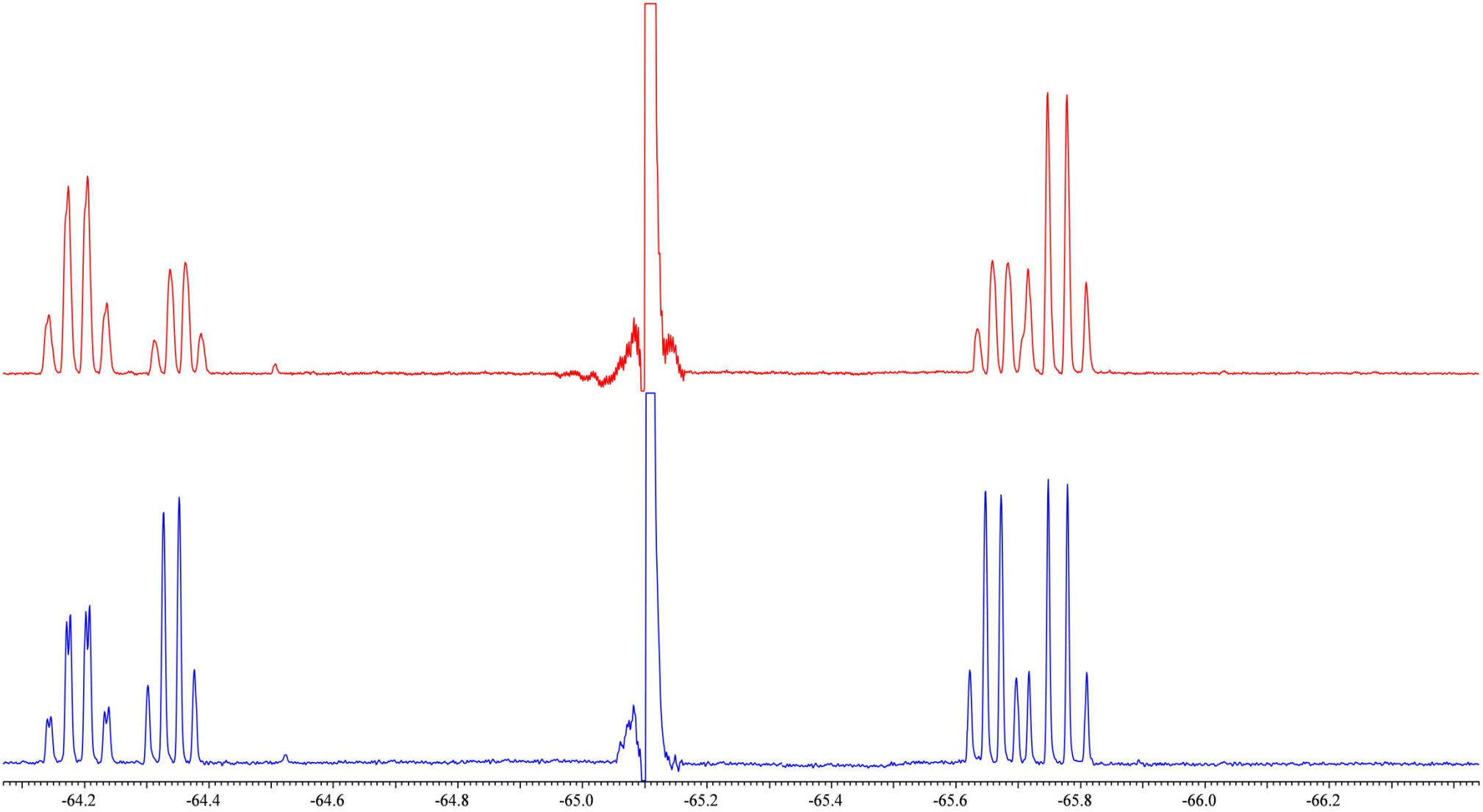

Figure 106. The –66÷–64 ppm region of ^{19}F NMR spectra (376.3 MHz, CD_2Cl_2, 5°C, the next day, red; 5°C, in two days, blue) of compound (**5b**); minor quartets belong to compounds (**3b**, **5b**).

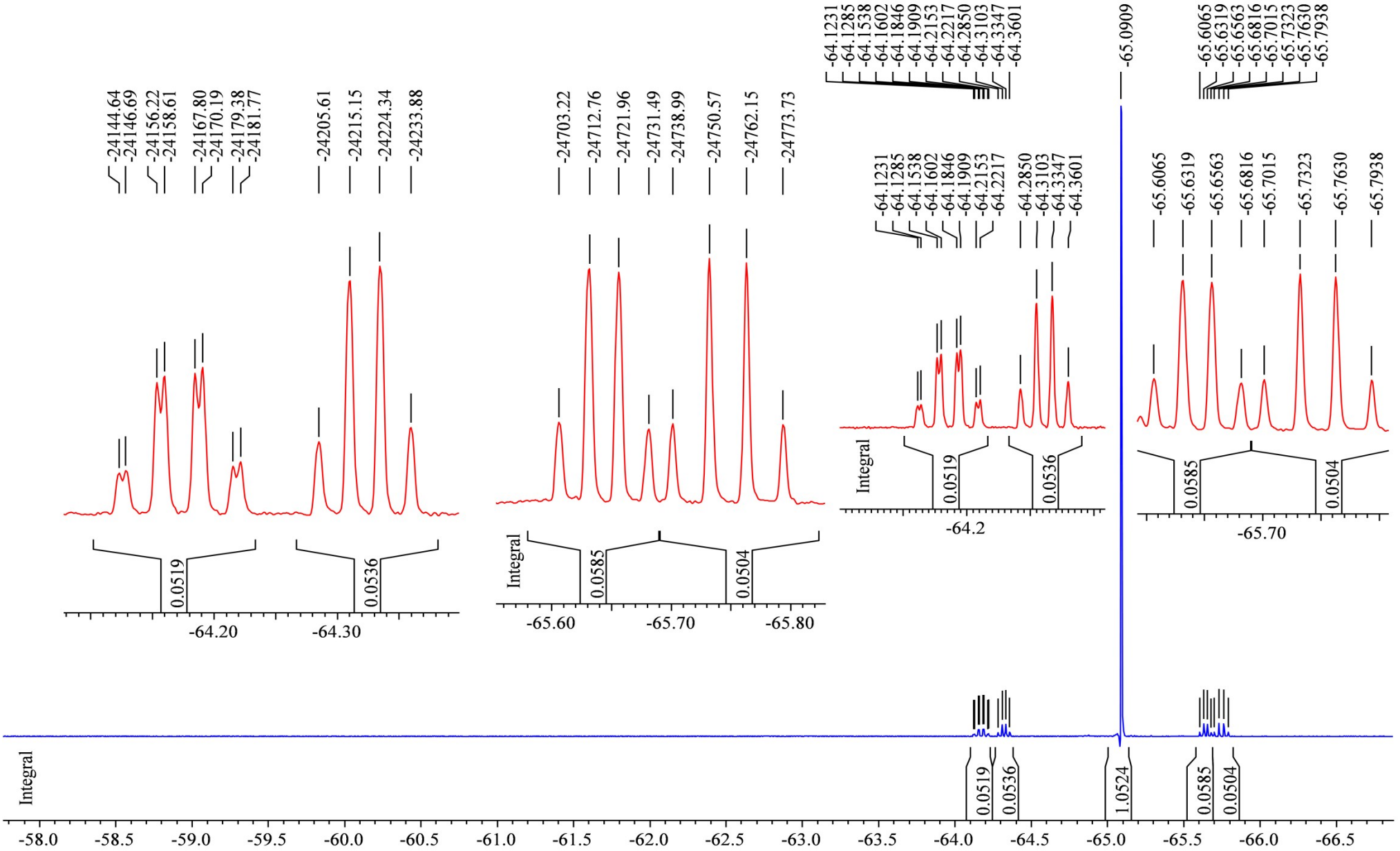

Figure 107. ^{19}F NMR spectrum (376.3 MHz, CD_2Cl_2, 5°C, in two days) of the phosphole (**1b**) and perfluorodiacetyl reaction mixture. The main compound is (**4b**), and minor quartets belong to compounds (**3b**, **5b**).

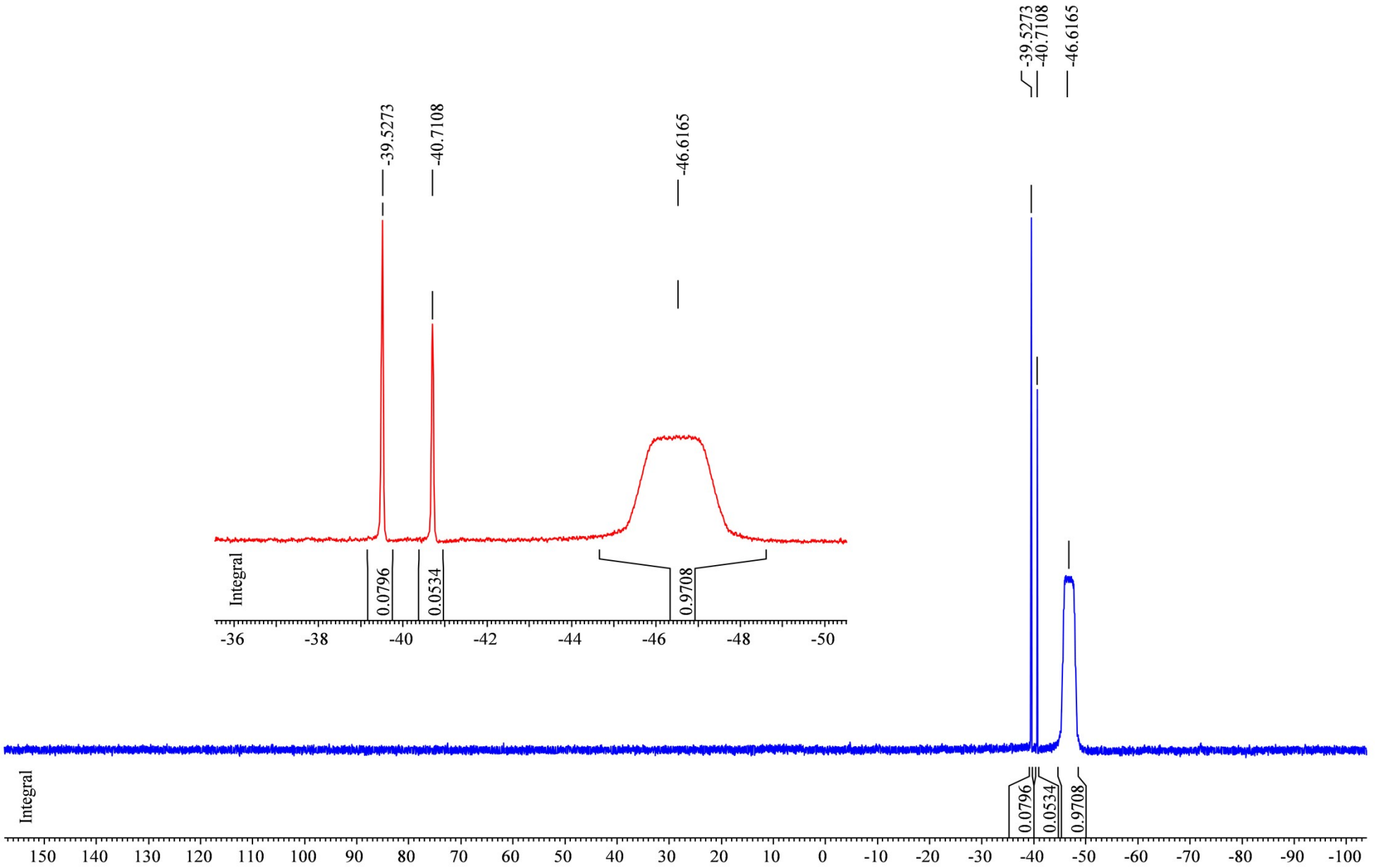

Figure 108. ^{31}P-{^{1}H} NMR spectrum (162.0 MHz, CD_2Cl_2, 5°C; after 3 days at 5 °C) of compound (**4b**); minor signals belong to compounds (**3b**) and (**5b**).

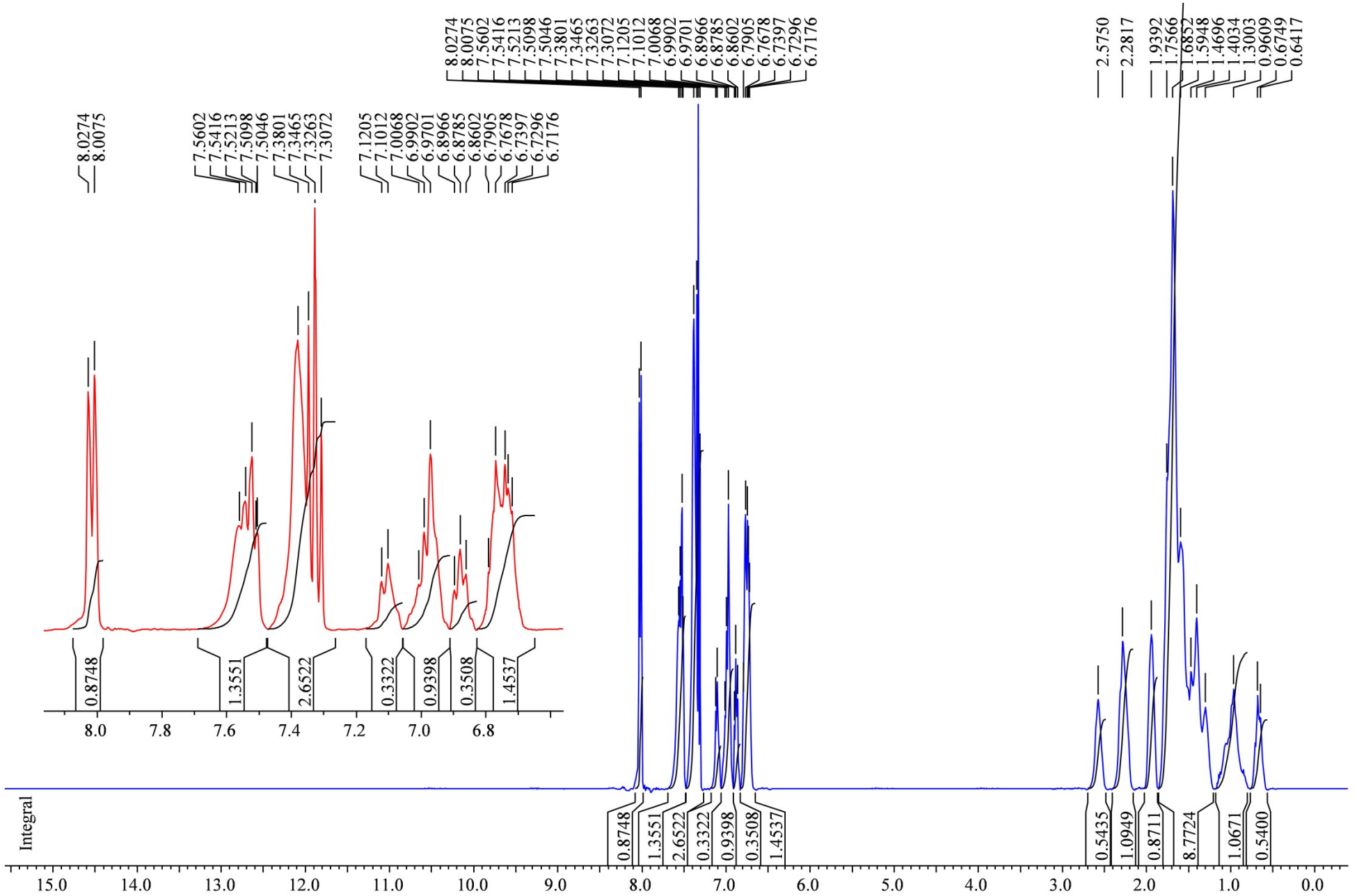

Figure 109. ^{1}H NMR spectrum (400.0 MHz, CD_2Cl_2, 5°C) of the compounds (**4b**, **5b**) mixture.

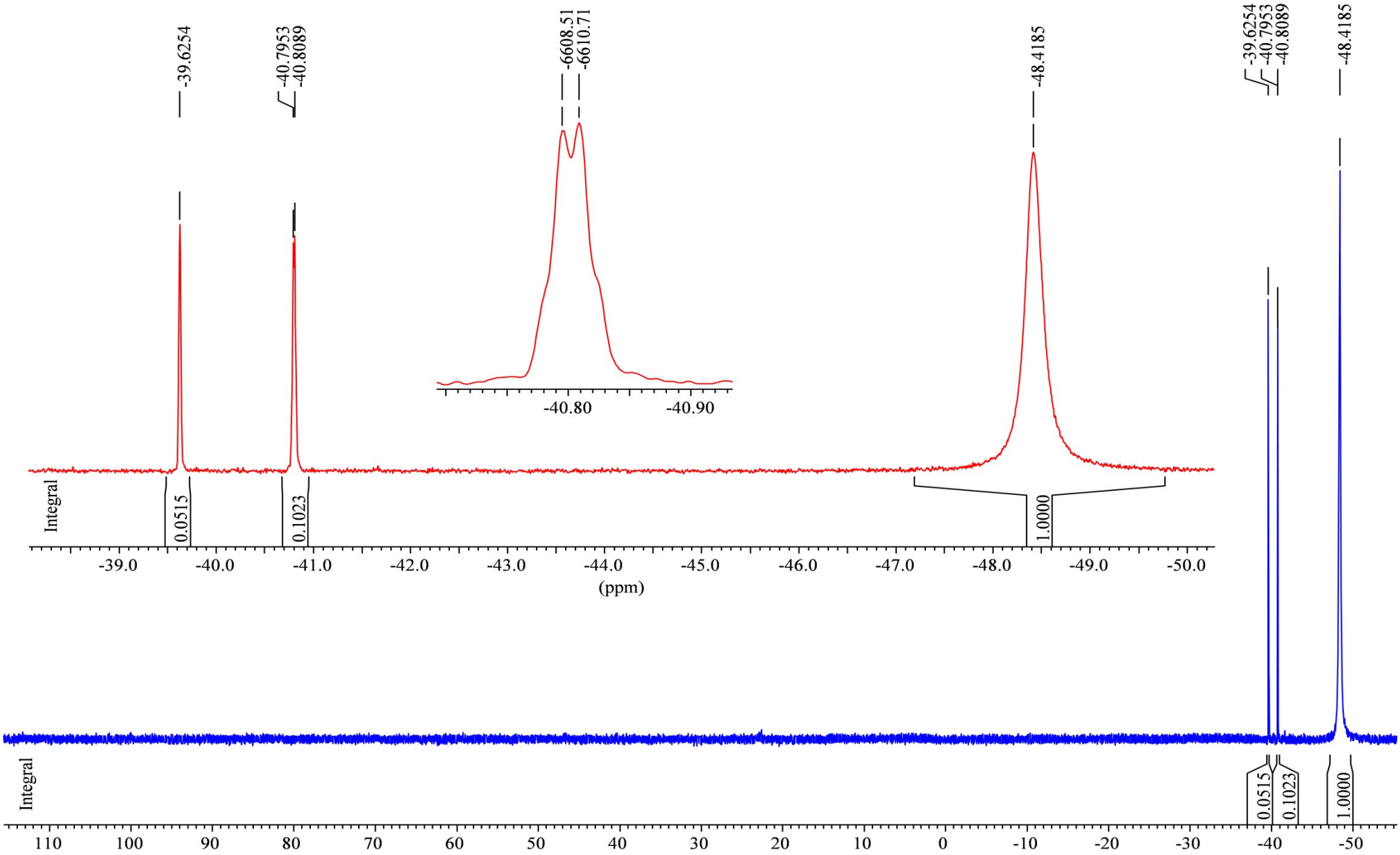

Figure 110. ^{31}P-{^{1}H} NMR spectrum (162.0 MHz, CD_2Cl_2, 25°C; in three days at 5 °C) of compound (**4b**); minor signals belong to compounds (**3b**) and (**5b**).

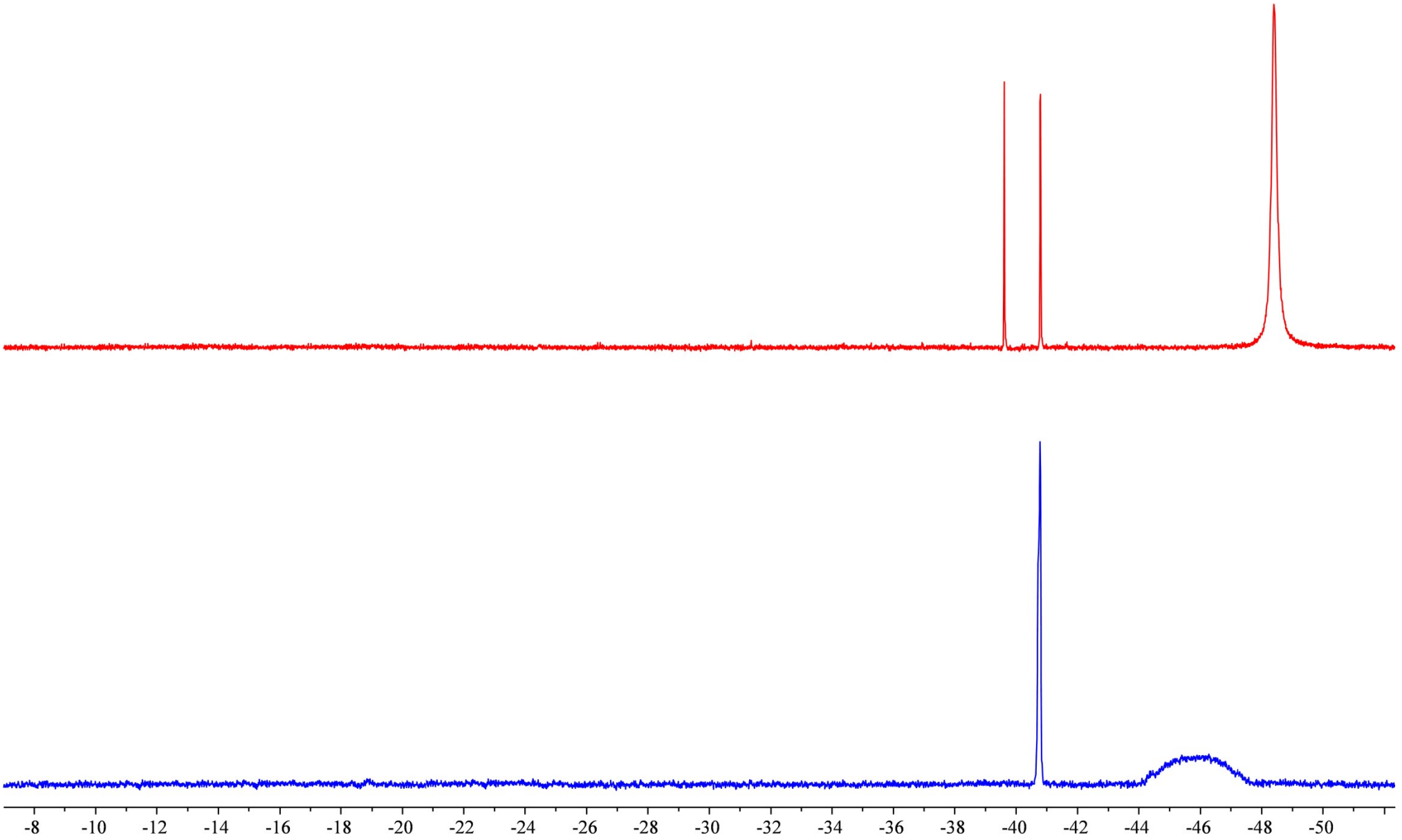

Figure 111. ^{31}P-{^{1}H} NMR spectra (162.0 MHz, CD_2Cl_2, 25°C, in three days at 5 °C, red; in one day at 5 °C, blue) of compound (**4b**).

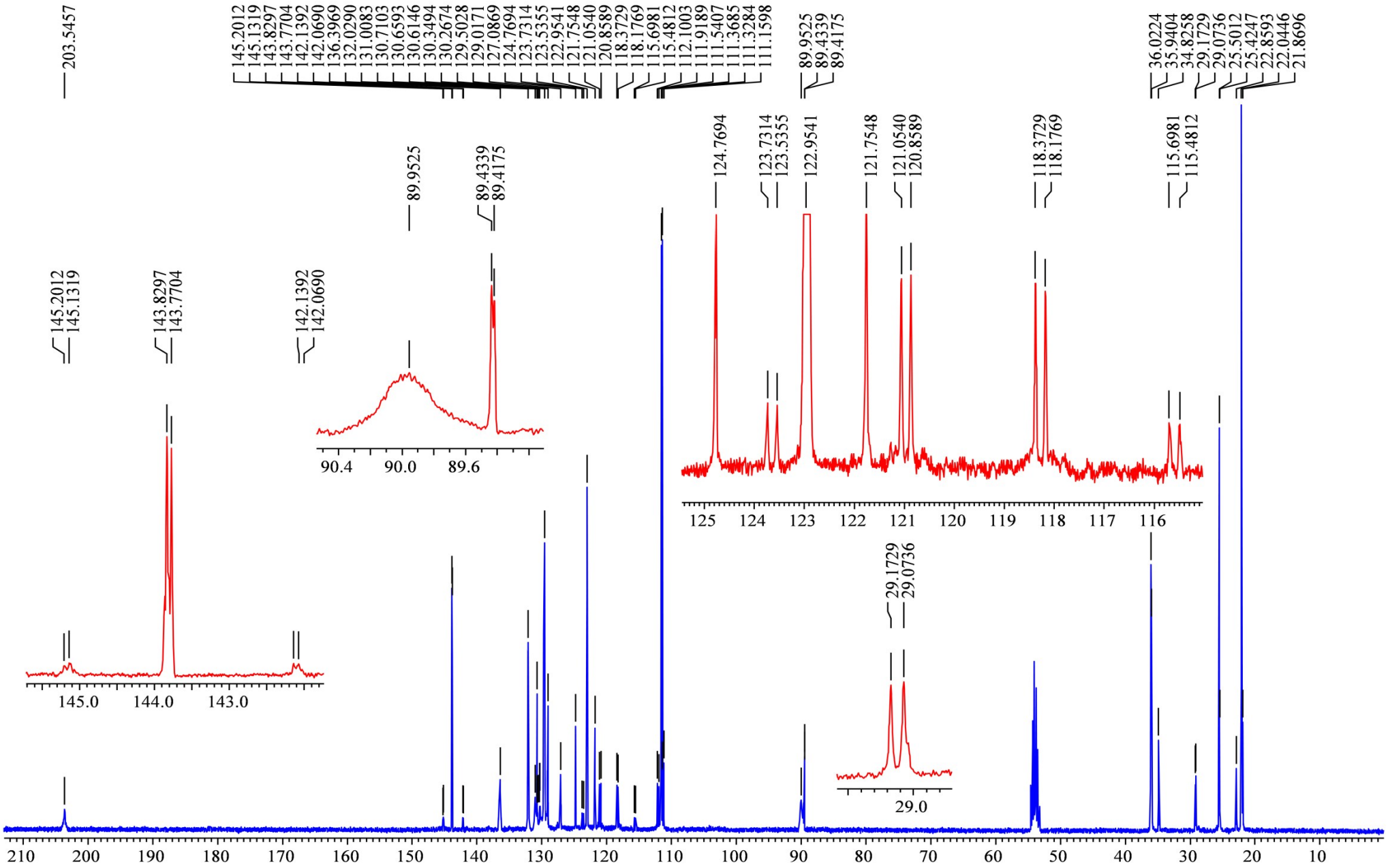

Figure 112. ^{13}C-{^{1}H} NMR spectrum (100.6 MHz, CD_2Cl_2, 5°C) of compound (**4b**); minor signals belong to compound (**5b**).

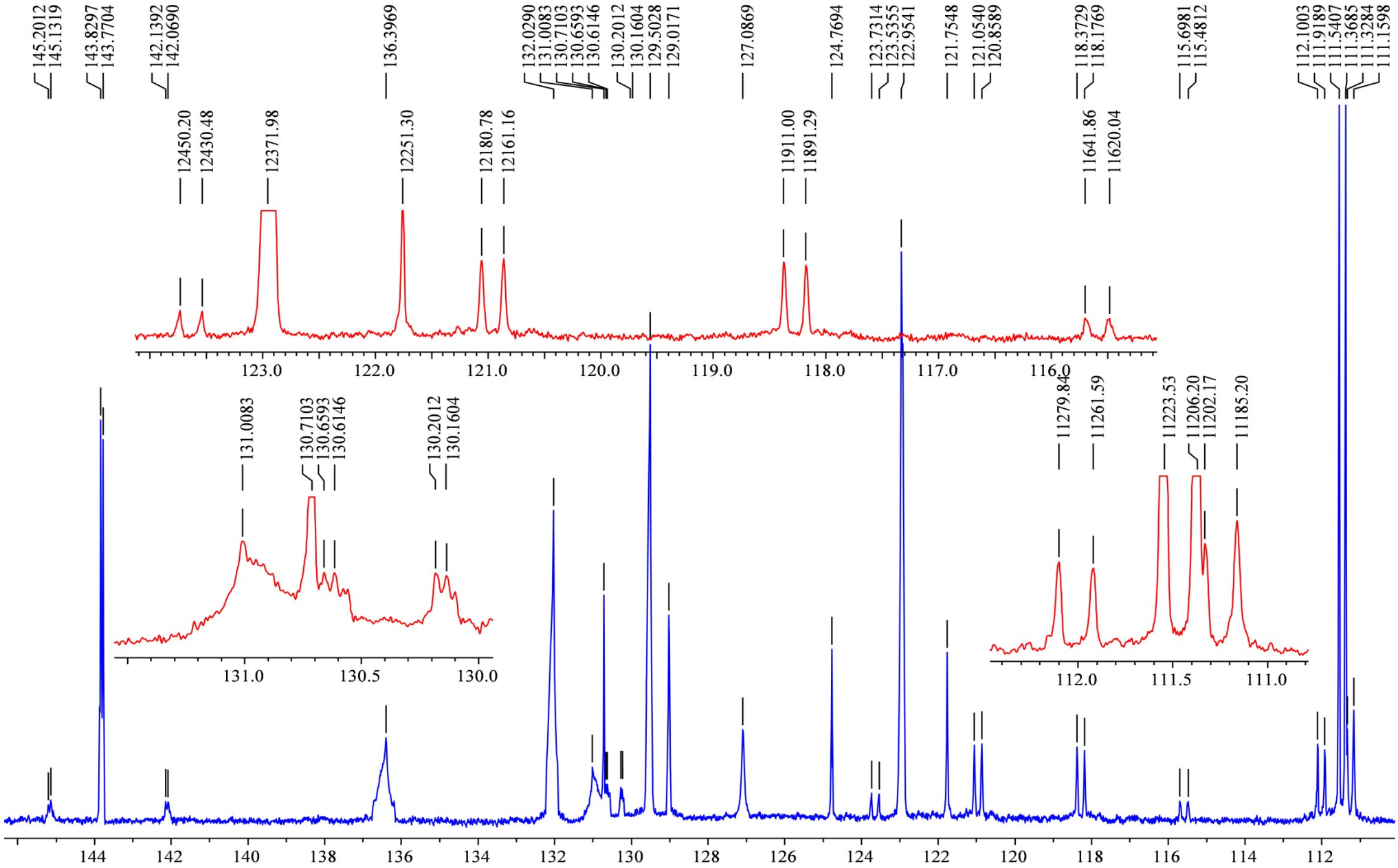

Figure 113. Low-field region of ^{13}C-{^{1}H} NMR spectrum (100.6 MHz, CD_2Cl_2, 5°C) of compound (**4b**); minor signals belong to compound (**5b**).

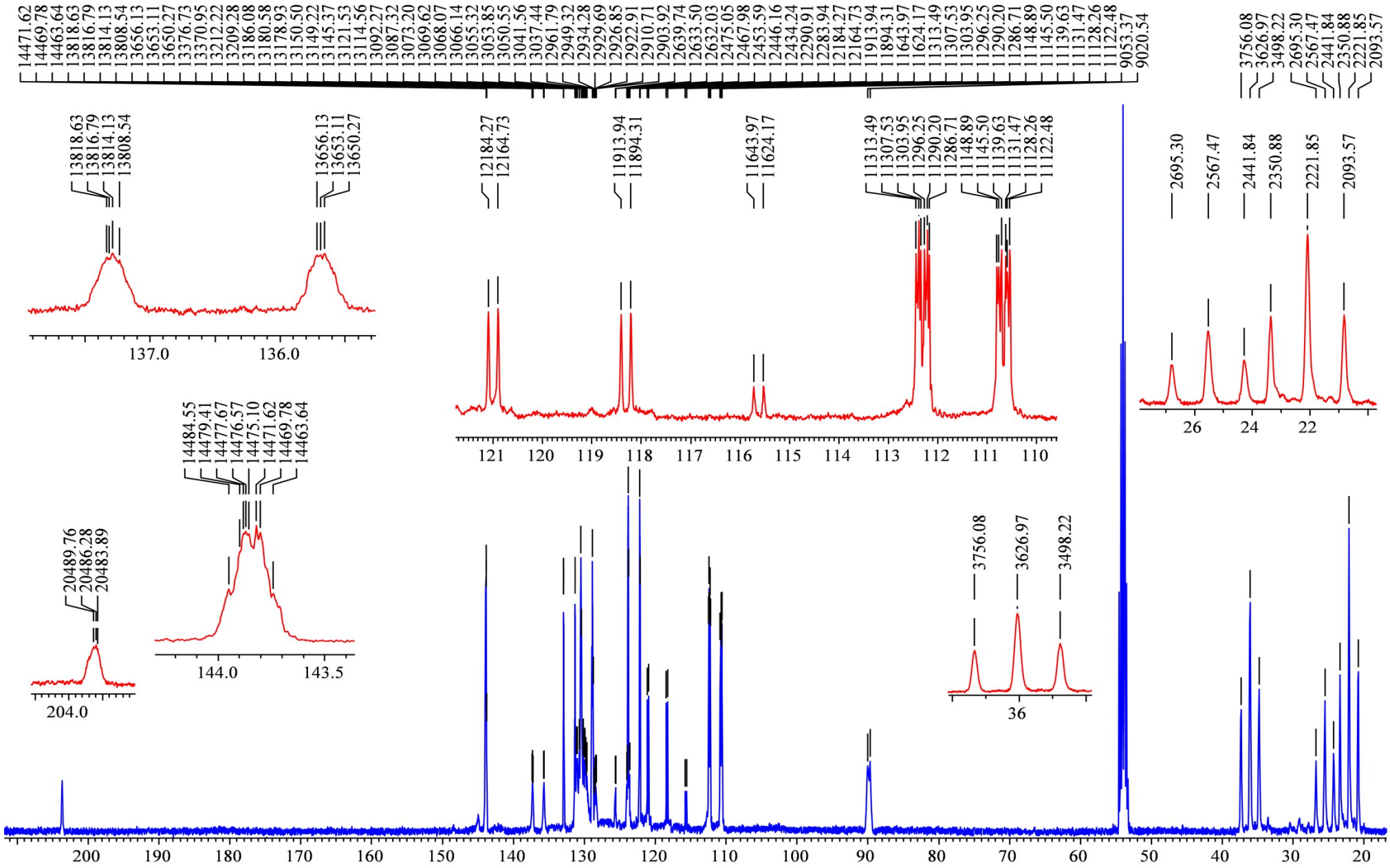

Figure 114. ^{13}C NMR spectrum (100.6 MHz, CD_2Cl_2, 5°C) of compound (**4b**); minor signals belong to compound (**5b**).

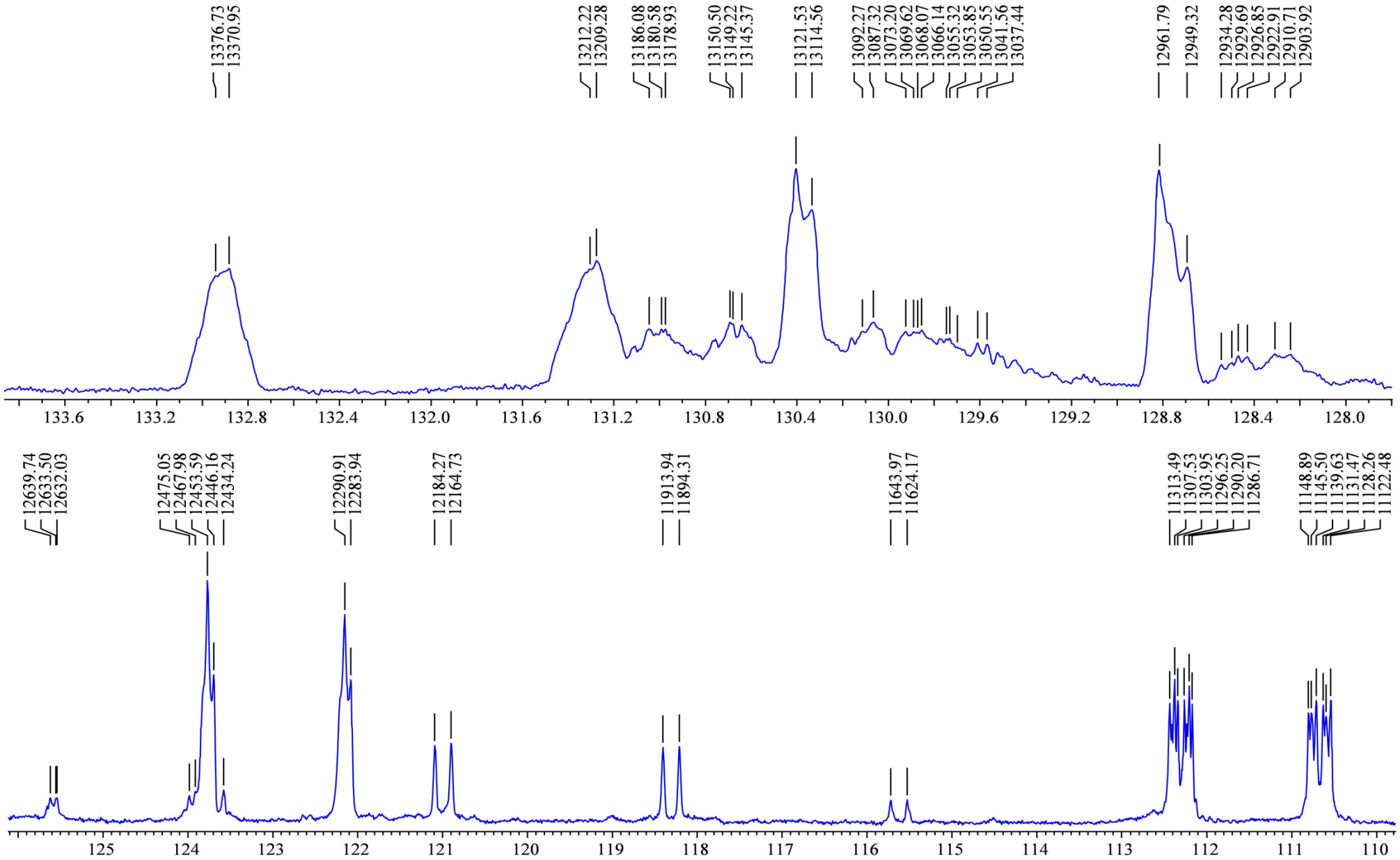

Figure 115. Low-field fragments of ^{13}C-{^{1}H} NMR spectrum (100.6 MHz, CD_2Cl_2, 5°C) of compound (**4b**); minor signals belong to compound (**5b**).

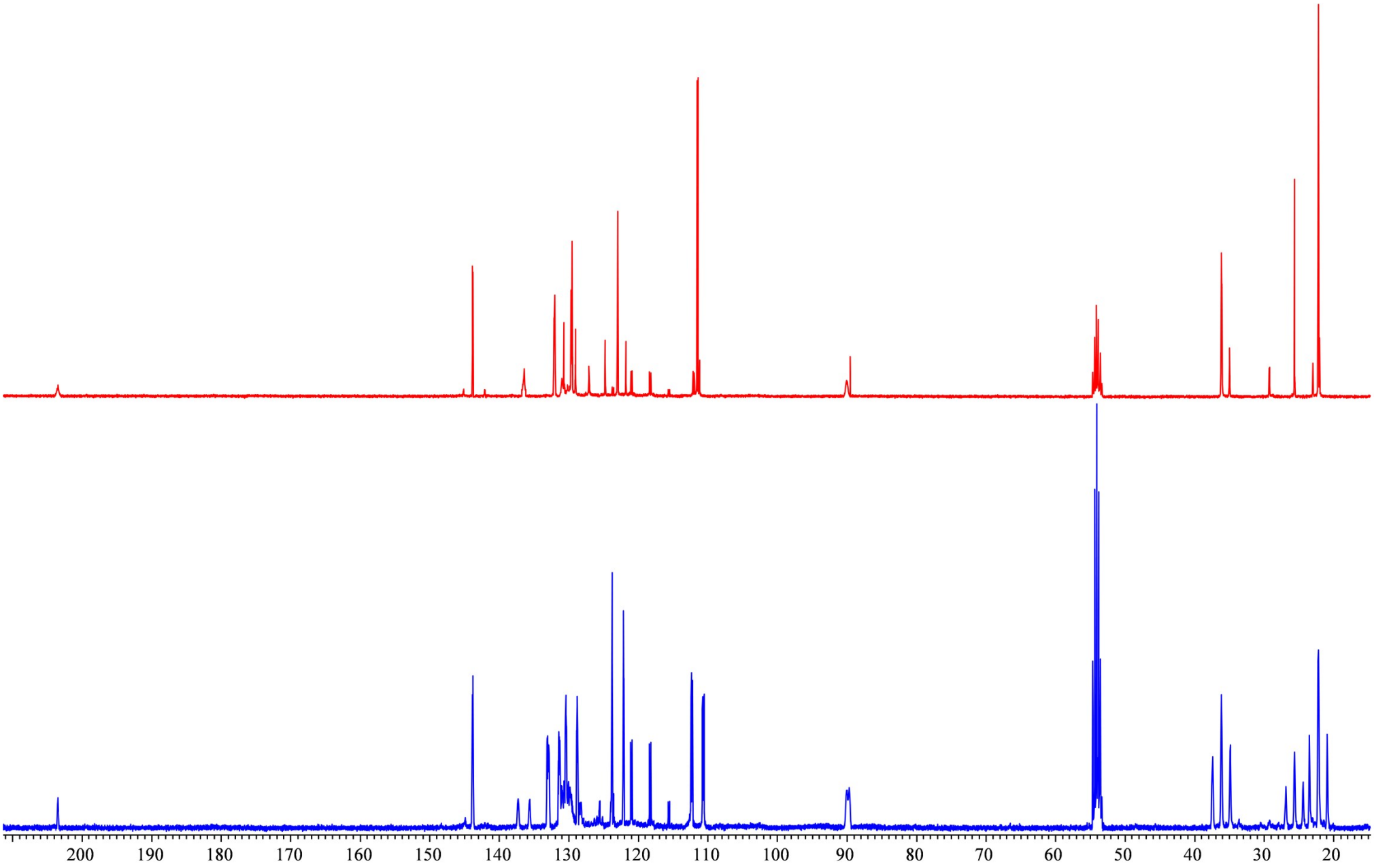

Figure 116. ^{13}C-{^{1}H} and ^{13}C NMR spectra (100.6 MHz, CD_2Cl_2, 5°C) of compound (**4b**); minor signals belong to compound (**5b**).

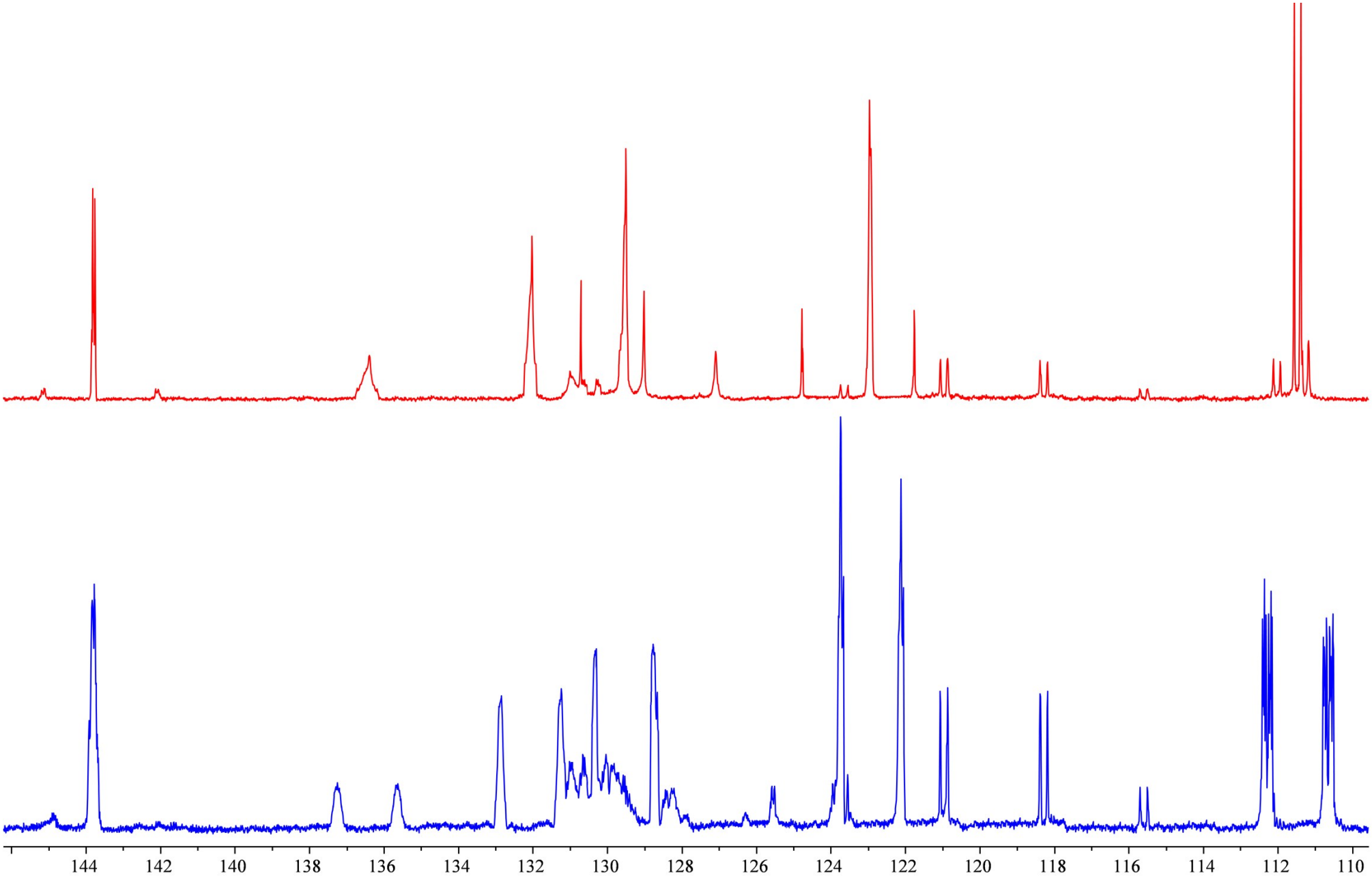

Figure 117. Low-field region of ^{13}C-{^{1}H} and ^{13}C NMR spectra (100.6 MHz, CD_2Cl_2, 5°C) of compound (**4b**); minor signals belong to compound (**5b**).

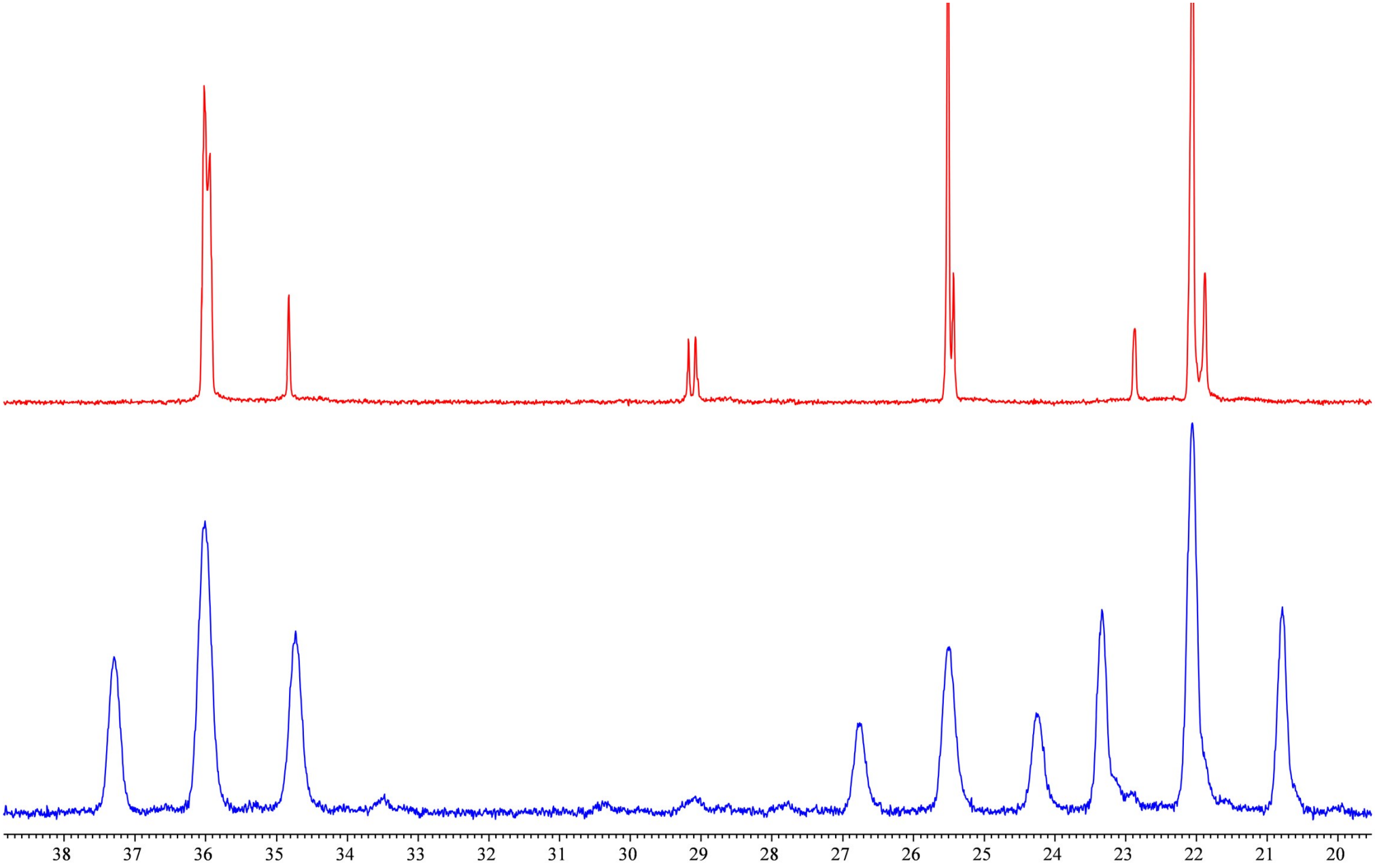

Figure 118. High-field region of ^{13}C-{^{1}H} and ^{13}C NMR spectra (100.6 MHz, CD_2Cl_2, 5°C) of compound (**4b**); minor signals belong to compound (**5b**).

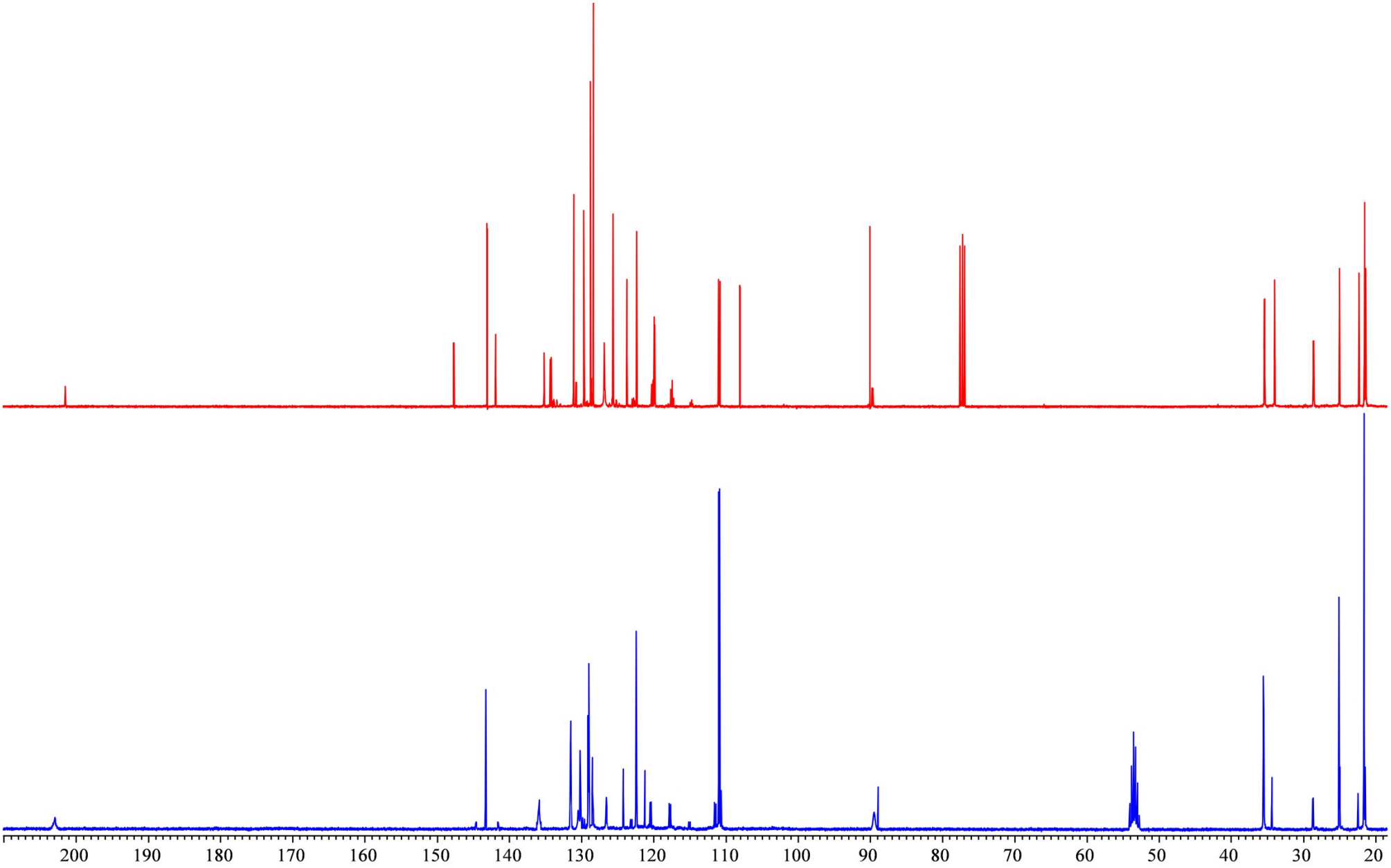

Figure 119. ^{13}C-{^{1}H} NMR spectra (150.9 MHz, $CDCl_3$, 25°C, red; 100.6 MHz, CD_2Cl_2, 5°C, blue) of the compounds (**3b**, **4b**) (red) and (**4b**, **5b**) mixtures. Here and below (Fig. 120, 121), the lower spectrum is shifted to the right until the signals of the benzo fragment of compound (**4b**) coincide.

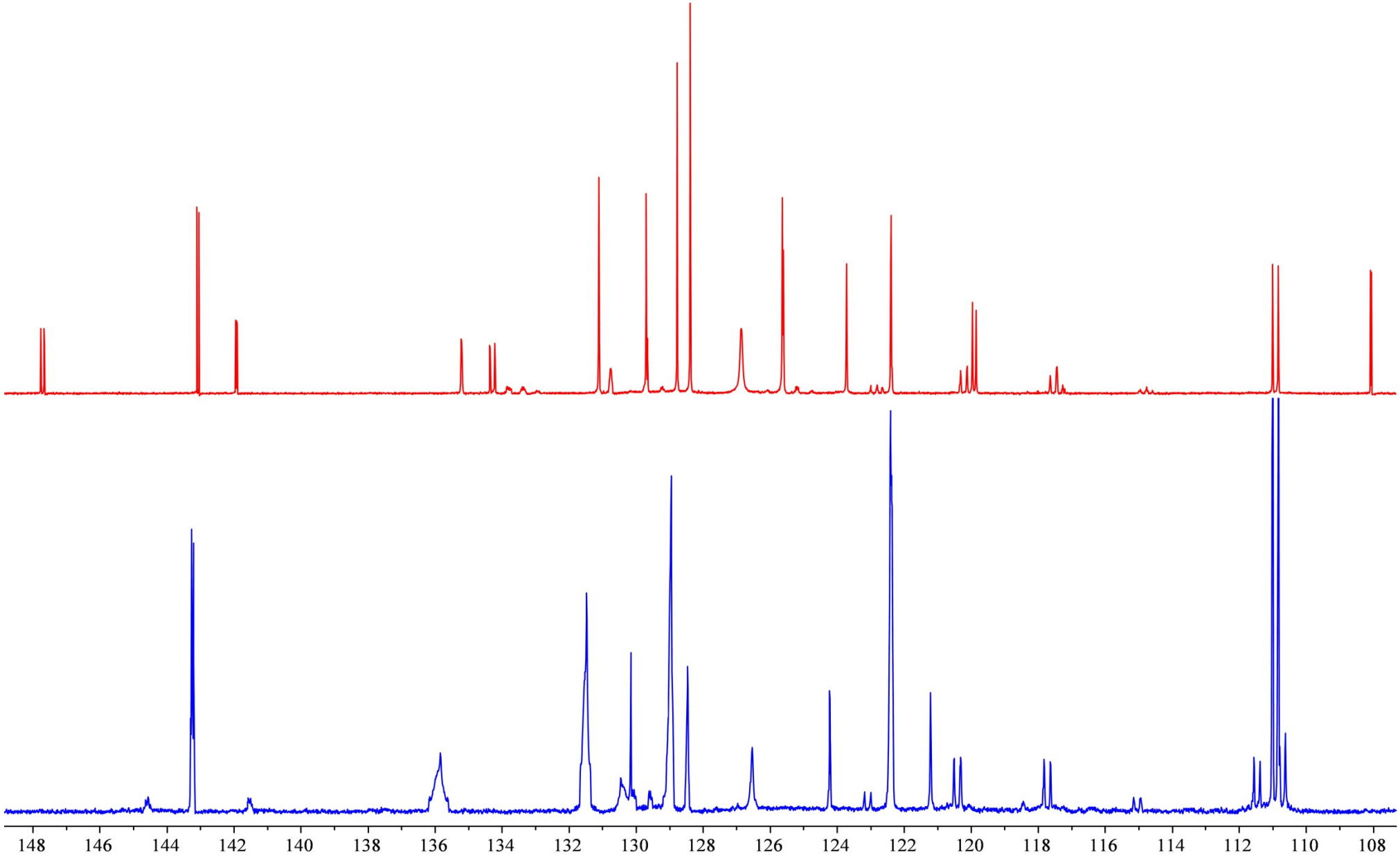

Figure 120. Low-field fragment of ^{13}C-{^{1}H} NMR spectra (150.9 MHz, $CDCl_3$, 25°C, red; 100.6 MHz, CD_2Cl_2, 5°C, blue) of the compounds (**3b**, **4b**) (red) and (**4b**, **5b**) mixtures (blue).

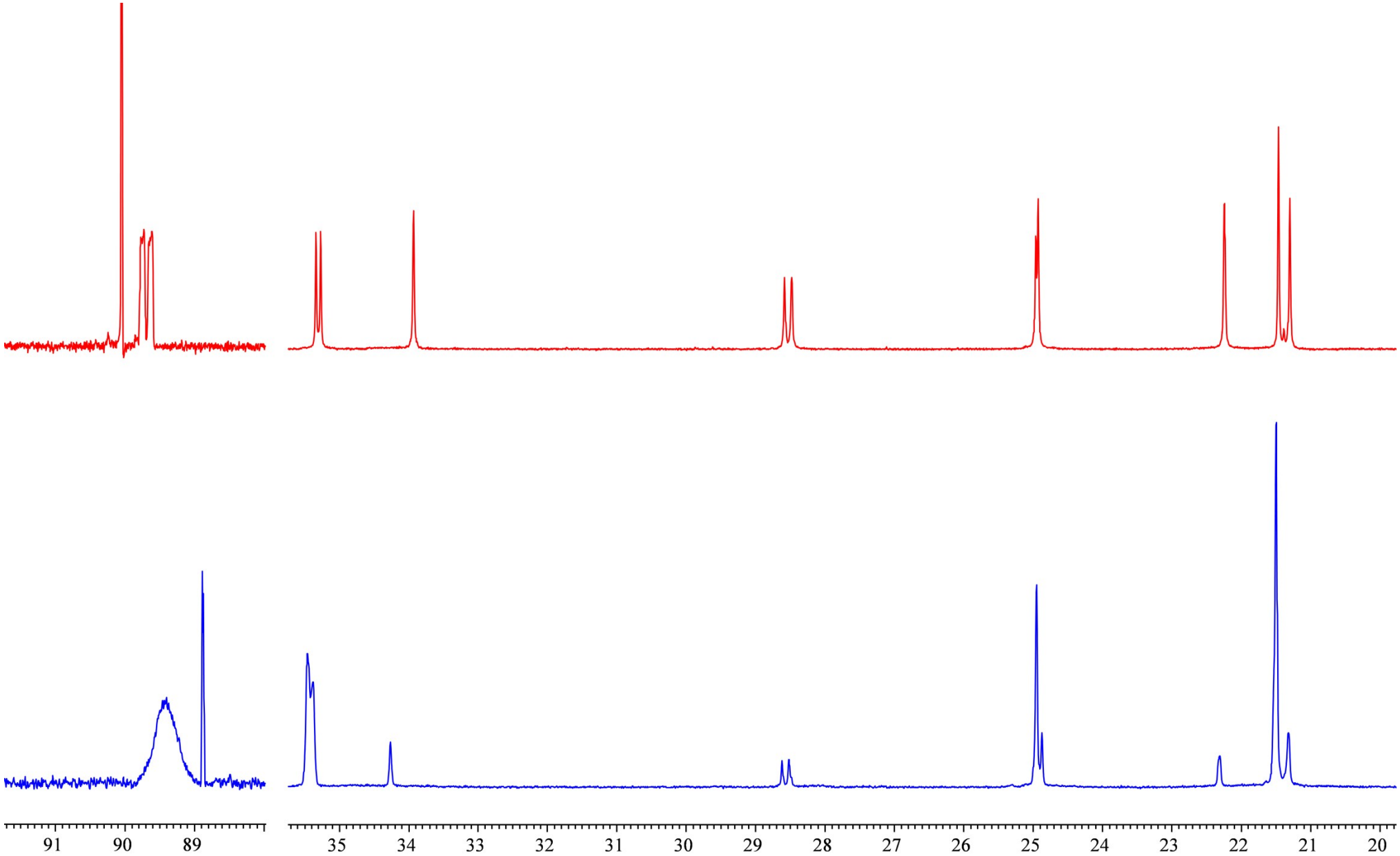

Figure 121. High-field fragments of ^{13}C-{^{1}H} NMR spectra (150.9 MHz, $CDCl_3$, 25°C, red; 100.6 MHz, CD_2Cl_2, 5°C, blue) of the compounds (**3b**, **4b**) (red) and (**4b**, **5b**) mixtures (blue).

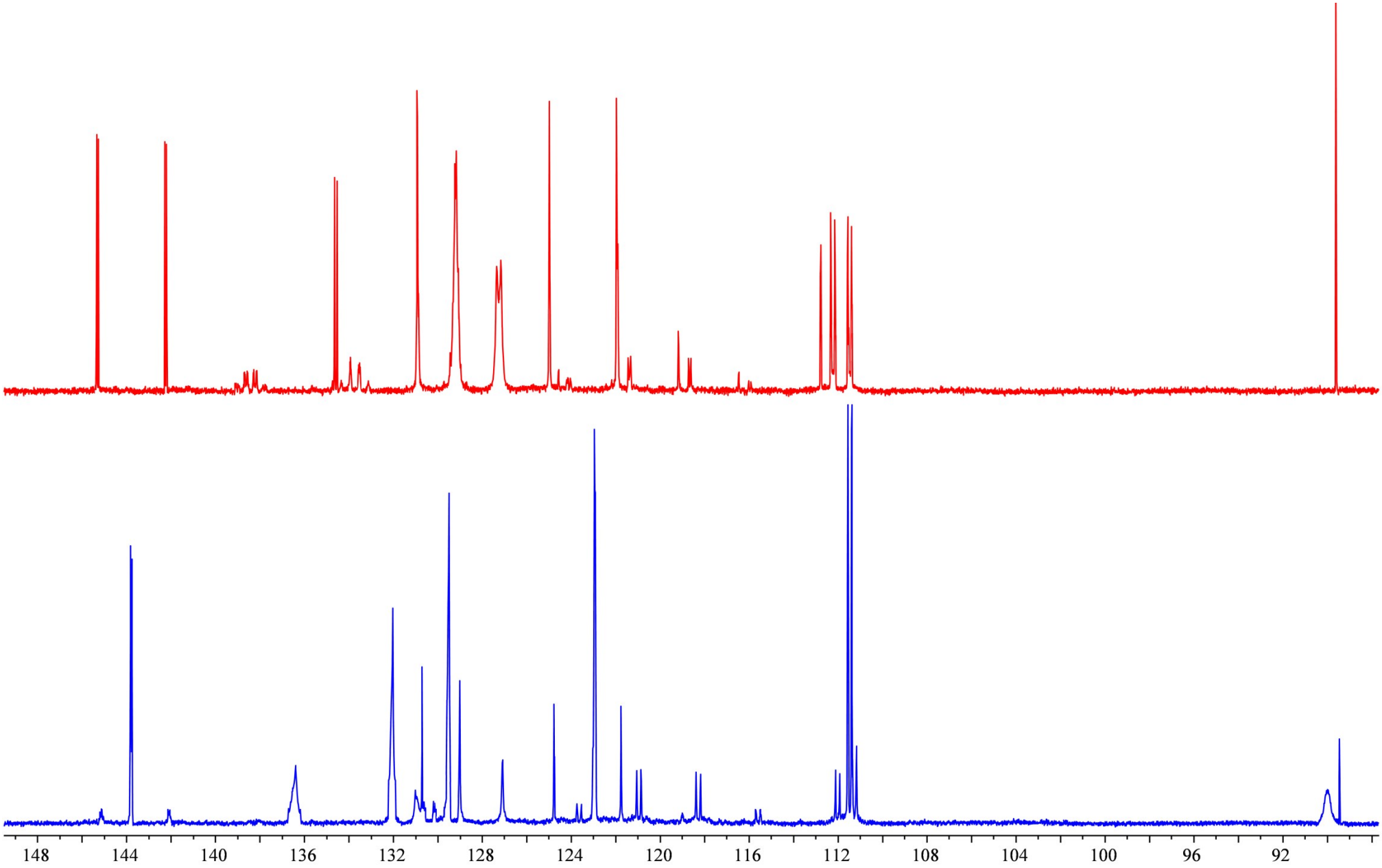

Figure 122. Low-field fragment of ^{13}C-{^{1}H} NMR spectra (100.6 MHz, CD_2Cl_2, –5°C, red; CD_2Cl_2, 5°C, blue) of compound (**5b**) (red) and the compounds (**4b**, **5b**) mixture. Here and below (Fig. 123, 124) the lower spectrum is shifted to the left until the signals of the benzo fragment of compound (**5b**) coincide.

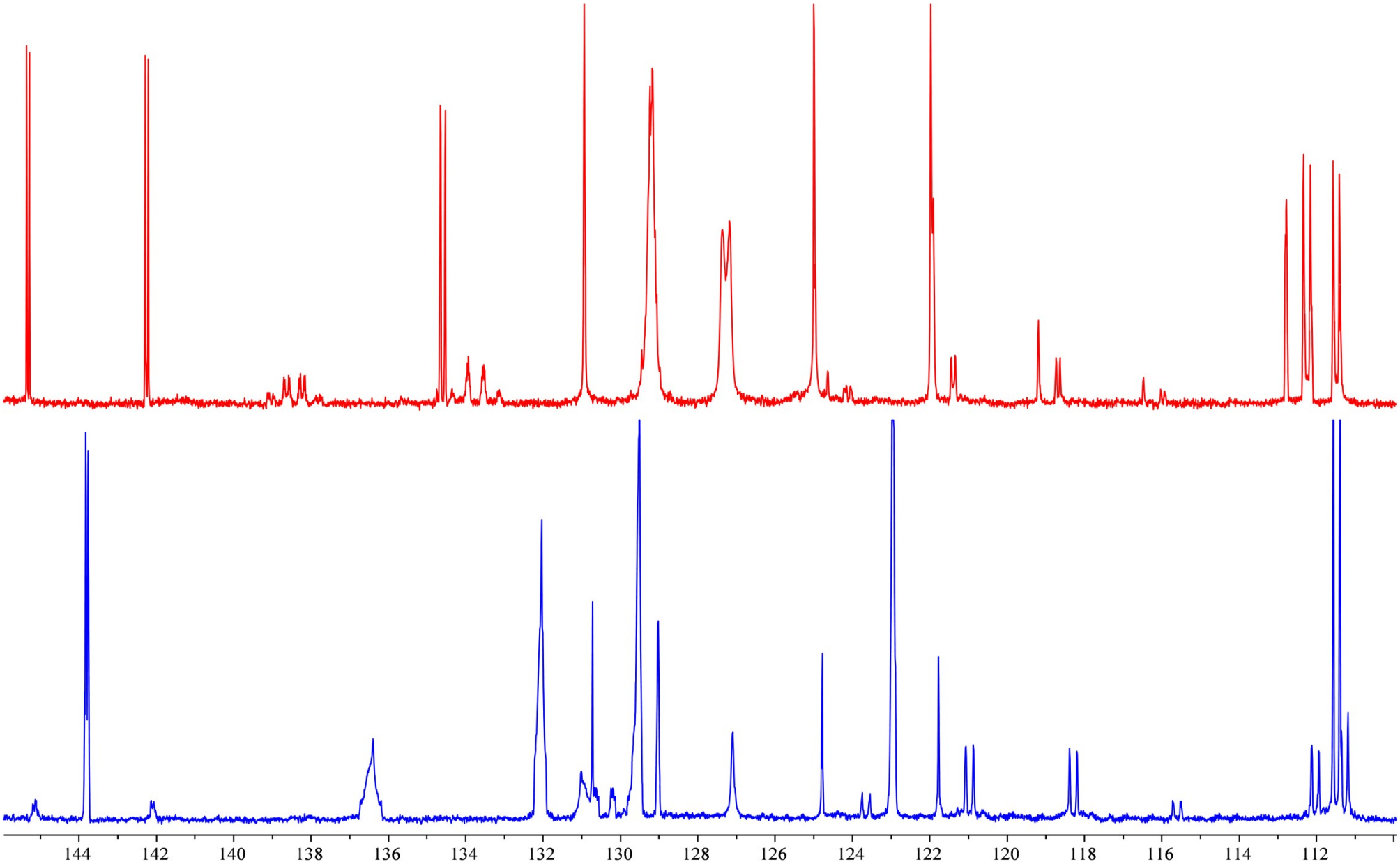

Figure 123. 111-145 ppm region of ^{13}C-{^{1}H} NMR spectra (100.6 MHz, CD_2Cl_2, –5°C, red; CD_2Cl_2, 5°C, blue) of compound (**5b**) (red) and the compounds (**4b**, **5b**) mixture (blue).

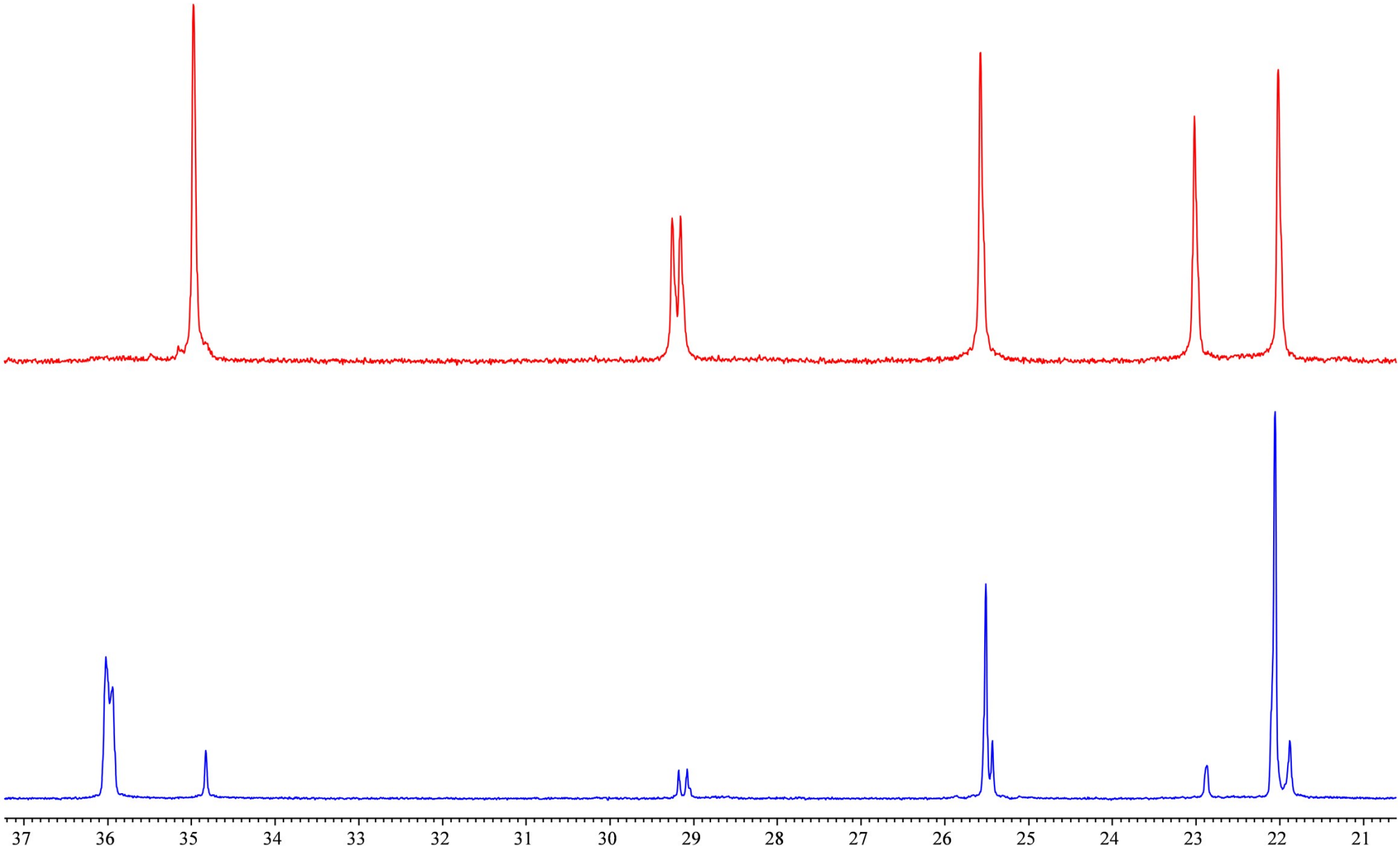

Figure 124. High-field fragments of ^{13}C-{^{1}H} NMR spectra (100.6 MHz, CD_2Cl_2, –5°C, red; CD_2Cl_2, 5°C, blue) of compound (**5b**) (red) and the compounds (**4b**, **5b**) mixture.

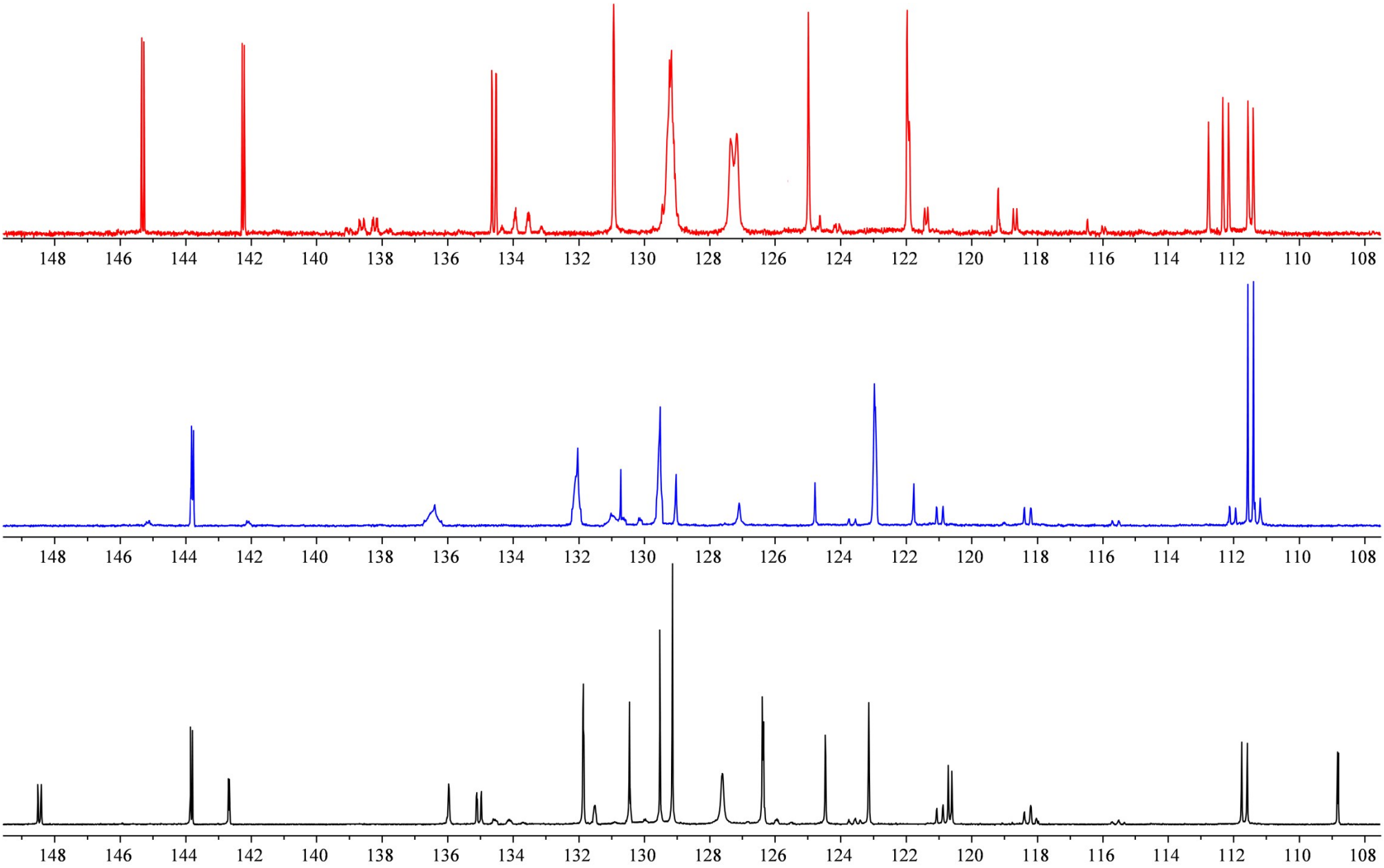

Figure 125. Low-field fragment of ^{13}C-{^{1}H} NMR spectra (100.6 MHz, CD_2Cl_2, –5°C, red; 100.6 MHz, CD_2Cl_2, 5°C, blue; 150.9 MHz, 25°C, black) of compound (**5b**) (red), the compounds (**4b**, **5b**) and (**3b**, **4b**) mixtures (blue and black, respectively).